FSTC-HT-23-539-71

US ARMY FOREIGN SCIENCE AND TECHNOLOGY CENTER

PRINCIPLES OF THE THEORY OF AVIATION

GAS TURBINE ENGINES

by

I. I. Kulagin

Subject Country: USSR

This document is a rendition of the original foreign text without any analytical or editorial comment.

TECHNICAL TRANSLATION

FSTC-HT-23- 539-71

ENGLISH TITLE: PRINCIPLES OF THE THEORY OF AVIATION GAS TURBINE ENGINES

FOREIGN TITLE: OSNOVY TEORII AVIATSIONNYKH GAZOTURBINNYKH DVIGATELEY

AUTHOR: I. I. Kulagin

SOURCE: Military Publishing House of the Ministry of Defense of the USSR, Moscow, 1967

Translated for MID by Translation Consultants, Ltd.

NOTICE

BLANK PAGE

Today aviation for the most part uses gas-turbine engines as replacements for the reciprocating engines which have exhausted their developmental potential. There is no practical way to attain any significant increase in airspeed, let alone at supersonic speed, with reciprocating engines driving air screws, that is, with a reciprocating propeller-engine installation (VMU).

The reasons are as follows. The shaft power developed by the reciprocating engine, that is, the engine's effective power, N_e, in hp, is expended in rotating the air screw, the propeller of the propeller-engine system. When the propeller rotates and drives the surrounding mass of air back at a speed greater than the airspeed, it imparts acceleration to this mass. And the reactive force developed is directly absorbed by the propeller blades and is then transmitted through the shaft, bearings, and engine block to the aircraft as propeller tractive force, P_p.

Thus, a propeller on an aircraft moving at speed V, in m/sec, pulls the aircraft with force P_p, in kg, and consequently imparts to the aircraft a net power equal to P_pV, kg m/sec, and lends it forward motion in the air. However, the power expended in turning the propeller is always greater than the net power because of unavoidable losses usually taken into consideration in propeller efficiency: $\eta_p < 1$. Therefore, we can write:

$$P_pV = 75N_e \cdot \eta_p,$$

from whence:

$$P_p = 75\ N_e/V \cdot \eta p.$$

Since the effective power of a reciprocating engine is practically independent of airspeed, and since the efficiency of a propeller is reduced significantly at Mach numbers close to one, it will be seen from the relationship obtained above that under these conditions propeller thrust must decrease rapidly with increasing airspeed While the thrust developed by the propeller-engine system is decreasing, the thrust required for the aircraft to fly will increase significantly with increasing airspeed.

Therefore, a sharp increase in the power of a reciprocating engine is required at high speed to provide the necessary thrust. But this leads to an unacceptable increase in the weight and size of the aircraft power plant. As a result, the weight of a reciprocating power plant proves to be about the same as the weight of the aircraft, so it becomes impossible to use this type of power plant and, consequently, achieve high airspeeds with it.

This obstacle can be completely overcome by making the transition to jet engines capable of developing thrust required for very high airspeeds at completely acceptable weights and sizes, many times less than those of comparable reciprocating engines with a propeller.

The use of jet engines made possible a significant increase in aircraft speed and altitude within a short period of time. In 1948, a turbojet aircraft flew at 1079 km/h whereas the previous (1939) maximum speed of a special-purpose aircraft with a reciprocating engine designed to establish a record was only 755 km/h.

The officially recorded world records for jet aircraft were 1822 km/h in 1956, and 2259.8 km/h in 1958. A new world record of 2388 km/h was established in 1959, by the Soviet Ye-66. The maximum speed recorded while this record was being established was even higher, 2504 km/h. In that same year, 1959, the Soviet T-431 set a world altitude record (28,852 m above sea level). Today jet aircraft fly at even greater speeds and altitudes.

The principal, characteristic feature common to jet engines, regardless of design or working principle, is that the thrust they develop is the reactive force of a flow of fuel combustion products accelerated in the engine proper and discharged from it into the surrounding medium at a speed greater than the airspeed. This reactive force is opposite in direction to that of the gas exhaust flow, is directly absorbed by the structural elements of the engine, transferred to the aircraft through the engine mount, and used as the thrust required to achieve flight.

The acceleration of the gas flow in a jet engine is dependent on the heat imparted to it during fuel combustion and the subsequent conversion (during the expansion process) of the potential energy of the combustion products into kinetic energy. Consequently, in a jet engine the chemical energy of the fuel, transformed into the kinetic energy of the combustion products, can be used to obtain thrust directly, without an intermediate propulsive unit reacting with the surrounding medium such as a propeller, for example.

Thus, the jet engine combines the engine proper, the thermal engine in which the chemical energy of the fuel is converted into mechanical energy (in this case into the kinetic energy of the gas jet), and the propulsive unit which creates thrust as a result of the reaction of the gas jet escaping from the engine. Jet engines are therefore called direct reaction engines, as distinguished from engines with propeller thrust, which are called indirect reaction engines.

All jet engines can be divided into the following two classes:

air-breathing engines (VRD);

rocket engines.

Air-breathing engines, in turn, are divided into two types:

solid injection, or ramjet; (PVRD);

gas turbine engines (GTD).

Gas turbine engines, as was indicated above, are most widely used in modern aviation and have a compressor driven by a gas turbine to compress the air fed into the combustion chamber. These engines have been highly perfected within a relatively short period of time.

Gas turbine engines are subdivided into turbojet engines (TRD), turboprop engines (TVD), and turbofan, or dual-flow engines (DTRD).

Whereas in the TRD the gas turbine only turns the compressor, in the TVD it turns the compressor and the propeller, and in the DTRD it turns the compressor and the fan, which is enclosed in an annular duct.

In the TRD, the only thrust is that of the direct reactive force of the gas jet discharged from the engine into the atmosphere. In the TVD and DTRD, thrust is a combination of the reactive force of the gas jet discharged from the engine, and the thrust created by the propeller, or by a special fan.

Turbojet engines are the principal engines used in the different types of military aircraft flying at both supersonic and very much lower than subsonic speeds. These engines are beginning to find ever increasing use in fast civilian aircraft (passenger and cargo) flying at approximately 800 km/h,and faster.

Turboprop engines are widely used in relatively slow (subsonic) (600 to 700 km/h) passenger and cargo aircraft. At these speeds they are more economical than other types of gas turbine engines.

Dual-flow jet engines are more economical at subsonic speeds than TRD's, and therefore are used in many cargo aircraft, despite their more complicated design. Even at supersonic speeds the DTRD can, under certain conditions, be more advantageous to use than the TRD (weightwise,for example).

Different turbine engine designs are also used for helicopter rotor drives in many cases.

Rocket engines can be subdivided into the following two groups:

liquid-fuel rocket engines (ZhRD), in which an oxidizer, such as liquid oxygen, nitric acid, hydrogen peroxide, and others, is used to burn the liquid fuel;

solid fuel rocket engines (RDTT) using special powders, and other solid fuels, that include the oxygen required for combustion.

BLANK PAGE

Liquid-fuel rocket engines (ZhRD) are installed in various types of ballistic missiles. ZhRD's are also used to launch and accelerate different types of unmanned aircraft. ZhRD thrust is independent of airspeed and, what is particularly important, will not decrease but will even increase markedly with an increase in altitude. The special feature of the ZhRD is that there is no need for atmospheric air for fuel combustion. Therefore, missiles equipped with ZhRD can develop airspeeds and reach altitudes completely unattainable by aircraft with other types of engines. Clear proof of this are the speeds and altitudes reached by Soviet satellites and space ships using ZhRD rocket carriers.

Liquid-fuel rocket engines can also be used in high-speed aircraft with a requirement for high speed, high rate of climb and high ceiling for a relatively short flight fixed by the amount of oxidizer and fuel the aircraft can carry in its tanks. These engines can also be used in conjunction with a TRD as auxiliary systems used to reduce the time to altitude, to increase speed for short periods of time, and increase the ceiling for the aircraft, or as booster systems to facilitate take-off, that is, to shorten the take-off run.

Solid-fuel rocket engines are distinguished by a short period of continuous operation fixed by a short combustion period for the fuel in the engine is combustion chamber. This is why the RDTT is only used in aviation in boosters (booster rockets) that facilitate the take-off for some aircraft. In addition, the RDTT is widely used, independently, and as an auxiliary (boost and acceleration), in various types of ballistic and winged missiles, missiles , etc.

Principles of the theory of gas turbine engines will be reviewed in this book. Attention in the main is devoted to the physical significance of the phenomena and behavior patterns reviewed, and especially to those questions of theory directly associated with engine operation in the aircraft, and with bench testing.

In concluding his introduction, the author expresses his great appreciation to Professor Yu. N. Nechayev, Doctor of Technical Sciences, for his valuable advice and comments given upon reviewing the manuscript of this book.

CHAPTER 1

NECESSARY DATA FROM THE THERMODYNAMICS OF FLOW AND GAS DYNAMICS

1. Gas Flow and the Equation of Continuity

The equations under consideration in this chapter are derived as applicable to an elementary gas filament; in other words, to that stream filament, the lateral dimensions of which are so small that all gas parameters, velocity, pressure, temperature, and density, can be taken as constants within each of its cross-sections.

These equations are also used in this form in the theory of aviation gas turbine engines, regardless of type.

When these gas parameters are not identical within the limits of a flow cross-section the actual parameters in each specific flow cross-section are replaced by their averaged values. This makes it possible to use all the equations obtained for the elementary stream filament in these cases as well by using corresponding correction factors.

In what follows we will consider only the steady (stationary) fluid flow, a characteristic feature of which is that at each point in the flow the gas velocity, and the parameters for the state of the gas (pressure, temperature, volume) have completely defined values that do not change over time. In a fluid flow such as this the particle trajectories are called lines of flow, and the lateral surface of the elementary stream filament is called the surface of flow. In the case of steady motion, the velocities at which the particles move are in a direction tangent to the surface of flow, so there is no gas leakage, and the surface of flow is, as it is usually spoken of, gas impermeable.

Let us consider a section of a gas stream filament between its cross-sections, 1 and 2, normal to the surface of flow (fig.1), and assuming that the gas moves from cross-section 1 to cross-section 2.

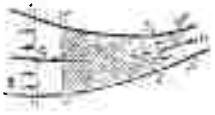

Fig. 1: Derivation of the equation of continuity.

After some (very short) time interval $\Delta\tau$, the separated section of the stream filament is displaced from position 1 2 to a new position 1' 2'. The gas displaced from area 1 1' flows into shaded volume 1' 2, and at the same time some gas flows from

this volume (1' 2) and fills area 2 2'.

Obviously, the weight of gas ΔG_1 entering volume 1 2 in time $\Delta\tau$ will equal

$$\Delta G_1 = \gamma_1 F_1 \Delta l_1,$$

where

γ_1 is the specific weight of the gas in cross-section 1;

F_1 is the area of cross-section 1;

Δl_1 is the distance between cross-sections 1 and 1'.

Distance Δl_1 can be represented as the product of velocity c_1 in cross-section 1 and time $\Delta\tau$; $\Delta\tau_1 = c_1 \Delta\tau$, so,

$$\Delta G_1 = \gamma_1 F_1 c_1 \Delta\tau,$$

or

$$\frac{\Delta G_1}{\Delta\tau} = \gamma_1 c_1 F_1.$$

But $\Delta G_1/\Delta\tau$ is the weight flow of the gas per unit time, G_1 kg/sec, through cross-section 1, so

$$G_1 = \gamma_1 c_1 F_1,$$

and, in general, for any cross-section of the flow

$$G = \gamma c F. \tag{1.1}$$

This relationship is called the flow equation.

$$\frac{G}{F} = \gamma c. \tag{1.2}$$

is obtained from the flow equation.

The product γc is called the flow density. It is easily seen that the flow density is the weight flow per unit cross-sectional area.

The amount of gas by weight, ΔG_2, displaced from volume 1' 2 in the same time, $\Delta\tau$, and the weight flow of the gas, G_2, per unit time through cross-section 2, by analogy with the foregoing, will equal, respectively,

$$\Delta G_2 = \gamma_2 F_2 \Delta l_2 = \gamma_2 F_2 c_2 \Delta\tau$$

and

$$G_2 = \frac{\Delta G_2}{\Delta\tau} = \gamma_2 c_2 F_2,$$

where γ_2 is the specific weight of the gas in cross-section 2;

F_2 is the area of cross-section 2;

c_2 is the velocity of the gas in cross-section 2.

In the case of steady motion, and no discontinuities in the flow, the same amount of gas (liquid) by weight passes through each of its cross-sections; that is, the inflow of gas equals its consumption and $G_1 = G_2 = G$

or, on the basis of (1.1),

$$\gamma_1 c_1 F_1 = \gamma_2 c_2 F_2 = \gamma c F. \tag{1.3}$$

This is also the equation of continuity, or the equation of constancy, for the weight flow of a compressible gas.

For an incompressible liquid the specific weight is a constant $\gamma_1 = \gamma_2 = \gamma$, so equation (1.3) assumes a simpler form,

$$c_1 F_1 = c_2 F_2 = cF. \qquad (1.4)$$

What follows from the foregoing is that for an incompressible liquid the velocity in any two cross-sections of the flow is inversely proportional to the areas of these cross-sections.

2. The Energy Equation.

Let us compile the energy balance for a moving gas relative to a fixed system of coordinates.

Let some mass of gas, initially filling volume 1 2 (fig. 1), be displaced into a position bounded by cross-sections 1' and 2' in an infinitely short period of time, $\Delta\tau$. The velocity of the gas, and its pressure in cross-section 1 are equal to c_1 and p_1, respectively, and to c_2 and p_2 in cross-section 2.

A change in any type of energy equals the difference between the amounts of the given type of energy in positions 1' 2' and 1 2. Readily noted is that volume 1' 2 is common to both positions and that the energy of the mass of gas filling this volume does not change over time $\Delta\tau$ because gas motion is steady. Therefore, the change in energy when the mass of gas is displaced from position 1 2 to position 1' 2' will be determined only by the difference between the amounts of energy in the infinitely small volumes 2 2' and 1 1' for a gas weight flow, ΔG, in time $\Delta\tau$. Accordingly the change in kinetic energy will equal

$$\Delta E_k = \frac{\Delta G (c_2^2 - c_1^2)}{2g},$$

and the change in the internal (thermal) energy will equal

$$\Delta U = c_v (T_2 - T_1) \Delta G,$$

where T_2 and T_1 are the gas temperatures in cross-sections 2 and 1, respectively;

c_v is the specific heat capacity of the gas at constant volume.

During the gas displacement under consideration, the external pressure forces applied to the stream filament in sections 1 and 2, and equal to $p_1 F_1$ and $p_2 F_2$, perform work which is expended in displacing the given volume of gas. The external pressure forces acting on the lateral surface of the stream filament (on the surface of flow) do no work because they are normal to it.

In time $\Delta\tau$ the work performed by pressure force $p_1 F_1$, the direction of which is the same as that of the gas motion, will equal

$$p_1 F_1 c_1 \Delta\tau = p_1 v_1 \Delta G,$$

because the product $F_1 c_1 \Delta\tau = v_1 \Delta G$ is the volume of element 1 1', and v_1 is the specific volume of the gas in cross-section 1.

Similarly, the work performed by pressure force p_1F_2, the direction of which is opposite to that of the gas motion, will, in the same time period $\Delta\tau$, correspondingly equal

$$p_2F_2c_2\Delta\tau = p_2v_2\Delta G.$$

Consequently, the work absorbed by the gas and expended in its displacement (or the work required to push the gas through) as a result of the drop in pressure from position 1 2 to position 1' 2' must be equal to the difference between the work done by the pressure forces under consideration in sections 1 1' and 2 2'

$$\Delta L_{1-2} = \Delta G(p_1v_1 - p_2v_2).$$

In the general case heat of amount Δ Q can be added to (or removed from) the gas in time $\Delta\tau$ during its movement. Moreover, during this same period mechanical work, Δ L, can be introduced into the gas from the outside by a compressor impeller installed between cross-sections 1 and 2, for example, or, conversely, the gas can do (deliver) external mechanical work by rotating a turbine rotor located between the same cross-sections. Finally, that amount of energy, ΔL_r, expended in overcoming the friction which develops during the gas flow (friction work) must be taken into consideration.

The law of conservation of energy has it that all the energy introduced into the gas, that is, the sum of the heat added to the gas, the mechanical work, and the work done by pressure forces, must equal the change in the kinetic and internal energy of the gas, plus the friction work. Consequently, the energy balance for a moving gas applicable to the stream filament flow section between cross-sections 1 and 2 must be written in the following form:

$$\frac{\Delta Q}{A} + \Delta L + \Delta L_{1-2} = \Delta E_\kappa + \frac{\Delta U}{A} + \Delta L_r$$

where A = 1/427 is the heat equivalent of the mechanical work.

Dividing all the terms in the expression obtained by ΔG, and using the above relationships, we obtain the energy equation equated to 1 kg of moving gas

$$Q + AL + A(p_1v_1 - p_2v_2) = A\frac{c_2^2 - c_1^2}{2g} + c_v(T_2 - T_1) + AL_r, \qquad (1.5)$$

where Q = Q/Q is the heat introduced per 1 kg of gas in flow section 1 2;

L = L/G is the external mechanical work transmitted by 1 kg of gas in flow section 1 2;

$L_r = L_r/G$ is the friction work done during the movement of 1 kg of gas in flow section 1 2.

We can now take it that in the general case heat can be added to a moving gas in two ways; as a result of a heat exchange with an outside medium (or, for instance, as a result of fuel combustion in the flow), in amount Q_H, and as a result of the conversion of

friction work L_r into heat Q_r which is absorbed by the gas. Since it is obvious that $Q_r = AL_r$, $Q = Q_H + AL_r$, so after substituting in formula (1.5) and making the reduction,

$$Q_H + AL + A(p_1v_1 - p_2v_2) = c_v(T_2 - T_1) + A\cdot\frac{c_2^2 - c_1^2}{2g}. \quad (1.5a)$$

Moreover, from thermodynamics the sum $c_vT + Apv = i$ is the enthalpy (heat content), that is

$$i_1 = c_vT_1 + Ap_1v_1 = c_pT_1;$$
$$i_2 = c_vT_2 + Ap_2v_2 = c_pT_2,$$

where c_p is the specific heat at constant pressure.

Thus, equation (1.5a) may be represented in the following form

$$Q_H + AL = A\cdot\frac{c_2^2 - c_1^2}{2g} + c_p(T_2 - T_1). \quad (1.6)$$

If the heat is expelled from the gas to an outside medium, or if the gas performs external work (if the gas yields energy), the terms Q_H and AL in equation (1.6) will have a minus sign, so in the general case, we can write

$$\pm Q_H \pm AL = c_p(T_2 - T_1) + A\cdot\frac{c_2^2 - c_1^2}{2g}. \quad (1.7)$$

In this form this equation, sometimes called the <u>heat content equation</u>, is widely used in gas turbine and jet engine theory. It, by itself, expresses the thermal form of the energy balance for a moving gas, associating its temperature with the velocity at which it is moving, and takes into account the energy exchange between the gas flow and the outside medium.

This equation is distinguished by a significant feature; it contains no friction work magnitudes, and is correct for flows with, and without, friction. This is explained by the fact that the work expended in overcoming friction is completely converted into heat that is absorbed by the gas. Therefore, friction only leads to the conversion of one form of energy into another in the flow, and can have no effect on the overall energy balance.

Let us consider certain special cases of equation (1.7).

1. Air flows through a passage in a centrifugal impeller in which work (+L) is added to the air from without in flow section 1 2, compressing the air, and increasing its temperature. At the same time, air velocity is kept constant, $c_2 = c_1$. The air simultaneously expels some heat, $(-Q_H)$, to the surrounding medium, through the passage walls. Under these conditions, and in accordance with the foregoing, we write

$$AL = c_p(T_2 - T_1) + Q_H. \quad (1.8)$$

This equation shows that in this case the work done from without is expended in increasing the enthalpy of the air, and on heat transfer to surrounding medium.

2. The gas in section 1 2 flows through the passage between turbine rotor blades, expanding and performing external work (- L) transmitted to the turbine shaft. Heat transfer from the gas through the passage walls to the external medium is negligible and can be disregarded ($Q_H = 0$). The gas temperature falls as the gas expands ($T_2 < T_1$), so from equation (1.7) we obtain

$$c_p(T_1 - T_2) = AL + A\cdot\frac{c_2^2 - c_1^2}{2g}. \qquad (1.9)$$

This equation indicates that the external work performed by the gas, and the increase in kinetic energy (in the turbine, $c_2 < c_1$), are the result of a reduction in its enthalpy.

3. The gas flow process in section 1 2 is energy isolated, that is, neither heat nor work is added or rejected. ($Q_H = 0$ and $L = 0$). Now, we obtained from equation (1.7)

or

$$c_p(T_1 - T_2) = A\cdot\frac{c_2^2 - c_1^2}{2g}$$

$$i_1 + \frac{Ac_1^2}{2g} = i_2 + \frac{Ac_2^2}{2g}. \qquad (1.10)$$

Thus, the sum of the enthalpy and the kinetic energy is a constant for an energy isolated process and change in enthalpy, and the corresponding change in gas temperature is simply a result of change in velocity.

The energy equation for a quiescent gas is simpler than that for a moving gas, because if the gas is not flowing there is no change in its kinetic energy and friction work, and the work done by external forces can only be associated with change (deformation) in gas volume, that is, with its expansion or compression.

In this context the energy equation for 1 kg of quiescent gas is in the following form, known from thermodynamics (the equation for the first law of thermodynamics)

$$Q = c_v(T_2 - T_1) + AL_a, \qquad (1.11)$$

where Q is the heat involved in the process;

$c_v(T_2 - T_1)$ is the change in the internal energy of the gas;

L_a is the absolute work done in expanding or compressing the gas (work done in deforming its volume).

This equation indicates that in a quiescent gas all the heat, for example the heat added to the gas, is expended in simply changing its internal energy and on the work required to expand the gas.

Equation (1.11) is also applicable to a moving gas if the energy balance is equated to a system of coordinates that moves with the flow and at the same velocity; that is, together with the center of gravity of a separate element of the gas volume. Here we must keep in mind that in the general case the friction

work is $AL_r = Q_r > 0$ for a moving gas and that as a result the heat involved in the process will equal $Q = Q_H + AL_r$. Therefore, equation (1.11) should be written as follows for 1 kg of moving gas

$$Q_H + AL_r = c_v(T_2 - T_1) + AL_a. \tag{1.12}$$

The work done by the gas, L_a, can be measured in the pv-coordinates of the area located between the curve depicting the change of state process and the axis of volumes; the shaded area 1 2 3 4 in Figure 2. The absolute magnitude of this work can be computed through formulas derived in thermodynamics. One of these formulas for the general case of polytropic expansion has the following form

$$L_a = \frac{1}{n-1}(p_1v_1 - p_2v_2), \tag{1.13}$$

where n is the exponent of the polytropic expansion (or compression).

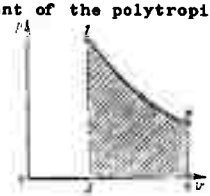

Figure 2. Establishing the absolute work done by a gas.

If no heat is added to or expelled by the gas ($Q = 0$) the polytropic exponent n in formula (1.13) can be replaced by the adiabatic exponent k.

3. Bernoulli's Equation

There is yet another form of energy equation for a moving gas. Let us, for this purpose, take equation (1.5 a)

$$Q_H + AL + A(p_1v_1 - p_2v_2) = c_v(T_2 - T_1) + \frac{A}{2g}(c_2^2 - c_1^2)$$

and let us substitute in it the expression for external heat, Q_H, from equation (1.12)

$$Q_H = c_v(T_2 - T_1) + AL_a - AL_r$$

Then, after combining similar terms, and making a simple transformation we obtain

$$L + L_a + (p_1v_1 - p_2v_2) = \frac{c_2^2 - c_1^2}{2g} + L_r$$

The sum of the absolute work of expansion (or compression) of a gas, L_a, and the work $L_{1-2}(p_1v_1 - p_2v_2)$ done in displacing its volume, is called the total work of polytropic expansion (or compression) of the gas, L_t, and, in accordance with (1.13), is equal to

$$L_t = L_a + L_{1-2} = \frac{n}{n-1}(p_1v_1 - p_2v_2). \tag{1.14}$$

In graphical form and in pv-coordinates this work can be represented by the shaded area a 1 2, b in Figure 3.

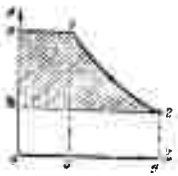

Figure 3. Establishing the total work done by a gas.

Thus, retaining the previous sign rule for the external work L, we can finally write

$$-L + L_t = \frac{c_2^2 - c_1^2}{2g} + L_r. \qquad (1.15)$$

This is the so-called <u>generalized Bernoulli equation</u>, and represents the energy balance in mechanical form for 1 kg of moving compressible gas. The equation explains the connection between gas velocity, change in its pressure and specific volume, friction work, and external mechanical work. As will be seen, external heat, Q_H, does not enter into the Bernoulli equation, so this latter has the same form for the processes involved in expelling (or adding) heat as it does for processes without heat exchange with the external medium. However, the intensity and the direction of heat exchange between a moving gas and the external medium have a direct effect on the nature of the thermodynamic change in the state of the gas; that is, on the magnitude of the polytropic exponent and, consequently, can be taken into consideration when computing the total work done in expanding (or compressing) a gas.

Let us consider certain special cases of the Bernoulli equation.

1. Air flows through a compressor impeller, where, in section 1 2, work (+L) is added to the air from without, as a result of which the air is compressed and forced into an area of higher pressure than that prevailing at the impeller inlet. Air velocity is unchanged ($c_2 = c_1$). We also have friction work ($L_r > 0$) and heat exchange with the external medium ($Q_H > 0$). Under these conditions, we obtain the following from formula (1.15)

$$L + L_t = L_r,$$

or

$$L = -L_t + L_r = \frac{n}{n-1}(p_1 v_2 - p_1 v_1) + L_r. \qquad (1.16)$$

This equation demonstrates that in this case the external work is expended on polytropic compression, in forcing the air through, and for overcoming friction (hydraulic resistance).

2. Gas flows through a turbine rotor where, expanding in section 1 2, it does external work (-L) against friction ($L_r > 0$). Let us disregard the heat exchange with the external medium. In this case we obtain the following from formula (1.15)

$$L_t = L + \frac{c_2^2 - c_1^2}{2g} + L_r \qquad (1.17)$$

or $$\frac{n}{n-1}(p_1v_1 - p_2v_2) = L + \frac{c_2^2 - c_1^2}{2g} + L_r.$$

Equation (1.17) demonstrates that the total work of polytropic expansion (the potential energy of the gas) is expended in the turbine in doing external work, increasing the kinetic energy of the gas, and overcoming friction.

3. Air flows through a pipeline, expanding against friction ($L_r > 0$). No external work is performed ($L = 0$). Now we obtain the following from equation (1.15)

$$L_t = \frac{c_2^2 - c_1^2}{2g} + L_r. \tag{1.18}$$

Consequently, when $L = 0$ the potential energy of the gas is expended in changing its kinetic energy and in overcoming friction.

4. External work is $L = 0$, friction work is $L_r = 0$. The air flow through section 1 2 is slowed by the corresponding change in the pipe cross-section; the velocity is $c_2 < c_1$. In this case equation (1.15) will obviously be in the form

$$\frac{c_1^2 - c_2^2}{2g} = -L_t + L_r$$

or

$$\frac{c_1^2 - c_2^2}{2g} = \frac{n}{n-1}(p_2v_2 - p_1v_1) + L_r \tag{1.19}$$

Thus, when $L = 0$ the kinetic energy of a decelerating gas is expended on its compression, on forcing it through, and on overcoming friction.

5. The gas flow process is energy isolated ($L = 0$; $Q_H = 0$), and there is no friction ($L_r = 0$); that is, process is adiabatic and $n = k$. For these conditions, we obtain the following through equation (1.15) and formula (1.14)

$$\frac{k}{k-1}(p_1v_1 - p_2v_2) = \frac{c_2^2 - c_1^2}{2g}. \tag{1.20}$$

Consequently, in an energy isolated process an increase in velocity must be accompanied by a reduction in gas pressure (expansion), and a decrease in gas velocity must be accompanied by an increase in its pressure (compression). It is easily seen that equations (1.10) and (1.20) are identical. Actually, based on the known equation of state, $pv = RT$ (where R is the gas constant), we can write

$$\frac{k}{k-1}(p_1v_1 - p_2v_2) = \frac{k}{k-1} \cdot R(T_1 - T_2). \tag{1.20 a}$$

However, from Mayer's equation, $c_p - c_v = AR$, $kR/k-1 = c_p/A$, so

$$\frac{k}{k-1}(p_1v_1 - p_2v_2) = \frac{c_p}{A}(T_1 - T_2),$$

which after substitution in equation (1.20) again leads to equation (1.10).

Comparing equations (1.18), (1.19), and (1.20) it is readily seen that friction (hydraulic resistance) reduces the potential

energy (pressure) when kinetic energy is converted into potential energy, and will reduce kinetic energy (velocity) when potential energy is converted into kinetic energy.

6. For an incompressible liquid, $v = 1/\gamma = \text{constant}$, so

$$L = v_1(p_1 - p_2) = \frac{p_1 - p_2}{\gamma_1},$$

and if L = 0, equation (1.15) will take the following form, known from hydraulics,

$$\frac{p_1 - p_1}{\gamma_1} = \frac{c_2^2 - c_1^2}{2g} + L_r. \tag{1.21}$$

If, morecver, $L_r = 0$, we obtain

$$\frac{p_1}{\gamma_1} + \frac{c_1^2}{2g} = \frac{p_2}{\gamma_2} + \frac{c_2^2}{2g}. \tag{1.22}$$

Consequently, when L = 0 and $L_r = 0$, the sum of the potential and kinetic energies is a constant. Equations (1.21) and (1.22) are also applicable to the motion of a compressible gas if its pressure drop is insignificant, with the result that we can take $\gamma_1 \approx \gamma_2$ without significant error.

4. Stagnation Parameters. Special Features Involved in Heating Bodies in a Gas Flow.

What follows from the energy equation at (1.10) for an energy isolated flow is that gas temperature and enthalpy increase with a decrease in gas velocity and reach their maximum values when the flow velocity euqals zero; that is, when the flow is completely stagnated.

The temperature of a completely stagnated flow is called the stagnation temperature, and the corresponding enthalpy is called the total enthalpy. In what follows enthalpy, temperature, and other state parameters of a completely stagnated flow will be indicated by the corresponding letters and an asterisk.

Thus, if the flow velocity of an energy isolated flow is reduced from $c_1 = c$ to $c_2 = 0$, the energy equation at (1.10) can be written

$$i + A \cdot \frac{c^2}{2g} = c_p T^* = i^* = \text{const},$$

from whence is found the stagnation temperature

$$T^* = T + A \cdot \frac{c^2}{2gc_p} = \text{const}, \tag{1.23}$$

where T* is the stagnation temperature (c = 0);

T is the true (thermodynamic) temperature of a gas moving at velocity c > 0.

For air $c_p = 0.24$, so

$$T^*_{air} \approx T + c^2/2000. \tag{1.23 a}$$

These relationships demonstrate that total enthalpy i* and stagnation temperature T* are constants for energy isolated flows and are completely independent of the nature of the process of flow stagnation.

Let us turn to the following example to explain the physical significance of stagnation temperature. The leading edge of a solid body placed in a gas flow will deflect the flow from its initial direction. However, there is always one among the traveling stream filaments on the body that is not deflected, but approaches normal to the body and upon impact loses all its kinetic energy (velocity); that is, is completely stagnated. That point on the surface of the body where this phenomenon occurs is called the stagnation point, or the zero velocity point. The gas temperature at the stagnation point, where the gas velocity becomes zero, and will exactly equal the stagnation temperature, is determined through equation (1.23) if, of course, the very insignificant heat exchange between adjacent stream filaments is disregarded.

What follows from the Bernoulli equation at (1.2) for an energy-isolated flow when there is no friction (for an adiabatic flow) is that a reduction in velocity ($c_2 < c_1$) will increase gas pressure because the gas is being compressed, and will reach its maximum upon complete stagnation, when the velocity is reduced from some magnitude $c_1 = c$ to zero; that is, to $c_2 = 0$. Now the equation at (1.20) will take the following form

$$\frac{k}{k-1} p_1 v_1 \left(\frac{p_2 v_2}{p_1 v_1} - 1 \right) = \frac{c^2}{2g}, \tag{1.24}$$

but the following relationship for pressures and specific volumes is known for an adiabatic process

$$\frac{v_2}{v_1} = \left(\frac{p_1}{p_2} \right)^{\frac{1}{k}}.$$

In addition, let us use the gas state equation $p_1 v_1 = RT_1$. Substituting this relationship in the equation at (1.24) and transforming, we can write it in the following general form

$$\frac{k}{k-1} RT \left[\left(\frac{p^*}{p} \right)^{\frac{k-1}{k}} - 1 \right] = \frac{c^2}{2g}, \tag{1.25}$$

where T and p are the actual temperature and pressure (static pressure) in the flow at a flow velocity equal to c, p* is the pressure in a completely adiabatic, stagnant flow (when c = 0), and called the total pressure or the stagnation pressure.

From the equation at (1.25) total pressure equals

$$p^* = p \left(1 + \frac{k-1}{2} \cdot \frac{c^2}{kgRT} \right)^{\frac{k}{k-1}}. \tag{1.26}$$

For air k = 1.4, R = 29.3, and k/k-1 = 3.5, so

$$p^*_{air} = p \left(1 + \frac{c^2}{2000T} \right)^{3,5}. \tag{1.26 a}$$

We note that the effective pressure obtained upon total stagnation of the gas flow is usually lower than the total pressure established through the formula at (1.26). This is explained by the fact that, actually, flow stagnation is accompanied by friction (hydraulic losses); it is not an adiabatic process.

In many cases the introduction of stagnation parameters greatly simplifies the computations since by so doing there is no need for a separate calculation for change in the kinetic energy of the flow.

What follows from the foregoing is that a solid body located in a gas flow and causing it to stagnate will, as was explained above, result in compression and a consequent increase in gas temperature. Now, let there be a gas flow incident to a plate perpendicular to the flow. In the center of the flow, in front of the plate itself, where flow stagnation is total, all its kinetic energy is converted into heat and the gas temperature is increased, becoming equal to stagnation temperature.

As a result, there will be supplemental heating of the plate to a temperature higher than that of the moving gas. At the same time, plate temperature will be somewhat lower than the temperature of the completely stagnant gas because some of the heat will have been expelled from the plate and because of heat radiation from its surface. However, in many cases it is possible to assume without appreciable error that a plate perpendicular to the flow has the temperature of a completely stagnant gas.

Another cause of flow stagnation, and of increase in gas temperature, when the flow washes a body is associated with gas viscosity. Actually, if a plate is placed lengthwise in a forward flow the gas too will be stagnated at its side, longitudinally washed surfaces, and its temperature will be increased accordingly. In this case, this is because the gas viscosity forms a thin, so-called boundary layer of stagnated gas at the surface of bodies washed by a gas.

Gas velocity at the boundary layer increases gradually from zero on the very surface of the plate (where the gas is immobilized by the friction on the plate surface) to the value of the velocity in the forward flow (at the outer limit of the boundary layer).

This gradual increase in velocity at the boundary layer is explained by the presence of internal friction between adjoining gas layers at the boundary layer, the result of gas viscosity.

Internal friction heats the gas, and boundary layer temperature rises above that of the forward flow.

Since, for the reasons indicated above, almost all the kinetic energy of the gas (from 85 to 100 %) is converted into heat at the boundary layer along a longitudinally washed plate, its temperature right at this plate will be found to be close to stagnation temperature. Correspondingly, the plate itself assumes the increased temperature.

Thus, any body washed by a gas flow will be heated to a temperature in excess of the actual (thermodynamic) temperature of the gas in a forward flow undisturbed by the effect of that body (provided, of course, that special cooling is not used). It is this, in particular, that complicates considerably measurements of the true temperature of a moving gas. If a thermometer (thermocouple, or other) is placed in the gas flow, the gas temperature at the thermometer will be highest at the stagnation point and equal to stagnation temperature.

$$T^* = T + \frac{v^2}{2gc_p}.$$

The gas temperature at the thermometer in the boundary layer will be slightly lower than the stagnation temperature, but still close to it. Therefore, the thermometer will indicate some average elevated temperature, T_m, of the gas stagnated near it, and not the true, lower temperature, T, of the gas in the forward undisturbed flow. Consequently, we can write the following for the temperature measured by the thermometer:

$$T_m = T + r\frac{v^2}{2gc_p},$$

where $r = T_m - T/T^* - T$ is the temperature recovering factor, established experimentally.

This factor depends on thermometer (temperature sensor) design and shape, viscosity, and heat conductivity of the gas. Special temperature measuring devices have a factor $r \approx 0.97$ to 0.98.

Consequently, in order to determine the true temperature of a moving gas it is necessary to know gas velocity and its specific heat, as well as r.

5. Sound Velocity and Mach Number

Experience shows that any so-called local perturbation, such as an increase in pressure (density)developing somewhere in a gaseous medium, will be propagated in all directions at a predetermined velocity.

A perturbation is called small if the changes in the parameters (pressure, density, etc.) caused by it are very small compared to the values of these parameters for a gas in a state of equilibrium.

Small perturbations propagating in a gaseous medium are called weak waves, or small perturbation waves. Sound waves are a characteristic example of this type of wave.

A sound wave consists of regularly alternating domains of increased and decreased density (and pressure) which can be propagated in a gas mass at a velocity called the sound velocity.

All the other small perturbations not perceived by the human ear as sound [1] can be propagated in a gaseous medium at precisely the same velocity. Therefore, in gas dynamics sound velocity is understood to be the velocity at which, in general, all small perturbations in density and pressure are propagated in a gas (air), regardless of whether or not they are perceived as sound by the human ear.

It is known from physics that sound velocity equals

$$a = \sqrt{gk\frac{p}{\gamma}} = \sqrt{gkRT}, \tag{1.27}$$

that is it depends solely on the temperature, and the type of gas. If we insert k = 1.4, g = 9.81, and R = 29.27 in this formula, we obtain the following expression for the velocity of sound in air

$$a \approx 20{,}1\sqrt{T}.$$

Since sound velocity depends on temperature it can differ in the same gas. Sound velocity in a gas increases with increase in temperature.

As altitude increases (up to 11,000 m above sea level), the temperature and the velocity of sound in air, decrease.

The ratio between the velocity at which a gas moves, c, and the sound velocity in a gas flow, a, is called the Mach number

$$M = \frac{c}{a}.$$

Using the formula at (1.23) and the expression at (1.27) for sound velocity, we can express the stagnation parameters in terms of the Mach number as follows

$$T^* = T\left(1 + \frac{k-1}{2} \cdot M^2\right), \tag{1.28}$$

$$p^* = p\left(1 + \frac{k-1}{k} \cdot M^2\right)^{\frac{k}{k-1}}, \tag{1.29}$$

where p, as before, is the static pressure at a specified point in the flow.

If the Mach number is M < 1 flow is called subsonic, if M > 1, supersonic. There can also be a flow regime when the gas velocity coincides with the local sound velocity in the flow; M = 1. This gas flow regime is called the critical regime, and, in accordance with (1.28) the critical temperature in the flow corresponds to it.

$$T_{crit} = 2/k + 1 \cdot T^*. \tag{1.30}$$

The gas velocity, which is thus equal to the local sound velocity in the flow, is called the critical velocity, or critical sound velocity. It is obvious that this velocity is equal to

$$c_{crit} = a_{crit} = \sqrt{gkRT_{crit}}$$

---

[1] The ear perceives as sound only those small perturbations transmitted at frequencies from 20 to 20,000 oscillations per second.

or, expressing T_{crit} in terms of stagnation temperature through the equation at (1.30):

$$c_{crit} = \sqrt{2g \cdot k/k+1 \cdot RT^*}. \qquad (1.31)$$

In an energy isolated flow a change in gas temperature is associated only with a change in the velocity at which the gas is moving. Sound velocity in a given gas depends only on its temperature. Therefore, in a given case the sound velocity in a gas should change with change in the velocity at which the gas is moving, the result of the corresponding change in its temperature.

Accordingly, in the case under consideration the Mach number will increase with an increase in the velocity at which the gas is moving, as well as a reduction in the local sound velocity in the process and if there is flow stagnation the Mach number will be reduced as a result of the reduction in the velocity at which the gas is moving and the increase in the local sound velocity.

In the case of a gas flow without energy exchange with the surrounding medium, the stagnation temperature at each point, or section of the flow, is a constant, as is the critical sound velocity. This follows from the formula at (1.31).

The relationship between the velocity at which a gas is moving and the critical sound velocity is called <u>velocity coefficient λ</u>:

$$\lambda = c/a_{crit} \qquad (1.32)$$

It is obvious that in the critical gas flow regime (when $c = a_{crit}$) the velocity coefficient, as well as the Mach number, equal one; $\lambda_{crit} = M_{crit} = 1$.

It is readily seen that, unlike the Mach number, this coefficient is only proportional to the velocity at which the gas is moving because a_{crit} is a constant.

In many cases simpler relationships can be obtained by using λ, instead of the Mach number. Therefore, in gas dynamics, as well as in jet engine, compressor, and turbine theory, the velocity coefficient, λ, is widely used, in addition to the Mach number.

6. Propagation of Weak Perturbations in a Gas. Shock Waves.

As was explained above, weak perturbations propagated in a quiescent gas do so from their origin in all directions in the form of low-amplitude compression waves of identical velocity, equal to sound velocity.

Therefore, if a perturbation source is in the form of a mass point (a body of insignificant dimensions) surrounded on all sides

by a quiescent gas, the leading front of the weak compression wave created by it (the perturbation boundary) will be a sphere (spherical wave) which can be represented by a circle on a plane.

If the perturbation source somehow generates a single local perturbation (compression) in the surrounding quiescent gas, by rapidly increasing its volume, for example, the leading front of the low-amplitude compression wave created moves in all directions, covering a distance after one second numerically equal to the sound velocity a, after two seconds a distance equal to 2a, etc. Thus, the radius of the spherical, low-amplitude wave will increase by a meters per second and in quiescent air these waves will be propagated symmetrically with respect to the perturbation source (which, in a plane can be represented by concentric circles centered at the source).

The picture is different when weak perturbations are propagated in a gas that is moving relative to the perturbation source.

Figure 4 Propagation diagram of sound waves in a subsonic gas flow.

Now the perturbation wave is not only propagated in radial directions, but is also carried along in its entirety by the gas flow. After the first second the radius of the spherical wave will become numerically equal to the sound velocity a, just as in the case of the quiescent gas, but after the same period the entire spherical wave, and consequently its center as well, is carried along by the flow, moving from the perturbation source for a distance numerically equal to the gas velocity c. After two seconds the wave radius will equal 2a, and the distance between the center of the wave and the perturbation source will become equal to 2c, etc. Obviously, wave propagation can no longer be symmetrical relative to the perturbation source.

The propagation velocity of these waves will be highest and equal to c + a in the direction of gas motion, and lowest and equal to c - a in the direction opposite to the gas flow.

Consequently, in a subsonic gas flow, when velocity is $c < a$, the compression waves must propagate in all directions

from the perturbation source, in the direction of flow, and opposite to it, but asymmetrically with respect to their source A, as shown in Figure 4. Now the perturbations are finally propagated throughout the flow and do not attenuate until some distance from their source, the result of the viscosity of the gas.

In sonic and supersonic gas flows, when $c \geq a$, the drift velocity of compression waves due to the flow is respectively equal to or greater than the propagation velocity (sound velocity a) of the waves along the radii. Therefore, in supersonic (and sonic) flows small perturbations, compression waves that is, cannot be propagated against the gas flow but will be concentrated exclusively in a particular section extending in the direction of the gas flow, as shown in figures 5 and 6. The domain in which weak perturbations can be propagated in a supersonic flow in an expanse (fig. 6) shaped like a cone the apex of which is in the perturbation source, and is called the weak perturbation cone. The surface of this cone is the boundary dividing the flow into two parts, the perturbed part (inside the cone) and the unperturbed part (outside the cone). This boundary surface is called the perturbation wave boundary, or simply the perturbation boundary. The angle, α_0, between the generatrix AB of the perturbation boundary (cone) fig. 6) and the velocity direction, c, of the gas flow is called the perturbation angle. It is easily apparent that this angle can be established through

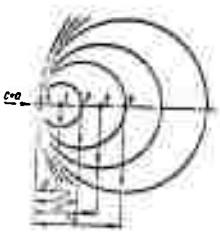

Figure 5 Schematic diagram of the propagation of sound waves in a sonic gas flow.

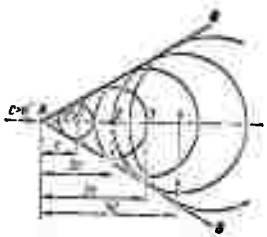

Figure 6 Schematic diagram of the propagation of sound waves in a supersonic gas flow.

What follows from this relationship is that with an increase in the Mach number there is a reduction in the perturbation angle, and that the domain filled by the perturbations is even more constructed and extended along the flow in the direction of the gas motion. This angle will increase with a decrease in the Mach number, and when $M = 1$ ($c = a$) will equal 90°; the perturbation boundary will develop into a plane.

Practically speaking, any minor obstacle, such as a shallow bend in a surface washed by the gas, a scribe mark, or protruberance, on this surface, a thin tapered body, the leading edge of which has a very small cone angle (and which, strictly speaking, has an infinite span), etc., can be the source of small perturbations. These obstacles generate a small compression which too can be propagated in the flow as described above.

In all cases where a supersonic flow washes bodies with lateral dimensions such as to cause them to become definite and significant obstacles to the gas flow there is strong perturbation, a strong pressure wave, or so-called shock wave developed in front of the body as a result of flow stagnation. Experiments have shown that strong perturbations propagate in a gas at supersonic velocity. This is explained, in particular, by the fact that a shock wave generated in front of a body washed by a supersonic steady-state flow is stationary relative to the body.

The generation of a shock wave when a supersonic gas (air) flow washes any body, such as a bullet, rocket, aircraft wing, etc. (or when the bodies move relative to a quiescent gas at supersonic speed), can be explained as follows.

Small perturbations in the gas (an increase in pressure) caused by each surface element of a body washed by a supersonic flow are superimposed and added, so strong perturbation, a shock wave, is generated ahead of the body. The shock wave has its greatest intensity directly in front of the body. As the distance from the body increases the intensity of the perturbations it causes in the gas decrease, the result of gas viscosity, and well away from the body the shock wave gradually merges into the boundary wave of the weak perturbations.

The basic feature of the shock wave is that its front is very narrow (about 10^{-5} mm), so it undergoes an abrupt, shock-type increase in gas pressure, temperature, and density, in addition to an abrupt reduction in velocity.

The shock wave is also the boundary dividing the flow into two parts: the unperturbed (ahead of the shock front) and the perturbed (behind the shock front). A gas interlayer of much higher pressure is enclosed between the shock front and the leading face of the body and has the same effect as if the inflowing, unperturbed stream had hit an unexpected obstacle, experiencing

gas shock (at the shock wave) upon contact. This shock resembles the shock of a jet striking a solid obstacle, accompanied by sudden loss of velocity in the direction of the normal, and a corresponding increase in pressure. The difference between these two situations is that in the case of the solid obstacle the jet velocity in the direction of the normal is lost completely, whereas flow velocity in the direction normal to the shock wave is reduced considerably, but not lost completely. Consequently, it can be said that a supersonic flow appears to "strike" the obstacle suddenly and begins to adapt to the shape of the body, that is it will not begin to wash it behind the front of the shock wave (fig. 7 b).

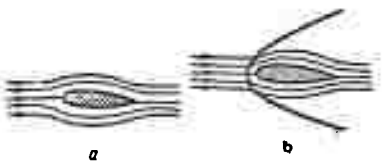

Figure 7 Diagrams of flows around bodies at subsonic (a) and supersonic (b) velocities.

However, if the body is washed by a gas flow at subsonic velocity, the perturbation caused by it associated with flow stagnation will propagate in the form of a pressure wave in the direction against the flow far ahead of the leading part of the body. The gas flow begins to deform gradually, and accomodate to washing the body long before it approaches the body (fig. 7 a).

Shock waves can be normal or oblique. A shock wave is called normal if its surface (front) is perpendicular to the direction of the velocity of the inflowing unperturbed stream, that is, if it contains the angle $\alpha = 90^{\circ}$.

Flow stagnation for a normal shock wave is so great that flow velocity behind it is always less than sound velocity, no matter how large it was in front of the shock waves.

A shock wave is called oblique if its surface forms an acute angle ($\alpha < 90^{\circ}$) with the direction of the inflowing, unperturbed stream. An oblique shock wave is obtained when a supersonic gas flow intersects a shock front and is forced to deviate from its original direction by some angle ω as when it flows around a wedge-shaped body, for example (fig. 8).

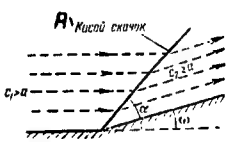

Figure 8 Diagram of an oblique shock wave
A oblique shock wave

The oblique shock wave is always weaker than the normal shock wave, at the same velocity of the inflowing, unperturbed stream; the oblique shock wave velocity decrease and pressure increase are always less than in the case of the shock wave. The velocity of the gas flow behind an oblique shock wave can be either less or greater than sound velocity.

Gas dynamics has proved that the angle of tilt of a shock wave, α (fig. 8) depends on the angle ω of the leading edge of the washed body, and on the Mach number of the inflowing stream. With increasing angle ω and M = constant, the angle of tilt α of the wave increases, and when angle ω becomes greater than some specific value for the velocity in question, the shock wave separates from the body and its front bends, the shock wave curves in the general case (fig. 7 b). There is, in the leading part of such a shock wave, a section close to a normal shock wave, but with increase in distance from the body, the angle of tilt of the curved shock wave is reduced, approaching the weak perturbation angle. An increase in the Mach number of the inflowing stream, ω = constant, will reduce the angle of tilt α of an oblique shock wave.

Gas compression associated with subsonic flow stagnation, that is, with compression in a sonic wave, takes place with practically no loss, and without heat exchange with the external medium; that is, adiabatically. This is explained by the fact that in sonic (weak) waves propagating in a gas, the processes of compression and expansion proceed so rapidly that it is practically impossible for heat exchange to take place between that part of the gas where these waves proceed and its other parts, as well as with the external medium. In addition, because of the small change in the gas state involved, the effect of internal gas friction is not manifested perceptibly. Therefore, the kinetic energy lost by the gas is completely expended in increasing its pressure, and gas entropy does not change, so that pressure and density are linked by the well-known adiabatic equation

$$\frac{p_2}{p_1} = \left(\frac{\rho_2}{\rho_1}\right)^k.$$

In the case of shock waves gas compression, associated with supersonic flow stagnation, heat exchange with the external medium can, as before, be disregarded. However, gas entropy increases, and this is associated with the irreversible, shock-type nature of the shock wave compression process. When gas stagnation occurs in this manner some of its kinetic energy is irreversibly converted directly into heat at the shock wave. This energy is absorbed by the gas and is not consumed in increasing gas pressure.

Thus, in the case of flow stagnation in a shock wave not all

the kinetic energy in the gas is consumed in its compression. Some of it is converted irreversibly into heat and simply heats the gas, the while reducing its compression (pressure is increased).

Gas compression, and the simultaneous introduction of heat into the gas (in this case the result of the direct conversion of some of the kinetic energy into heat), must also result in an increase in the entropy, as we know from thermodynamics. Therefore, the pressure behind the shock wave (both static and total pressure) always proves to be lower than the pressure that would prevail for the same reduction in flow velocity but with no shock wave present; that is, for conventional adiabatic compression taking place without change in entropy. The more intensive the shock wave, in terms of degree of change in flow velocity in it, the greater will be the pressure loss characteristic of it.

Given the same increase in pressure, the increase in gas density (the magnitude of the gas compression) at the shock wave too will always prove to be less than it would be under conventional adiabatic compression. This is explained by the fact that in the first case the gas temperature increases to a greater extent than in the second case, because of the gas being heated.

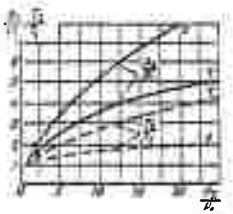

Figure 9 Comparison of shock (Y) and ordinary adiabats (A).

Consequently, some association between gas pressure and gas density other than that for the conventional adiabat must be obtained for the process of shock compression at the shock wave, specifically

$$\frac{p_2}{p_1} > \left(\frac{\rho_2}{\rho_1}\right)^k \qquad \text{instead of} \qquad \frac{p_2}{p_1} = \left(\frac{\rho_2}{\rho_1}\right)^k.$$

The graphical representation of the relationship between gas pressure and gas density under shock compression at the shock wave is called the shock adiabat.

Figure 9 compares a shock adiabat Y, and an ordinary adiabat A, and makes it clear that for the shock adiabat an increase in the pressure ratio p_2/p_1 will be accompanied by a significantly slower increase in the density ratio ρ_2/ρ_1, and that the increase in the temperature ratio T_2/T_1 is correspondingly faster than for the ordinary adiabat. Moreover, regardless of how large

the pressure ratio p_2/p_1 may be, the density ratio ρ_2/ρ_1 cannot be larger than some predetermined value (no larger than 6 in the case of air). The reason is the above established great heating of the gas at the shock wave, that is, the great increase in the temperature ratio T_2/T_1.

7. The Momentum Equation.

The law of momentum, known from theoretical mechanics, can be stated as follows.

The change in the momentum of a body over some period of time equals the momentum imparted by the resultant of all the forces acting on the body during that period.

The momentum of a force equals the product of the force times its action time, and the momentum is the product of the mass of a body times its velocity; so, the law of momentum can be expressed through the following equation:

$$P\Delta\tau = \Delta(mc),$$

where

P is the projection of the resultant of all forces applied to a mass m on some coordinate axis;

c is the projection of the velocity of the motion of mass m on the same axis;

$\Delta\tau$ is force P action time on mass m;

$\Delta(mc)$ is the change in the momentum of mass m during time $\Delta\tau$.

This is the form the momentum equation takes as used in solid mechanics. There is another, more convenient equation, the so-called hydrodynamic form of the momentum equation, applicable to a gas flow. Let us, in order to derive the momentum equation in hydrodynamic form, consider the steady motion of an elementary gas filament by dividing section 1 2 into two sections normal to its axis (fig. 10).

Let us assume that the motion of the filament occurs in plane xOy, that external forces whose resultant equals P act on the separated gas volume 1 2, and that the projections of this resultant on the x and y axes equal P_x and P_y, respectively. Let the separated section of filament 1 2 assume the position 1' 2' after an infinitely short period of time $\Delta\tau$, under the effect of these forces.

Figure 10 The derivation of the moment equation.

Given steady motion, the state and velocity of the gas enclosed in volume 1' 2 will not change. Therefore, the momentum of the mass of gas in this volume too remains unchanged. Consequently, change in the momentum of the gas mass during the displacement of the separated volume 1 2 under consideration will be determined only by the difference between the momentums of the gases in volumes 2 2' and 1 1'. In other words, the change in momentum during time $\Delta\tau$ in the direction of the x-axis will equal

$$\Delta (mc)_x = \Delta m_2 c_{2x} - \Delta m_1 c_{1x},$$

where

m_2 and m_1 are the gas masses enclosed in volumes 2 2' and 1 1';

c_{2x} and c_{1x} are the projections of the flow velocities through sections 2 2 and 1 1 on the x-axis.

Expressing the mass of the gas, Δm, through its weight, ΔG, and the acceleration due to gravity, g, and keeping in mind that for steady motion $\Delta G_2 = \Delta G_1$, we can write

$$\Delta (mc)_x = \frac{\Delta G}{g} (c_{2x} - c_{1x}).$$

However, the gas weight flow per second, G, equals $\Delta G/\Delta\tau$, and, $\Delta G = G\Delta\tau$, so

$$\Delta (mc)_x = \frac{G}{g} (c_{2x} - c_{1x}) \Delta\tau.$$

Equating the change in momentum obtained to the momentum of the force p_x acting on the flow in the direction of the x-axis, and cancelling the equality $\Delta\tau$ on both sides, we obtain

$$P_x = \frac{G}{g} (c_{2x} - c_{1x}). \tag{1.33}$$

We can obtain the following in the direction of the y-axis similarly

$$P_y = \frac{G}{g} (c_{2y} - c_{1y}). \tag{1.34}$$

Equation (1.33), or (1.34), is the momentum equation in hydrodynamic form, or the first Euler equation, which states that for a steady flow, the projection, in any direction, of the resultant of all external forces applied to the gas stream in any of its flow sections is equal to the change in momentum per second at that section in the same direction.

In the general case, the external forces applied to the gas at the flow section under consideration will be the hydrodynamic pressure forces acting from the inflow (p_1F_1), as well as the outflow (p_2F_2) sides, such as the gas friction force against the wall, P_r, directed against the motion of the flow, and the force of the surfaces of the solid walls acting on the gas and which limit the flow or are inside the flow (in the latter case this can be turbine or compressor blades, and the like, washed by the gas.)

Let us explain what has been said through the following examples.

1. An air flow moves at subsonic velocity through a diffuser (fig. 11), that is, through a duct 1 2, the cross-sectional area of which increases in the direction of flow ($F_2 > F_1$), so that air velocity is reduced ($c_2 < c_1$), but pressure increases ($p_2 > p_1$).

Disregard air friction. The forces acting on the flow will be the hydrodynamic pressure forces in the inlet and outlet sections; that is, forces p_1F_1 (with the flow) and p_2F_2 (against the flow) and the force of the inclined walls of the diffuser acting on the gas, p_a.

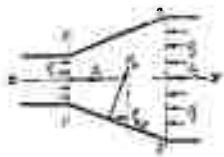

Figure 11 Forces acting on the walls of a diffuser.

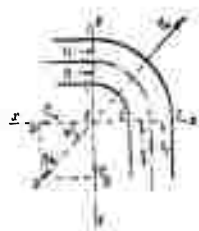

Figure 12 Forces acting on an elbow.

Taking the flow direction as positive, we can write the momentum equation with respect to the longitudinal axis of the diffuser, x - x, in the following form

$$P_x = R_x + p_1F_1 - p_2F_2 = \frac{G}{g}(c_{2x} - c_{1x}),$$

from whence, keeping in mind that $c_{2x} = c_2$; $c_1 > c_2$; $c_{1x} = c_1$, we obtain

$$R_x = p_2F_2 - p_1F_1 - \frac{G}{g}(c_1 - c_2). \qquad (1.35)$$

2. Air is flowing through an elbow (fig. 12) of constant cross-section bent at an angle of 90°. At the elbow inlet the pressure is p_1, the air velocity is c_1, and the cross-sectional area is F_1. At the outlet the pressure is p_2, the velocity is c_2, and the area is $F_2 = F_1$.

Let us compare the momentum equation with respect to the x - x and y - y axes parallel to the straight sections of the elbow, again taking the direction of air flow as positive.

In the case of the projection on the x - x axis, the projection of the pressure force p_1F_1 is obtained equal to this force and flow direction, while the projections of the pressure force p_2F_2, and of velocity c_2 prove to be equal to zero ($c_{2x} = 0$). Therefore, in terms of the projections on the x - x axis, the momentum equation can be written

$$P_{a_x} + p_1F_1 = -\frac{G}{g} \cdot c_{1x}$$

or

$$P_{a_x} = -\left(p_1F_1 + \frac{G}{g} \cdot c_{1x}\right),$$

that is, the horizontal component of the force of the elbow walls acting on the flow, p_{a_x}, is directed against the air flow and obstructs its motion in the original direction.

The projection of force $p_1 F_1$ equals zero when projected on the y - y axis; the projection of force p_2F_2 equals this force, and is opposite in direction to the flow ($-p_2F_2$). The projection of the velocity is $c_{1_y} = 0$. Consequently, for projections on the y - y axis the momentum equation will have the following form

$$P_{a_y} = p_2F_2 + \frac{G}{g} \cdot c_{2y},$$

that is, the vertical component of the force of the walls acting on the flow is with the air flow and lends itself to assisting movement in the new direction. The component forces p_{a_x} and p_{a_y}, and their resultant, p_a, are indicated by dotted arrows in figure 12.

The resultant of forces p_{a_x} and p_{a_y}, that is, the wall force acting on flow p_a, is the hypotenuse of the right triangle aOb and equals

$$P_a = \sqrt{P_{a_x}^2 + P_{a_y}^2}.$$

The direction of force p_a is determined by angle φ (fig. 12). It is obvious that the tangent of this angle will be equal to the ratio of legs ab and a0 of triangle aOb

$$\tan \varphi = ab/a0 = p_{a_y}/p_{a_x}$$

Given $F_2 = F_1$. If moreover, it is taken that $p_1 = p_2$ and $c_1 = c_2$, then $p_{a_x} = p_{a_y}$. Now, from the preceding equations, we obtain

$$P_a = \left(p_1F_1 + \frac{G}{g} \cdot c_1\right)\sqrt{2}$$

and

$$\tan \varphi = 1, \text{ or } \varphi = 45^\circ,$$

The force p'_a, with which the flow acts on a bent pipe is equal in magnitude to the force found, p_a, but is directly opposite direction to it (solid arrow in fig. 12).

3. A flow of air proceeds from section 1 1 to section 2 2 through a straight section of pipe of constant cross-section (fig. 13). Now, if there is no friction, there are no forces interacting between the pipe walls and the flow in the axial direction ($p_{a_x} = 0$ and $p_r = 0$). If we take the direction of air flow

as positive, the momentum equation with respect to the pipe axis can be written

$$F(p_1 - p_2) = \frac{G}{g}(c_2 - c_1),$$

from whence

$$p_2 = p_1 - \frac{G}{gF}(c_2 - c_1).$$

Since, from the flow measurement equation

$$G = c_1\gamma_1 F,$$

then

$$p_2 = p_1 - \frac{c_1\gamma_1}{g}(c_2 - c_1).$$

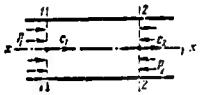

Figure 13 Air flow in a cylindrical pipe.

What follows from this expression is that the pressure in a pipeline of constant cross-section can change even when there is no friction, and no external work is being done. It is sufficient to have a change in air flow velocity, however achieved, say, by heating or cooling the air. In fact, if the air is heated its specific gravity will be reduced and, consequently, its velocity will increase, and this follows from the continuity equation, written for the condition $F_1 = F_2$

$$c_1\gamma_1 = c_2\gamma_2 \qquad \text{or} \qquad c_2 = \frac{c_1\gamma_1}{\gamma_2}.$$

The momentum equation makes it extremely simple to solve many important problems associated with establishing forces acting from the gas flow side on the surface of solid bodies that either confine the flow, or are located in the flow. In addition, one of the main problems in jet engine theory, that of determining the thrust developed by any type of jet engine, can be solved by using this same equation, as will be demonstrated in what follows.

An important, special feature of the momentum equation, is that it can be used to determine the forces that are acting merely from the known gas state and velocity parameters within a loop that limits a given flow section, without taking into account directly the substance of the processes originating outside this loop.

8. Moment of Momentum Equation

The following law of moments of momentum is known from theoretical mechanics. The moment of the resultant of all the forces applied to a body relative to some axis equals the change in the moment of momentum of that body relative to the same axis during the time these forces are acting

$$M\Delta\tau = \Delta(mcr),$$

where M is the moment of the resultant of all the forces applied to a body of mass m;

$\Delta\tau$ is the time during which the forces acted on mass m;

r is the moment arm;

mcr is the moment of momentum.

Let us apply this law to the steady motion of an elementary filament (fig. 14), keeping in mind that the moments of the radial components of the forces, and the momentums with reference to point O, are equal to zero.

Filament section 1 2 is displaced to position 1' 2' in an infinitely short period $\Delta\tau$. The change in the summed moment of the momentum of the gas mass enclosed in the volume between sections 1 1 and 2 2 will after time $\Delta\tau$, be equal to the difference in the moments of the momentum of the gas enclosed in the elementary volumes 1 1' and 2 2' (for the reasons stated earlier, the moment of momentum of the gas mass in volume 1' 2 is canceled upon subtration)

$$M\Delta\tau = c_{2u}r_2\Delta m_2 - c_{1u}r_1\Delta m_1,$$

where M is the moment of the circular component of the resultant of all the external forces applied to the separated section of filament 12;

m_1 and m_2 are the masses of gas in elementary volumes 1 1' and 2 2';

c_{2u} and c_{1u} are the circular components of absolute gas velocities c_2 and c_1 in sections 2 2 and 1 1 (on radii r_2 and r_1).

Since, in the case of steady motion $\Delta G = G\Delta\tau$, and since $\Delta m_2 = \Delta m_1 = \frac{\Delta G}{g}$, after the corresponding substitutions and reductions

$$M = \frac{G}{g}(c_{2u}r_2 - c_{1u}r_1). \tag{1.36}$$

This equation is the moments of momentum equation in hydrodynamic form, and is called the second Euler equation.

Equation (1.36) demonstrates that in the case of a steady flow, and with respect to some axis, the moment of the resultant of all the external forces applied to any gas flow section (gas loop) equals the difference in the moments, with respect to this same axis, of the momentums per second of the outflowing and inflowing gas.

Figure 14 The derivation of the moments of momentum equation.

It is easy to preceed from moment M to external work L done by the flow, or introduced into it from the outside, equated to 1 kg of gas. For this purpose, equation (1.36) must be multiplied by the angular velocity ω of the displacement of the moment arm (radius r), and divided by the rate of flow per second, G

$$L = \frac{M\omega}{G} = \frac{\omega}{g}(c_{2u}r_2 - c_{1u}r_1). \qquad (1.36\ a)$$

In this case of inertial flow motion without friction the moment of the external forces equals zero (M = 0), and, from equation (1.36), we obtain

$$c_{2u}r_2 = c_{1u}r_1 \qquad \text{or} \qquad \frac{c_{2u}}{c_{1u}} = \frac{r_1}{r_2},$$

that is, the circular velocity component will increase with a decrease in the radius.

CHAPTER 2

TURBOJET ENGINES

1. General Information

Figure 15 is a diagrammatic layout of a turbojet engine with the principal design cross-sections of its flow section as shown.

Section HH, ahead of the engine intake, marks the boundary of external air unperturbed by the engine effect. This means that through section HH, and to the left of it (on the side away from the engine), pressure and temperature, p_{un} and T_N, are equal to atmospheric, and that the air velocity relative to the engine is equal to the airspeed, V, or to zero, if the engine is at rest. The parameters for conditions and air velocity through section HH are taken as the initial parameters when making thermal and gas dynamics computations for the engine.

The principal elements of a turbojet engine are (in the order of their location, beginning with the intake section a' a'): the engine intake section, or intake device, 1 (the section from a' to a); the compressor, 2 (the section from a to k); the combustion chambers, 3 (from k to z); the gas turbine, 4 (from z to 2 2) used for compressor 2, and auxiliary (lube oil and fuel pumps, etc.) drive only, and not shown in the layout; the exhaust pipe, or transition chamber 5 (from 2 2 to e); and the jet nozzle, 6 (from e' to e).

The turbojet engine operates as follows. Outside air is compressed by the compressor, 2, and fed uninterruptedly into the combustion chamber, 3, into which a continuous fine spray of liquid fuel is injected simultaneously by injectors, 1. The combustion product formed as a result of uninterrupted fuel combustion pass through the turbine, 4, rotating it, and then pass through the exhaust pipe, 5, and the jet nozzle, 6, and are discharged at high velocity into the atmosphere in a direction opposite to that of flight.

The corresponding changes in pressure, temperature, and velocity of the gas-air flow inside a turbojet engine running at rest are shown in Figure 16 (below).

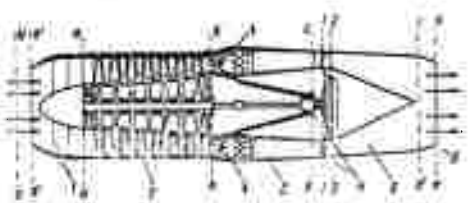

Figure 15 Diagrammatic layout of a turbojet engine.

1 - engine intake section, or intake device; 2 - compressor;

3 - combustion chambers; 4 - gas turbine; 5 - exhaust pipe, or transition chamber; 6 - jet nozzle.

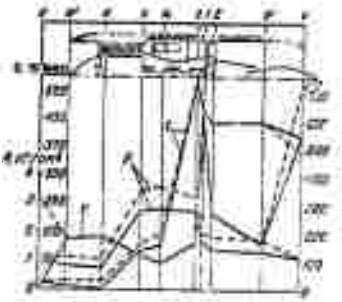

Figure 16 Change in air and combustion product parameters inside a turbojet engine.

When an engine is running at rest the air movement from section a' a' to the compressor inlet, a a, is subject to reduction in pressure and temperature, the result of the gradual increase in flow velocity. Too, the air pressure in section a' a is reduced because of the hydraulic resistances offered by the engine intake section.

Air pressure is increased significantly during the compression process in the compressor (4 to 16 times for a turbojet engine running at rest in the design regime). Air temperature is increased accordingly. There is usually little change in the axial air velocity lengthwise through the compressor, however.

Average gas temperature increases significantly in the combustion chambers as a result of fuel combustion, and can reach 1150 to 1200° K at the turbine inlet, that is, through section z z. Higher temperatures are usually not acceptable because turbine blade destruction can result unless special internal turbine blade cooling is used. The pressure is slightly reduced through the combustion chambers, the result of hydraulic resistances, and the acceleration of the gas flow, explained by the increase in its specific volume, associated with heating.

The gas expands in the turbine (between sections z z and 2 2), so its pressure and temperature are reduced. The absolute gas velocity increases significantly in the turbine nozzle assembly (between sections z z and 1 1). However, the absolute gas velocity decreases in the turbine rotor (between sections 1 1 and 2 2), because some of the kinetic energy acquired by the gas during its expansion is imparted to the rotor and consumed in driving the compressor and the auxiliaries. The axial component

of the gas velocity continues to increase through the turbine, reaching 300 to 400 m/sec at the turbine outlet (in section 2 2). This is explained by the increase in the specific volume of the gas, associated with its expansion.

The gas flows from the turbine into the exhaust pipe, which must be designed to deliver the gas flow to the jet nozzle with least possible losses. This is why the exhaust pipe is shaped to reduce the gas flow velocity between sections 2 2 and e' e'. In other words, the duct between these sections is given the configuration of a small diffuser (the flow section areas increased from 2 2 to e' e').

Further gas expansion takes place in the jet nozzle between sections e' e' and e e. Gas pressure is reduced, either to atmospheric, or to greater than atmospheric (see below), temperature is reduced, but velocity continues to increase, reaching 550 to 650 m/sec at the engine outlet (section e e) when running on the ground in the design regime.

In flight, the velocity head compresses the air in front of the engine intake, with the result that air entering an engine in flight has pressure and temperature higher than atmospheric. Consequently, when all other conditions are equal, the pressure throughout the engine flow section is increased accordingly, the pressure drop across the jet nozzle is increased, and the result is an increase in the escape velocity of the gas from the jet nozzle. The air temperature too will increase through the length of the flow section, including the combustion chambers. However, the gas temperature maintained at the combustion chamber outlets, that is, ahead of the turbine (section z z) is not in excess of the magnitude acceptable for reliable turbine operating conditions. This is done by regulating fuel delivery, and in some engines by changing the area of the outlet section of the jet nozzle simultaneously.

Thus, in the turbojet engine some of the potential energy of the combustion products, acquired during the preliminary air compression process and subsequent delivery of heat to the engine during the combustion process, is converted into mechanical work in the turbine, transferred to the turbine rotor, and then used to drive the compressor and the auxiliaries. The kinetic energy not used in the turbine causes a significant increase in the velocity of the gas flowing through the turbine. The potential energy unused in the turbine is additionally converted into kinetic energy during subsequent gas expansion in the jet nozzle. The result is a high engine gas escape velocity, one that is

nigher than the airspeed. Consequently, the gas-air flow through the turbojet engine is accelerated. This causes the reactive forces absorbed by the engine elements, that is, the jet thrust. Widely used as well are afterburner type turbojet engines. A diagrammatic layout of this engine is shown in Figure 17. It differs from the preceding type in that it has a second combustion chamber located between the turbine and the jet nozzle, a so-called afterburner, in which additional fuel is burned. In both these engines all the air from the compressor enters the combustion chambers in front of the turbine and in which the main fuel burns in an environment containing a significant excess of air. However, upon leaving the turbine, the combustion products first enter the afterburner, into which additional fuel is fed and which burns when mixed with the air that was unused in the combustion chambers in front of the turbine. The gas temperature in front of the jet nozzle is increased, leading to an increase in the velocity with which the gas escapes from the nozzle.

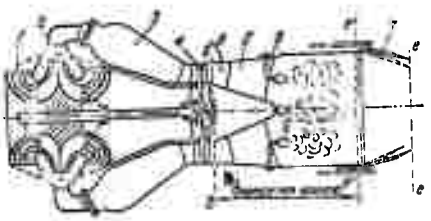

Figure 17 Diagrammatic layout of the afterburner type turbojet engine.
A - afterburner; 1 - intake device; 2 - centrifugal compressor; 3 - combustion chambers; 4 - turbine; 5 - diffuser; 6 - flame stabilizers; 7 - controllable jet nozzle; 8 - thermocouple; 9 - afterburner fuel line.

All modern turbojet engines burn fuel continuously at approximately constant pressure. These conditions also establish the principal special features of the working principle of these engines.

Characteristic layouts of existing turbojet engines are also shown in Figure 18, 19, and 20. Multi-stage axial-flow compressors, and occasionally single-stage, double-entry and single-entry centrifugal compressors, are used in these engines. Axial-flow compressors are most often used in modern turbojet engines. The turbines used are single-stage, two-stage, and three-stage axial-flow turbines.

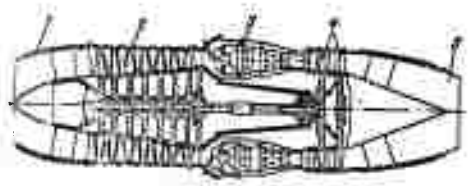

Figure 18 Layout of a turbojet engine with an axial-flow compressor.
1 - inlet section; 2 - axial-flow compressor; 3 - combustion chambers; 4 - two-stage turbine; 5 - jet nozzle.

There are also engines with twin-shafts (figure 19). These engines have two axial-flow compressors, one a low, the other a high pressure, built in tandem, with no mechanical coupling, each driven by its own turbine (so-called compound compressor).

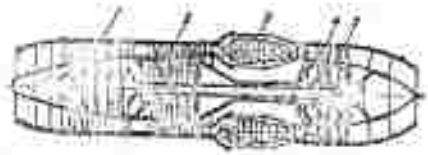

Figure 19 Layout of a twin-shaft turbojet engine.
1 - low-pressure compressor; 2 - high-pressure compressor; 3 - combustion chamber; 4 - turbine high-pressure compressor turbine; 5 - low-pressure compressor turbine.

The jet nozzles in the engines, the layouts of which are shown in figures 15, 18, 19, and 20, have the configuration of simple convergent nozzles, and have a constant, non-adjustable area of least exit section. However, many modern turbojet engines use jet nozzles with an adjustable (changed during engine operation) exit area, and in many cases also have expansion, or "supersonic", jet nozzles (see below).

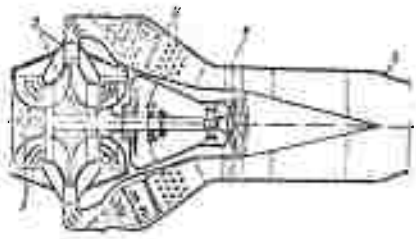

Figure 20 Layout of a turbojet engine with a double-entry, centrifugal compressor.
1 - intake section; 2 - compressor; 3 - combustion chambers; 4 - turbine; 5 - jet nozzle.

Let us, briefly, consider yet other special features of turbojet engine working principles.

Compressor and turbine shafts are made separately, or integral, and are mounted in two, three, and four anti-friction bearings, journal roller bearings, and journal thrust ball bearings. The latter, in addition to taking the radial forces, also take the axial forces generated during turbine and compressor rotation. The bearings are mounted in the inner strength housing of the engine, called the crank case, or the support.

All auxiliaries (fuel and lube oil pumps, governors, generators, etc.) are driven off the compressor shaft through a system of geared transmission and small, intermediate shafts. All turbojet engines use governors that automatically maintain specified rpm, or limit any increase in rpm and gas temperature ahead of the turbine above their maximum permissible values. Plunger, or gear pumps are used to deliver the fuel to the injectors at the pressure required to atomize the fuel (as high as 80 to 100 kg/cm^2).

Engine parts subject to greatest heating, such as turbine blades, wheels, and bearings, combustion chamber walls, exhaust piping, and the like, are air-cooled. In turbojet engines with axial-flow compressors, air-cooling is usually accomplished by bleeding air from an intermediate compressor stage. In turbojet engines with centrifugal compressors, the cooling air is bled from the cavity at the compressor outlet, or supplied by a special, separate, impeller, mounted on the shaft between the compressor and the turbine (figure 20). The air consumed for cooling usually will not exceed 2 to 4 % of the toal air flow through the engine. As a rule, about 2 to 3 % of turbine shaft power is consumed in driving all auxiliaries and supplying cooling air.

Engine bearings are lubricated and cooled by oil sprayed on them by special metering injectors (nozzles), to which the oil is pumped at a pressure of 2 to 4 kg/cm^2 by a lube oil pump, usually a gear type. The oil drains from the bearings into oil sumps in the engine housing and is returned to the oil tank by scavenging pumps.

Lube oil consumption is considerably lower in turbojet engines than in reciprocating engines, because there are not as many working surfaces and because their temperatures are lower, as well as because anti-friction bearings are used.

2. Turbojet Engine Thrust

The effective thrust produced by a turbojet engine equals the axial component of the resultant of the forces acting on the engine and originating in the gas and air flow within the engine

and in the external air flow washing the engine.

Let us use the momentum equation to determine the effective thrust, P_{eff}. For this purpose, let us isolate that coaxial cylindrical separation around the engine (figure 21), the forward edge, 1 1, and side (generators), 1 2, the boundaries of which lie completely beyond the limits of the air perturbed by the engine, and the trailing edge boundary surface of which, 2 2, coincides with the plane of the jet nozzle exit section, e e.

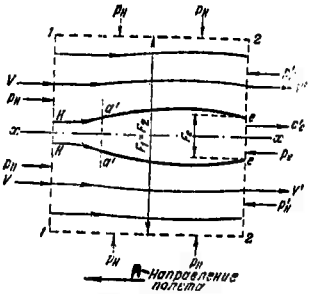

Figure 21 Determination of the thrust produced by a turbojet engine.

Key: A - direction of flight.

The pressure at the end 1 1, and side, 1 2, surfaces of this cylindrical separation will be equal to the pressure, P_{un}, of the unperturbed outside air, and its velocity with reference to the engine will be equal to the airspeed V.

But at the trailing boundary of the edge surface, 2 2, outside the jet of exhaust gases (beyond section e e), that is, at the annular surface with area equal to $(F_2 - F_e)$, the pressure and velocity of the outside air with reference to the engine will not be equal to the pressure P_{un}, or to the airspeed V, because of the perturbation (stagnation) effect of the engine on the external flow. For the same reason, the air pressure and velocity through the radius of the annular area $(F_2 - F_e)$ will be variable. The gas has pressure p_e, which, in the general case does not equal pressure P_{un} of the outside air (see below), in the jet nozzle exit section e e, and an axial discharge velocity equal to c'_e.

Let us now derive the momentum equation applicable to the entire flow through the separated cylindrical area between its normal sections 1 1 and 2 2 equating it to x-x, the axis of symmetry of the engine and of the flow, assuming that this axis coincides with the direction of flight (at speed V).

It was shown in Chapter 1 that the projection in any direction of the resultant of all external forces applied to the gas flow in any section of it, equals the change in the same direction of the momentum per second in that flow section.

The external forces acting on the flow under consideration in the direction of the x-x axis are:

the engine force acting on the internal part of the cylindrical flow that passes through the engine, and on the external part that washes it. Based on the law of the equality of action and reaction in mechanics, this force is equal in magnitude but opposite in direction to, the sought for effective thrust, P_{eff};

the pressure force on end surface 1 1, equal to the product of the pressure of the unperturbed outside air times the area of this surface, or $p_{un}F_1$;

the pressure force on the end surface e e, equal to the product of the pressure in the jet nozzle exit section times its area, p_eF_e;

the pressure force on the end surface 2 2, beyond the jet nozzle exit section F_e, that is on the annular surface. This force can be represented by the product $p'_{un}(F_2 - F_e)$, where p'_{un} is the average value of the variable pressure through the radius of the annular section $(F_2 - F_e)$.

The change in the momentum of the entire air mass moving between sections 1 1, and 2 2 in the cylindrical area under consideration in one second and caused by the forces listed above can be represented in the form of a sum

$$(m_{com}c'_e - m_{air}V) + M(V' - V)$$

where $(m_{com}c'_e - m_{an}V)$ is the change in momentum in the internal part of the flow passing through the engine and bounded by the contour Ha'eea'H;

m_{com} is the mass of combustion products escaping from the engine per second at velocity c'_e;

m_a is the mass of the air entering the engine per second at an initial velocity equal to the airspeed;

M is the mass of the air per second flowing past the outside of the engine through the annular areas $(F_1 - F_{un})$ and then $(F_2 - F_e)$;

V' is the average value of the variable velocity of the external air through the radius of the annular section $(F_2 - F_e)$.

Thus, if we take the direction of movement of the flow as positive with respect to the engine, and keep in mind that area $F_1 = F_2$, the sought for momentum equation can be written in the following form

$$P_{eff} + p_{un}F_1 - p_eF_e - p'_{un}(F_1 - F_e) = m_{com}c'_e - m_{air}V + M(V' - V).$$

If we now add $+ p_{un}F_e$ and $- p_{un}F_e$ to the left side of the equality thus obtained, after a simple transformation we have

$$P_{eff} = m_{com}c'_e - m_{air}V + F_e (p_e - p_{un}) -$$
$$- [(p_{un} - p'_{un}) (F_1 - F_e) - M (V - V')].$$

or

$$P_{eff} = m_{com}c'_e - m_{air}V + F_e (p_e - p_{un}) - X, \qquad (2.1)$$

where

$$X = (p_{un} - p'_{un}) (F_1 - F_e) - M (V - V'). \qquad (2.2)$$

The sum designated X is the engine force acting on the external flow of air washing the engine and causing the change in pressure and momentum (velocity) in this flow[1]. This force is equal in magnitude and opposite in direction to the external flow force acting on the engine, that is, the engine drag force which reduces effective thrust.

The external engine drag X is composed of the drag caused by air friction on the outer surface of the engine housing (or on the engine nacelle in which it is located), of the wave drag caused by the engine intake, which is the force originating from the outside flow and acting on the engine through the intake flow, which is shaped by engine effect (contour Ha'a'H in figure 21), and of the engine wave drag (its nacelle); that is, the force exerted by the excess pressure from the external flow on the external surface of the engine (nacelle).

The magnitude of the external engine drag depends on the airspeed, on engine shape and dimensions, on where and how the engine is installed in the aircraft, on the effect created by adjacent aircraft parts, etc. The magnitude of this drag is found through experimental data, and in many cases can be approximated by computation and theoretically.

The relationships obtained demonstrate that the effective thrust produced by a turbojet engine is the result of the internal engine operation process that establishes the value of the velocity, c'_e, and the pressure, p_e, in the jet nozzle exit section, and the flow of air and combustion products through the engine, as well as of external engine drag, that is, the result of the conditions under which the external washing of the engine takes place. Moreover, effective thrust, as will be seen, depends on airspeed and altitude (on atmospheric pressure, p_{un}).

If we disregard external engine drag, assuming X = 0, we obtain the so-called internal thrust, equal to

---

1) Expression (2.2) for force X can be obtained from the momentum equation written for the outer, annular part of the flow under consideration, limited from within by the contour Ha'eea'H, and from without by the contour 1 2 2 1 (figure 21).

$$P = m_{com}c'_e - m_{air}V + F_e (p_e - p_{un}$$

or, passing from mass flow to weight flow,

$$P = G_{air}/g \ (G_r/G_{air} \cdot c'_e - V) + F_e(p_e - p_{un}), \quad (2.3)$$

where G_{air} and G_{com} are the mass flows of air and combustion products, respectively, through the engine;

$g = 9.81$ is the acceleration of gravity.

Wave drag is negligibly low at subsonic airspeeds, and air friction is slight, so, as a practical matter, $p \approx p_{eff}$. However, at supersonic airspeeds the effective engine thrust becomes a good deal less than the internal thrust, primarily the result of high engine wave drag (by its intake), and can be 85 to 70 %, or less, of the internal engine thrust.

It is readily seen that the internal engine thrust for a given airspeed and altitude is the direct result of just the engine operating process. We will, in what follows, consider just the internal engine thrust, and refer to it simply as thrust.

Let the weight of fuel burned in the engine in one second equal G_f, kg. The weight of the combustion products will then be $G_{com} = G_f + G_{air}$, kg/sec, and the corresponding weight of air consumed will equal $G_{air} = \alpha\, l_o G_f$, kg/sec, and

$$G_{com}/G_{air} = 1 + \alpha l_o/\alpha\, l_o,$$

where l_o is the quantity of air theoretically required for the complete combustion of 1 kg of fuel;

α is the excess of air coefficient, $\alpha = G_{air} / l_o G_f$.

Therefore, equation (2.3) can be rewritten

$$P = G_{air}/g \ (1 + \alpha l_o/\alpha\, l_o \cdot c'_e - V) + F_e(p_e - p_{un}). \quad (2.4)$$

Ordinarily $\alpha \geq 3$, and $l_o = 14$ to 15 for a turbojet engine, so $1 + l_o/\alpha\, l_o \approx 1$, providing a simpler, and sufficiently accurate formula for establishing the thrust

$$P = G_{air}/g \ (c'_e - V) + F_e(p_e - p_{un}). \quad (2.5)$$

Accordingly, we obtain the following for engine operation at rest when $V = 0$

$$P_o = G_{air}/g \cdot c'_e + F_e \ (p_e - p_{un}) \quad (2.6)$$

If the expansion of combustion products in the jet nozzle is completely terminated, the discharge velocity, c_e, will be higher than the discharge velocity, c'_e, for incomplete expansion, all other conditions being eqqal, and a pressure equal to the external pressure will be established in the jet nozzle exit section. Now, because $p_e = p_{un}$, the expression for the thrust will assume the following form

$$P = G_{air}/g \ (c_e - V). \quad (2.7)$$

Accordingly, when the engine in running on the ground

$$P_o = G_{air}/g \cdot c_e. \quad (2.8)$$

When combustion product expansion in the jet nozzle is incomplete, the thrust reduction the result of the reduction in their discharge velocity ($c'_e < c_e$) is not completely compensated for by the supplemental force $F_e(p_e - p_{un})$, so engine thrust is reduced, as compared with that found in the case of full expansion.

3. Turbojet Engine Efficiencies.

The losses incurred during the processes of converting the heat introduced into a jet engine in the form of chemical fuel energy into external work performed by the engine thrust (imparting movement to the flying machine) are evaluated successively in terms of three efficiencies: effective efficiency η_e, propulsion efficiency η_p, and economic, or total, efficiency η_t.

Effective efficiency is the ratio of the heat, equivalent to the increase in the kinetic energy of the gas and air flow in the jet engine, and to the consumed heat, that is, to the heat introduced into the engine in the form of chemical fuel energy.

When gas expansion in the jet nozzle is complete, when the discharge velocity from the nozzle equals c_e, the increase in the kinetic energy of the gas and air flow in the engine is the difference $c_e^2 G_{com}/2g - V^2 G_{air}/2g$, and the heat consumed equals the fuel consumption, G_f, multiplied by the calorific value, H_u, so effective efficiency will equal

$$\eta_e = A\,(c_e^2 G_{com} - V^2 G_{air})/2g G_f H_u, \qquad (2.9)$$

where $A = 1/427$ is the thermal equivalent of the mechanical energy.

But if, as before, and for the sake of simplicity, we assume that $G_{com}/G_{air} \approx 1$, and substitute $G_{air}/G_f = a$ we obtain

$$\eta_e \approx \frac{A}{2g} \cdot \frac{c_e^2 - V^2}{H_a}, \qquad (2.10)$$

where $H_a = \frac{H_u}{a l_0}$ is the amount of heat consumed per kg of air flowing through the engine.

When the engine is running at rest, that is, the velocity is $V = 0$,

$$\eta_{e_0} \approx \frac{A}{2g} \cdot \frac{c_e^2}{H_a}. \qquad (2.11)$$

When gas expansion in the jet nozzle is incomplete, the effective efficiency, as well as the efficiencies that will be discussed below, can be established conveniently with respect to the equivalent discharge velocity.

The equivalent discharge velocity, c_{eq}, is here understood to mean the velocity that would be required in the event of complete gas expansion in the jet nozzle to obtain thrust equal to the thrust provided when gas expansion is incomplete, but air flow, G_{air}, and airspeed, V, are the same. Accordingly, in order

to establish the equivalent discharge velocity, c_{eq}, we must equate the right sides of the expressions at (2.5) and (2.7) to each other, and obtain

$$c_{eq} = c'_e + gF_e/Gair\ (p_e - p_{un})$$

and further, for the effective efficiency: $\eta_e = \frac{A}{2g} \cdot \frac{c_{eq}^2 - V^2}{H_u}$.

The effective efficiency takes into account all the losses that take place during the conversion of heat into kinetic energy in the engine:

the heat carried away from the engine by the combustion products, which leave the engine at a temperature considerably higher than that of the surrounding medium;

heat losses in the combustion chambers due to incomplete fuel combustion;

heat losses to the surrounding medium directly through the combustion chamber walls, turbine housing, the walls of the exhaust pipe and jet nozzle, as well as the heat given off to the air that cools the engine parts (turbine blades, turbine wheel, etc.), and to the oil that cools the engine bearings;

energy consumed in driving the auxiliaries;

energy consumed in overcoming hydraulic resistance in the flow section of the engine, and the friction in its bearings, which in the long run leads to some increase in the temperature of the gas departing the engine, and in that of the oil flowing through its bearings and mechanisms.

Thus, the effective efficiency establishes the percentage of consumed heat converted into kinetic, that is, into the energy of the gas flowing through the engine. The effective efficiency describes the efficiency of a turbojet engine as a heat engine, so from this standby can in essence be compared to the effective efficiency of the reciprocating engine, for example.

For existing turbojet engines running the ground, the heat carried off by the combustion products leaving the engine is 65 to 75 % of the heat introduced into the engine with the fuel, and all other heat losses amount to about 3 to 5 %. Accordingly, under these conditions the effective efficiency is in the ηe_o = 0.20 to 0.30 range, reaching appreciably greater values under flying conditions (see below).

Propulsion efficiency is the ratio of the external work performed by the engine thrust to the increase in the kinetic energy of the gas flow it picks up in the engine

$$\eta_p = PV / G_{air}/2g\ (c_e^2 - v^2) \qquad (2.12)$$

where PV is the external work performed by the thrust in flight in one second, or the engine power.

If we establish the thrust through the formula at (2.7), the expression for propulsion efficiency will be in the following form after reduction $\eta_p = \frac{2V(c_e - V)}{c_e^2 - V^2}$,

or, after reduction by the difference $(c_e - V)$:

$$\eta_p = \frac{2V}{c_e + V} = \frac{2}{1 + \frac{c_e}{V}}. \qquad (2.13)$$

The external work performed by the thrust and imparted to the flying machine is the direct result of the use of the kinetic energy acquired by the gas flow in the engine. But, not all the kinetic energy of the flow is converted into thrust work. Actually, the gas flow leaving the engine has an absolute velocity (the velocity relative to the ground) obviously equal to the velocity difference $(c_e - V)$. Consequently, that part of the kinetic energy of each kilogram of gas leaving the engine not converted into thrust work, that is, the lost part, equals $\frac{(c_e - V)^2}{2g}$ Propulsion efficiency also takes this loss of kinetic energy into account.

As will be seen from the expression at (2.13), propulsion efficiency is only dependant on the discharge velocity of the gases from the engine and on the airspeed. Propulsion efficiency will increase with a reduction in this ratio. This is understandable because the closer the discharge velocity, c_e, approximate the airspeed, V, the lower the absolute velocity at which the gas flow leaves the engine, and the less will be that part of the kinetic energy remaining unused.

When the gas discharge velocity relative to the engine, c_e, equals the airspeed, V, propulsion efficiency equals unity because the absolute gas velocity as it leaves the engine, $(c_e - V)$, equals zero. But, according to the formula at (2.7) engine thrust becomes zero.

When the engine is running on the ground and airspeed is V = 0, the propulsion efficiency is $\eta_p = 0$, because no thrust work is performed, and all the kinetic energy of the gas flow at the engine outlet is unused.

Thus, propulsion efficiency indicates how much of the kinetic energy acquired by the gas flow in the engine is converted into external thrust work. Propulsion efficiency describes the efficiency of the turbojet engine as a propelling device, that is, as a device designed to generate thrust. Therefore, the propulsion efficiency of the jet engine should be compared to the efficiency of an aerial propeller.

The propulsion efficiency, η_p, of existing turbojet engines ranges over broad limits, depending on airspeed, altitude, and engine operating conditions, but as a rule will not exceed 0.60 to 0.65.

Economic, or total, efficiency is the ratio of the heat converted into external thrust work to the heat consumed, that is, introduced into the engine by the fuel

$$\eta_t = APV/G_T H_u = APV/G_{air} H'_u \qquad (2.14)$$

from whence, and based on the preceding relationships,

$$\eta_t = \eta_e \eta_p \qquad (2.15)$$

Thus, total efficiency equals the effective efficiency multiplied by the propulsion efficiency and, thus takes into account all the energy losses listed above as the chemical energy of the fuel consumed is converted into external thrust work. Total efficiency establishes the percentage of the consumed heat converted into external thrust work transferred to the flying machine, thus completely describing the efficiency of an engine in flight.

The total efficiency of an engine running at rest is zero, because the propulsion efficiency is $\eta_p = 0$. The total in-flight efficiency of existing turbojet engines can have values $\eta_t = 0.20$ to 0.30.

4. Specific Parameters of Turbojet Engines

The in-flight operational qualities of jet engines are most conveniently evaluated through specific parameters.

The principal specific parameters of turbojet engines are:

specific thrust;

specific fuel consumption;

specific weight;

specific drag.

Specific thrust, P_{sp}, is the ratio of the engine thrust to the weight flow per second of air through the engine

$$P_{sp} = P/G_{air} \left[\text{kg} \cdot \text{sec/kg of air} \right]. \qquad (2.16)$$

Now, using the formulas at (2.6) and (2.7), we can write the following for specific thrust

$$P_{sp} = c'_e - V / g + F_e/G_{air} (p_e - p_{un}). \qquad (2.17)$$

If $p_e = p_{un}$ (complete gas expansion in the jet nozzle)

$$P_{sp} = c_e - V / g . \qquad (2.18)$$

If $V = 0$

$$P_{sp_o} = c_e/g . \qquad (2.19)$$

Specific thrust can be expressed in terms of the effective efficiency of the engine by establishing the discharge velocity of the gas from the jet nozzle through the formula at (2.10) and, substituting the result in the formula at (2.18), obtain

$$P_{sp} = \frac{1}{g} \sqrt{\frac{2g}{A} \cdot H_u \eta_e + V^2} - \frac{V}{g},$$

and for engine operation at rest

$$P_{sp_o} = \sqrt{\frac{2H'_u}{gA} \cdot \eta_e}.$$

Consequently, the specific thrust of a turbojet engine depends on its effective efficiency, and on the amount of heat given up to one kilogram of air flowing through the engine. The greater H_u' and η_e, the greater will be the specific thrust of an engine at a given airspeed.

But, the greater the specific thrust, the smaller will be the weight flow per second of air through the engine required for a given engine thrust p, because $p = p_{sp}G_{air}$, and, consequently the smaller the diametric dimensions and weight of the engine, all other conditions being equal.

Specific fuel consumption, C_{sp}, is the ratio of the fuel consumption per hour for an engine to it's thrust,

$$C_{sp} = G_{f_{hr}}/p \quad [\text{kg/kg of thrust hour}]. \tag{2.20}$$

Specific fuel consumption for a turbojet engine can be expressed in terms of specific thrust, based on the following relationships. It is obvious that

$$C_{sp} = G_{f_{hr}}/P_{sp}G_{air} = 3600\ G_f/P_{sp}G_{air},$$

where G_f and G_{air} are the weight flows per second of fuel and air, respectively.

But, the ratio of fuel consumption to air flow is

$$G_f/G_{air} = 1/\alpha l_0,$$

so we can finally write

$$C_{sp} = 3600/\alpha l_0 P_{sp}. \tag{2.21}$$

Specific fuel consumption is also associated with engine efficiency. In fact, from the formula at (2.14)

$$P_{sp} = H_u \eta_t/\alpha l_0 AV.$$

Now, after substituting this expression for P_{sp} in the formula at (2.21), we obtain $C = \frac{3600\,AV}{H_u \eta_t}$. (2.22)

from whence it follows that specific fuel consumption, C_{sp}, describes the thermal efficiency of an engine in flight only for a given airspeed.

Specific fuel consumption is an important operational magnitude. All other conditions being equal, the smaller C_{sp} the greater will be the aircraft's range and flying time.

Specific engine weight, γ_{en}, is the ratio of engine weight, G_{en}, to its maximum thrust

$$\gamma_{en} = G_{en}/P \quad [\text{kg/kg of thrust}]. \tag{2.23}$$

The lower specific engine weight, the lower the weight of the engine installation for a specified amount of thrust, and this, in turn, can to a considerable degree be reflected in such important aircraft data as ceiling, payload, range, and speed.

Specific drag, P_{drag}, is the ratio of maximum engine thrust to the area of its greatest cross-section

$$P_{drag} = P/F_{drag} \quad [kg/m^2]. \tag{2.24}$$

Specific drag indirectly characterizes the aerodynamic drag of the engine installation in flight. The greater the specific drag, the smaller the percentage of engine thrust expended in flight in overcoming the drag caused by engine installation in the aircraft.

The specific parameters for the same type of engine will change with change in airspeed, altitude, and atmospheric conditions, because thrust, weight flow of air, and fuel consumption per hour change (see below). Too, the magnitudes of the specific parameters depend on aircraft operating conditions. Therefore, specific parameters obtained for engine operation at rest (V = 0), on the ground (H = 0), and under standard atmospheric conditions, that is, at an atmospheric pressure of p_o = 760 mm mercury column, and an air temperature of t_o =+15°C (288°K), are usually taken as the initial magnitudes. Given these conditions, existing turbojet engines have a maximum specific thrust of P_{sp_o} = 50 to 70 kg · sec/kg of air, and a specific fuel consumption of C_{sp_o} = 0.76 to 1.10 kg/kg of thrust hour, depending on engine operating conditions.

The values for the specific weight and specific drag for modern turbojet engines are γ_{sp_o} = 0.2 to 0.4 kg/kg of thrust and P_{drag_o} = 2500 to 8000 kg/m², respectively.

CHAPTER 3

THERMODYNAMIC PRINCIPLES OF TURBOJET ENGINE OPERATION

1. General Considerations

Let us, in order to develop and analyze the principal properties and special features of the turbojet engine, start out by using ideal thermodynamic cycles.

An ideal cycle is understood to mean a simplified, conditional way of combining the operating processes that take place in an engine, one that is a closed, and reversible, cycle consisting of highly simplified thermodynamic processes.

Accordingly, the following simplifying assumptions are made for ideal cycles: air is the working substance throughout the cycle; the heat capacity of this air does not depend on its temperature; there are no losses (thermal, hydraulic, or mechanical) in any element in the engine, with the exception of the necessary removal of heat to a cold source, without which and in accordance with the second law of thermodynamics, the continuous conversion of heat into work would be impossible.

As a result of these assumptions, all engine parameters in the case of the ideal cycle have limits, and the degree to which these same parameters for the real engine approximate these limits is what determines the efficiency of the latter.

The combustion stages in all existing turbojet engines (as well as in other types of gas turbine engines) are based on the thermodynamic cycles during which heat is supplied at constant pressure. Realization of these combustion stages requires no special gas distribution devices, and results in a simple, reliable, and quite efficient engine design, in which all elements function with the flow of air and gas continuous and steady. Then too, the design of these engines can be improved, if desired.

The simple cycle with adiabatic air compression and expansion, and the cycle with staged heat supply and adiabatic air compression and expansion, are the principal thermodynamic cycles, with heat supplied at constant pressure, in modern turbojet engines. A cycle with isothermic air compression and adiabatic air expansion is used in some instances as the basis for the turbojet engine combustion stage.

In considering these cycles as applicable to gas turbine engines, one must be aware of the kinetic energy of the working substance, as well as of its potential energy, because its flow velocity in the engine flow section is quite high. With this in mind, we will take it that the air flow is stagnated at all points in the cycles, with the exception of their initial points (the

external, unperturbed air condition; that is, section H H in fig. 15) and their end points (the condition of the air, or gas, at the engine exhaust; that is, section e e), so that air flow pressure and temperature are higher than static pressure and temperature, respectively.

Moreover, magnitudes like work, amount of heat, and kinetic energy will be equated in all cases to one kg of air flowing through the engine, and it will be assumed that the air expands to atmospheric pressure in the jet nozzle.

In what follows ground pressure and temperature of atmospheric air will be designated by p_o and T_o, and at an altitude of H>0 will be designated by p_H and T_H.

Finally, it is appropriate to note that the cycles, and the basic conclusions considered and arrived at in this chapter can also be applied to turboprop and dual-flow turbojet engines.

2. Cycle with Heat Input at Constant Pressure and with Adiabatic Compression and Expansion

The ideal cycle with heat input at constant pressure and adiabatic compression is shown by the pv and TS diagrams in figure 22 for the case of engine operation in flight, and in figure 23 for in situ engine operation. This cycle consists of the following sequential processes.

1. Air compression along the adiabat Hk, achieved in flight initially as a result of air stagnation by the engine, that is, as a result of the velocity head of the meeting flow of air (section Ha), and subsequently in the compressor (section ak).

2. The input from without of heat Q_1 to the air along the isobar kz in the combustion chambers.

3. Air expansion along the adiabat ze, initially in the turbine (section z2) and subsequently in the jet nozzle (section 2e). Point 2 establishes the condition of the stagnated air beyond the turbine driving the compressor.

4. Heat Q_2 given up by the air along the isobar eH (according to the second law of thermodynamics) to the cold source that is the surrounding medium. This process, a closed cycle, is conditional for the engine because it actually takes place outside the engine and corresponds to the heat transfer from the gases leaving the engine to the surrounding air.

In the pv diagrams all of the work done to compress the air, L_c, is depicted by the area Hk41, consisting of area Hal'1, corresponding to the compression work L_{cc} done by the velocity head, and the area ak41', corresponding to the compression work L^s_{ad} done in the compressor (fig. 22). When the engine is running in situ the compression work done by the velocity head obviously

equals zero, and the total compression work in the cycle is depicted by area Ok41 (fig. 23).

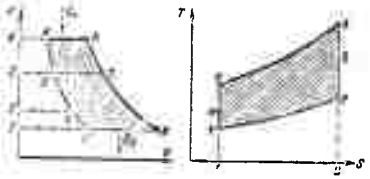

Figure 22: Cycle with heat input when p = const and with adiabatic compression (V > 0).

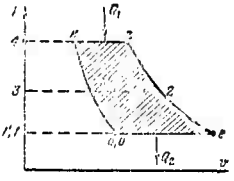

Figure 23 Cycle with p = const when V = 0.

Total air expansion work, L_{ex}, is depicted in the pv diagram by the area 14ze, consisting of area 34z2, the expansion work done in the turbine, and of area 32e1, the expansion work done in the jet nozzle.

Since the turbine in a turbojet engine drives the compressor, and if there are no losses, something that is characteristic of the ideal cycle, the expansion work done in the turbine should equal the compression work done in the compressor and, consequently, area 34z2 equals area ak41'.

The useful work done in the cycle, L_t, equals the difference

$$L_t = L_{ex} - L_c$$

and is depicted in the pv diagrams by the area Hkze.

The heat, equivalent to the useful work of the cycle, equals

$$AL_t = Q_1 - Q_2$$

and is depicted by the area Hkze in the TS diagram. The area 1kz2 in the same diagram corresponds to the heat added to the cycle Q_1 and the area 1He2 corresponds to the heat removed from the cycle, Q_2.

In a turbojet engine, and in accordance with its principle of operation, the work of the cycle goes to increase the kinetic energy of the air flowing through the engine. This can be established through the pv diagram in figure 22, based on the following considerations. The total work done during the expansion of the air from full pressure beyond the turbine p_2, (point 2) to atmospheric

pressure, p_H, (point e), and depicted by area 132e, goes to increase the kinetic energy of the air in the jet nozzle at the exchange of which the air velocity equals c_{e_t}, so we can write

$$c_{e_t}^2 / 2g = \text{area } 132e.$$

Area 132e can be represented in the form of a sum of areas

area 132e = area H3'2e + area 1'33'a + area 11'aH.

But the equality of areas ak41' and 34z2, established above, that is, the equality of the work done by the turbine and the compressor, also makes areas 1'33'a and 3'kz2 equal, and the sum of area H3'2e + area 3'kz2 = area Hkze = L_t, so

$$c_{e_t}^2/2g = L_t + \text{area } 11'aH.$$

Since area 11'aH is compression work L_{cc} done by the velocity head, that is, the result of the kinetic energy of the meeting flow, $V^2/2g$, in the case of complete stagnation

$$\frac{c_{e_t}^2}{2g} = L_t + \frac{V^2}{2g},$$

from whence we also obtain

$$L_t = \frac{c_{e_t}^2 - V^2}{2g}, \tag{3.1}$$

and, for in situ operation, when V = 0

$$L_{t_0} = \frac{c_{e_t}^2}{2g},$$

where c_{e_t} is the velocity of the flow from the jet nozzle when there are no engine losses, that is, the ideal velocity;

V is the initial velocity of the air relative to the engine, equal to the airspeed.

Thus, the work of the cycle, L_t, in a turbojet engine can be used to accelerate the air flow through the engine, and thrust is obtained as a direct result of this process.

The efficiency of the ideal cycle, or the degree to which the heat input is converted into useful work, can be evaluated by the thermal efficiency η_t, which equals the ratio between the heat converted into useful work, L_t, for the ideal cycle, and the heat expended, Q_1,

$$\eta_t = \frac{AL_t}{Q_1} = \frac{Q_1 - Q_2}{Q_1}$$

or

$$\eta_t = 1 - \frac{Q_2}{Q_1}. \tag{3.2}$$

For the cycle under consideration (equating all magnitudes to one kg of air) we can write

$$Q_1 = c_p (T_3' - T_{c'}');$$
$$Q_2 = c_p (T_{e'} - T_{H'}),$$

where c_p is the specific heat at constant pressure.

Substituting these expressions in the formula at (3.2), and converting, we obtain

$$\eta_t = 1 - \frac{T_H}{T_c^*} \cdot \frac{\frac{T_e}{T_H} - 1}{\frac{T_z^*}{T_c^*} - 1}.$$

From the equations for the expansion, ze, and the compression, Hk, adiabats, we have

$$\frac{T_z^*}{T_e} = \left(\frac{p_z^*}{p_e}\right)^{\frac{k-1}{k}};$$

$$\frac{T_c^*}{T_H} = \left(\frac{p_c^*}{p_H}\right)^{\frac{k-1}{k}},$$

however, $p_z^* = p_c^*$ and $p_e = p_H$, so

$$\frac{T_z^*}{T_c^*} = \frac{T_e}{T_H}.$$

On this basis,

$$\eta_t = 1 - \left(\frac{p_H}{p_c^*}\right)^{\frac{k-1}{k}}$$

or

$$\eta_t = 1 - \frac{1}{\pi_c^{*\frac{k-1}{k}}}. \qquad (3.3)$$

The ratio of the total pressure, p_c^*, at the compressor outlet to the pressure, p_H, of the external, unperturbed air, that is is called the <u>summed compression ratio</u> and is one of the most important turbojet engine operating parameters. The summed compression ratio can be represented by the following product

$$\pi_c^* = \frac{p_c^*}{p_a^*} \cdot \frac{p_a^*}{p_H} = \pi_c^* \pi_{cc}^*$$

where $\pi_c^* = \frac{p_c^*}{p_a^*}$ — is the compressor compression ratio;

$\pi_{cc}^* = \frac{p_a^*}{p_H}$ — is the velocity compression ratio;

p_a^* — is the total air pressure at the compressor inlet (through section a a).

The assumption for the ideal cycle is that velocity compression (stagnation) of the air, and its flow through the engine are loss-less, adiabatic. Therefore, in the ideal cycle the total pressure, p_a^*, at the compressor inlet equals the total pressure, p_H^*, in the external, unperturbed air, and the velocity compression ratio can be established through the already known formula for the pressure of an adiabatically stagnated flow

$$\pi_{cc}^* = \frac{p_H^*}{p_H} = (1 + 0{,}2M_H^2)^{3{,}5}, \qquad (3.4)$$

where $M_H = V/a_H$ is the Mach number for the flight;

$a_H = \sqrt{kgRT_H}$ — is the velocity of sound in an unperturbed atmosphere, where the air temperature equals T_H.

As will be seen from the formula at (3.4), the velocity compression ratio, π^*_{cc}, increases with an increase in airspeed, V, when a_H = const (that is, T_H = const), as well as with a decrease in the external temperature (that is, in a_H) when V = const, and consequently with an increase in altitude (so long as temperature T_H decreases with altitude).

There is no velocity air compression during in situ engine operation (V = 0 or M_H = 0), and in accordance with the formula at (3.4), and with no losses, π^*_{cc} = 1, so, in this case

$$\pi^*_c = \frac{p^*_c}{p_H}$$

and

$$\eta_t = 1 - \frac{1}{\pi^{*\frac{k-1}{k}}_c}. \qquad (3.5)$$

Turning now to the dependencies obtained above for the thermal efficiency, η_t, we can draw the following important conclusions for the cycle under consideration.

1. The thermal efficiency of the cycle depends only on the summed air compression ratio and increases steadily with the increase (fig. 24) in the ratio, because with an increase in π^*_c there is an increase in the air ratio after heat Q_1 is added, and as a result the relative amount of heat, Q_2, transferred to the surrounding medium is reduced.

2. The thermal efficiency increases with an increase in airspeed and altitude, as well as and only with a decrease in the outside temperature, because the velocity compression ratio and, consequently, the summed compression ratio increase.

The thermal efficiency of compressor compression ratios in existing modern turbojet engines is η_t = 0.38 to 0.48, increasing to η_t = 0.5 to 0.6 and higher in flight (reaching these values at M_H = 1 and H = 11,000 m, thanks to the corresponding increase in the summed compression ratio, π^*_c).

We note, for purposes of comparison, that aviation piston engines that operate on the ideal cycle principle wherein heat input and heat transfer occur at constant volume, have a thermal efficiency not in excess of η_t = 0.5 to 0.6 for compression ratios used and this does not depend, as we know, on airspeed and altitude.

The useful work, L_t, of the cycle not only depends on thermal efficiency, but also on the amount of heat, Q_1, added to the cycle, since from the foregoing

$$L_t = \frac{Q_1}{A} \cdot \eta_t.$$

The work of the cycle increases continuously with increase in the compression ratio, π_c^*, when Q_1 = const, the result of the increase in the thermal efficiency, η_t. However, since

$$Q_1 = c_p(T_z^* - T^*) = c_p\left(T_z^* - T_H \pi_c^{*\frac{k-1}{k}}\right),$$

the increase in π_c^* when Q_1 = const and T_H = const will be accompanied by a simultaneous increase in the maximum temperature, T_z, of the cycle, that is, in the temperature in front of the turbine.

However, if the maximum temperature of the cycle remains constant with an increase in the compression ratio π_c^*, an increase in thermal efficiency will be accompanied by a simultaneous reduction in the amount of heat, Q_1, added, the result of the rise in temperature T_c^*, when T_z^* = const. The result will be an initial increase in the useful work of the cycle with increase in the compression ratio, π_c^*, when T_z^* = const, caused by the intensive increase in the thermal efficiency, η_t, reaching a maximum at some optimum compression ratio $\pi_{c\,opt}^*$. Work L_t will then decrease because the increase in the thermal efficiency increases with less and less intensity (fig. 24) with the considerable increase in π_c^*, while Q_1 continues to decrease.

Calculations show that

$$\pi_{c\,opt}^* = \sqrt[k]{\left(\frac{T_z^*}{T_H}\right)^{\frac{k}{k-1}}}.$$

What follows from the foregoing is that the optimum summed compression ratio does not depend on airspeed (Mach number, M_H) and increases with increase in altitude, that is, with a decrease in the temperature, T_H, of the atmospheric air. In addition, the higher the temperature, T_z^*, in front of the turbine the higher will be $\pi_{c\,opt}^*$, all other conditions being equal.

The simple cycle, with heat input at constant pressure and with adiabatic compression and expansion, reviewed here is at the basis of the combustion stage in all presently existing turbojet engines, as well as in other types of aviation gas-turbine engines (dual-flow and turboprop engines).

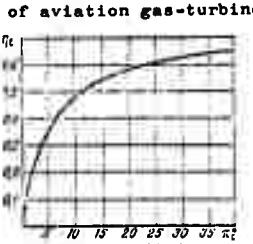

Figure 24 Dependence of thermal efficiency on compression ratio π_c^*.

3. Cycle with Two-Stage Heat Input at Constant Pressure

The ideal cycle for a turbojet engine with two-stage heat input at constant pressure and with adiabatic compression is depicted by the pv and TS diagrams in figure 25. This cycle comprises the following processes:

air compression along the adiabat Hk as a result of the velocity head and in the compressor;

first heat input, Q_1' , along the isobar kg in the first combustion chamber ahead of the turbine; in the TS diagram this heat is depicted by the area 1kz2';

air expansion along the adiabat z2 in the turbine;

second heat input, Q_1'', along the isobar 22f (depicted in the TS diagram by the area 2'22f3) in the combustion chamber between the turbine and the jet nozzle;

final expansion along the adiabat 2fe in the jet nozzle;

heat transfer, Q_2, along the isobar eH (depicted by the area 1He3 in the TS diagram) to the outer medium.

The useful work, L_t, in the cycle under consideration is depicted by the area Hk22fe in the pv diagram, and its heat equivalent by the area bounded by the outline with the same designations as in the TS-diagram. In this diagram the area 1kz22f3 corresponds to the total heat input, $Q_1 = Q_1' + Q_1''$.

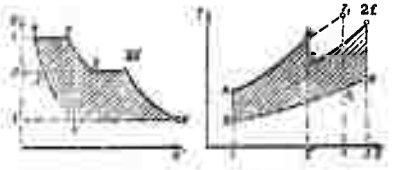

Figure 25 Cycle with two-stage heat input.

The thermal efficiency of a cycle with two-stage heat input is obviously equal to

$$\eta_t = 1 - \frac{Q_2}{Q_1' + Q_1''}.$$

The amounts of heat, Q_1' and Q_1'', added in a two-stage cycle, are equal to

$$Q_1' = c_p(T_z^* - T_c^*);$$
$$Q_1'' = c_p(T_{2f}^* - T_z^*).$$

A detailed analysis reveals that the thermal efficiency of the cycle with staged heat input not only depends on the compressor compression ratio π_c^*, but also on the temperature, T_z^*, in front of the turbine, or on the amount of heat, Q_1', and on the temperature T_{2f}^*, at the end of the secondary heat input, Q_1'', or on the amount of that heat.

The corresponding calculations will permit drawing the following conclusions for the cycle with staged heat input.

1. The thermal efficiency of the cycle will increase continuously with increase in the compression ratio, π_c^*, if at the same time the condition that $Q_1' = \text{const}$ and $Q_1'' = \text{const}$ is observed (curve 2 in fig. 26), because the amount of heat transferred, Q_2, is reduced as a result of the reduction in the end temperature, T_e, of the cycle.

2. The thermal efficiency has a maximum with respect to π_c^* (curve 2' in fig.26) when there is an increase in the compression ratio, π_c^*, and constant temperatures, T_z^*, in front of the turbine and, T_{2f}^*, in front of the jet nozzle, all other conditions being equal.

3. Thermal efficiency decreases continuously with an increase in temperature, T_{2f}^*, that is, with the amount of heat input, Q_1'', when $\pi_c^* = \text{const}$ and $T_z^* = \text{const}$ (fig. 27). This effect of T_{2f}^* (or Q_1'') on thermal efficiency is explained by the fact that the heat input, Q_2'', is accomplished at reduced pressure $p_2 < p_c$, so the summed amount of heat, $Q_1 = Q_1' + Q_1''$, increases at a slower rate than does the amount of heat, Q_2, transferred, the result of the increase in Q_1''.

Figure 26 Dependence of thermal efficiency on compression ratio for a two-stage cycle.

Legend:

A - $Q_1' = \text{const}$ and $Q_1'' = \text{const}$

A more detailed analysis reveals that with all other conditions being equal, the thermal efficiency of the cycle under consideration increases with an increase in airspeed and altitude (with a decrease in temperature, T_H), just as did the efficiency of the simple cycle, because of the increase in the summed compression ratio.

This is the basis for the conclusion that the cycle with staged heat input is always less efficient, given the same compression ratios, than is the simple cycle, that is, the cycle with single-stage heat input. This can be seen, in particular, from the curves in figure 26, where dashed curve 1 indicates the change in the thermal efficiency of the simple cycle. One can be persuaded of this fact by superposing both cycles in a TS diagram, as was done in figure 25 in the case of identical π_c^*, for equal

amounts of heat input Q_1 (areas 1kz22$_f$3 and 1kz$_1$4 are equal) and for the same initial conditions. As will be seen, in this case the staged cycle is actually less efficient than the simple cycle (Hkz$_1$e$_1$), because of the great magnitude of heat transferred, Q_2 (area 1He3 is larger than area 1He$_1$4). However, as we see, the first cycle takes place at a lower temperature, T_z^*, in front of the turbine.

If the comparison of the cycles in question takes into consideration the fact that they have identical compression ratios, and identical maximum temperatures in front of the turbine, the advantage with respect to efficiency will, as before, go to the simple cycle. This even follows from the curves in figure 27, where points 1 are the magnitudes of the thermal efficiency for the simple cycle. But then the useful work of the staged cycle proves to be greater in this case than the work of the simple cycle, as will be seen from the diagram in figure 25.

Thus, the use of the staged cycle results in a significant increase in useful work, L_t, and, consequently, in the specific thrust of the engine, without increasing the temperature in front of the turbine. This is why the staged cycle is widely used today as the basis for the combustion stage in turbojet engines (with afterburner), despite the fact that its efficiency is lower than that of the turbojet engine with the simple cycle.

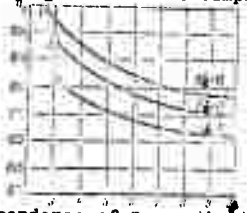

Figure 27 Dependence of η_t on the temperature in front of the jet nozzle for the two-stage cycle.

4. Cycle with Heat Input at Constant Pressure and with Isothermic Compression

The ideal cycle with heat input at constant pressure and with isothermic compression is depicted in the pv and TS diagrams in figure 28. This cycle differs from the preceding ones in that the compression process does not take place along an adiabat but along an isotherme, Hk, and is a simple diagram of the combustion stage for a turbojet engine with air cooling in the compressor.

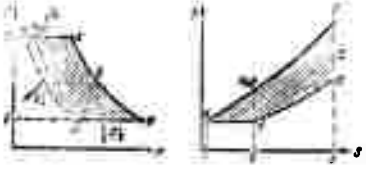

Figure 28 Cycle with isothermic compression.

The useful work, L_t, of the cycle, and its heat equivalent, AL_t, are depicted, respectively, by the areas defined by the contours Hkze in the pv and TS diagrams.

The heat added to the cycle, Q_1, is depicted by the area 1kz3 in the TS diagram, and the heat removed, Q_2, is depicted by the area 1kHe3. Heat Q_2 is composed of heat Q_2' (area 2He3) removed along the isobar He, and heat Q_2'' (area 1kH2) removed during the isothermic compression process, Hk.

Accordingly, we can write the following for the thermal efficiency of the cycle:

$$\eta_t = 1 - \frac{Q_2' + Q_2''}{Q_1}.$$

Since the temperature is constant during isothermic compression ($T_c^* = T_H$)

$$Q_1 = c_p(T_z^* - T_H) = c_p T_H(\delta - 1),$$

where $\delta = \frac{T_z^*}{T_H}$.

The amount of heat expelled during isothermic compression is precisely equal to the work of isothermic compression, expressed in thermal units

$$Q_2'' = ART_H \ln \frac{p_c^*}{p_H}.$$

Now, substituting the dependencies for Q_1, Q_2'', and Q_2' in the expression for η_t, we can, after simple transformations, obtain

$$\eta_t = 1 - \frac{1}{\delta - 1}\left(\frac{\delta}{\pi_c^{*\frac{k-1}{k}}} - 1 + \ln \pi_c^{*\frac{k-1}{k}}\right).$$

This expression is the basis for the following conclusions with respect to the cycle with isothermic compression.

1. The thermal efficiency of the cycle depends on the compression ratio, and on the temperature ratio $\delta = T_z^*/T_H$, that is, on the amount of heat, Q_1, added to the cycle.

2. The thermal efficiency increases with increase in the compression ratio, when δ = const, reaches a maximum for some value $\pi_{c\,opt}^*$, and then decreases.

This is explained by the fact that heat Q_2', expelled along the isobar eH, decreases with increase in π_c^*, when δ = const, the result of the reduction of the end temperature, T_e, of the cycle, and that heat Q_2'', expelled during compression, increases simultaneously. Initially, the effect of heat Q_2' predominates, the expelled heat, Q_2, is reduced despite the increase in Q_2'', and η_t increases. Then, because of the significant increase in π_c^*, the increase in heat Q_2'' begins to predominate, resulting in an increase total expelled heat, Q_2, and η_t is reduced.

3. The thermal efficiency increases continuously with the increase in δ (or T_z^*, when T_H = const), that is, with an increase in the amount of added heat, Q_1, when π_c^* = const. This is explained by the fact that here the expelled heat, Q_2, increases at a slower rate than the added heat, Q_1, because heat Q_2 increases only because of the increase in Q_2', while its other

component, Q_2^*, remains constant because π_c^* = const.

Given the same compression ratio, and any value of δ, the thermal efficiency of the cycle with isothermic compression is always lower than the efficiency of the simple cycle with adiabatic compression.

However, given identical π_c^* and T_z^*, the useful work of the cycle with isothermic compression proves to be greater than the useful work of the simple cycle with adiabatic compression, despite its lower efficiency, the result of the greater amount of heat, Q_1, thus added to the cycle with isothermic compression (greater by a magnitude proportional to the area Hkk_{ad} in the diagram in fig. 28).

As a result of the positive aspects mentioned above, the cycle with isothermic compression is used in individual cases as the basis for the combustion stage in turbojet engines in which compressor air cooling is by water injection (see below).

5. Cycle with Thermal Regeneration

Thermal regeneration can substantially increase the efficiency of gas turbine engine cycles without exceeding practically permissible temperatures and pressures.

Thermal regeneration is understood to mean the use of some of the waste heat, Q_2, to heat the compressed air fed into the combustion chamber from the compressor.

A diagrammatic layout of a gas turbine engine with thermal regeneration is shown in figure 29. In this engine, the air is compressed in compressor 1, and flows into heat exchanger 2, where it is heated by the hot gases leaving the turbine. The heated air then flows into combustion chamber 3, into which pump 5 injects fuel. Correspondingly, combustion products from combustion chamber 3, after flowing through turbine 4, the prime mover of compressor 1 and propeller 6 (or another energy consumer), flow into heat exchanger 2, and from there are discharged to atmosphere after giving up some of their heat to the compressed air.

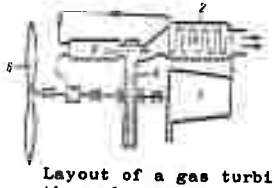

Figure 29 Layout of a gas turbine engine with thermal regeneration.
1 - compressor; 2 - heat exchanger; 3 - combustion chamber; 4 - turbine; 5 - pump; 6 - propeller.

Figure 30 shows the cycle with heat input when p = const, and with maximum possible thermal regeneration in the ideal case, that is, if the compressed air has been heated in the heat exchanger to the temperature of the combustion products at the turbine exhaust, and in which

ok is the air compression process in the compressor along the adiabat;

kk' is the isobaric process of heating the compressed air with exhaust gases in the heat exchanger;

k'z is the process of external heat, Q_1, input along the isobar;

ze is the process of adiabatic expansion of gases in the turbine;

ee' is the cooling of the waste gases in the heat exchanger, that is, the isobar of the heat output, Q_p, from the gases to the compressed air being heated;

e'O is the process of yielding heat, Q_2, to the external medium.

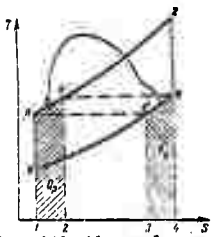

Figure 30 Cycle with thermal regeneration in the case of adiabatic compression.

The heat Q_p yielded by the exhaust gases to the compressed air they are heating in the heat exchanger, is represented by the shaded area 3e'e4 in the TS diagram, or what is the same thing, by the area 1kk'2. So far as the cycles are concerned, this is internal heat in constant circulation, as if in a closed circle.

Heat, Q_1, added to the cycles from the outside with thermal regeneration, is represented by the area 2k'z4 in the TS diagram.

The heat not used in these cycles (after subtraction of heat Q_p), that is, heat Q_2 expelled to a cold source (external medium) in accordance with the second law of thermodynamics, is represented by the area 10e'3.

Without studying cycles with thermal regeneration in detail, let us use two examples to show that regeneration increases the thermal efficiency of the gas turbine cycle.

Let us assume that a cycle with thermal regeneration in the case of adiabatic compression, and a cycle of the same type, but without thermal regeneration, have identical initial conditions, equal compression ratios, and maximum temperatures. Obviously, these conditions will result in complete coincidence between all points of the cycles being compared, so the cycle okze, depicted in the diagram in figure 30, will be the cycle with thermal regeneration and the cycle without regeneration, at one and the same time. The useful work of both cycles (with and without regeneration) can be measured by the same area, okze. However, in the cycle with thermal regeneration the consumed heat Q_1, measured

by the area 2k'z4, is less than it is in the cycle without regeneration, in which Q_1 is measured by the area 1kz4. The obvious conclusion is that the thermal efficiency of the cycle with thermal regeneration is higher than that of the cycle without regeneration.

We will arrive at the same conclusion if we compare cycles with adiabatic compression under identical initial conditions, equal compression ratios, and equal amounts of input heat Q_1, which is equivalent to equality in the areas 1kz4 and $2k'z_15$ in figure 31. As will be seen, in this case the useful work in the cycle with thermal regeneration, corresponding to the area okz_1e_1, is greater than it is in the cycle without regeneration, okze. But a greater magnitude of useful work in the cycle for the same amount consumed heat Q_1, also results in higher thermal efficiency.

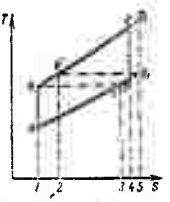

Figure 31 Comparison of a cycle with thermal regeneration.

The amount of heat, Q_p, that can be communicated to the air in the heat exchanger will be greater the greater the difference between the temperature of the combustion products leaving the turbine, Te, and the temperature of the air leaving the compressor, T_c. Obviously, thermal regeneration is impossible if these temperatures are equal.

The temperature of the compressed air in an engine with compressor cooling is lower, for the same ratio of pressure increase, than it is in an engine with an uncooled compressor. Therefore, if the temperature of the combustion products at the turbine exhaust, Te, is identical in both cases, a greater degree of thermal regeneration is possible in the first engine than in the second.

Thermal regeneration in engines with uncooled compressors is limited by the fact that for a constant magnitude of the temperature in front of the turbine, T_z, the temperature difference $T_e - T_c$ will decrease with increase in the compression ratio because of the rise in temperature T_c and the drop in temperature T_e. At some predetermined value for the compression ratio this temperature difference equals zero, and, generally speaking, precludes the possibility of using thermal regeneration.

Detailed calculations show that in aviation gas turbine engines with uncooled compressors with low temperatures in front of the turbine, $T_z^* = 1050^\circ$ to 1150°K, thermal regeneration

becomes impossible when the compression ratio in the compressor reaches $\pi_c^* = 9$ to 10.

But, if the compression ratio is low ($\pi_c^* \leq 3$ to 5), considerable thermal regeneration is possible, and can increase the efficiency of these engines to approximately 25 to 20 % if the internal hydraulic resistance of the heat exchanger is sufficiently low.

The use of a heat exchanger increases the weight and size of the power plant as a whole. This is not decisive for stationary gas turbine engines, so thermal regeneration is usually used in these engines, and a very significant economic effect results when use is in conjunction with compressor cooling.

Thermal regeneration in aviation gas turbine engines can be desirable, but only when the saving in fuel is such as to warrant the increase in engine weight, while at the same time increasing aircraft range or payload for a specified range, all other conditions being equal.

The difficulties involved in building heat exchangers with the required heat exchange surface and low internal resistance, light in weight, and small in size, as well as with respect to the limited possibility of thermal regeneration in the case of the uncooled compressor, hamper the use of thermal regeneration in aviation gas turbine engines.

6. The Real Turbojet Engine Cycle

The real, or combustion stages in all elements of a turbojet engine take place in the presence of hydraulic resistances and of heat exchange between the air and the combustion products flowing through the engine and the outside medium. At the same time, the temperature, and the change in the chemical composition (during the combustion process) of the working substance, also have an effect on the engine's thermal capacity. Therefore, the nature of the change in the parameters for the state of the gas-air flow, the absolute values of these parameters, and the end results of the processes in a real turbojet engine, and in the ideal cycle, which is at the basis of the combustion stages in the engine, are considerably different.

The sequential change that takes place in the parameters for the state of the gas-air flow in a real turbojet engine can be conventionally depicted by the pv and TS diagrams. The set of thermodynamic processes obtained as a result is called the real engine cycle, depicted by the contours Hakze in figure 32. Here the ideal cycle, with heat input when p = const and adiabatic compression with the same compression ratio and amount of heat input as for the real cycle, is indicated by the dotted outline for purposes of comparison.

The real cycle of an in-flight turbojet engine is composed of the following main processes (fig. 32):

air compression along a polytrope because of the velocity head; this process is represented by the curve Ha;

air compression in the compressor along the polytrope aK;

the combustion process kz at a somewhat reduced pressure (see below);

expansion of the combustion products in the turbine along the polytrope z2;

expansion of the combustion products in the jet nozzle along the polytrope 2e;

the closed isobaric process, eH, corresponding to the dissipation into the surrounding medium of the heat carried away by the combustion products leaving the engine; this process takes place outside the engine.

In the real cycle the total work of polytropic expansion of the combustion products is depicted by the area 5kzel in the pv diagram (fig. 32) and is made up of the work of expansion in the combustion chambers (area 5kz4), in the turbine (area 4z23), and in the jet nozzle (area 32e1).

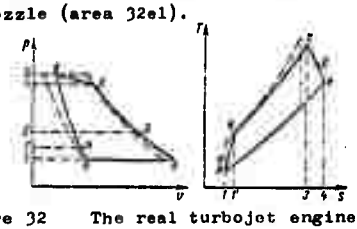

Figure 32 The real turbojet engine cycle

The total work of air compression can be depicted by the area 5kH1. In flight this work is equal to the sum of the work of ram compression (area 1'aH1) and polytropic compression in the compressor (area 5ka1'), and for engine operation in situ it equals the work of compression in the compressor.

The useful, or internal work of a real cycle, L_i, is equal to the difference between the total work of polytropic expansion of the combustion products in the engine, and the total work of air compression.

The internal work, L_i, is depicted by the area HakzeH in the pv diagram, and its thermal equivalent, AL_i, by the area with the same designations in the TS diagram.

The heat delivered to the air during the combustion process in the real cycle and leading to an increase in its enthalpy, is depicted by the area 1'kz3 in the TS diagram, while the heat carried away from the engine into the surrounding medium with the combustion products is depicted by the area 1He4 (fig. 32).

Moreover, area 3z2e4 in the TS diagram is the heat absorbed by the gas during its expansion. This heat is equal to the

difference between the heat equivalent to the work of hydraulic resistances in the turbine, exhaust pipe, and jet nozzle, and the heat transferred from the gas to the outside medium through the walls of these engine elements. Accordingly, area 1Hk1' is the heat absorbed by the air as it is compressed in the compressor. This heat is equal to the difference between the heat equivalent to the work of the hydraulic resistances in the compressor, and the heat given off to the atmosphere through the compressor housing.

Designating the total work of polytropic expansion of one kilogram of combustion products by $L_{p\ e}$, and the total work of compression of one kilogram of air by $L_{t\ c}$, and taking into consideration the fact that one kilogram of burned fuel contains αl_o kg of air and $(1 + \alpha l_o)$ kg of combustion products, we can write the following for the internal work, L_i, of the cycle, equated to 1 kg of fuel

$$L_{i_1} = (1 + \alpha l_o) L_{pe} - \alpha l_o L_{tc}.$$

After dividing this expression by αl_o, we obtain the internal work, equated to 1 kg of air flowing through the engine

$$L_i = \frac{1 + \alpha l_o}{\alpha l_o} \cdot L_{pe} - L_{tc}$$

or

$$L_i \approx L_{pe} - L_{tc}.$$

The internal work done by a turbojet engine goes to increase the kinetic energy of the gas-air flow through the engine and, in addition, is partially expended in overcoming the hydraulic resistances in all engine elements, friction of the end surfaces of compressor and turbine wheels and the air and gas, friction in the bearings, and driving the auxiliaries.

If we subtract from the internal work, L_i, that part, L_r, expended on all of the resistances indicated above, we obtain the effective work as

$$L_e = L_i - L_r.$$

The effective work done in a turbojet engine goes in full to the increase in the kinetic energy of the gas-air flow through the engine. On this basis, we can write the following energy relationship

$$L_e = \frac{c_e^2}{2g} - \frac{V^2}{2g}, \tag{3.6}$$

where L_e is the effective work, equated to 1 kilogram of air flowing through the engine (assuming $\frac{1 + \alpha l_o}{\alpha l_o} \approx 1$).

For engine operation in situ, when V = 0, we obtain

$$L_{e_s} = \frac{c_e^2}{2g}.$$

The expression at (3.6) provides the velocity at which the gas flows from the jet nozzle

$$c_r = \sqrt{2gL_e + V^2}.$$

We can therefore write the specific thrust in the form

$$P_{sp} = \frac{1}{g}(\sqrt{2gL_e + V^2} - V),$$

and for in situ operation

$$P_{sp_o} = \frac{1}{g}\sqrt{2gL_e}.$$

Thus, the effective work done in the real turbojet engine cycle is used only to create reactive thrust.

The efficiency of the real turbojet engine cycle evaluates its effective efficiency, η_e, which takes into consideration, as was explained earlier, all the losses incurred during the conversion of the heat contained in the fuel into the kinetic energy of the gas-air flow through the engine, that is, into effective work, L_e. Consequently, on the basis of the dependencies obtained earlier, we can write

$$\eta_e = \frac{AL_e}{H_u}. \tag{3.7}$$

Losses in the real cycle always result in a lower effective efficiency, η_e, for a given compression ratio, than the thermal efficiency, η_t, of the ideal cycle. Therefore, $L_e < L_t$ for the same amount of delivered heat.

CHAPTER 4

TURBOJET ENGINE INLETS

1. Air Compression at the Engine Inlet By the Ram Effect

The inlets of turbojet engines, as well as those of other types of aviation gas turbine engines, are used to obtain precompression of the air by the ram effect and then deliver the air to the compressor.

The inlets, usually referred to as inlet diffusers, must provide:

minimum loss in the case of stagnation (ram compression) of the meeting flow of air;

minimum hydraulic losses in the diffusor flow section;

an adequately uniform velocity field at the compressor inlet;

the weight flow of air required by the engine under all possible operating conditions;

stable operation, that is, operation without flow separations and pressure pulsations, under all operating conditions;

a minimum of external drag.

After passing through the inlet, the air enters the compressor, which has stagnation temperature T_a^*, stagnation pressure p_a^*, and, correspondingly, actual temperature T_a, and static pressure p_a, across its inlet section.

When we determine the air stagnation temperature, T_a^*, at the compressor inlet, we can completely disregard heat exchange with the external medium, because it is insignificant. In this case, as we know, we can only establish a temperature increase by a reduction in air velocity, and this increase does not depend on the magnitude of the losses when there is air flow stagnation. Therefore, the air stagnation temperature, T_a^*, at the compressor inlet is practically equal to the external air stagnation temperature T_H^*.

Temperature T_a^* can be expressed in terms of the Mach number, M_a, at the compressor inlet

$$T_a^* = T_a(1 + 0.2M_a^2), \tag{4.1}$$

where $T_a^* = T_H^*$.

The actual air temperature at the compressor inlet can be established through the formula at (1.23,a)

$$T_a = T_H^* - \frac{c_a^2}{2gJ}, \tag{4.2}$$

where c_a is the air velocity at the compressor inlet.

For in situ engine operation, $T_H = T_0$, so $T_a^* = T_0$ and, consequently

$$T_a = T_0 - \frac{c_a^2}{2gJ}. \tag{4.3}$$

Stagnation pressure, p_a^*, at the compressor inlet is always less than the stagnation pressure p_H^*, that would be present in the case of adiabatic (lossless) air stagnation for a given Mach number M_H, that is, when k = 1.4

$$p_a^* = \sigma_{in} p_H^* = \sigma_{in} p_H (1 + 0{,}2M_H^2)^{3{,}5}, \tag{4.4}$$

where $\sigma_{in} < 1$ is a factor that takes into consideration all pressure losses in the case of ram compression in the inlet, or the so-called stagnation pressure recovery factor.

Correspondingly, the ram air compression ratio, with inlet loss taken into consideration, will equal

$$\pi^*_{ram} = \frac{p_a^*}{p_H} = \sigma_{in}(1 + 0{,}2M_H^2)^{3{,}5}. \tag{4.5}$$

When engine operation is in situ $M_H = 0$, so

$$\pi^*_{ram_0} = \frac{p_a^*}{p_0} = \sigma_{in} < 1. \tag{4.6}$$

Static pressure, p_a, at the compressor inlet can be established through the adiabat equation $\frac{p_a}{p_a^*} = \left(\frac{T_a}{T_a^*}\right)^{\frac{k}{k-1}}$,

from whence, and reminded that $p_a^* = \sigma_{in} p_H^*$ and $T_a^* = T_H^*$, and using the formula at (4.3), we obtain

$$p_a = \sigma_{in} p_H^* \left(1 - \frac{c_a^2}{2000 T_H^*}\right)^{3{,}5} \tag{4.7}$$

and, correspondingly, for in situ operation

$$p_a = \sigma_{in} p_H \left(1 - \frac{c_a^2}{2000 T_H^*}\right)^{3{,}5}.$$

The velocity, c_a, at the compressor inlet is assigned when the engine is designed and is based on the required diametrial dimensions and weight for the compressor, while taking into consideration the effect of the velocity, c_a (Mach number M_a), on compressor capacity and efficiency. In modern turbojet engines at the design point, c_a = 180 to 200 m/sec, and higher.

When the engine is installed in the aircraft, the engine inlet section proper is often preceded by air feeders that are part of the aircraft structure (when the engine is located in the fuselage), or that are formed by special housing-fairings (when the engine is located in the wing, or under the wing, etc.). The hydraulic losses incurred in these feeders differ from aircraft to aircraft of different types and designs, so pressure losses in the aircraft air feeders are disregarded in the engine design, but are taken into consideration separately when fitting the engine to a specific aircraft.

2. Simple Inlets

Simple inlets, often referred to as subsonic diffusers, are used at subsonic airspeeds. Their layouts are shown in figures 33 and 34. In order to reduce losses during ram compression, subsonic diffusers are shaped in such a way that stagnation of the meeting air takes place completely, or partially, before the air enters the diffuser, that is, in front of it. All, or a considerable part of the internal duct in these diffusers is directly butted to the compressor, and is slightly convergent. The ratio between areas, F_a/F'_a, usually equals 0.75 to 0.85. As a result, the air picks up some acceleration inside the diffuser and this lends itself to there being a more uniform velocity field at the compressor inlet and to a reduction in hydraulic losses. The intake lips of these diffusers are smoothly rounded, providing for a flow with extremely small losses under all engine operating conditions.

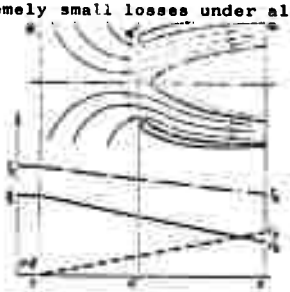

Figure 33 Flow diagram in a subsonic inlet diffuser when V = 0.

When the engine is running in situ (fig. 33) the air velocity in front of the inlet diffuser increases gradually, the result of the compressor suction effect, rising from zero outside the diffuser, that is, at the boundary of the air undisturbed by compressor operation (section H H), to some velocity, c_a, at the compressor inlet (section a a). Since no external energy is added to the air flow in this section, its pressure and temperature are reduced.

Figure 34 Flow diagrams in a subsonic diffuser in the case of subsonic flight.

In subsonic flight ($M_{fl} < 1$), when airspeed V, is greater than velocity c'_a across the initial section, a'a', of the inlet diffuser (fig. 34), ram air compression (stagnation), causing the increase in air pressure and temperature, takes place in front of the diffuser, outside it (before section a'a') and

beginning at the free air boundary, HH. This external ram compression is practically lossless. The air then enters the internal contracting duct in the diffuser, where its velocity increases somewhat, beginning at section a'a' and ending at the compressor inlet. There is a corresponding reduction in pressure and temperature (fig. 34 a). If the contracting section of the diffuser's internal duct is preceded by a divergent section, ram compression will terminate in this section of the internal duct, as shown schematically in figure 34 b. The pressure losses due to ram air compression are small during subsonic flight because they are caused only by the hydraulic resistances in the inlet ducts of the inlet assembly, or $\sigma_{in} = \sigma_{rf} = 0.95$ to 0.98, where σ_{rf} is the stagnation pressure recovery factor in these ducts.

In supersonic flight ($M_H > 1$) a shock wave with, generally speaking, a curved front (fig. 35), forms at some distance before the subsonic diffuser under discussion. However, experience shows that that section of the shock front intersected by the air flow subsequently entering the engine is practically perpendicular to the flow; there is a normal shock wave (shock section 1 1 in fig. 35). The air velocity becomes subsonic immediately at this shock, and this is accompanied by a shock-type increase in pressure and temperature. Consequently, there is a subsonic flow of air between the shock front and the inlet diffuser, and its subsequent flow schematic remains the same as that reviewed above.

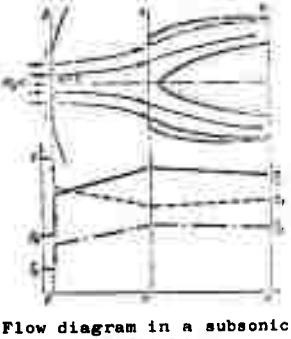

Figure 35 Flow diagram in a subsonic diffuser in supersonic flight

When the supersonic air flow stagnates some of its kinetic energy is irreversibly converted into heat at the shock wave and is not used to increase the air pressure. Therefore, beyond the shock wave the stagnation pressure p_c^* (and, correspondingly, static pressure p_c), is always lower than pressure p_H^*, which would have been obtained for the same reduction in flow velocity if there were no shock wave, that is for the case of conventional adiabatic (lossless) flow stagnation. This is why the stagnation pressure recovery factor, $\sigma_c = \frac{p_c^*}{p_H^*}$, at the shock wave is always

less than unity. The higher the supersonic flow velocity, or the larger the flight Mach number, M_H, with respect to unity, the more intensive the normal shock, and the greater will be that part of the kinetic energy converted into heat. As a result, the loss in stagnation pressure at the shock increases with increase in the flight Mach number M_H, while the coefficient σ_c decreases. It is obvious that when there is a shock wave, the pressure loss involved in ram compression at the engine inlet will be established by the product $\sigma_{in} = \sigma_c \cdot \sigma_{rf}$.

Curve 1 in figure 36 shows the dependence of the stagnation pressure recovery factor at the normal shock on the flight Mach number M_H. As will be seen, the factor σ_c decreases rapidly with an increase in the Mach number, M_H, and that when $M_H = 2.5$ it is 0.5. This means that when $M_H = 2.5$, stagnation and static air pressures at the engine inlet (after the normal shock) will be approximately half what they would be in the case of adiabatic stagnation of a supersonic flow, that is, when there is no normal shock wave in the flow.

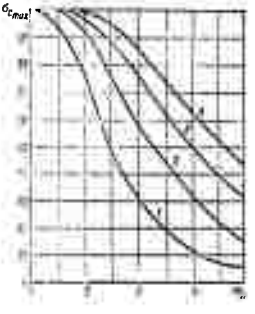

Figure 36 Dependence of the loss in stagnation pressure on the flight Mach number, M_H, for different types of inlet diffusers

The loss in pressure at the normal shock wave is comparatively small ($\sigma_c = 0.92$ to 0.93) in the case of relatively slow supersonic speeds, that is, when $M_H = 1.4$ to 1.6. This is why the simple subsonic inlets reviewed above are used, but with tapered inlet lips, for aircraft with these airspeeds as well as for subsonic aircraft.

3. Supersonic Inlet Diffusers

Special inlets, called supersonic diffusers, must be used at high speed supersonic flights in order to reduce the significant pressure losses characteristic of air stagnation at a single, normal shock wave. These diffusers cause air stagnation by multiple oblique shock waves which, for a given flight Mach number $M_H >> 1$, is accompanied by significantly smaller pressure losses than those encountered in the case of stagnation of this flow at a single, normal shock wave. The greater the supersonic

airspeed, and the number of oblique shocks, the greater will be the gain obtained in the magnitude of the ram compression ratio, as with the compression at a single, normal shock.

Supersonic diffusers used in turbojet engines are designed in the form of an axisymmetrical duct with sharp inlet lips, inside which there is a central cone with a straight or broken-line generatrix or one in the form of a flat duct formed by two asymmetrical wedges, the larger of which performs the same function as does the central cone in the axisymmetrical diffuser, depending on the location of the engine in the aircraft.

Diagrammatic layouts of axisymmetrical supersonic diffusers with one and two incident shocks are shown in figure 37, and those of flat supersonic diffusers with two and three oblique shocks are shown in figure 38. The oblique shocks formed by the tip of, and the breaks in, the central cone, or by the upper wedge, are indicated in figures 37 and 38 by the straight lines Oa', ba', and ca', and their angles of inclination to the longitudiaal axis of the diffuser are designated by α. Air velocity remains supersonic with respect to the engine after these multiple incident shocks. Further reduction in air velocity to subsonic takes place in a complicated, and little-studied system of primary and reflected shocks also located inside the diffuser duct. In order to simplify research and design, this system of shocks is usually replaced by a single, weak, normal breakdown shock wave, shown by the wavy lines a'd, bd, and dc in these diagrams. Practical experience shows that this substitution is completely acceptable.

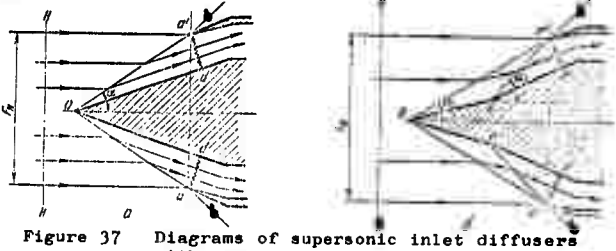

Figure 37 Diagrams of supersonic inlet diffusers with one and two oblique shocks

The operational design point for a supersonic inlet diffuser is that point at which conditions are such that the front of the first external oblique shock formed by the tip of the central cone (the first external shock) touches the leading edge of the cowling as shown in figures 37 and 38, which show the air flow diagrams for the operational design points of a supersonic diffuser.

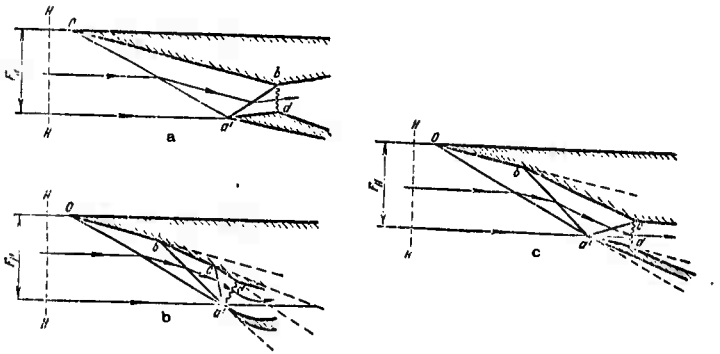

Figure 38 Diagrams of supersonic inlet diffusers with two and three oblique shocks

Henceforth, the flight Mach number, M_H, corresponding to the diffuser design point will be designated $M_{H_{ddp}}$.

If all the oblique shock waves formed by the central cone are outside the internal diffuser duct, that is, before it, and if the normal breakdown shock is in the plane of the inlet section of that duct (figures 37 and 38 b), the diffuser in question is called a diffuser with external compression. However, in some of the oblique shocks and the normal breakdown shock are located in the internal duct (figure 38 a and b), the diffuser is called a diffuser with mixed compression (with partly external, and partly internal compression).

The curves plotted in figure 36 show the dependence of the maximum possible stagnation pressure recovery factors, σ_c on the flight Mach number, M_H, for the following shock systems: 1 - a single normal (simple diffuser as per the diagram in figure 35); 2 - one oblique + one normal (as per the diagram in figure 37 a); 3 - two oblique + one normal (as per the diagrams in figures 37 b and 38 a); 4 - three oblique + one normal (as per the diagrams in figures 38 b and 38 c). These dependencies, obtained from investigations made by G. I. Petrov and Ye. P. Ukhov, show that when $M_H \gg 1$ the use of supersonic diffusers provides a very significant gain over the simple diffuser, that is by a single normal shock. For instance, when $M_H = 2$ the ram pressure after a single normal shock is $p_c^* = \sigma_c p_H^* = 0.75\ p_H^*$ (curve 1 in fig. 36), whereas a pressure of $p_c^* = 0.9\ p_H^*$ is obtained after a system of two shocks (one oblique + one normal) (curve 2 in fig. 36), or 20% higher. But if $M_H = 3$, $p_a^* = 0.3\ p_H^*$ is obtained for a single normal shock, at the same time that we have a pressure after a system of three shocks (two oblique + one normal) greater by a factor of 2.5, that is, $p_a^* = 0.75\ p_H^*$ (curve 3 in fig. 36).

All other conditions being equal, an increase in pressure after the system of shocks in the inlet diffuser will cause the pressure to increase at the turbojet engine compressor inlet and, consequently, there will be an increase in the ram compression ratio, in the resultant compression ratio, and in the air flow through the engine. The result is a corresponding increase in engine efficiency, and an increase in specific and total thrust. This is why supersonic inlet diffusers are absolutely necessary in turbojet engines designed for high-speed supersonic flight.

The principal geometric parameters of supersonic inlet diffusers (fig. 39) are:

diffuser intake area F_{in} (section a'a');

throat area, F_t, the area of the smallest flow section, tt, of the internal diffuser duct, normal to the flow;

the number of breaks on the surface of the central cone (or upper wedge), establishing the number of external incident shocks;

the vertex angle, and angles of the breaks, w_1, w_2, etc., on the surface of the central cone (wedge);

stagger of the central cone, l;

distance between its breaks, l_1, l_2, etc.;

area of diffuser outlet, F_d, section d,d);

frontal area (drag area) of the diffuser, F_f;

inner and outer cowling angles, σ_{cowl_i} and σ_{cowl_o}.

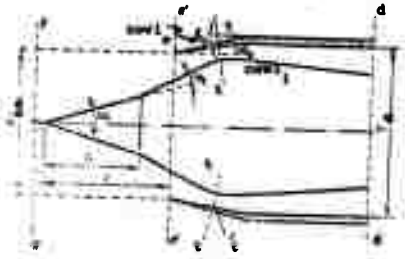

Figure 39.
Geometric parameters of a supersonic inlet diffuser

The resultant pilot loss in a supersonic diffuser can be evaluated by the factor $\sigma_d = \frac{p_d^*}{p_H^*}$, or

$$\sigma_d = \frac{p_c^*}{p_H^*} \cdot \frac{p_d^*}{p_c^*} = \sigma_c \sigma_{d.d}$$

where p_d^* is the ram pressure at the diffuser outlet (section d,d);

p_c^* is the ram pressure beyond the system of shocks;

$\sigma_{d.d}$ is a factor that takes into consideration the pressure loss in the internal duct of a supersonic diffuser; usually the average is $\sigma_{d.d} = 0.86$ to 0.88.

The maximum air flow through the diffuser occurs at the design point because the cross-sectional area, F_H, of the free air subsequently entering the diffuser (fig. 37) equals the inlet area, F_{in}, of the diffuser (fig. 39). Actually, we can write

$G_a = \gamma_H F_H V$, where γ_H is the specific weight of the external free air, and V is its velocity relative to the diffuser, that is, the airspeed for the air flow through the area F_H. However, for given values of γ_H and V, the maximum for this flow will occur when $F_H = F_{in}$, that is, $G_{a_{max}} = \gamma_H F_{in} V$.

The capacity, or the output, of a supersonic inlet diffuser, for given γ_H, is evaluated by the discharge coefficient, φ_d, which equals the ratio between the actual air flow, G_a, and the maximum air flow, $G_{a_{max}}$

$$\varphi_d = G_a/G_{a_{max}} = F_H/F_{in},$$

from whence

$$G_a = \varphi_d F_{in} V \gamma_H.$$

It is obvious that $\varphi_d = 1$ at the design point. We note that the external drag of a supersonic inlet diffuser, X_d, is least at the design point.

The diffuser throat area should have a magnitude such that, at the design point all the air passing through the system of external shocks can pass through it, that is, $\varphi_d = 1$. If the throat area is selected such that the air velocity in it equals the speed of sound, this throat area will be called the optimum throat area $F_{t_{opt}}$, because here the pitot loss in the diffuser will be least all other conditions being equal.

If the throat area at the diffuser is comparable to that shown in figures 38 a or 38 b, and is made greater than optimum, ($F_t > F_{t_{opt}}$), that is, it is oversized, and the other conditions remain the same, the air in the throat will become supersonic (the normal breakdown shock will be located beyond the throat), and the velocity beyond the throat will increase accordingly. This is why the pitot loss in the diffuser duct will increase. The same result will be obtained when $F_t \gtrsim F_{t_{opt}}$ for the diffusers in figures 37 and 38 b, the result of flow separation and eddy formation in the throat region.

If the throat area is less than optimum and all other conditions remain unchanged, the throat will be unable to pass all the air flowing through the external incident shocks. In that case a so-called deflected forward shock wave develops before the diffuser duct inlet, destroying the multiple external oblique shocks near the cowling, as shown in figure 40.

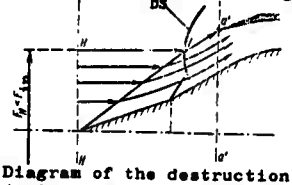

Figure 40 Diagram of the destruction of designed multiple shocks by a deflected shock (DS)

This causes external air leakage near the cowling, so the discharge coefficient, φ_d, is reduced and becomes less than unity. In addition, pitot losses in the diffuser increase, as does external diffuser drag.

The internal diffuser duct is made wider beginning at the throat (downstream), then, immediately before the engine, the inlet section is made in the form of a slightly converging duct, as was mentioned earlier, in order to equalize the flow at the compressor inlet.

4. Off-Design Points and Unstable Operation (Surging) of a Supersonic Diffuser

Let us now consider the special features of the operation of a fixed-area (invariable geometry) supersonic inlet diffuser at the off-design points. The diffuser can deviate from its design point as a result of a change in the flight Mach number M_H, or of a change in the backpressure at the diffuser outlet, caused by a change in engine operation.

If there is a change in flight Mach number, M_H, compared with that value of $M_{H_{ddp}}$ for which the supersonic diffuser was designed and configurated, the designed multiple shocks will be destroyed, causing a change in the coefficients σ_d and φ_d, and in the external diffuser drag.

We know that the angle of inclination of the oblique shocks is reduced, but that their intensity increases, when the flight Mach number, M_H, increases beyond $M_{H_{ddp}}$. Therefore, the external oblique shocks, instead of converging at the leading edge of the cowling, flow inside the diffuser duct (figure 41), where they produce a series of additional reflected shocks. This results in an increase in the pitot losses in the diffuser and in a corresponding reduction in σ_d (even when compared with σ_d for a diffuser designed for this other, higher Mach number, $M_H > M_{H_{ddp}}$). Moreover, as will be seen from the diagram in figure 41, when $M_H > M_{H_{ddp}}$, the discharge coefficient does not change, but remains $\varphi_d = 1$, that is, diffuser output remains the maximum possible.

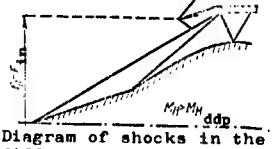

Figure 41 Diagram of shocks in the supersonic diffuser when $M_H > M_{H_{ddp}}$

If the flight Mach number, M_H, is reduced as compared with the design point for the diffuser, that is, when $M_H < M_{H_{ddp}}$, the external oblique shocks will fall away from the leading edge of the cowling (fig. 42 a), all other conditions unchanged, because angle of inclination, α, of these shocks will increase with a decrease in the Mach number, M_H. The result is external air leakage, the area F_H of the undisturbed jet becomes smaller than that of F_{in}, as will be seen in figure 42, and the discharge

coefficient is reduced; it becomes $\varphi_d < 1$, and external diffuser drag increases. The pressure-recovery factor, σ_d, increases because of the reduction in the intensity of the shocks when the flight Mach number, M_H, is reduced. But even so, a lower σ_d is obtained than would be the case for a diffuser designed for this lower Mach number $M_H < M_{H_{ddp}}$.

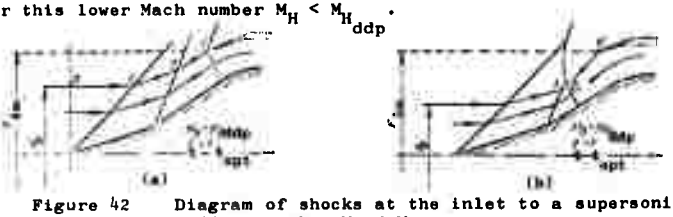

Figure 42 Diagram of shocks at the inlet to a supersonic diffuser, when $M_H < M_{H_{ddp}}$

Calculations show that the smaller the flight Mach number, M_H, the greater will be the required optimum diffuser throat area $F_{t_{opt}}$, that is, the minimum throat area providing for an air flow without a deflected forward shock, as in the diagram in figure 42 a. Physically speaking, this can be explained by the fact that with a decrease in the Mach number, M_H, comes a reduction in the ram air compression ratio in the diffuser, and the density of the air in the throat is reduced accordingly, so throat discharge capacity is reduced, and this requires an increase in $F_{t_{opt}}$ when the flight Mach number, M_N, is reduced. Fixed-area supersonic diffusers have a constant throat area. Therefore, if the throat area is selected as optimum when $M_{H_{ddp}}$, this area will become less than optimum for lower flight Mach numbers, M_H, that is, the throat capacity will become less than the capacity of the oblique shocks falling away from the cowling (when $\varphi_d < 1$). When $M_H < M_{H_{ddp}}$, this results in the appearance of a deflected forward shock as shown in figure 42 b, so that φ_d is reduced, and the external drag of the diffuser increases at a greater rate than in the case of the air flow shown in figure 42 a. Therefore, the throat area in fixed-area diffusers is usually made oversized ($F_t > F_{t_{opt}}$) for the diffuser design point when $M_H = M_{H_{ddp}}$, that is, the throat area is made optimum for $M_H < M_{H_{ddp}}$. As was explained earlier, this will reduce σ_d at the design point, but then σ_d and φ_d will increase and diffuser drag at flight Mach numbers, M_H, below $M_{H_{ddp}}$ will decrease.

In subsonic flight ($M_H < 1$), and particularly in slow subsonic flight ($M_H << 1$), the discharge capacity of a fixed-area supersonic diffuser proves to be considerably less than that of simple subsonic inlets, but the pressure losses in it are greater. This is primarily explained by the fact that under these conditions, ($M_H << 1$) the flow over the sharp edges of supersonic diffuser cowlings is accompanied by flow separation and eddy formations, causing air jet contraction in the diffuser duct, as shown schematically in figure 43.

Figure 43 Diagram of the air flow in a supersonic diffuser when $M_H < 1$ (a), and $M_H = 0$ (b).

The backpressure at the supersonic diffuser outlet for a given Mach number, M_H, depends on turbojet engine compressor capacity. If the compressor's capacity is increased by increasing its speed to the point where the air flow through the compressor is greater than the diffuser throat can handle at a given flight Mach number M_H, pressure at the compressor inlet, and, correspondingly, the backpressure at the diffuser outlet, will be reduced. On the other hand, if the flow of air through the compressor becomes less than the flow of air into the diffuser because of a reduction in speed (reduction in capacity), the pressure before the compressor, that is, the backpressure at the diffuser outlet, will increase. Thus, a change in the capacity of a compressor positioned after a supersonic diffuser is equivalent to a change in the air throttling ratio at the diffuser outlet. Let us see what the effect of a change in backpressure at the diffuser outlet section is on the operation of a supersonic diffuser, when the flight Mach number, M_H, is unchanged.

The cross-sectioned areas of the internal duct in supersonic diffusers are always selected such that at the design point after the throat, downstream in some section of the duct, there is acceleration and a supersonic air flow as in a supersonic expansion nozzle. Further downstream the flow stagnates, the result of the backpressure, and the supersonic flow terminates in an almost normal shock wave, after which the air velocity becomes subsonic. This supersonic region after the throat in the diffuser duct naturally increases the pressure loss in the duct. At the same time, this region protects the external shock formations against the penetration of pressure fluctuations (perturbations) from the throat caused by the compressor, the propagation velocity of which is less than the air velocity in this region.

The extent of the protective supersonic region in the diffuser duct, and the air velocity in this region, increase with decrease in the backpressure at the diffuser outlet (with increase in turbojet engine compressor rpm and M_H = const). Its breakdown shock is displaced downstream, toward the diffuser outlet, and becomes more intense, causing an increase in pressure loss, and σ_d is reduced. However, the shock formation at the diffuser inlet is not disrupted, so φ_d = const.

When the backpressure after the diffuser is increased

(reduction in turbojet engine compressor rpm and M_H = const) the breakdown shock at the protective supersonic region is displaced upstream, toward the throat, becomes less intense, and the extent of this region is reduced. As a result, the pressure loss in the diffuser duct is reduced, and σ_d increases. At the same time, the shock formation at the diffuser inlet is retained and φ_d = const.

This keeps recurring until the increase in backpressure at the diffuser outlet results in the complete disappearance of the protective supersonic region after the diffuser throat. After this, further increase in backpressure results in the normal breakdown shock being displaced outside the diffuser duct (upstream), so that a deflected forward shock appears before the diffuser inlet, moving ahead from the edge of the cowling in a manner comparable to that shown in figure 40.

At the same time, however, the aspect of deflected forward shock proves to be unstable, the result of a variety of complex phenomena accompanying the air flow in a supersonic diffuser. The mechanism of this instability in the deflected shock can be explained schematically as follows. Then a deflected forward shock develops, σ_d is reduced, the air flows outward at edges of the cowling, and the flow of air into the diffuser is reduced (φ_d is reduced), so there is a pressure drop in the duct. This moves the deflected shock backward (downstream) into the diffuser duct, and the whole shock formation is restored. But this causes an increase in the supply of air to the diffuser (increase in φ_d), there is an increase in σ_d, and a corresponding increase in pressure in the diffuser duct, again resulting in the formation of a deflected forward shock and at the same time, the disruption of the shock formation at the diffuser inlet. The shock formation is again restored in accordance with the pattern described above, after which it is destroyed, etc. In other words, these processes are repeated, alternating rapidly in the process. The result is unstable operation, or surging in the diffuser, accompanied by heavy pressure fluctuations and return air currents in the diffuser duct.

The frequency of the pressure fluctuations during diffuser surging is approximately 100 Hz, and their intensity, that is, the ratio between the total amplitude of a pressure fluctuation and its average magnitude reaches 75 %.

Surging of a supersonic diffuser is not acceptable during engine operation because it causes vibration and jarring that impairs the strength of the inlet assembly, and other elements, in the power plant, as well as fluctuations in pressure in the combustion chambers and corresponding fluctuations in thrust, and can lead to flame attenuation and flameout in the combustion chambers, that is, to self-shutdown of the engine.

What follows from the foregoing is that the supersonic region between the diffuser throat and the diffuser outlet provides some protection against surging. The greater its length, the greater will be the delay before surging begins as the backpressure increases at the diffuser outlet, that is, the broader will be its range of stable operation, or the greater its "stability margin". However, the pressure loss increases and σ_d decreases with increase in the length of this region. Therefore, the "stability margin" for the fixed-area, supersonic diffuser can be evaluated by the magnitude $\Delta_{st} = \sigma_{max}/\sigma_d$, where σ_d is the pressure-recovery factor in the diffuser when there is a supersonic region after the throat, and σ_{max} is the pressure-recovery factor when there is no such region, and all other conditions are equal.[1)] It is obvious that the greater Δ_{st}, the greater will be the stability margin for the diffuser. As a rule, at the design point Δ_{st} = 8 to 10 %.

However, this cannot always prevent surging in supersonic diffusers of turbojet engines, because of the broad range over which operating conditions change in flight. This is why it is usually necessary to use special antisurging devices in these diffusers, one of which is the discharge for some of the air from the diffuser duct into the atmosphere through a duct located between the supersonic region and the turbojet engine compressor inlet. This prevents the pressure at the diffuser outlet from building up high enough to destroy the protective supersonic region in the diffuser duct and cause surging, regardless of operating conditions.

5. The Supersonic Diffuser Characteristic Curves And Regulation Concept

The dependencies of the stagnation pressure recovery factor, σ_d, and the discharge coefficients φ_d and X_d on the backpressure (resistance) at the outlet of a supersonic diffuser for a constant flight Mach number, M_H, are called the throttling characteristic curves. These curves are constructed from experimental data obtained with the diffuser in a supersonic wind tunnel and with different settings of the throttling device installed after the diffuser outlet section.

The throttling curves can be constructed as functions of any parameter that is uniquely associated with the magnitude of the resistance at the diffuser outlet for a constant flight Mach number, M_H, value.

The throttling curves for a supersonic diffuser can be constructed using the following relationships.

[1)] The "stability margin" for a supersonic diffuser is also often described by the relationship $\Delta_{st} = (\sigma_d/\varphi_d)_{bound}/\sigma_d/\varphi_d$, where $(\sigma_d/\varphi_d)_{bound}$ is the ratio between the coefficients σ_d and φ_d at the diffuser surge boundary (see fig. 44).

From the relationships cited above, the weight flow of air through the diffuser equals $G_a = \varphi_d \rho_H V F_{in} = \varphi_d \rho_{in} V \frac{p_H}{RT_H}$,

but since $V = M_H \sqrt{kgRT}$ and for air $\sqrt{\frac{kg}{R}} = 0{,}685$, то

$$G_a = 0{,}685 \varphi_d F_{in} M_H \frac{p_H}{\sqrt{T_H}}.$$

Now, after dividing both sides of this equality by the ram pressure in the diffuser outlet section, $p_d^* = \sigma_d p_H^*$, and multiplying by $\sqrt{T_H^*}$, we obtain

$$\frac{G_a \sqrt{T_H}}{p_d^*} = 0{,}685 \cdot \frac{\varphi_d}{\sigma_d} \cdot F_{in} M_H \cdot \frac{p_H}{p_H^*} \sqrt{\frac{T_H}{T_H^*}}.$$

On the basis of the formulas at (1.28) and (1.29), and after a simple transformation, we can substitute

$$\frac{p_H}{p_H^*} \sqrt{\frac{T_H}{T_H^*}} = \frac{1}{(1 + 0{,}2M_H^2)^3}.$$

Finally, we can write

$$\frac{G_a \sqrt{T_H}}{p_d^*} = \frac{\varphi_d}{\sigma_d} \cdot \frac{0{,}685 F_{in} M_H}{(1 + 0{,}2M_H^2)^3}. \qquad (4.8)$$

The left side of this relationship is called the air weight flow parameter for the diffuser outlet section. As the resistance at the outlet of a fixed-area diffuser increases (with an increase in the air throttling ratio), the pressure p_d^* and (p_d) increases, when M_H = const, and the air flow, G_a, remains unchanged, as was explained above, until the deflected forward shock develops. Any subsequent increase in p_d^* is accompanied by a decrease in φ_d and by a corresponding decrease in air flow G_a. Accordingly, with M_H = const, any increase in diffuser outlet resistance, that is, any increase in p_d^*, will result in a reduction in $\frac{G_a \sqrt{T_H}}{p_d^*}$. So it is possible to construct the throttling curves for the diffuser in the form of the dependencies of φ_d and σ_d on the flow parameter for any given flight Mach number, M_H. For this purpose, a series of values for G_a, p_d^*, T_H^*, and σ_d are found experimentally for each given Mach number, and the corresponding magnitudes of φ_d are computed through the expression at (4.8). The shapes of these throttling curves, constructed for a supersonic, fixed-area diffuser for four different flight Mach numbers, M_H, are shown in figure 44. The shading indicates the diffuser surge boundary. The operating points of the diffuser with deflected forward shock are located in the region between the surge boundaries and the dotted curves plotted in the field of the characteristic curves. The closer these points are to the surge boundary, the more intensive they will be. It is readily seen that the nature of the change in φ_d and σ_d in figure 44 corresponds completely to the special operating features of the fixed-area diffuser with changing backpressure at its outlet when M_H = const discussed in the preceding paragraph.

The throttling curves for the diffuser make it possible to establish its points (that is, σ_d, φ_d, and X_d) for any operating conditions for the turbojet engine for which the diffuser is intended. Needed for this purpose in addition to the flight Mach number, M_H, is the air flow parameter at the turbojet engine compressor inlet, that is, $\frac{q_a\sqrt{T_H}}{p_H^*}$ (where p_a^* is the ram pressure at the compressor inlet), and the pitot loss factor, σ_k, in the duct between the diffuser outlet and the compressor inlet. Since $p_a^* = \sigma_k p_d^*$, it is obvious that $\frac{q_a\sqrt{T_H}}{p_d^*} = \frac{\sigma_k q_a\sqrt{T_H}}{p_a^*}$

The throttling curves for fixed-area, supersonic diffusers are very often constructed in the form of the dependencies of σ_d on φ_d, as shown in figure 44 b. These dependencies are obtained by the simple reconstruction of the curves shown in figure 44a, or directly, through the relationship at (4.8).

The dependencies of the coefficients φ_d and σ_d, as well as of X_d, on the flight Mach number, M_H, are called the Mach curves, or the diffuser velocity curves. These curves have been constructed as dotted curves in figure 45 for a fixed-area, supersonic diffuser in which the designed shock wave formation as well as the optimum throat area correspond to a design Mach number, $M_{H\,des.d} = 3$. As will be seen, in this case the discharge capacity of the diffuser, φ_d, drops off radically with a decrease in the Mach number, M_H, but its external drag, X_d, increases sharply. This is the result of the destruction of the designed shock wave formation by the deflected forward shock that develops because when $M_H < M_{H\,des.d}$, the throat area becomes too small, less than optimum, as was explained earlier. If the throat area in this same diffuser is increased to the optimum for $M_H = 2$ (that is, made oversized for $M_H = 3$), there will be some loss in σ_d, but overall the curves can flow more favorably than in the preceding case, as is shown by the solid lines in figure 45.

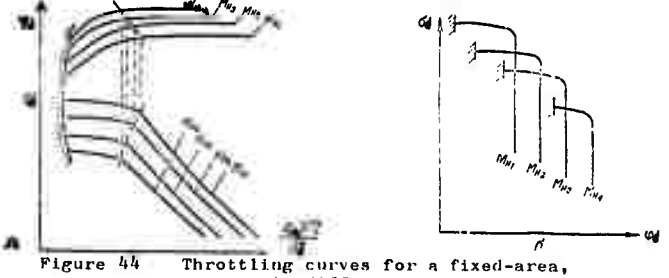

Figure 44 Throttling curves for a fixed-area, supersonic diffuser.

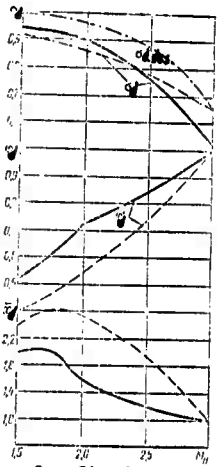

Figure 45 Velocity curves for fixed-area, supersonic diffuser.

In the general case, the turbojet engine in a supersonic aircraft should operate over a wide range of flight Mach numbers, M_H, and under greatly variable engine operating conditions (rpm). Therefore, because of its off-design points and characteristic curves the supersonic diffuser in this turbojet engine should be made adjustable. Otherwise the reduction in φ_d and σ_d, and the increase in external diffuser drag, that accompany appreciable deviations from the design point will cause very significant losses in effective thrust and engine efficiency, as well as the danger of diffuser surging and its unacceptable consequences.

What follows from the foregoing is that regulation of supersonic inlet diffusers can be accomplished by:

longitudinal displacement of the central cone to prevent the falling away of the external oblique shock waves from the leading edge of the cowling (the cone is displaced backward with increase in the flight Mach number, M_H);

changing the throat area; for example, by increasing it with decrease in the flight Mach number, M_H, in order to prevent the development of the deflected forward shock; the throat area can be changed, by displacing the central cone, for example;

feeding additional external air into the duct, bypassing the throat as shown in figure 46, in order to increase the capacity of the diffuser and reduce losses in it when $M_H < 1$, and during take-off;

discharging some of the air to the outside from beyond the throat in order to prevent diffuser surging, as was explained above.

Figure 46 Diagram of the regulation of a supersonic diffuser by delivering additional air, when $M_H < 1$

There are other ways to regulate supersonic diffusers, including changing the angles of the wedges forming the duct, changing the cowling angles, etc.

CHAPTER 5

AVIATION COMPRESSORS

1. Principles of Compressor Arrangement and Operation

The purpose of the compressor is to compress air, and this is necessary to obtain better conversion of the heat added to the air in the combustion chamber into useful work.

Multistage, axial-flow compressors are used in the main in turbojet engines. Radial-flow compressors are used in certain cases.

Diagrammatic layouts of the multistage, axial-flow compressor, and of one of its stages, are shown in figures 47 and 48.

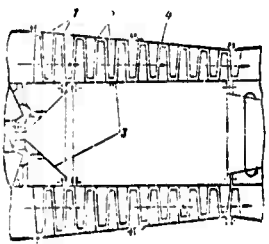

Figure 47: Layout of an axial-flow, multistage compressor:
1 - rotor blades; 2 - straightener blades;
3 - drum; 4 - compressor casing.

The multistage, axial-flow compressor consists of several rows of shaped, moving (rotor) and stationary (straightener) blades in an alternating sequence in the axial direction and distributed around the periphery. The rotor blades, 1, are secured to the outer surfaces of individual wheels mounted on a common shaft, or to a surface formed by a drum, 3, common to all blades (fig. 47). The ends of the straightener blades, 2, are clamped in outer and inner rings. The outer ring in turn is secured in place inside the stationary compressor casing, 4.

Each row of rotor blades, together with its supporting element(wheel, drum section) is called a rotor wheel. The entire rotating part of the compressor is called the rotor. Each row of stationary blades is called a straightener rig. The entire stationary part of the compressor is called the stator.

The grouping made of the rotor wheel and the straightener rig after it (in the direction of air flow) is called the compressor stage.

When the compressor rotor rotates, the blades act on the air like propeller blades, twisting it and forcing it to move in an axial direction toward the compressor outlet (toward the combustion

chamber). This results in a drop in pressure at the compressor inlet, providing a constant inflow of air from the surrounding medium. The convex sides of the rotor blades face in a direction opposite to that of rotor rotation. Therefore, the flow in the channels between the rotor blades is in the direction of rotation but the moment of the aerodynamic forces acting on the rotor blades is correspondingly opposite to rotor rotation. This requires the expenditure of mechanical energy to rotate the rotor, and this energy is then transferred by the rotor blades to the air flowing between them.

As a result of the input of external energy into the rotor wheel, static pressure, p, and absolute air velocity, c, increase simultaneously (fig. 48).

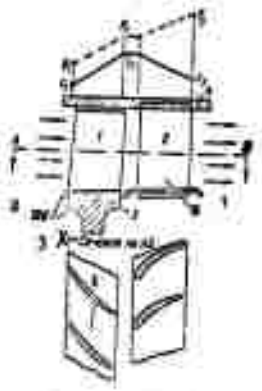

Figure 48: Schematic diagram of a stage in an axial-flow compressor (position as in fig. 47)

Legends:
1 - SR - straightener rig
2 - RW - rotor wheel
3 - X - section through AB;

The air velocity acquired in the wheel is converted into pressure in the stationary straightener rig installed after the rotor wheel (as a result of the diffusive shape of the channels between the blades) without external energy input, resulting in an additional increase in air pressure, and a corresponding reduction in air velocity (fig. 48). In addition, the straightener rig turns the flow against rotor rotation, providing it with the direction required for entering the next compressor stage. The air is given an axial direction in the last (output) straightener rig, for which purpose it is often necessary to use several

successive straightener rigs after the last rotor wheel (losses would increase considerably if only one were used).

In the axial-flow compressor the air moves approximately along cylindrical surfaces, the axes of which coincide with the axis of rotor rotation, which also explains the name of the compressor.

The flow areas of the successive stages in the axial-flow compressor are made successively smaller, since the air is compressed as it moves through the compressor, and its density increases. The axial velocity of the air usually remains constant in all stages, or decreases slightly at the compressor outlet. This is done so the blades in the last stages will not be too short and cause an increase in losses.

The reduction in the flow area of the flow section of a compressor is accomplished by reducing the outside diameter of the rotor, keeping the drum diameter constant, or by increasing the diameter of the drum (of the wheels)while keeping the outside diameter of the rotor constant, or, finally, by increasing both rotor and drum diameter. The first solution simplifies rotor blade installation and securing, and the important thing, reduces the danger of obtaining too short blades in the last compressor stages. In the second and third solutions the blades in the succeeding stages function at higher average circumferential velocities than do the blades in the preceding stages. This makes it possible to increase the compression ratio in the compressor for the same number of stages. An increase in the circumferential velocity in succeeding stages is permissible because the temperature, and consequently the speed of sound as well, is higher at the inlet to these stages than it is at the inlet to the first stage.

The higher circumferential velocities of the blades in succeeding stages as compared with the velocities of the blades in the first stages, are readily provided for by using dual-rotor or compound compressors (fig. 19), in which the second rotor runs at higher rpm than the first rotor. These compressors have other advantages, and this will be discussed later on.

The increase in pressure provided by one stage in an axial-flow compressor is small, so these compressors are always made multi-stage. Axial-flow compressors used in existing aviation gas turbine engines have from 6 to 17 stages.

The diagrammatic layout of the centrifugal compressor is shown in figure 49.

The centrifugal compressor includes the inlet duct 5, the impeller wheel, 1, with vanes 2, the diffuser 3, and the outlet ducts 4.

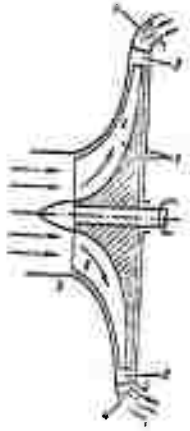

Figure 49: Layout of a centrifugal compressor:
1 - impeller heel; 2 - impeller vane; 3 - diffuser;
4 - outlet ducts; 5 - inlet duct.

The main part of the centrifugal compressor is the impeller wheel, or impeller, which is a wheel with a row of straight (radial) vanes, 2. The wall of the impeller wheel and the vanes form channels through which air flows. The impeller wheel is fitted on a shaft and is surrounded by a fixed cover, to which intake duct 5 is connected.

The diffuser, 3, is a flat or conical, annular expanse formed by the walls of the fixed cover and located concentrically around the impeller wheel. The flow area of this expanse increases in the direction of flow of the air leaving the impeller wheel. In many designs, the diffuser has fixed vanes in separate, curved channels. These diffusers are called vaned diffusers. A vaned diffuser is always preceded by an annular slot with no vanes.

The outlet ducts, through which the compressed air is directed into the combustion chambers, are located after the diffuser.

The centrifugal compressors for turbojet engines with high air consumption are usually of the double-entry type.

The use of double-entry compressors makes it possible to reduce the inlet diameter and, correspondingly, the outside diameter, and thus reduce the diametral size of the compressor as a whole, without increasing the air velocity at the impeller wheel inlet.

When the compressor impeller rotates the air between the impeller vanes is also rotated relative to the impeller axis, and moves to the periphery (to the diffuser) under the effect of centrifugal forces. As a result, a vacuum is created at the impeller inlet, providing for an inflow of external air into the compressor through the inlet duct.

External mechanical work is transferred to the air by the impeller vanes, causing the pressure and velocity of the air flowing through the channels between the impeller vanes in the compressor to increase. A good part of the kinetic energy acquired by the air in the impeller is converted into potential energy in the diffuser, where the air pressure continues to rise as a result of the corresponding reduction in its velocity.

In this type of compressor, the air is compressed and moved by centrifugal forces, and it is this feature which gives the compressor its name of centrifugal compressor.

2. Air Compression in a Compressor

The most important magnitude establishing the efficiency and specific thrust (power) of an engine is the air compression ratio in the compressor.

As has already been noted, the air compression ratio in the compressor π_c^* equals the ratio of the total pressure at the compressor outlet p_c^* to the total pressure at the compressor inlet p_a^*

$$\pi_c^* = p_c^*/p_a^* = p_c^*/\sigma_{in}p_o^* \tag{5.1}$$

and when the airspeed is V = 0

$$\pi_{c_o}^* = p_c^*/\sigma_{in}p_o .$$

If we assume for simplicity that no heat exchange with the environment takes place in the compressor ($Q_{en} = 0$), and that there are no hydraulic losses ($L_{hyd} = 0$), the compressor will be called an ideal non-cooled compressor. The energy equation at (1.7) can be written as follows for this type of compressor:

$$L_{ad_c}^* = c_p/A\,(T_{c_{ad}} - T_a) + c_c^2 - c_a^2/2g \tag{5.2}$$

where $T_{c\,ad}$ is the temperature at the outlet of the compressor under consideration.

The work, $L_{ad\,c}^*$, required for adiabatic compression and changing the kinetic energy of the air in the ideal non-cooled compressor is called the adiabatic head for the compressor.

If we introduce the parameters of the stagnated flow, it is obvious that the equation at (5.2) can be rewritten as

$$L_{ad_c}^* = c_p/A\,(T_{c_{ad}}^* - T_a^*) \tag{5.2,a}$$

Since $T_a^* = T_o^*$, and $C_p/A = kR/k\text{-}1$, and since, in addition, because of the adiabatic equation

$$T_{c_{ad}}/T_a^* = \left(\frac{p_c^*}{p_a^*}\right)^{\frac{k-1}{k}} = (\pi_c^*)^{\frac{k-1}{k}},$$

we finally obtain

$$L_{ad_c}^* = \frac{k}{k-1} \cdot RT_o^* \left(\pi_c^{*\frac{k-1}{k}} - 1\right). \tag{5.3}$$

From whence, substituting k/k-1·R = 102.5 and k/k-1 = 3.5 , we obtain

$$\pi_c^* = (1 + L^*_{ad_c}/102.5\ T_o^*)^{3.5}. \qquad (5.4)$$

Consequently, π_c^* not only depends on the magnitude of the adiabatic head, but also on T_o^*, that is, on the airspeed and altitude (and on the outside air temperature T_o). Therefore, when we assign a magnitude to the compressor's compression ratio, we must also indicate the conditions under which it applies. As a rule, π_c^* is given for standard air temperature on the ground, $T_o = 228^\circ K$ ($t_o = +15^\circ C$) and for airspeed of $V = 0$ ($M_o = 0$). A single-stage centrifugal compressor provides a $\pi^*_{c\,o}$ of 4.5 to 4.8, and one stage (subsonic, see below) of an axial-flow compressor can provide a $\pi^*_{c\,st}$ of 1.25 to 1.35. This latter also serves to explain the necessity of using multi-stage axial-flow compressors mentioned above.

The pv-diagram (fig. 50) can be used to measure the adiabatic head, as well as the total work of adiabatic air compression in the compressor, by measuring the area contained within the lines for the compression process and the pressure axis. Consequently, if ac_{ad} is the adiabatic compression from pressure p_a^* to a pressure p_c^*, the adiabatic head, $L^*_{ad\,c}$, will be represented by the area $Obc_{ad}a$.

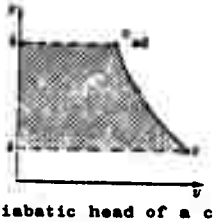

Figure 50: Adiabatic head of a compressor in the pv-diagram.

In the TS-diagram (fig. 51) the compression adiabat is represented by the segment ac_{ad}, parallel to the temperature axis, and limited by the isobars corresponding to the initial pressure p_a^* and the terminal pressure p_c^* of compression in the compressor. The adiabatic head (its thermal equivalent)can be represented in this same diagram. Actually, as will be seen from the equation at (5.2,a), the adiabatic head (in thermal units) equals the heat of the isobaric process taking place in the temperature interval from T_a^* to $T^*_{c\,ad}$. At the same time, it is obvious that in this case the isobaric process can be represented by the curve cc_{ad} (fig. 51), and the heat of this process by the area $Oc_{ad}b$. Consequently, the adiabatic head will be represented by the area $Occ_{ad}b$ in the TS-diagram.

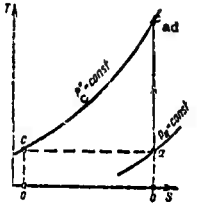

Figure 51: Adiabatic head in the TS-diagram.

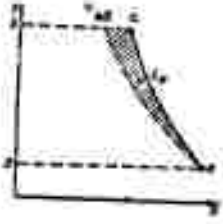

Figure 52: pv-diagram for air compression in a compressor.

A real compressor, and particularly an uncooled one, differs from the ideal compressor by the hydraulic resistances ($L_{hyd} \neq 0$). Moreover, in the real compressor some heat is transferred from the compressed air to the environment through the walls of the compressor housing because the temperature of the air in the compressor is higher than the outside temperature. However, the amount is relatively small, and can be disregarded in the compressor calculation without incurring any appreciable error, assuming that $Q_0 = 0$.

The external work that must be added to 1 kg of air to compress it in a real compressor, or the so-called internal work done by the compressor* can be determined through an equation similar to that at (5.2,a) after substituting the real temperature at the end of compression T_c^* (at the outlet of the real compressor) for the adiabatic temperature $T_{ad\ c}^*$.

$$L_c = \frac{k}{k-1} \cdot R(T_c^* - T_0^*). \tag{5.5}$$

The work done by the hydraulic resistances, L_r, is converted into heat $AL_{hyd} = Q_{hyd}$, and absorbed by the compressed air, so that the compression process in a real, uncooled compressor takes place along a polytrope with an exponent n larger than the exponent, k, of the adiabat, and therefore

$$L_c = \frac{k}{k-1} \cdot RT_0^* \left(\pi_c^{*\frac{n-1}{n}} - 1 \right). \tag{5.6}$$

On the other hand, the internal work done by the compressor expended on polytropic air compression and in overcoming the hydraulic resistances, so can also be determined through the Bernoulli equation at (1.16), which can be written in the following form

$$L_{i\ c} = L_{p\ c} + L_r \tag{5.7}$$

where L_r is the work done by the hydraulic resistances;

*This work is sometimes called the theoretical head for the compressor.

$L_{p\ c}$ is the total work done by the polytropic compression (polytropic head) from the initial pressure p_a^* to full pressure p_c^* at the compressor outlet.

The value of n, the polytrope exponent, for centrifugal compressor used in aviation gas turbine engines operating under designed operating conditions, ranges approximately from 1.52 to 1.62, and for axial-flow compressors ranges from 1.46 to 1.52.

For a given compression ratio, and the same initial conditions, the total work of polytropic air compression $L_{p\ c}$ (the polytropic head) is greater than the adiabatic head, $L^*_{ad\ c}$, by some magnitude L_v, because in the real compressor the air is heated by heat equivalent to the work done by the hydraulic resistances, L_r (the compression polytrope with exponent n > k is located above the adiabat)

$$L_{p\ c} = L^*_{ad\ c} + L_v \ . \qquad (5.8)$$

The air compression process in a real compressor is represented in the pv-diagram in figure 52, where ac is the compression politrope with n > c, and ac_{ad} is the adiabat of compression to the same pressure, p_c^*. In this diagram the total politropic compression work, $L_{p\ c}$ is represented by the area ObSa, the adiabatic head, $L^*_{ad\ c}$, by the area $Obc_{ad}a$, and the additional work, L_v, by the area $ac_{ad}c$. This additional work is a secondary result of the effect of the hydraulic resistances occasioned by heating and the resultant increase in volume. The increase in air compression work it is not solely additional work. Most of the additional work added to the air in the real compressor, that is, the work of the hydraulic resistances, L_r, is not represented in the pv-diagram, since it is not a function of change in air state.

In the TS-diagram (fig. 53) the polytropic compression process with index n > c is represented by the curve ac which slopes to the right of the adiabat, ac_{ad}. The area below the ac curve is the heat added to the air during polytropic compression. In this case this heat is equivalent to the work of the hydraulic resistances. Therefore, the work of the resistances, L_r (in thermal units AL_r) is represented in the TS-diagram by the area bacd. Area $Occ_{ad}b$ in turn represents the adiabatic head, $L^*_{ad\ c}$, and the area $ac_{ad}c$ represents the additional compression work, as is obvious from a comparison of the pv- and TS-diagrams.

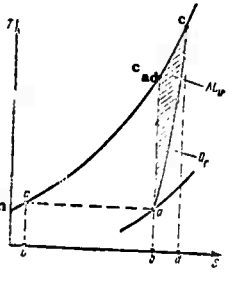

Figure 53: The air compression process in a TS-diagram.

Based on the equations at (5.7) and (5.8), the internal work done by a real compressor can be represented in the form of the sum

$$L_{i\,c} = L^{*}_{ad\,c} + L_{v} + L_{r} \qquad (5.9)$$

so will be represented in the TS-diagram by the sum of the areas listed above, that is, by the area occd.

Thus, the internal work done by a real compressor, as well as all components of this work, can be represented very clearly in the TS-diagram.

Let us now consider some special features of air compression in the multistage compressor.

The process of changing the air state during air compression in a multistage compressor is shown in the pv-diagram in figure 54. Air compression in the ideal compressor will take place along the adiabat ac_{ad}, and the compression adiabats in the individual stages, a1", 1"2", and $2"c'_{ad}$ coincide with it.

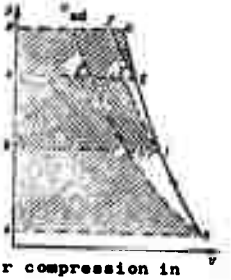

Figure 54: Diagram of air compression in a multistage compressor.

The adiabatic head of the compressor as a whole is represented by the area $Odc_{ad}a$, and the adiabatic heads of the individual stages of the ideal compressor are represented by the areas Ob1"a, bc2"1", and $cdc_{ad}2"$, respectively.

In the real multistage compressor the compression process will take place along the adiabat with index n, which in general, will be different for the different stages. In the special case when n is identical for all stages the compression polytropes for the compressor as a whole, as well as for its individual stages, will be common (will coincide).

Figure 54 shows the compression polytrope for a multistage compressor as the curve ac. Sections a1, 12, and 2c of this curve are the compression polytropes for the individual compressor stages.

The actual air state at the outlet of the first stage is established at point 1, at the outlet of the second stage at point 2, etc. Accordingly, the compression adiabats for the individual stages will be the curves a1", 12", 23', etc. (these adiabats must be developed from the points establishing the actual air state at the inlet to the stage in question).

The total polytropic compression work done by the individual stages is described by the areas Obla, bc21, cdc2, while the total polytropic work done by the compressor as a whole is area Odca, equal to the sum (designated by Σ), of the polytropic work done by the individual stages

$$L_{p_c} = \Sigma L_{p_{st}}.$$

The adiabatic heads, $L^*_{ad\ st}$, in the individual stages of the real compressor, are areas Obl"a, bc2'1, and cdJ'2. It is readily seen that the sum of these areas is greater than area $Odc_{ad}a$; so, the adiabatic head for the compressor as a unit is less than the sum of the adiabatic heads in the individual stages

$$L^*_{ad_c} < \Sigma L^*_{ad_{st}}.$$

This difference is explained by the fact that the actual temperature at the outlet of each preceding stage is higher than the temperature at the end of the adiabatic compression in that stage up to the same pressure. In other words, the discrepancy between $L^*_{ad\ c}$ and $\Sigma L^*_{ad\ st}$ is explained by the greater heating of the air in each stage than would be encountered in the ideal compressor.

It is obvious that the discrepancy between $L^*_{ad\ c}$ and the sum $\Sigma L^*_{ad\ st}$ will increase with an increase in the number of stages, as well as with an increase in the hydraulic resistance in each stage.

The internal work, $L_{i\ c}$, done by the multistage compressor as a unit can, naturally be fixed as the sum of the internal work done by the individual stages

$$L_{i_c} = \Sigma L_{i_{st}}.$$

However, the compression ratio in a multistage compressor depends on the magnitudes of the compression ratios in each stage, and is equal to their product.

3. Compressor Efficiency and Rating

As a rule, the efficiency of the real compressor is arrived at by comparing it with the ideal compressor.

The measure of comparison used for uncooled compressors in particular, and the compressors used in aviation gas turbine engines are of this category, is the ideal uncooled compressor in which the internal work done is equal to its adiabatic head, and is the minimum required to compress the air to a given pressure in an uncooled compressor.

The ratio of the adiabatic head, $L^*_{ad\ c}$, corresponding to air compression to a given pressure, to the internal work, $L_{i\ c}$, (exclusive of mechanical losses) actually done in the compressor to compress the air to that same pressure, is called the compressor adiabatic efficiency

$$\eta_{ad\ c} = L^*_{ad\ c}/L_{i\ c}. \qquad (5.10)$$

Since, according to the preceding equation,

$$L^*_{ad\ c} = L_{i\ c} - (L_r + L_v),$$

then

$$\eta_{ad\ c} = 1 - L_r + L_v/L_{i\ c} \qquad (5.11)$$

The adiabatic efficiency only takes into consideration those energy losses (work done) associated with the presence of hydraulic resistances. The greater these resistances, the lower the adiabatic efficiency. However, the magnitude of the work done by the hydraulic resistances in a compressor cannot be established directly by the adiabatic efficiency. For example, if $\eta_{ad\ c} = 0.8$, 20 % of the work done, $L_{i\ c}$, is lost (as compared to the ideal compressor) simply because of the presence of the hydraulic resistances. But, as will be seen from the equation at (5.11), the work, L_r, done to properly overcome the hydraulic resistances is less than 20 % of work $L_{i\ c}$. The magnitude of the hydraulic resistances in a compressor can only be determined indirectly from the value of $\eta_{ad\ c}$.

After substituting the expression for work $L_{i\ c}$ in the equation at (5.5) in equation (5.10), we obtain

$$\eta_{ad\ c} = L^*_{ad\ c}/102.5(T^*_c - T^*_a). \qquad (5.12)$$

From whence we find the actual increase in the temperature in the compressor

$$\Delta t_c = T^*_c - T^*_a = L^*_{ad\ c}/102.5\ \eta_{ad\ c} \qquad (5.13)$$

The adiabatic efficiency of a multistage compressor is less than the adiabatic efficiency of its individual stages. The following discussion will be the basis for the statement.

Let us assume, for simplicity's sake that the adiabatic efficiencies and heads for all compressor stages are identical. This being so, the internal work done in each stage will be the same and if z is the number of stages

$$\Sigma L^*_{ad\ st} = zL^*_{ad\ st}$$

$$\Sigma L_{i\ st} = zL_{i\ st} = L_{i\ c}.$$

Hence, we can write the following for the adiabatic efficiency of a stage

$$\eta_{ad\ st} = L^*_{ad\ st}/L_{i\ st} = \Sigma L^*_{ad\ st}/L_{i\ c},$$

that is, the adiabatic efficiency of a stage will be equal to the ratio of the sum of the adiabatic heads for all stages to the internal work done by the compressor as a unit. At the same time, the adiabatic efficiency of the compressor is $\eta_{ad\ c} = L^*_{ad\ c}/L_{ic}$.

But it was shown above that $L^*_{ad\ c} < \Sigma L^*_{ad\ st}$, so $\eta_{ad\ c} < \eta_{ad\ st}$, and this discrepancy increases with increase in the number of stages.

The magnitude of compressor adiabatic efficiency for present day aviation gas turbine engines is (at the design point):

$\eta_{ad\ c}$ = 0.84 to 0.88 for axial-flow, multistage compressors;

$\eta_{ad\ c}$ = 0.86 to 0.90 for individual stages in axial-flow compressors;

$\eta_{ad\ c}$ = 0.72 to 0.78 for centrifugal (single-stage) compressors.

The polytropic efficiency too is often used to assess compressor efficiency.

Compressor polytropic efficiency is defined as the ratio of the total polytropic work, $L_{p\ c}$, required to compress the air to pressure p^*_c, to the internal work done by the compressor, $L_{i\ c}$, to compress the air to that same pressure

$$\eta_p = L_{p\ c}/L_{i\ c} \tag{5.14}$$

According to the equation at (5.7),

$$L_{p\ c} = L_{i\ c} - L_r$$

so

$$\eta_p = 1 - L_r/L_{i\ c} \tag{5.15}$$

from whence

$$L_r = (1 - \eta_p)\, L_{i\ c}.$$

So we see that the convenience of using the polytropic efficiency resides in the possibility of making a direct determination of the hydraulical losses in the compressor and, consequently, of the index of the compression polytrope as well.

It is readily seen that the polytropic efficiency is always greater than the adiabatic efficiency, because $L_{p\ c} > L^*_{ad\ c}$.

For modern axial-flow compressors, η_p = 0.86 to 0.90 (in individual cases as high as 0.92), and for centrifugal compressors η_p = 0.76 to 0.80.

The work, $L_{i\ c}$, added to the air in the compressor is always slightly less than the work done in driving the compressor because the compressor has mechanical losses associated with friction in its bearings and in the transmission (if any). These losses are taken into consideration in the compressor mechanical efficiency, established through the relationship

$$\eta_{m\ c} = L_{i\ c}/L_c \tag{5.16}$$

where L_c is the effective work done by the compressor, that is, the work done in driving the compressor, and including mechanical losses equated to 1 kg of compressed air.

For modern centrifugal and axial-flow compressors, $\eta_{m\ c}$ = 0.98 to 0.99. High $\eta_{m\ c}$ is explained by the fact that aviation gas

turbine engine compressor shafts are mounted in anti-friction bearings, and the compressor rotors are usually driven directly off the turbine shaft, without intermediate transmissions.

All energy losses in the compressor, mechanical, as well as those associated with the hydraulic resistances, are taken into consideration in the overall, or effective efficiency of a compressor, η_c. This efficiency is equal to the ratio of the adiabatic head to all the work done by the compressor, that is, to the effective work done by the compressor

$$\eta_c = L^*_{ad\ c}/L_c \tag{5.17}$$

or

$$\eta_c = \eta_{ad\ c}\eta_{m\ c}. \tag{5.18}$$

Knowing the magnitude of the effective efficiency, it is possible to find the required compressor rating for a given air flow and a known magnitude of adiabatic head.

Since the work done per second to drive the compressor can be established by multiplying the weight flow per second of air, G_a, through the compressor by work L_c, the rating, N_c, required for the compressor will be

$$N_c = G_a L_c/75 = G_a L^*_{ad\ c}/75\eta_{ad\ c}\eta_{m\ c} \tag{5.19}$$

Compressors in modern turbojet engines have extremely high ratings, from approximately 10,000 to 15,000, to as high as 40,000 to 45,000, hp, and higher.

4. Fundamentals of Axial-Flow Compressor Theory

Velocity Plan and Internal Work Done by a Stage

A schematic diagram of an axial-flow compressor is shown in figure 55. The principal compressor dimensions are:

D_w is the outside diameter of the rotor wheel;

D_{hub} is the hub diameter;

$\xi_{hub}=D_{hub}/D_w$ is the relative hub diameter;

$D_{mean}=D_w+D_{hub}/2$ is the mean diameter of the rotor wheel;

h is the blade height.

If the blades of an axial-flow compressor are made to intersect a cylindrical surface at some diameter D concentric to the compressor axis, and if the intersection surface is developed on the plane of a drawing the development will provide so-called cascades of rotor wheels and pre-rotation vanes (fig. 56), and the cascades of rotor wheels appear to us as moving at velocity u, equal to the circumferential velocity of the rotor wheel at given diameter D.

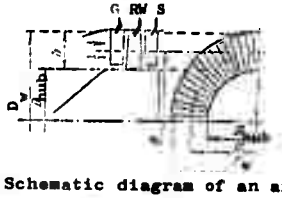

Figure 55: Schematic diagram of an axial-flow compressor.

A cascase is defined as a series of identical aerodynamic profiles arranged on some surface equidestant from each other. If the profiles are arranged parallel to each other on the plane the cascade is called rectilinear. However, if the profiles are arranged on a cylindrical surface, as in an axial-flow compressor for example, the cascade formed by them is called a circular cascade.

The set of rotor wheel cascades and the pre-rotation vanes following them are called an elementary stage.

The principal geometric and aerodynamic parameters of a cascade are (fig. 57):

$t = \pi D/z$	is the cascade pitch for a given diameter, D, and number of blades, z;
b	is the profile chord;
b/t	is the cascade solidity;
β_1' and β_2'	are the angles at which the profiles are installed at inlet and outlet, respectively;
β_1 and β_2	are the air flow inlet and outlet angles;
$i = \beta_1' - \beta_2'$	is the incidence for the profile;
$\theta = \beta_2' - \beta_1'$	is the blade-camber angle;
c	is the maximum profile thickness.

The principal cascade parameters in an axial-flow compressor generally change in a radial direction, that is, with the height of the blades. Consequently, an axial compressor stage (a complete stage) is a set of individual, elementary stages.

Let us consider the air movement through an elementary stage in an axial-flow compressor (fig. 56). Air moving at velocity c_a approaches the guide vane (G) located in front of the first stage rotor wheel, moving axially.

The air at the guide vane outlet will not only be moving axially, but circumferentially as well. In other words, the guide vanes impart an entry spin to the air, the magnitude of which is determined by the circumferential component, c_{1u}, of the absolute velocity, c_1, at the guide vane outlet.

The entry spin in the guide vane can be imparted in the direction the rotor wheel is moving (in the direction of rotation, $+c_{1u}$), as well as against that direction (against the direction of rotation, $-c_{1u}$). Both types of entry spin are found in existing axial-flow compressors, as is a purely axial entry of air (in which case there are no guide vanes).

Thus, the air approaches the rotor blades with absolute velocity c_1, and at some angle relative to the compressor axis in the general case.

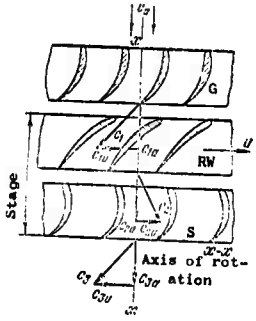

Figure 56: Schematic diagram of the vane cascades in an axial-flow compressor.

The air, while in the rotor, is exposed to the effect of the moment of the external forces caused by the action of the rotor blades on the flowing air, so that its angular momentum relative to the axis of rotation of the rotor (of the compressor rotor) is increased; that is, the air is whirled in the direction of rotor rotation. The air leaves the rotor with absolute velocity c_2, the circumferential component of which, c_{2u}, usually coincides with the direction of rotation of the rotor.

The air enters the straightener(s) beyond the rotor wheel with velocity c_2, and leaves it with velocity c_3. If velocity c_3 is less than velocity c_2, the air pressure in the straightener is increased (due to the conversion of kinetic energy into potential energy), and the straightener functions in this respect like a diffuser. However, if velocities c_3 and c_2 are equal in magnitude, the straightener functions like a simple flow deflector and there is no conversion of velocity into pressure.

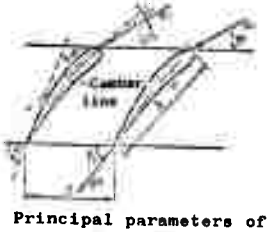

Figure 57: Principal parameters of a cascade.

The axial-flow compressor stage is very often designed so velocities c_3 and c_1 are equal in magnitude and direction. Now there is no change in the kinetic energy of the air in the stage, an the external work input is only used to compress the air and to overcome the hydraulic resistances in the stage.

The magnitude and direction of absolute and relative air velocities in the stage, as well as their circumferential and axial components, are established through velocity triangles. Figure 58 shows the velocity triangles at the inlet to the rotor cascade, and at its outlet when the entry open given the air is in a direction opposite to that of the rotor.

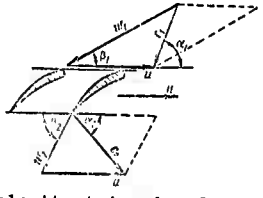

Figure 58: Velocity triangles for a rotor cascade.

It has already been pointed out that the axial velocity of the air flow in a compressor is kept constant, or is slightly reduced, from the first to the last stage. However, even in the latter case, the axial velocity in an individual stage can be taken as constant; $c_{1a} = c_{2a} = c_{3a}$. Moreover, the circumferential blade velocities at the rotor inlet and outlet are equal for a given diameter ($u_1 = u_2$). Therefore, it is convenient to consider the velocity triangles as congruent. Congruent velocity triangles for a rotor, called a velocity plan, are shown in figure 59, where (as in fig. 58):

c_1 and c_2 are the absolute air velocities before and after the rotor;

c_{1u} and c_{2u} are the circumferential components of velocities c_1 and c_2;

$c_a = c_{1a} = c_{2a}$ is the axial component of the absolute air velocity in the compressor;

w_1 and w_2 are the relative air velocities at the rotor inlet and outlet;

w_{1u} and w_{2u} are the circumferential components of velocities w_1 and w_2;

α_1 and α_2 are the angles between the directions of velocities c_1 and c_2, and the direction of the circumferential velocity;

β_1 and β_2 are the angles between the directions of velocities w_1 and w_2, and the direction of the circumferential velocity;

u is the circumferential velocity of the rotor for a given diameter;

$\Delta c_u = c_{2u} - c_{1u}$ is the air spin acquired in the rotor for a change in velocity (with respect to direction) from c_1 to c_2.

What follows from the plan is that

$$c_{2u} = u - w_{2u};$$
$$c_{1u} = w_{1u} - u,$$

from whence, and remembering that the entry open was opposite to the direction of operation, we obtain

$$\Delta c_u = c_{2u} - (-c_{1u}) = w_{1u} - w_{2u}$$

or putting it another way, we can also determine the air spin, Δc_u, in the rotor through the difference in the circumferential components of the relative velocities.

If the axial velocity, c_a, at the rotor inlet, the entry spin, c_{1u}, the circumferential velocity u, and the air spin, Δc_u, in the rotor are known, all the other velocities in the stage, and their directional angles, can be found from the velocity plan.

In order to determine the circumferential velocity, u, and the air spin, c_u, in the rotor, we must know the relationship between these magnitudes and the external work added to 1 kg of air in the rotor, that is, the internal work, $L_{i\ st}$, done in the stage. This relationship can be established on the basis of the equation for angular momentums, which can be written as follows with reference to the axis of rotation of the compressor rotor, and as applicable to 1 kg of air flowing through the rotor blades in a stage with radius r.

$$M_{st} = \frac{rc_{2u} - rc_{1u}}{g}.$$

Now, multiplying the torsional moment M_{st}, by the angular velocity, ω, of rotor rotation, we obtain the sought for internal work done in the stage

$$L_{i\ st} = \omega M_{st} = \frac{r\omega}{g}(c_{2u} - c_{1u}),$$

but $r\omega = u$ and $(c_{2u} - c_{1u}) = \Delta c_u$, so

$$L_{i\ st} = \frac{u\Delta c_u}{g}. \qquad (5.20)$$

From whence it is seen that for a given circumferential velocity u, the air spin, Δc_u, in the rotor and, consequently, the internal work (head, compression ratio) done in the stage as well, will increase with a decrease in the entry spin along the path $(+c_{1u})$. The spin, Δ_{cu}, in the rotor will increase to an even greater degree if, for the same velocity, u, an entry spin in the opposite direction $(-c_{1u})$ is imparted to the air, since in this case $\Delta c_u = c_{2u} - (-c_{1u}) = c_{2u} + c_{1u}$ (fig. 59). At the same time, the relative inlet velocity, w_1, will also increase (for given values of velocities c_a and u).

If there is no entry spin ($c_{1u} = 0$), and if the circumferential component of the absolute outlet velocity is $c_{2u} = u$, $\Delta c_u = u$, and the work done in the stage will be

$$L_{i\ st} = u^2/g. \qquad (5.21)$$

The ratio between the adiabatic head for the stage and this work is usually called the head pressure coefficient (relative head) for an axial-flow compressor stage, and is designated $\bar{H}$

$$\bar{H} = L^*_{ad\ st}/u_2/g \ . \qquad (5.22)$$

Knowing the head pressure $L^*_{ad\ st}$, and given the coefficient $\bar{H}$, we can find the required circumferential velocity for the stage through the formula

$$U = \sqrt{gL^*_{ad\ st}}/\bar{H} \qquad (5.23)$$

Axial-flow compressors used in turbojet engines have $\bar{H}$=0.15 to 0.30, and u = 240 to 300 m/sec, for the mean diameter of the rotor (in individual cases $\bar{H}$ will reach 0.35 to 0.40, and u 350 to 370 m/sec).

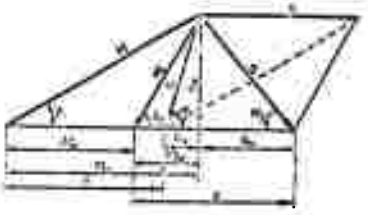

Figure 59: Velocity plan for a rotor cascade.

Compressor Stage Reaction Ratio

The work, $L_{i\ st}$, done in a stage is expended on polytropic air compression, on increasing the air's kinetic energy (if $c_3 > c_1$), and in overcoming resistance in the stage. The same work done in the stage to compress the air and associated with increasing the air pressure can be distributed in different ways between the rotor and the straightener after it (air compression occurs in the latter as a result of the reduction in air velocity).

In order to describe the distribution of all the compression work done in a stage (or the tototal increase in pressure) between the rotor and the straightener, we will introduce the concept of a compressor stage reaction ratio.

The compressor stage reaction ratio p_c is the relationship between the adiabatic work done to compress the air in the rotor, $L_{ad\ wh}$ and the internal work done in the stage $L_{i\ st}$ (the theoretical head) i.e.

$$p_c = g \cdot L_{ad\ wh}/u\Delta c_u . \qquad (5.24)$$

If there are no losses in the rotor ($L_{r\ wh} = 0$) work $L_{i\ st}$ will be expended in the adiabatic compression and in increasing the kinetic energy of the air flowing through the rotor. Therefore, in this case the adiabatic air compression work done in the rotor will be

$$L_{ad\ wh} = \frac{u\Delta c_u}{g} - \frac{c_2^2 - c_1^2}{2g} \ . \qquad (5.25)$$

Let us express velocities c_2 and c_1 in terms of their circumferential and axial components, assuming that the axial components are equal; $c_{1a} = c_{2a}$. Then,

$$c_2^2 - c_1^2 = c_{2u}^2 - c_{1u}^2 = (c_{2u} + c_{1u})(c_{2u} - c_{1u}).$$

Moreover, $c_{2u} - c_{1u} = \Delta c_u$, and $c_{2u} = c_{1u} + \Delta c_u$, so we can write

$$L_{ad\ wh} = \frac{u\Delta c_u}{g} = \frac{\Delta c_u}{g}(\Delta c_u + 2c_{1u}). \tag{5.26}$$

Substituting this dependence in the expression for the reaction ratio (5.24), and reducing, we obtain

$$\rho_c = 1 - \frac{\Delta c_u}{2u} - \frac{c_{1u}}{u}. \tag{5.27}$$

What follows now is that for specified values of rotor circumferential velocity, u, and air spin, Δc_u, in the rotor, the reaction ratio p_c, and consequently the distribution of the total air compression work done in the stage between the rotor and the straightener wall, depend only on the magnitude and direction of the entry spin, c_{1u}, before the rotor.

The less the entry spin in the direction of flow ($+c_{1u}$), or the greater the spin in the opposite direction ($-c_{1u}$), the higher the stage reaction ratio, that is, the greater will be the amount of total compression work done in the rotor, and the smaller will be that done in the straightener.

If the reaction ratio is $p_c = 1$, all air compression (all the pressure increase) takes place in the rotor, and there is no pressure increase in the straightener. Now ($p_c = 1$) through the formula at (5.27) we find

$$c_{1u} = -\frac{\Delta c_u}{2}. \tag{5.28}$$

in other words the entry spin, c_{1u}, given the air should be opposite in direction to rotor rotation.

If the reaction ratio is $p_c = 0$, only the kinetic energy of the air is increased in the rotor, and pressure is not increased (there is no compression). All the air compression, and the corresponding increase in air pressure, takes place in the straightener (because of the reduction in the air velocity that occurs in it).

Now, from the formula at (5.27), we have

$$c_{1u} = u - \frac{\Delta c_u}{2}. \tag{5.29}$$

Since it is usual for $\Delta c_u < u$, the initial air spin in this case should be directed in the direction of rotation of the rotor ($+c_{1u}$).

The two extreme cases considered above ($p_c = 1$ and $p_c = 0$) are never encountered in practise. Existing axial-flow compressors usually have intermediate reaction ratios, and very often $p_c \approx 0.5$, that is the total air compression work is divided evenly between the rotor and straightener.

The preliminary spin providing $p_c = 0.5$ is, according to the formula at (5.27)

$$c_{1u} = -\frac{u - \Delta c_u}{2} \tag{5.30}$$

and should be directed with compressor rotation because $u > \Delta c_u$.

When $p_c = 0.5$, the velocity plan is symmetrical, and the corresponding velocities and flow angles prove to be identical in the rotor and the straightener. Therefore, the rotor and straightener are identically loaded and can have completely identical blade shape and dimensions. In addition, minimum losses (profile losses) are obtained in the rotor and straightener cascades. As a result, $p_c = 0.5$, or a so-called 50% reaction ratio is used in many axial-flow compressors for aviation gas turbine engines.

Concept of the Supersonic Stage in an Axial-Flow Compressor

A reduction in diameter and, consequently, a reduction in the weight, of an axial-flow compressor for a given air flow, that is, an increase in compressor capacity for the air flow through its first stage, is obtained by increasing the axial velocity, c_a, of the air at the compressor inlet.

Another important way to reduce compressor weight is to increase the head pressure developed, or the degree to which the pressure in one stage is increased, and the number of stages associated with this reduction for given π_c^*, which is in turn achieved by increasing the circumferential velocity, u_c, of the compressor rotor, all other conditions being equal.

However, a simultaneous increase in velocities c_a and u_c is extremely limited, because the relative velocity, w_1, of the air washing the blades, which have conventional profiles, rapidly approaches the speed of sound. The result is a sharp increase in losses in the stage, causing an unacceptable reduction in stage efficiency.

In order to achieve a significant increase in the circumferential velocity of the compressor blades, and at the same time ensure high compressor capacity by high values of inlet velocity, c_a, and retain acceptable magnitudes of compressor efficiency while doing so, a transition must be made to so-called supersonic stages.

A supersonic axial-flow compressor stage is defined as a stage in which the relative air velocity at the rotor inlet or at the straightener inlet (or at both at the same time) exceeds the local speed of sound. And the circumferential velocity of the rotor is limited only by structural strength, and can be increased significantly as compared with the permissible velocity for a conventional subsonic stage.

The characteristic difference in the supersonic stage is that shock waves develop in the vane channels of the cascade carrying the supersonic flow. These channels also cause the transition from supersonic air velocity to subsonic air velocity. In addition, in

the supersonic stage the profiles of the blades carrying the supersonic flow should have pointed leading edges, because only in this way can the shock waves be inside the vane channels and can a large area of the profile surface be washed by the subsonic flow. On the other hand, if conventional subsonic profiles with blunt leading edges are used for these blades, a shock wave with a curvilinear front will develop in front of each profile (blade). A zone of subsonic velocity will follow this shock wave. But the velocity will increase again further on in the direction toward the cascade, so that during subsequent washing of the profiles in the cascade (the blades of the rotor or straightener) almost all of their surfaces will be subjected to supersonic velocity. This will result in an unacceptable increase in stage losses.

Generally speaking, an elementary supersonic stage for an axial-flow compressor can be designed in different ways. As an example, let us consider the conventional design employed, wherein the relative supersonic velocity, w_1, at the rotor inlet ($w_1 > a_1$, that is, $M_1 > 1$) is subsequently transformed into a subsonic velocity by one normal shock wave, two oblique shock waves, or one normal and one oblique shock wave. Velocity c_2 at the inlet to the straightener too is subsonic ($c_2 < a_2$). Moreover, let us simplify the example by assuming that the direction of the relative velocity of the air does not change in the rotor ($\beta_1 = \beta_2$).

The profile cascades of the guide, rotor, and straightener in this supersonic stage design are shown in figure 60, and the corresponding velocity triangles in figure 61. In this case the air is given a preliminary counterrotational spin in the guide (G) and approaches the rotor at an absolute subsonic velocity, c. However, relative velocity, w_1, becomes supersonic as a result of the high value of the circumferential velocity, u, and the effect of the direction of the preliminary spin. The transition from a relative supersonic velocity, w_1, to a subsonic velocity, w_2, takes place in the shock waves inside the vane channels of the rotor. The air leaves the latter at an absolute subsonic velocity c_2, which is subsequently reduced to magnitude c_3 in the straightener. Thus of all the velocities only one velocity, w_1, exceeds the local speed of sound. All others are subsonic.

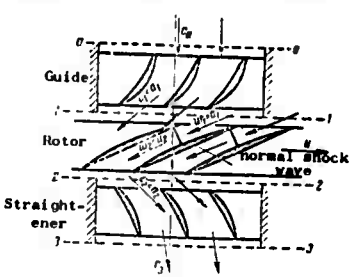

Figure 60: Schematic diagram of a supersonic stage.

Let us note in conclusion that a normal shock wave or a system of oblique and normal shock waves in the vane channels of a supersonic stage in an axial-flow compressor will cause no significant reduction in the stage efficiency, because at relatively low supersonic velocities, the losses in the shock waves are small compared to the other types of losses in the stage, such as, for example, compared with flow separation after the shock wave, and the other types of losses discussed earlier.

Figure 61: Velocity plan for a supersonic stage when $\beta_1 = \beta_2$.

5. Centrifugal Compressor Theory in Brief

The principal dimensions of a centrifugal compressor are (fig. 62):

D_2 is the outside diameter of the impeller;
D_1 is the impeller inlet diameter;
D_o is the impeller hub diameter;
D_{av} is the average diameter at the impeller inlet;
D_3 and D_4 are the inlet and outlet diameters of the vaned diffuser, respectively;
b_2 is the width of the vane at the impeller outlet;
b_3 and b_4 are the widths of the vaned diffuser at inlet and outlet, respectively.

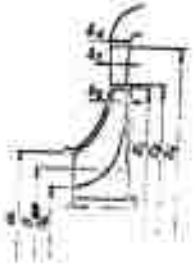

Figure 62: Schematic diagram of a centrifugal compressor.

As a rule, centrifugal compressors in turbojet engines have the following ratios:

$\frac{D_o}{D_1} = 0.6$ to 0.7; $\frac{D_o}{D_2} = 0.25$ to 0.30.

Let us intersect the compressor impeller by a cylindrical surface of diameter D_1, coaxial with the impeller, and let us develop the intersection surface on the plane of a drawing relative to axis A (fig. 63). In this development the section of the impeller disk, a, together with the sections of its vanes, b, appear tobe moving at velocity u_1, equal to the circumferential velocity of the impeller at the inlet radius, $r_1 = D_1/2$.

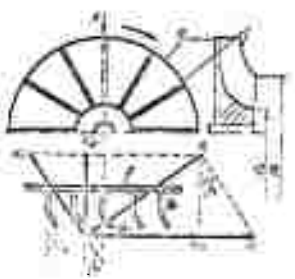

Figure 63: Velocity triangle at the inlet to the centrifugal compressor impeller.

Immediately after entering the vane formed by the intake lips of the impeller vanes the air begins a complex motion; it rotates with the impeller at circumferential velocity $u_1 = \pi D_1 n/60$ (n is impeller rpm), and moves relative to the impeller at some velocity w_1.

The relative air velocity, w_1, is found from the inlet velocity triangle shown in figure 63, where c_1 is the absolute air velocity at the impeller inlet, and c_{1a} and c_{1u} are the axial and circumferential components of velocity c_1. For an axial impeller input, the circumferential component is $c_{1u} = 0$, and $c_{1a} = c_1$.

The divergence between the direction of relative air velocity and the direction of the intake lips of the vanes, that is, the significant inequality between angles β_1 and β_1', results in an air flow separation at the impeller inlet which is associated with the loss of energy and, consequently, with a reduction in the head pressure generated by the compressor.

As a rule, a so-called rotating guide is used in centrifugal compressors in aviation engines to prevent the separation flow over the intake lip of the impeller vanes mentioned above. The intake lips of the vanes are bent in the direction of impeller rotation so they coincide approximately with the direction of relative air velocity w_1 (fig. 63). The angle is usually $\beta_1' = \beta_1 - (2^\circ \text{ to } 4^\circ)$.

The angle to which the intake lips of the impeller vanes is bent can be reduced by using a stationary guide consisting of stationary vanes fastened to the compressor casing in front of the impeller inlet. These vanes give the air its preliminary spin

in the direction of impeller rotation, so the angle α_1 between the directions of absolute velocity, c_1, and circumferential velocity, u_1, can be reduced and, consequently, so can angle β_1 if all other conditions remain unchanged (same c_1 and u_1). At the same time, the magnitude of the relative velocity, w_1, can be reduced, as will be seen from the velocity triangle, helping to reduce the losses in the intake section of the impeller.

The air at the impeller outlet will be in complex motion, just as it was at the impeller inlet. As will be seen from the outlet velocity triangle in figure 64, its absolute velocity, c_2, can be found by the magnitude and direction of the movable and relative velocities.

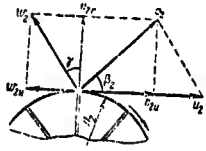

Figure 64: Velocity triangle at the compressor impeller outlet.

The movable air velocity at the impeller outlet equals the circumferential velocity of the impeller at its periphery

$$u_2 = \frac{\pi D_2 n}{60}. \tag{5.31}$$

The relative air velocity, w_2, at the impeller outlet is deflected from the radial direction by some angle γ in a direction opposite to impeller rotation, despite the radial vane arrangement. This is explained by the fact that air entering the vanes of the rotating impeller attempts to use its inertia to remain in its initial state, one in which it was not rotated relative to the surrounding, stationary, environment. As a result, the air mass in the impeller is slightly displaced in a direction opposite to its rotation, so that a circumferential component, w_{2u}, of the relative velocity, w_2, in a direction opposite to that of impeller rotation appears. The magnitude of velocity w_{2u} will be less the narrower the openings between the vanes and, consequently, the greater the number of vanes in the impeller. This magnitude can be found through the equation

$$w_{2u} = u_2(1-\mu), \tag{5.32}$$

where μ is a coefficient derived experimentally.

As will be seen from the outlet velocity triangle (figure 64) and from the equation at (5.32), the circumferential component c_{2u} of the absolute velocity c_2 can be expressed in terms of the circumferential velocity u_2.

$$c_{2u} = u_2 - w_{2u} = \mu u_2. \tag{5.33}$$

The work input to the air in the compressor can be divided

into two parts. One part (L_z), is transferred to the air flowing through the vane channels in the form of mechanical work by the impeller vanes. The other, (L_f), is absorbed by the air in the form of heat released as a result of the friction between the end surfaces of the impeller disk and the surrounding air*. Thus

$$L_{i\ c} = L_z + L_f. \tag{5.34}$$

The dependence of work L_z on the circumferential velocity u_2 of the impeller is found through the momentum equation at (1.36) which can be written as follows with reference to the axis of rotation of the impeller and as applicable to the air flow through the impeller (between inlet section 1 1 and outlet section 2 2):

$$M_c = G_a/g\,(c_{2u}r_2 - c_{1u}r_1), \tag{5.35}$$

where M_c is the torque required to rotate the impeller of a compressor carrying G_a kg of air per second; that is, the moment of forces of the effect of the impeller vanes on the air.

Knowing the moment with which the impeller vanes act on the air, we can also determine the work L_z which they transmit to 1 kg of air. For this purpose we must multiply the torque M_c by the angular velocity, ω, of impeller rotation, and divide by the air flow, G_a. We obtain

$$L_z = \omega M_c/G_a = \frac{c_{2u}r_2\omega - c_{1u}r_1\omega}{g}. \tag{5.36}$$

Remembering that

$$\left.\begin{aligned} c_{2u} &= \mu u_2;\\ r_2\omega &= u_2;\\ r_1\omega &= u_1. \end{aligned}\right\} \tag{5.37}$$

we can reduce the equation at (5.36) to the form

$$L_z = \frac{\mu u_2^2 - c_{1u}u_1}{g}. \tag{5.38}$$

The friction work, L_f, done by the end surfaces can be found through the following formula

$$L_f = f\cdot\frac{u_2^3}{g}, \tag{5.39}$$

where f is the coefficient of "end losses", or the coefficient of friction work for the impeller.

Centrifugal compressors in existing turbojet engines have f = 0.06 to 0.10 for single-entry impellers, and f = 0.03 to 0.05 for double-entry impellers.

Now, if we replace L_z and L_f in the equation at (5.34) for the internal work, $L_{i\ c}$, done by the compressor by the expressions found for them, we obtain

$$L_{i\ c} = (\mu + f)\frac{u_2^2}{g} - \frac{c_{1u}u_1}{g}. \tag{5.40}$$

---

*The work L_f was disregarded in the axial-flow compressor stage because of its insignificance.

If there is no preliminary air spin, that is, if $c_{1u} = 0$,

$$L_{i\ c} = (\mu + f)\frac{u_2^2}{g}. \tag{5.41}$$

The ratio between the adiabatic head, $L^*_{ad\ c}$, corresponding to the actual increase in pressure in the compressor, and the adiabatic head that can be obtained for optimum utilization of the circumferential velocity of the impeller, u_2^2/g is called the <u>hydraulic efficiency of a centrifugal compressor</u>, η_h:

$$\eta_h = L^*_{ad\ c}/u_2^2/g\ . \tag{5.42}$$

The hydraulic efficiency η_h, often called the head pressure coefficient, establishes the degree to which the circumferential velocity, u_2, of the impeller is used to increase pressure in the compressor. Centrifugal compressors in existing turbojet engines have $\eta_h = 0.65$ to 0.75, and $u_2 = 400$ to 480 m/sec.

Passing through the compressor impeller, the air enters the diffuser. As has already been mentioned, the diffuser can be either vaneless or vaned. Vaned diffusers are usually used in the centrifugal compressors in turbojet engines. They always have an annular clearance of about 20 to 30 mm (on one side) ahead of them. This clearance is, in essence, a small vaneless diffuser. The air flow in a vaneless diffuser, and the air's velocity triangles, are shown in figure 65.

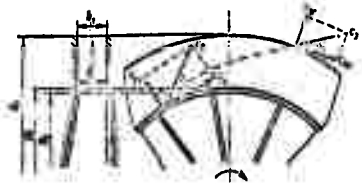

Figure 65: Schematic diagram of a vaneless diffuser.

The increase in the air pressure in the diffuser depends on the degree to which the absolute air velocity is reduced in it. Obviously, the increase in the air pressure will be greater the lower the absolute velocity, c_3, at the diffuser outlet with respect to the absolute velocity, c_2, at the diffuser inlet.

The magnitude of the velocity ratio, c_3/c_2, depends on the relative dimensions of the diffuser and on the nature of the air motion in it. The ratio between these velocities can be found through the equation of continuity for the inlet and outlet sections of the diffuser $\frac{c_3}{c_2} = \frac{\gamma_2 F_2}{\gamma_3 F_3}$,

(5.43)

where $F_2 = \pi b_2 D_2 \sin\beta_2$ and $F_3 = \pi b_3 D_3$ are the areas of the inlet and outlet sections of the diffuser, respectively, normal to the direction of the absolute air velocities, c_2 and c_3.

The ratio between areas F_3 and F_2 is called the diffuser divergence ratio.

$$\frac{F_3}{F_2} = \frac{b_3 D_3 \sin \beta_3}{b_2 D_2 \sin \beta_2}. \tag{5.44}$$

Any substantial increase in the pressure in a vaneless diffuser would require large diameters $\left(\frac{D_3}{D_2} = 1{,}7 \text{ to } 2\right)$ and this would increase compressor size and weight. Moreover, the path covered by the air particles in this diffuser will be longer, resulting in a significant increase in losses. This is why vaneless diffusers are not used alone in centrifugal compressors in turbojet engines, but instead are usually intermediate devices intended for aligning the velocity field and reducing the velocity of the air flow approaching a vaned diffuser. This reduces hydraulic losses at the inlet to a vaned diffuser. The divergence ratio for an intermediate vaneless diffuser such as this (the annular clearance) must provide for the admission of air to the vanes of the vaned diffuser after it at an acceptable velocity.

What follows from the expression for the diffuser divergence ratio at (5.44) is that the divergence ratio can be increased for given diameters if the angle of the air flow from the diffuser is increased. This is one purpose of the stationary vanes in a vaned diffuser, for they force the air flow to straighten out so that the outlet angle, β_4, (fig. 66) becomes greater than the inlet angle, β_3. Now the path covered by the air particles is fixed by the vane configuration.

Figure 66: Schematic diagram of a vaned diffuser.

A schematic diagram of, and the velocity triangles for a vaned diffuser are shown in figure 66, where it represents the stationary vanes.

Existing designs of centrifugal compressors in turbojet engines have $\frac{D_4}{D_2} = 2 \text{ to } 3$; $\frac{D_4}{D_2} = 1{,}25 \text{ to } 1{,}35$; $\frac{b_4}{b_3} = 1{,}0 \text{ to } 1{,}25$.

6. Compressor Characteristic Curves

When installed in an engine a compressor not only operates under designed conditions, but under conditions differing from designed conditions as well.

As a rule, compressor operating conditions are determined by air pressure and temperature at the inlet (atmospheric conditions), by the rpm (circumferential velocity of the impeller), and by its capacity (weight or volume flow of air through the compressor). Depending on these factors, or combinations of them, the compressor will produce some compression ratio, will have different efficiency ratings, and will require some amount of power.

Compressor characteristic curves are used to evaluate the operational qualities of a compressor, that is, to develop basic data on the compressor when operating under different sets of operating conditions. A distinction is made between normal and universal compressor curves, depending on the method of presentation.

Normal characteristic curves are defined as the dependencies of the compression ratio developed by a compressor, and of its efficiency, on the air flow and rpm for specified conditions at the compressor inlet (atmospheric conditions). These dependencies are obtained during tests performed on a compressor in a special installation.

During these tests the compressor is run at predetermined rpm (for instance, by an electric motor), and the necessary measurements are taken as the air flow is changed by throttling the air at the compressor outlet. Air pressure and temperature at compressor inlet and outlet, and torque at the compressor shaft, are usually measured. The compressor's compression ratio and efficiency (and if necessary capacity as well) are computed from the measured data, thus establishing the dependence of π_c^* and $\eta_{ad\ c}$ on the air flow at constant rpm. Compressor rpm are then changed and the same operation is repeated.

The result is a series of curves for the change in π_c^* and $\eta_{ad\ c}$ as a function of the air flow for different rpm, and these are the normal compressor characteristics shown in figures 67 and 68.

The shape of the air flow characteristic curves for an axial-flow compressor is fixed by the nature of the change in the lift factor, c_y, and in the coefficient of drag, c_x, for the profiles of the impeller vanes and straightener.

In reality, the axial velocity of the air at the impeller inlet, c_{1a}, decreases with a decrease in the volume flow of air, and as a result the angle of attack, i, of the vane profiles increases when n = const (u = const) (figure 69). Initially, the coefficient c_y increases significantly with an increase in the angle of attack, but subsequently drops sharply, beginning at some so-called critical angle of attack, and this is accompanied by a significant increase in the coefficient of drag, c_x (figure 70). In the axial-flow compressor this also results in the nature of the dependence of efficiency and compression ratio on the air flow being as mentioned above, and this is also the reason for

the greater sensitivity of the axial-flow compressor to changes in operating conditions (efficiency and compression ratio are greatly reduced when there is a deviation from designed air flow).

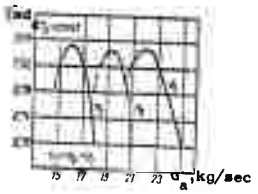

Figure 67: Change in η_{ad} as a function of G_a.

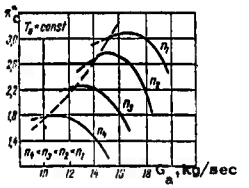

Figure 68: Change in π_c^* as a function of G_a.

In the case of the centrifugal compressor this shape of the characteristic curves is the result of a significant increase in hydraulic losses (primarily at the impeller inlet and in the vaned diffuser) when there is a deviation from air flows close to designed (for a given rpm).

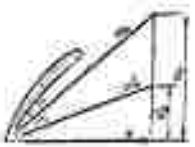

Figure 69: Change in vane angle of attack with change in air flow.

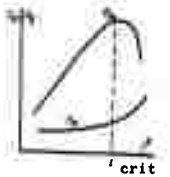

Figure 70: Dependence of coefficients c_y and c_x on the angle of attack.

The operational stability of a compressor is degraded when the air flow through the compressor is below a predetermined magnitude. Sharp, periodic, pressure and air velocity fluctuations develop; the air flow begins to pulsate. Compressor efficiency and average air pressure at the compressor outlet are greatly reduced. This phenomenon, called surging, is accompanied by a unique noise, one not inherent in the compressor when operation is stable, and by shaking (vibration) of the compressor (see below for details).

The line connecting the points on the compressor characteristic curves corresponding to the onset of surging for different rpm (dotted curve in figure 68) is called the limit of unstable compressor operation, or the surge limit. The area of unstable compressor operation is to the left of this line, and

the area of stable operation is to the right. The lower the rpm, the lower will be the air flow at which unstable compressor operation sets in.

Normal characteristic curves are valid only for those conditions at the compressor inlet (atmospheric conditions) for which they were found experimentally. Therefore, a thorough assessment of the operating qualities of a compressor requires a great many curves, constructed for different compressor operating conditions. Herein is a significant shortcomming in normal characteristic curves, and as a result they are practically not used for analyzing and evaluating compressor operating qualities, but instead are only a basis for constructing the so-called universal characteristic curves.

Unlike the normal characteristic curves, universal characteristic curves make it possible to evaluate the operational qualities of a compressor for different values of air pressure and temperature at the compressor inlet (for any atmospheric conditions), and therefore are widely used because they are more convenient for practical use.

The concept of similar compressor operating conditions which is based on the general theory of the similarity of gas flows, will be introduced for constructing universal characteristic curves.

Similar operating conditions for a compressor are defined as those under which the streams of air flowing through the compressor remain similar to each other, regardless of changing conditions at the compressor inlet (temperature, pressure), rpm, and air flow rate.

We know from aerodynamics that air streams flowing inside geometrically similar bodies, or washing them on the outside, are similar if they satisfy the conditions of kinematic and dynamic similarity.

In the event of any change in operating conditions for a given compressor, the condition of geometric similarity for its flow section will, of course, remain valid if we disregard the insignificant change in the geometric dimensions of the compressor that result from the change in its temperature, and if the compressor is not equipped with vanes that pivot during operation.

Kinematic similarity of air streams requires that similar points of their velocity triangles be similar to each other. In other words, in similar streams, the trajectories over which the air particles move, as well as the shapes of the flow passages and bodies (vanes) washed by the air, must be geometrically similar, and the air velocities must be proportional to each other at all similar points. Similar points in similar streams are points with identical locations with respect to the boundaries of these streams (for example, on the mean inlet diameter of the first compressor stage, etc.).

The condition for dynamic similarity of air streams is that the ratio between all comparable forces (inertia, gravity, pressure, and friction forces) acting on a volume element at similar points in these streams must be identical. This similarity condition is the determinant.

When air moves along a passage or washes different bodies (vanes) at high velocities, the condition of dynamic similarity of flows is expressed by the equality of the Mach numbers at similar points.

It should be noted that this definition of the similarity condition for air streams will be correct if we neglect the effect of heat exchange, and the dependence of the thermal capacity of air on temperature, and assume that the coefficients which define the magnitude of the hydraulic losses (friction) are constant. However, experience shows that in the majority of cases these assumptions will cause no significant errors, and that the relationships thus obtained are sufficiently accurate for practical purposes.

Thus, similar operating conditions for a given compressor are those operating conditions under which the Mach numbers (calculated for any speed) remain constant in all compressor sections.

It is obvious that similar operating conditions can apply not only to a given compressor, but also to a whole family of different compressors, if they are geometrically similar, that is, if all similar dimensions are proportional to each other.

Let us consider the conditions under which compressor operating conditions can be similar.

If all other conditions are equal, a change in air pressure at the compressor inlet will change the pressure in all compressor sections in proportion to inlet pressure, but air temperature and air velocity, and consequently the corresponding Mach number will remain constant. Therefore, in this case the similarity in compressor operating conditions is undisturbed.

Let us now suppose that for certain values of compressor inlet temperature, T_a, compressor rpm, n (circumferential velocity u), and axial air velocity, c_{1a}, at the inlet (volume flow of air), the inlet velocity triangle has the form shown in figure 71.

If the air temperature at the compressor inlet changes, but the rpm, n (circumferential velocity u) and axial velocity c_{1a} (volume flow of air) remain constant at the new temperature, T'_a, it is obvious that the velocity triangles for inlet temperatures T_a and T'_a will be identical, and therefore the condition of kinematic similarity of air streams at the compressor inlet, that is, similarity of velocity triangles, will be observed. However, it is readily seen that in this case the Mach number at the inlet will be different. In the first case the local sound velocity

equals $a \approx 20\sqrt{T_a}$ and in the second it is $a' \approx 20\sqrt{T_a'}$, while in both cases we have identical values for axial c_{1a} and circumferential, u, velocities and hence for the relative velocities, w_1, as well.

Consequently, if all other conditions are equal, a change in the temperature of entering air will upset the similarity of compressor operating conditions, since in this case the defining condition for dynamic similarity of the streams, that is, equality between Mach numbers at the compressor inlet, is not satisfied.

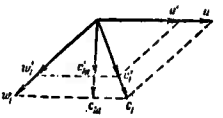

Figure 71: Velocity triangles at the compressor inlet for different initial temperatures.

In order to maintain a constant Mach number when there is a change in air temperature at the compressor inlet, and at the same time retain the similarity between the velocity triangles, the circumferential velocity, u_c (rpm), and the axial air velocity, c_{1a} (volume air flow) must be changed in proportion to the square root of inlet air temperature, that is, the following equality must be observed:

$$u_c'/u_c = \frac{c_{1a}'}{c_{1a}} = \sqrt{\frac{T_a'}{T_a}}. \qquad (5.45)$$

Since, at the same time, angle at which the stream leaves the stationary guide remains constant, and since the relationship between the circumferential and axial velocities are identical, the new velocity triangle for an inlet temperature equal to T_a' will be similar to the original velocity triangle for temperature T_a (figure 71).

Consequently, the relationships between all the other velocities will be identical,

$$\frac{c_1'}{\sqrt{T_a'}} = \frac{c_1}{\sqrt{T_a}};$$

$$\frac{w_1'}{\sqrt{T_a'}} = \frac{w_1}{\sqrt{T_a}};$$

$$\frac{u_c'}{\sqrt{T_a'}} = \frac{u_c}{\sqrt{T_a}}.$$

Each of these relationships is a magnitude proportional to a corresponding Mach number, so the Mach numbers at the compressor inlet will also be identical for both sets of operating conditions. It is easy to prove that in this case the equality of the Mach numbers, and the similarity of the velocity triangles, is observed in all the other compressor sections as well.

Thus, if the condition

$$\frac{u_c}{\sqrt{T_a}} = \text{const} \left(\text{or } \frac{n}{\sqrt{T_a}} = \text{const} \right)$$

is retained when there is a change in air temperature at the compressor inlet, and if

$$\frac{c_{1a}}{\sqrt{T_a}} = \text{const},$$

compressor operating conditions will be similar to each other. These relationships, like all the other relative magnitudes that remain constant for similar compressor operating conditions, are called <u>similarity parameters</u>.

Calculating the axial velocity, c_{1a}, we obtain, from the flow equation,

$$c_{1a} = \frac{G_a R T_a}{p_a F_a},$$

where F_a is the area of the flow area at the compressor impeller inlet;

R is the gas constant for air.

Since R/F_a = const for a given compressor, it is obvious that the similarity condition $c_{1a}/\sqrt{T_a} = \text{const}$ can also be replaced by

$$\frac{G_a \sqrt{T_a}}{p_a} = \text{const} \tag{5.46}$$

This relationship too is a similarity parameter, and is called the <u>weight flow parameter</u>, and the relationship $\frac{n}{\sqrt{T_a}}$ is called the <u>rpm parameter</u>.

The static temperature, T_a, and pressure, p_a, in the above relationships can be replaced by stagnation temperatures $T_a^* = T_o^*$ and total pressures p_a^*, and during in situ engine operation (V = 0) by $T_a = T_o$, respectively. This is explained by the fact that the dependencies between p_a^* and p_a, and between T_a^* and T_a, are determined uniquely by the Mach number, M_a, in the compressor, which remains constant under similar operating conditions.

Without going into the proofs, we now note the important fact that under similar operating conditions the compressor has identical compression ratios, efficiencies, ratios of work to initial temperature $L_{i\,c}/T_a$ and $L_{ad\,c}^*/T_a$, temperature ratios T_c^*/T_a, and other relative magnitudes (such as head pressure coefficient, $\bar{H}$, etc.).

When there is a change in the independent parameters $\frac{G_a \sqrt{T_o}}{p_a}$ and $\frac{n}{\sqrt{T_o}}$, the conditions of similarity of operating conditions are degraded and all the magnitudes listed above (π_c^*, $\eta_{ad\,c}$, etc.) will be changed. Therefore, these parameters, or the magnitudes proportional to them, characterize compressor modes and operating conditions, and we can examine the change in compressor efficiency and compression ratio as a function of their changes when we determine the operational qualities of a compressor.

The universal characteristic curves, or the characteristic curves in similarity parameters, too are a series of curves expressing the dependence of compressor efficiency and compression ratio on two independent similarity parameters.

The most frequently used procedure for constructing universal characteristic curves is to plot the weight flow parameter on the abscissa and the compressor compression ratio on the ordinate, and to plot curves in these coordinates that represent the dependence of π_c^* on $\frac{G_a\sqrt{T_0}}{P_a}$ for different values of the rpm parameter, $\frac{n}{\sqrt{T_0}}=\text{const.}$. Moreover, lines of constant efficiency, $\eta_{ad\ c}$, are plotted in the field of the compressor characteristic curves, and for this purpose the points on the different curves of $\frac{n}{\sqrt{T_0}}=\text{const}$, that correspond to identical efficiencies are connected by common lines.

Typical universal characteristic curves for compressors are shown in figure 72, where the surge limits are indicated by the shaded lines, and the constant efficiency lines by the dashed lines. Note that in these curves the lines for $\frac{n}{\sqrt{T_0}}=\text{const}$ are higher, the greater the magnitude of the rpm parameter.

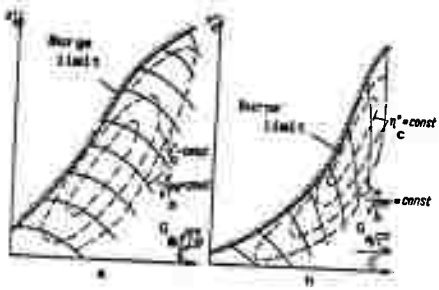

Figure 72: Typical compressor characteristic curves.
a - centrifugal compressor; b - axial-flow compressor.

7. Unstable Compressor Operation (Surging), and Preventive Measures

Mention has already been made of the fact that compressor operation becomes unstable when the air flow rate is reduced below a predetermined magnitude, that a phenomenon called surging develops.

When a compressor surges the blading vibrates, and the compressor shakes, the result of the flow pulsation inherent in surging. Compressor efficiency, and average air pressure at the compressor outlet, are reduced. The air from the compressor begins to enter the combustion chamber unevenly, with periodically fluctuating pressure and velocity. Normal operation of the engine as a whole is degraded, thrust drops, and efficiency deteriorates.

Heavy compressor surging can lead to flame interruption, to flameout in the combustion chambers and, consequently, to engine shutdown. The vibration and shaking that develops during heavy surging is transferred to the entire engine structure and can lead not only to the destruction of compressor elements, but to

the destruction of the power plant. This is why surging is unacceptable when an engine is running.

The substance of the origin and development of unstable compressor operation has not been completely studied as yet because of the great complexity of this process. However, investigations reveal that a primary role in the appearance of surging is played by the separation of the air flow from the compressor blading that develops at low air flow rates. Separation from the compressor blading develops at high air flow rates as well. However, the effect of separation on compressor operation is completely different in the two cases.

It has already been pointed out that in an axial-flow compressor a reduction in the air flow rate at constant rpm will result in a change in air velocity such that the angles of attack of the rotor and straightener blades are increased. This causes flow separation from the convex surfaces of the blades, accompanied by vortex formation. At the same time, the inertia of the air flow tends to cause separation from the convex side of the blades, lending itself to the formation and development of vortex regions. Therefore, if flow separation is great, these regions will grow and spread out inside the compressor, filling the compressor flow section. There is periodic, repetitive "choking" of the compressor's flow section by the vortex regions. The air, because of the compressor, also periodically shoots through these regions in the opposite direction, toward the inlet, and the result is autooscillation of the air column, leading to unstable operation, that is, to the entire compressor surging.

If the airflow rate and, consequently, the axial velocity, c_{1a}, at the inlet increase when n = const (or when velocity c_{1a} increases at a faster rate than the circumferential velocity), the angle of attack, i, decreases and then becomes negative (figure 69). This leads to flow separation from the concave side of the blading. At the same time, the air flow is pressed against the concave side of the blading by the effect of the inertial forces. Therefore, when there is an increase in the air flow rate, when separation regions are formed on the concave side of the blading, these regions cannot undergo strong development because they are pressed against the blading by the air flow and are local in nature, so do not degrade stable compressor operation. Similar phenomena occur when the intake lips of the impeller and the diffuser vanes in a centrifugal compressor are washed by light and heavy air flows.

It should be emphasized that the development of surging fluctuations ought not be considered as the result of the direct perturbation effect of the vortices stream off the blading when

separation develops. Actually, the connection between surging and flow separation is more complex, and does not occur spontaneously, but rather as a result of changes in such properties of the compressor as its energy sources caused by the separated flows.

Detailed experimental investigations of the flow structure in the axial-flow compressor at low air flow rates have also led to the discovery of the phenomenon known as the rotating stall. It has been established that flow separation never develops at all the rotor and straightener blading at the same time when the flow rate is reduced. The inevitable differences in blading configuration and positioning, and lack of a strictly axisymmetrical flow, cause the stall to appear initially in one or two places around the circumference, with each such zone encompassing a small number of vane channels. The stall occurs simultaneously along the entire length of the blading, or only over part of it, depending on the relative diameter of the rotor hub. In stages with short blading the stall immediately takes in the entire length. In this type of stall, referred to as a complete stall, one stall zone is usually formed in the annular section. In the case of relatively long blading, the stall zones are in part located only at the blade tips or, more rarely, near the rotor hub, and initially there are from one to three such zones. As the flow rate continues to decline the number of stall zones increases gradually, reaching seven or eight, and more. The stall meanwhile is propagating over more and more of the blading length, so is called a partial, or progressing, stall. When there are a great many stall regions they are distributed symmetrically around the circumference. However, at the start when there are no more than two or three zones, they can be distributed unevenly. At low flow rates the multizone, partial stall is often replaced by a single, broader zone of complete stall. When the flow rate is increased the phenomena described above are repeated in the inverse order, but with some delay.

Very significant is the fact that in a complete, as well as a progressive, stall, the separation zones are not localized around specific blades, but rotate continuously in the same direction as the impeller, and at a lesser angular velocity. The experiments found that the rotational velocities of the stall zones varied, and in the case of the progressive stall were from 40 to 85 % of the angular velocity of impeller rotation, and in the case of the complete stall, was 20 to 40 % of this same velocity. It proved to be independent of the number of stall zones, while changing in proportion to impeller rpm. The rotating stall was found to prevail to equal degree in impeller and straightener.

The following is an elementary explanation of how stall zones rotate. Flow separation in one, or in several rows of the installed vane channels results in a reduction in their discharge capacity.

Therefore, the air stream, encountering increased resistance in the stall zone, spills over into the axial clearance to both sides, trying to find its way through adjacent channels that are free of stalls. This reduces the angle of attack and, consequently, creates favorable conditions for flow around those blades located in front of the vortex-induced zone. On the other hand, the angle of attack for the blades located after the vortex-induced zone increases, causing flow separation at their convex surface. The stall zone now migrates in the rotational direction from one group of impeller channels to another, but at a velocity lower than that at which the impeller itself is moving, resulting in the rotating stall described above.

Since air velocity and air flow rate in the stall zones are much lower in value than their values in the rest of the annular channel, a rotating stall causes continuous flow pulsations which occupy either the entire area of the cross section, or only part of it, depending on the type of stall. Depending on the number of stall zones, and their rotational velocity, the pulsation frequency recorded by a stationary sensor is usually 0.2 n to 0.3 n in the case of a complete stall, and will reach 2 n to 3 n in the case of a multizone, progressive stall. The amplitude of the velocity pulsation can reach 70 % of the velocity in the flow core.

Even flow separation develops in just the first stage of a compressor, the rotating perturbation zone will propagate to the rest of the stages, causing velocity pulsations over the entire tract. However, according to the experimental data large amplitude velocity fluctuations are only observed in the first few stages, after which they decrease sharply.

Stall pulsations differ from surging pulsations by their incomparably greater frequency and smaller amplitude, as well as by only a nominal dependence of these magnitudes on network capacity. In addition, the rotating stall and surging differ with respect to the nature of their shift in phase during fluctuations; the former is associated with the pulsation phase displacement within the same section, while the latter is associated with it along the length of the flow section. The experimental data show that the rotating stall phenomenon will not cease, even when surging develops. At the same time large amplitude low-frequency flow oscillations characteristic of surging are simply superimposed on the rotating stall.

The rotating stall is just as unacceptable in operation as surging, primarily because it can be the source of excitation for dangerous oscillations and the compressor blading breakage associated with them. Since surging and rotating stall are both inherent in the operation of cascades at large angles of attack, and since the means for coping with them have a common basis, we shall henceforth not distinguish between these phenomena for simplicity's sake, but shall conventionally refer to them by the common term "surging" or "unstable operation".

Let us consider some special features of surging in the multistage, axial-flow compressor.

We know that the areas of the passages at the outlet of this compressor are much smaller than those at the inlet because of the gradual increase in the density of the air flowing through the compressor. The magnitude and the relationship between these areas are based on the change in the density and axial velocity of the air along the compressor when the compressor is running at the design point. The incidence of the profiles of the moving and straightener blades in each stage is selected for design point compressor operation and too is based on the corresponding design velocity triangles.

Thus, for design point operation there is a complete match between the areas of the flow cross-sections of the compressor's flow section, between the densities and velocities of the air moving through them, and between the blade incidence in all stages.

At other than the design point this match in the operation of the compressor stages will be upset unless special measures are taken, and the further away from the design point operation takes place, the greater will be the change in compressor operation as compared with that at the design point.

For example, if the compressor's compression ratio is reduced below its designed magnitude as a result of a reduction in rpm, axial velocity at the first stage inlet will not be reduced if there is no change in the designed air flow rate and all other conditions remain the same. But since circumferential velocity is reduced, the angles of attack of the first stage blading will be smaller.

The pattern observed in the following stages is a different one. Here the reduced compressor compression ratio causes a reduction in the air density in these stages, but their flow sections remain as before and have been designed for a given weight flow of air of greater density, one corresponding to the designed compression ratio. Therefore, in this case axial air velocity in succeeding stages increases, and in conjunction with a simultaneous reduction in circumferential velocity, results in reducing the angles of attack in these stages much more so than was the case in the first stages. For the same reasons, the angles of attack in the succeeding stages can even become negative if the compression ratio is reduced significantly from the designed ratio. At large negative angles of attack the air in the vane channels in the stage expands instead of being compressed. This condition in the last stages, which results in a drop in efficiency and in the compressor head, is called turbine operation.

If there is a simultaneous reduction in compression ratios below their designed values (due to a reduction in rpm) and in the air flow rate through the compressor, the axial velocity at the

first stage inlet will decrease at the same rate as the circumferential velocity. But if the axial velocity decreases more rapidly than the circumferential velocity, it is obvious that the blade angles of attack in the first stage will be increased, and can reach a value at which intensive flow separation from the backs of the blades, and surging, become possible.

The weight flow of air through the last stages will be reduced at the same ratio as in the case through the first stages, given the condition of continuity. However, at the same time the air density in the last stages will be reduced in the case of the change in compressor operating conditions considered because of the reduction in the compression ratio. As a result, the axial air velocity in the last stages changes little, if at all, and consequently the blade angles of attack in these stages will be reduced because of the reduction in circumferential velocity, and will then go negative.

So, in this case the last stages approach the turbine mode, while the first stages approach the surge mode.

Let us now increase the compressor compression ratio above the designed ratio by increasing compressor rpm, keeping the air flow rate, and, as a result the axial velocity at the inlet to the first stages, unchanged. Now the blade angles of attack in these stages will be increased because the circumferential velocity, u_c, increase when c_{1a} = const. At the same time, the axial velocity of the air in the last stages will be reduced because the air density increases with increase in the compression ratio. This causes the blade angles of attack in the last stages to increase much more quickly than is the case in the first stages, and this can then lead first to the appearance of severe stalling on the backs of the blades of these last stages, and to surging.

If the compressor compression ratio is increased above the designed ratio while simultaneously reducing the air flow rate, the axial velocity of the air in the first stages will be reduced. It will decrease at a faster rate in the last stages than it will in the first stages because the air flow rate is reduced and because the air density is increased as a result of the rise in the compression ratio. Therefore, the blade angles of attack in the last stages will increase at a faster rate (both when there is an increase in rpm and when n = const) than in the first stages. Now flow separation, associated with surging, can develop in this case as well, primarily in the last stages.

A mismatch in the operation of the first and the last compressor stages, and conditions for the development of surging in these stages, similar to those considered above, can also be observed when rpm are constant but the compressor compression ratio changes as a result of a change in the temperature of entering air (the rpm parameter $\frac{n}{\sqrt{T_0^*}}$ will change as a result of a change in T_0^*). In this case the only difference is that the circumferential

velocity u_c will remain constant, but the corresponding change in the blade angles of attack in the individual stages can be determined only by the change in the axial velocities of the air in these stages.

These examples, as well as the results of more detailed investigation of operating conditions for multistage axial-flow compressors at other than the design point lead to the following conclusion.

When surging develops at off-design points at which the compressor ratio remains below the design ratio, the first stages will usually prove to be the source of surging, and at off-design points at which the compression ratio exceeds the designed ratio, it will be the last stages.

It should be noted that degradation of the uniformity of the air flow at the compressor inlet very much lends itself to the development of surging. Flow uniformity can be degraded by flow separation, or the formation of turbulence in the engine intake section, the result of poor design configuration of the air intake ducts, sharp edges, dissimilar supports, deep indentations, nicks, and other causes (operational, design, and technological). Nonuniformity in the velocity field in front of the compressor can also be the result of large angles between the incoming flow of air against the compressor and the axis of the intake section when aircraft angles of attack are large, and can also result from engine exhaust from another aircraft flying close by entering the inlet, etc.

Any distortion in the designed distribution of the velocity at the compressor inlet, regardless of cause, considerably narrows the range of stable compressor operation and, consequently, accelerates the onset of surging. Therefore, everything that can be done to keep the air flow at the compressor inlet as uniform as possible must be done, in operation, as well as during design.

At the present time the following measures are taken to prevent surging, that is, to expand the limits of stable operation for axial-flow compressors.

1. Air is bypassed to the outside from one, or several intermediate stages through special ducts in the compressor housing. This is a very simple method, and is based on the fact that when all other conditions are equal, exhausting some of the air from an intermediate stage to atmosphere will cause an increase in the air flow rate and in the axial velocity of the air in the preceding, first stages. This results in a reduction in the blade angles of attack in these stages for a given circumferential velocity, thereby preventing air separation at the blades, associated with the onset of surging. At the same time, the air flow rate in the stages beyond the bypass will be reduced and, as a rule, the

compressor compression ratio will drop (for a given value of). In addition, the energy used to compress the air bypassed to atmosphere will be lost. Therefore, other conditions remaining unchanged, engine efficiency and thrust will be decreased when air is bypassed.

2. Rotatable guide (straightener) blades are used in one or in several stages. If these blades are slewed in the direction of impeller rotation the spin given the air flow in the direction opposite to that of the impeller is reduced, but is increased in the direction of rotation. As a result, the angles of attack of the impeller blades are reduced for a given impeller rotational velocity as will be seen from figures 57 and 59. But the reduction in the angles of attack of the blades, eliminating flow separation from their backs, lends itself to the prevention of surging, thereby extending the surge limit toward the lower air flow rates. At the same time, the compression ratio in the stage is reduced for given rpm, but its efficiency at the off-design point can be increased.

3. Twin-shaft (twin-rotor) compressors can be used to adjust the first and the last stages to different rpm levels when there is a transition to off-design points. Let us explain the advantages of this system by the following example. If a single-shaft compressor is shifted to a point at which the compression ratio drops below the designed ratio, the axial velocity in the first stages will be reduced at a faster rate than will the circumferential velocity, and this can lead to surging in these stages. But there is no danger of surging, in the last stages because the axial velocity in them will be reduced at a slower rate than will the circumferential velocity.

When a twin-shaft compressor is shifted to such lower points it is possible to reduce the first stage rpm (first rotor) faster than last stage rpm (second rotor). This can prevent a too rapid decrease in axial velocity relative to circumferential velocity, and in that increase in the angles of attack of the first stage blading associated with it that leads to surging in these stages.

In addition, the match in the operation of the individual stages of a multistage, axial-flow compressor at off-design points can be improved by using rotatable straightener blades and twin-shaft rotors. There are a number of cases when this results in an appreciable increase in efficiency and compressor head at these points.

All the methods listed above for extending the stability limits of axial-flow compressors are used in modern aviation engines, separately, and in combination with each other.

CHAPTER 6

COMBUSTION CHAMBERS

1. General Observations

The combustion chamber is one of the most important parts of an engine; the reliability, efficiency, and thrust-effective operation of the engine as a whole depend to a very large degree on the quality of combustion chamber operation.

Combustion chambers of aviation gas turbine engines must ensure the following:

stable fuel combustion (without flameouts or damping) over the entire range of engine operation and under all possible operating conditions;

trouble-free fuel ignition and combustion during engine start-up, both on the ground and in high-speed flight;

highly complete fuel combustion under all operating conditions;

low hydraulic resistance;

the specified temperature field at the outlet which is very important for reliable turbine blade operation;

reliable operation, and especially no deformations, burn-throughs, and cracks in the walls.

In addition, fuel chambers must have the minimum possible size and weight for a given air and fuel consumption.

By and large, modern combustion chambers satisfy these requirements. However, the creation of high-quality combustion chambers that are equally responsive to all the requirements imposed on them is a difficult task which requires theoretical and especially experimental investigations.

The principal elements of all types of combustion chambers for modern aviation gas turbine engines are (cf. figure 73): flame tube 2; flame stabilizers 4 and 5; fuel atomizer 1; outer casing 3.

Combustion chambers of modern turbojet engines are divided by type of design into tubular (individual), annular, and cannular combustion chambers.

Tubular combustion chambers (cf. figure 73) are installed around the engine casing and fastened each individually by their flanges to the compressor casing and to the gas header of the turbine. Each of these chambers can be removed easily for inspection or replacement with the engine in place on the aircraft. No cumbersome installations of high power and large air consumption are required for experimental investigations and empirical development of individual tubular combustion chambers, as this is the case for annular chambers.

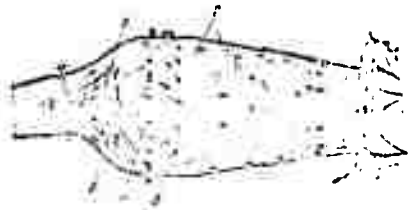

Figure 73: Schematic diagram of a tubular combustion chamber:
a - atomizer; 2 - flame tube; 3 - casing; 4 and 5 - flame stabilizers.

Annular combustion chambers (cf. figure 74) have one annular flame tube enclosed in an overall annular casing which in a number of cases is also a strength member of the engine structure. These chambers are distinguished by their lower weight and can provide a smaller engine diameter than tubular chambers for the same air consumption. However, inspections of internal parts and even more so the replacement of the flame tube of annular chambers usually requires engine disassembly.

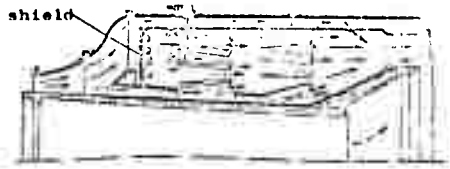

Figure 74: Schematic diagram of an annular combustion chamber.

Cannular combustion chambers (cf. figure 75) consist of a number of individual flame tubes located about the longitudinal axis of the engine and enclosed in a common annular casing. These combustion chambers combine the advantages of tubular and annular chambers and are employed at a continuously increasing rate today.

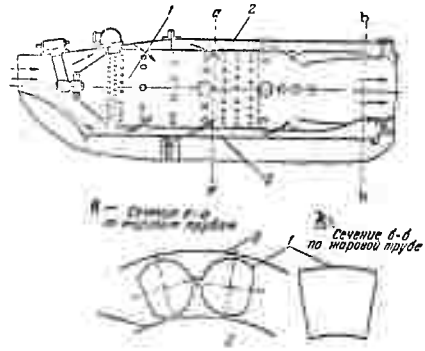

Figure 75: Schematic diagram of a cannular combustion chamber.
1 - flame tubes; 2 - common outer casing; 3 - inner casing.

Legends to figure 79:

A - section a-a through the flame tubes;
B - section b-b through a flame tube.

2. Special Features of Managing the Combustion Process

It was already mentioned that in modern aviation gas turbine engines the maximum acceptable temperature in front of the turbine will not usually exceed 1,150° to 1,200°K. Such a temperature is obtained when fuel is burned in air at a total excess air coefficient of α = 3.5 to 4.5. When the engine operates at reduced temperatures T_g in front of the turbine, and also at high temperatures T_g^* (high airspeed), the total excess of air coefficient necessary to ensure the required temperature in front of the turbine is increased to about α = 7 to 8 and more. Even greater values for the total excess of air coefficient are reached during a rapid shift by the engine from a higher rpm to a lower rpm, since in that case the supply of fuel in the combustion chamber is reduced at a faster rate than the air flow passing through the engine.

At such a high excess of air it is impossible to achieve stable fuel combustion, even more so in an air flow, since the considerably leaner mixture of fuel and air is difficult to ignite, and its combustion proceeds much more slowly and instable. As a result it is easy for the flame to be separated and blown out of the chamber by the flow of air passing through.

In order to ensure stable combustion and at the same time to obtain the required gas temperature in front of the turbine, the inflowing air from the compressor is divided into two parts in all combustion chambers of gas turbine engines.

The smaller part of this air, or primary air, is channeled directly into the combustion zone that occupies the forward part of the flame tube, where it primarily ensures the combustion of the entire mass of fuel. The quantity of primary air will not exceed 20 to 30 % of the total air flow passing through the engine and is so designed that the excess of air coefficient in the combustion zone amounts to α_1 = 1.2 to 1.5. At this excess of air the temperature in the combustion zone reaches 2,000° to 2,200°K and more, which also creates favorable conditions for rapid, stable, and sufficiently complete fuel combustion.

The remaining air, called secondary air, flows around the outside of the forward part of the flame tube, i.e. it bypasses the combustion zone, and then is gradually mixed with the combustion products departing from the combustion zone, ensuring the necessary temperature reduction prior to the turbine inlet (cf. figure 76).

The secondary air is mixed with the combustion products in the diluent zone located in the rear part of the flame tube (facing the turbine), which the air enters through a number of specially located apertures in the tube walls. This mixing process also

creates the most favorable temperature field in the gas flow moving toward the turbine. In addition to the reduction and equal distribution of gas temperatures the final combustion of unburned fuel particles and incompletely oxidized products takes place in the diluent zone, if these are carried from the combustion zone.

The secondary air, flowing around the outside of the flame tube, cools the tube and, in addition, forms a thermoinsulating layer between the high temperature zone and the outer combustion chamber casing, protecting it against excessive heat.

Continuous and stable combustion of the moving mixture of fuel and air is possible only if sufficient heat is added to the fresh mixture entering the combustion zone to heat it to igniting temperature, and if the velocity of the mixture in this zone does not exceed the propagation velocity of the flame.

Therefore, the mixture is enriched in the combustion zone and, in addition, so-called flame stabilizers or inlet devices are used in all combustion chambers of gas turbine engines that are located in front of the combustion zone in the flame tube. Behind these devices in the combustion zone an area filled by retrogressive turbulent streams of combustion gases and air is created where the progressive (axial) velocity of the gas and air flow does not exceed a mean of 15 to 25 m/sec (cf. figure 76).

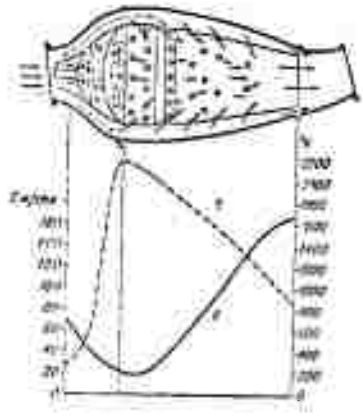

Figure 76: Temperature and velocity profile in the flame tube of a combustion chamber.

The retrogressive turbulent streams of combustion gases created by the stabilizers ensure a heat input from the combustion zone to the inflowing fresh mixture of fuel and air so that it is heated to the required temperature, is ignited continuously, and burns in a stable manner. And the turbulent motion of the inflowing air ensures that the air is properly mixed with the fuel and penetrates into the combustion zone.

The flame stabilizers are bodies of poor aerodynamic configuration installed in the path of the primary air. They are made in the form of diaphragms with a great number of small apertures through which the primary air passes, in the form of plates, hollow conical caps, annular slots, etc. The basic flow diagrams for the gas and air streams behind stabilizers with plate and conical configuration are shown in figure 77.

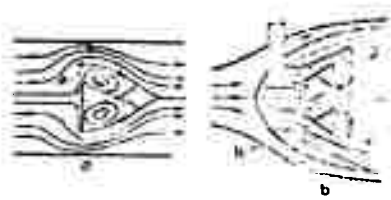

Figure 77: Flow diagram behind the stabilizer.
a - plate stabilizer; b - conical stabilizer.

In addition, special swirlers are used in many combustion chambers to achieve a better mixture of air and fuel and to create and strengthen the retrogressive streams of burning gases in the combustion zone. These are a number of radial nozzles installed at the flame tube inlet (cf. figure 73, item 5) under a certain angle to the direction of motion of the inflowing air. Up to 50% of the primary air enters the flame tube through the swirlers. The swirl imparted to this air by the swirling nozzles (cf. figure 78) ensures its intensive turbulization and rapid mixture with the fuel. And the centrifugal forces that develop when the air swirls create an outer region of increased pressure and an inner region of reduced pressure behind the swirlers, resulting in the formation of retrogressive turbulent streams of burning gases.

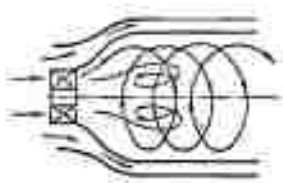

Figure 78: Diagram of air being swirled by a swirling nozzle.

The fineness of fuel atomization which is dependent on the magnitude of injection pressure and on the arrangement of the atomizer has a great effect on the combustion process. Fuel atomization is improved by increased injection pressure. Therefore, under designed operating conditions in modern aviation gas turbine engines the fuel injection pressure reaches 60 to 80 kg/cm^2 and more.

Good atomization and uniform fuel distribution in the flow are ensured, in particular, with the aid of centrifugal atomizers which are most frequently used. The cone of atomized fuel that is created by the atomizers varies within fairly broad limits for different engines, from 40° to 80°, and is selected experimentally according to type, shape, and dimensions of the combustion chamber.

The fuel is injected both with and against the air flow. The latter procedure, together with an appropriate type of combustion chamber, ensures good fuel atomization and stable fuel combustion.

Fuel prevaporization, i.e. "vaporizing" fuel atomization, can contribute to stable and adequately complete fuel combustion under a broad range of combustion chamber operating conditions, and also to a reduction in fuel injection pressure. For this purpose the fuel in some combustion chambers is channeled from the atomizer directly against surfaces whose outsides are washed by burning gases.

One of the possible schemes for a combustion chamber with "vaporizing" atomization is shown in figure 79. In this scheme the principal mass of air from the compressor enters the forward part of the flame tube, and from there the primary air is channeled into vaporizing tubes, i.e. burners, whose ends are bent into a U-shape and located in the combustion zone. The fuel is fed into these same tubes through the atomizer.

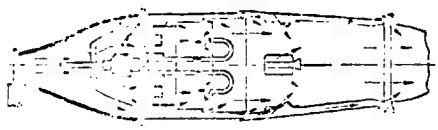

Figure 79: Schematic diagram of a combustion chamber with fuel vaporizing tubes.

The fuel is vaporized upon contact with the walls of the tubular burners, and the rich fuel-air mixture that is generated burns at the tube outlet where the admixture of secondary air begins.

A significant reduction of temperature and pressure, and an increase of air velocity in the combustion chambers render fuel ignition difficult, contribute to instable combustion, and can finally result in a flameout. Therefore, when the pressure and temperature of the inflowing air are reduced, which takes place at increased altitude and reduced engine rpm, the values for the excess o air coefficients are reduced under which fuel ignition and stable combustion chamber operation are possible (cf. figures 80 and 81).

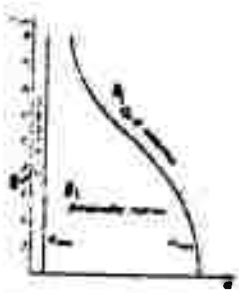

Figure 80: Stable combustion limits as a function of altitude.

Legends:
A - flameout;
B - stable combustion.

These circumstances also explain the difficulty involved in an air start with gas turbine engines at high altitudes, as well as the development of instable combustion chamber operation in a number of cases (especially at high altitudes and slow airspeeds), sometimes leading to flame damping and engine shut-down (especially under transient operating conditions).

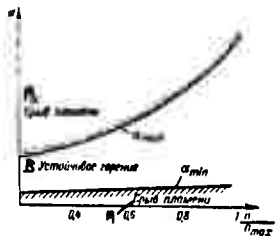

Figure 81: Stable combustion limits as a function of engine rpm.

Legends:
A - flameout;
B - stable combustion.

In addition, an air start of a shut-down engine at high altitudes can prove to be impossible because cold air at low pressure is blown through the combustion chambers of a shut-down engine at such a speed that under these conditions a flame, even if one develops, would be completely blown out immediately. In that case an engine air start requires a reduction in altitude and sometimes in airspeed, too.

An increase of the altitude for reliable starts and stable combustion chamber operation is achieved by increasing the capacity (heat intensity) and operating period of the igniters, reducing the air velocity in the combustion chambers by means of increasing their flow areas, using more intensive flame stabilizing devices, and other measures.

Air density drops with increasing altitude so that the weight flow of air through the engine is reduced, as it is under reduced engine rpm under otherwise equal conditions. At the same time, fuel consumption is reduced at a corresponding rate in order to maintain an acceptable gas temperature in front of the turbine. However, if the fuel flow through the atomizers is reduced while the area of their dosage openings remains unchanged, there will be a drop in injection pressure and the quality of fuel atomization will degenerate which can be a cause of degenerating combustion chamber operation, in other words a disruption of combustion stability and incomplete combustion.

Therefore, fuel atomizers with automatic flow area control are used in all modern aviation gas turbine engines: dual-nozzle atomizers, duplex atomizers, fuel-bypassing atomizers, and others. In addition, automatic minimum fuel pressure devices are used in front of the fuel atomizers that do not allow the fuel flow to drop below the minimum acceptable level where stable combustion without blowouts and flame damping is still ensured.

3. Principal Combustion Chamber Parameters

Let us consider the basic relationships and parameters that are characteristic for the combustion chambers of modern aviation gas turbine engines.

The combustion chamber volume is associated with fuel consumption and the calorific value of the fuel, or the quantity of heat released. This dependence is determined by the magnitude of the calorific intensity per unit of volume, q, equaling

$$q = G_{f\ hr} H_u / v_{c.c}\ p_c \ [kcal/m^3\ hr\ ata]$$

where $v_{c.c}$ is the combustion chamber volume, m^3;

p_c is the pressure in the combustion chamber, absolute atmospheres.

In combustion chambers with the same cross-sections and the same weight flows of air the quantity of heat released per unit of volume, or the calorific intensity per unit of volume, will rise with increasing pressure since in that case the axial gas velocity is reduced and, consequently, less combustion chamber length is required for the same time spent by the fuel particles in the chamber. Therefore, in a correct comparative evaluation of different chambers their calorific intensity per unit of volume is also referred, as we did above, to the magnitude of pressure in the combustion chamber.

Under otherwise equal conditions, combustion chambers with a small cross-section can be designed for a greater calorific intensity than chambers with a larger cross-section. This is explained by the shorter time required by the air to penetrate into the combustion zone as the cross-section of the chamber is reduced.

Under designed operating conditions the combustion chambers of existing aviation gas turbine engines have a calorific intensity per unit of volume of q = 30 to 50 x 10^6 kcal/m^3 hr ata. The maximum cross-section area of the combustion chamber is usually dimensioned so that the air velocity as determined by the aggregate air flow through the engine and by that area will not exceed 40 to 50 m/sec, which is necessary in order to ensure a stable combustion process.

The outlet cross-section area of the combustion chamber, or the cross-section at the inlet to the turbine nozzle assembly, depends on the mean diameter and length of the blades of the nozzle assembly that are determined when the turbine is designed.

The outlet gas velocity is increased when this area is reduced for a given gas temperature in front of the turbine and under otherwise equal conditions, and static pressure in front of the turbine nozzle assembly is correspondingly reduced. In existing designs the outlet gas velocity is 2 to 2.5 times greater than the air velocity in the maximum chamber cross-section, and about 1.5 times greater than the air velocity at the compressor outlet, which means that it is 170 to 180 m/sec.

The ratio of flame tube length to the maximum flame tube diameter in a tubular chamber, or to the difference between inner and outer diameter of the maximum cross-section of an annular chamber, ranges within the limits from 2.5 to 5 for existing designs.

Hydraulic resistance and an increase in gas velocity associated with a reduction in gas density due to an increase in temperature cause a reduction of static pressure p_g and total pressure p_g^* in the combustion chamber, compared to their values at the compressor outlet; in other words, it always applies that $p_g < p_k$ and that $p_g^* < p_k^*$. Here the total pressure decreases by about the same degree as the static pressure, since the Mach number M_g at the combustion chamber outlet usually differs little in magnitude from the Mach number M_k at the compressor outlet.

The total pressure drop in combustion chambers is evaluated by the pressure recovery factor

$$\sigma_{c.c} = p_g^* / p_c^*$$

this factor is determined by experience. Combustion chambers of modern aviation gas turbine engines have a factor of $\sigma_{c.c} = 0.95$ to 0.97.

In order to establish a connection between the required excess of air coefficient α and a given temperature T_g^* at the combustion chamber outlet, an energy equation is applied to the gas flow in the section located between the outlet cross-section kk of the compressor and the cross-section zz at the combustion chamber outlet (at the inlet to the turbine nozzle assembly). The gas flow absorbs heat in this section as a result of fuel combustion, but there is no internal work. Taking this into account we write the

energy equation in the following form, referred to 1 kg of burning fuel:

$$\alpha l_o i_k^* + Q_1 = (1 + \alpha l_o) i_z^* \qquad (6.1)$$

or

$$i_k^* + \frac{Q_1}{\alpha l_o} = \frac{1 + \alpha l_o}{\alpha l_o} i_z^*.$$

where αl_o is the weight of the air required for 1 kg of fuel;

i_k^* is the total enthalpy of 1 kg of air at the compressor outlet (at a temperature T_k^*);

Q_1 is the heat added to the gas flow as a result of the combustion of 1 kg of fuel and the associated increase in the enthalpy of the combustion products;

$(1 + \alpha l_o)$ is the weight of the combustion products generated by the combustion of 1 kg of fuel at an excess of air coefficient α;

i_z^* is the total enthalpy of 1 kg of combustion products at the combustion chamber outlet (at a temperature T_z^*).

The heat released during complete combustion of 1 kg of fuel is its net calorific value H_u. Part of this heat is lost to the outside medium through the walls of the combustion chamber, and part is not released if there is incomplete combustion. Therefore, the heat Q_1 that is absorbed by the combustion products is less than the calorific value H_u of the fuel, so that

$$Q_1 = \xi_{c.c} H_u,$$

where $\xi_{c.c} < 1$ is the heat release coefficient that takes into account the heat losses in the combustion chamber that were mentioned above.

This coefficient is determined by experience and is sufficiently great for combustion chambers of modern turbojet engines under designed operating conditions, where $\xi_{c.c} = 0.96$ to 0.98.

It was mentioned above that we can make the assumption $1+\alpha l_o/l_o \approx 1$ for combustion chambers of turbojet engines. Thus, we can now rewrite equation (6.1) as follows:

$$\xi_{c.c} H_u + i_k^* = i_z^* = c_p'(T_z^* - T_k^*), \qquad (6.2)$$

whence we obtain

$$T_z^* = T_k^* + \frac{\xi_{c.c} H_u}{c_p'(T_z^* - T_k^*)}, \qquad (6.3)$$

where c_p' is the mean specific heat in the temperature interval from T_k^* to T_z^* at constant pressure (as a rule, $c_p' = 0.26$ to 0.29).

CHAPTER 7

AVIATION TURBINES

1. Principles of Turbine Design and Operation

It was mentioned above that double-stage, single-stage, and sometimes even triple-stage axial-flow turbines are used in existing turbojet engines. Diagrams of typical turbines for turbojet engines are shown in figures 82 and 83, and a diagram of an axial-flow turbine stage and a cylindrical section through its blading, unfolded into a plane, in figure 84.

The principal parts of a turbine are: the nozzle or guide assembly formed by the fixed nozzle blades 1, fastened to the fixed turbine casing 2; the turbine wheel 3, secured to the turbine shaft, and the blade assembly or bucket ring formed by the rotor blades 4, fastened to the rim of the turbine wheel 3. All the rotating parts of the turbine make up its rotor.

The combination of the fixed nozzle assembly and the bucket ring that follows it is called a turbine stage.

The conversion of the pressure energy of the gas into kinetic energy takes place completely or partially in the nozzle assembly. Subsequently, part of the obtained kinetic energy is converted into work at the turbine shaft by means of the bucket ring.

If the pressure energy is converted into kinetic energy exclusively in the nozzle assembly so that the gas expands in it to the terminal pressure encountered behind the turbine, and if no gas expansion takes place in the spaces between the rotor blades, the turbine is called an action turbine.

If the conversion of pressure energy into kinetic energy takes place not only in the nozzle assembly but also at the rotor blades, simultaneously with the conversion of kinetic energy into external mechanical work, the turbine is called a reaction turbine.

In that case, gas expansion takes place in both assemblies, nozzle assembly and rotor blade assembly.

As a rule, all turbines used in aviation gas turbine engines are reaction turbines.

The gas velocity and gas pressure profile in a single-stage reaction turbine as well as the velocity triangles at the inlet and outlet of its rotor blading are shown in figure 84.

The gas flow approaches the nozzle assembly from the combustion chamber at a velocity c_z, a pressure p_z, and a temperature T_z.

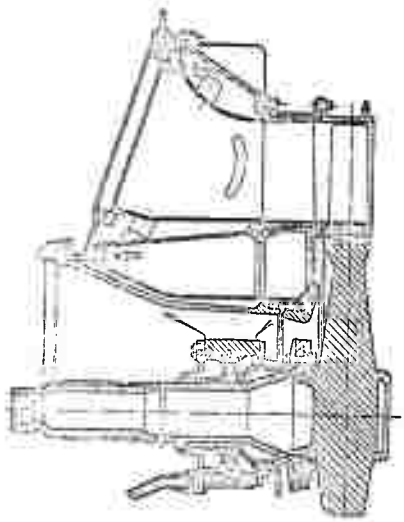

Figure 82: Diagram of a single-stage turbine for a turbojet engine.

The gas expands to a pressure p_1 in the spaces between the nozzle blading, and due to a corresponding drop in the enthalpy of the gas its absolute velocity increases from c_z to c_1. Thus, the gas departs from the nozzle assembly at a velocity c_1 and a direction enclosing an angle α_1 with the rotational plane of the turbine wheel. The gas enters the rotor blading at a relative velocity w_1 whose magnitude and direction are determined by the magnitude and direction of absolute velocity c_1 and the velocity of translational motion, i.e. the circumferential velocity u of the blades.

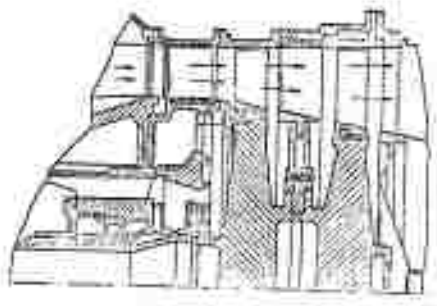

Figure 83: Diagram of a double-stage turbine for a turbojet engine.

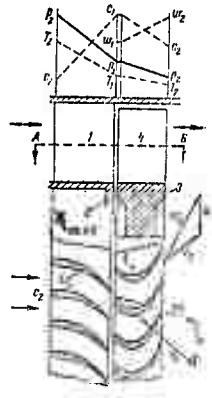

Figure 84: Diagram of a turbine stage:
1 - nozzle blade; 2 - turbine casing; 3 - turbine wheel; 4 - rotor blades;

Legend:
X - section through A-B

A further reduction in the enthalpy of the gas, or its expansion from a pressure p_1 to a terminal pressure p_2 behind the turbine, takes place in the spaces between the rotor blading, and as a result the relative velocity of the gas motion between the blades increases from w_1 to w_2. At the same time the absolute gas velocity decreases even then from c_1 to c_2, since a significant part of the kinetic energy acquired by the gas in the nozzle blading and rotor blading is transferred to the rotor blades and

through the turbine wheel to the turbine shaft, which means that it is converted into external mechanical work.

Plotting the outlet velocity triangle makes it possible to determine the magnitude and direction of the absolute gas velocity c_2 at the outlet of the turbine wheel. It is obvious that the greater the velocity c_2, the greater will be the kinetic energy of the gas that is not consumed in the turbine, or the greater will be the so-called turbine outlet loss $c_2^2/2_g$.

The acceleration of the gas flow during its relative motion through the spaces between the rotor blading of a reaction turbine results in a reaction force being applied to the rotor blading (reaction effect of the flow). In addition the rotor blades absorb the force that develops as a result of the change in the direction of the velocity of the gas motion around the blades (action effect of the flow). The circumferential components of these forces also yield the torsional moment on the turbine wheel.

There is no gas expansion in the spaces between the rotor blades of action turbines, and consequently no gas acceleration, either. Consequently, there is no reaction effect of the gas flow on the rotor blades, and the circumferential force applied to the rotor wheel results only from the action effect of the flow which means that it results from the change in the direction of gas velocity.

The difference between the enthalpies of 1 kg of gas in front of the turbine and behind it under adiabatic gas expansion from a total pressure p_z^* in front of the turbine to a terminal static pressure p_2 behind the turbine is the adiabatic heat drop h_T accomplished in the turbine. It is seen from the iS-diagram in figure 85 that

$$h_T = i_z^* - i_{2\,ad} = c_p'(T_z^* - T_{2\,ad})$$

or

$$h_T = c_p' T_z^* \left[1 - \left(\frac{p_2}{p_z^*}\right)^{\frac{k'-1}{k'}}\right], \tag{7.1}$$

where i_z^* and $i_{2\,ad}$ are the total enthalpy of the gas in front of the turbine and its enthalpy after adiabatic expansion in the turbine, respectively;

$T_{2\,ad}$ is the temperature upon completion of adiabatic expansion to a pressure p_2;

c_p' and k' are the specific heat under constant pressure and the adiabatic exponent of the combustion products during their expansion in the turbine.

The greater the part of total heat drop h_T that is accomplished at the rotor blading the greater will be the rate of increase of the relative gas velocity w_2, and the reaction effect of the flow

at the circumference of the rotor wheel will increase. The distribution of total heat drop h_T (cf. figure 85) between nozzle assembly and bucket ring is assumed to be described by the degree of reaction ρ of the stage, equal to the ratio between the adiabatic heat drop h_r accomplished at the bucket ring and the available heat drop h_T, in other words

$$\rho = h_r/h_T. \qquad (7.2)$$

It is obvious that for a reaction turbine, $\rho > 0$, since $h_r = 0$, $\rho = 0$.

With identical heat drops h_T the heat drop $h_T - h_r = h_n$ that is accomplished in the nozzle assembly of a reaction turbine and its corresponding gas exhaust velocity are less than they are in the nozzle assembly of an action turbine. At the same time the profiles of reaction turbine rotor blades also prove to be more favorable with respect to aerodynamics than the profiles of action turbine rotor blades. Therefore, the reaction turbine differs from the action turbine in that the energy losses incurred during the flow of the gas in the spaces between nozzle blading and rotor blading are less.

Moreover, the energy losses connected with radial gas leakage toward the periphery in the space between nozzle assembly and turbine wheel, and also with gas leakage in the rotor blade spaces that develops under the effect of centrifugal forces, can be eliminated or significantly reduced in a reaction turbine.

The degree of reaction for the mean diameter of the turbine wheel ranges approximately between 0.20 and 0.35 for turbines of existing turbojet engines.

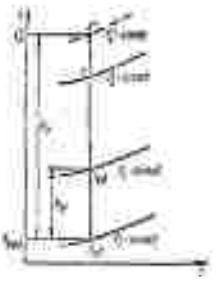

Figure 85: Determination of the available heat drop in a turbine.

If a significant heat drop (h_T > 75 to 80 kcal/kg) must be accomplished in a turbine, a sufficiently great efficiency (see below) must be ensured by dividing this heat drop between several stages, which means that a multi-stage turbine must be used.

A multi-stage turbine with pressure stages (see figure 86) consists of successively alternating nozzle assemblies a and

bucket rings b. The latter are fastened to a common drum (a wide turbine wheel, if there are two to three stages) or to individual disks secured to a common shaft.

In this type of turbine, gas expansion takes place gradually in the nozzle assemblies and bucket rings of each successive stage (see figure 86), and the heat drop and pressure drop attributed to each stage are reduced in comparison to a single-stage turbine.

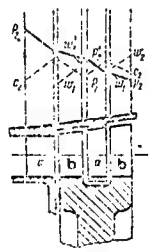

Figure 86: Diagram of a pressure stage turbine.

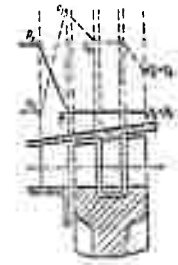

Figure 87: Diagram of a velocity stage turbine.

The degree of reaction of each stage of multi-stage turbine is determined by the ratio between the adiabatic heat drop at the rotor blades of that stage and the adiabatic heat drop attributed to the stage in question.

Also, a multi-stage turbine can be designed with velocity stages (see figure 87). In that case a fixed guide assembly is installed behind a first stage of the action type whose blades change the direction of the gas flow behind the first bucket ring and direct it to a second row of (action) rotor blades where the kinetic energy of the flow that departed from the first stage is partially exploited, too. If the absolute gas velocity still remains significant at the outlet of the second stage, a third stage can be installed, etc.

Velocity stages failed to find an application in aviation turbines because they cannot provide the required high values of efficiency.

2. Gas Outflow from the Nozzle Assembly of a Turbine

The gas outflow velocity from the nozzle assembly of a turbine is determined from the energy equation for the section between the inlet cross-section zz and the outlet cross-section 1,1 of the nozzle duct. This equation has the following form, if there is no heat exchange or resistance:

$$i_z^* = i_z + A \cdot \frac{c_z^2}{2g} = i_{1,1}^* + A \cdot \frac{c_{1t}^2}{2g},$$

whence

$$c_{1t} = \sqrt{2g \cdot \frac{i_z^* - i_{1\,ad}}{A}} \qquad (7.3)$$

where c_{1t} is the theoretical gas outflow velocity from the nozzle ducts;

$i_{1\,ad}$ is the enthalpy of 1 kg of gas at the end of adiabatic expansion in the nozzle ducts.

The true gas outflow velocity c_1 is less than the theoretical velocity c_{1t} because of losses in the nozzle assembly that are associated with flow deflection, vorticities, flow separation, and other causes. However, at the present time data based on experience that could be used to evaluate these losses individually by type are still inadequate. Therefore, an aggregate coefficient is used that takes into account a combination of all the losses, and the true outflow velocity is determined as the product $\varphi \cdot c_{1t}$, so that

$$c_1 = \varphi c_{1t}, \qquad (7.4)$$

where φ is the so-called velocity coefficient that takes into account the reduction in outflow velocity caused by all the losses inherent in the nozzle assembly.

Turbines of modern turbojet engines usually have a coefficient of $\varphi = 0.96$ to 0.98 (convergent nozzle ducts, see below).

The difference $i_z^* - i_{1\,ad}$ is the adiabatic heat drop h_n accomplished in the nozzle assembly during gas expansion from a pressure p_z^* to a pressure p_1 (see figure 85), so that in accordance with equation (7.2)

$$h_c = (1-\rho) h_n.$$

Moreover, $\sqrt{2gA} = \sqrt{2 \cdot 9{,}81 \cdot 427} = 91{,}5$. Consequently,

$$c_1 = 91{,}5\varphi\sqrt{(1-\rho) h_n}. \qquad (7.5)$$

The area of any cross-section f_n of a nozzle duct can be determined from the flow equation

$$f_n = G_g \cdot v/c \qquad (7.6)$$

where G_g is the gas flow rate through the nozzle, kg/sec;

c is the gas velocity in the given nozzle cross-section, m/sec;

v is the specific volume of the gas in the same cross-section, m^3/kg.

The dependence of the required area f_n of the nozzle cross-section on the pressure ratio p/p_z^* for otherwise unchanged constituent magnitudes is shown in figure 88.

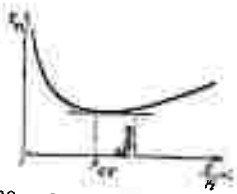

Figure 88: Dependence of the nozzle cross-section area on the pressure ratio.

It is seen that with decreasing pressure p (with decreasing ratio p/p_z^*) as the gas expands in the nozzle the nozzle area is initially reduced, achieving a minimum for some value p/p_z^* that is equal to $p_{cr}/p_z^* = \pi_{cr}$, and subsequently increases.

The nature of this change in nozzle cross-section along the length of the nozzle is explained as follows. During the first part of the expansion process, where $p/p_z^* \geq \pi_{cr}$, gas velocity increases faster than the specific volume of the gas; therefore, to the degree that the gas expands the required cross-section area is reduced. During the last part of expansion, where $p/p_z^* < \pi_{cr}$, gas velocity continues to increase, but at a slower rate than specific volume so that the nozzle cross-section area must be increased.

The pressure ratio that equals π_{cr}, or corresponds to the minimum nozzle cross-section, is called <u>critical pressure ratio</u>, and the pressure that equals $p_{cr} = p_z^* \pi_{cr}$ is called <u>critical pressure</u>.

It was demonstrated in thermodynamics that

$$\frac{p_{cr}}{p_i^*} = \pi_{cr} = \left(\frac{2}{k'+1}\right)^{\frac{k'}{k'-1}}, \tag{7.7}$$

in other words, the magnitude of critical pressure ratio depends only on the adiabatic exponent, and for $k' = 1.32$ to 1.35, which is characteristic for gas turbine engines, $\pi_{cr} = 0.55$ to 0.54.

Thus, if the pressure in the space into which the gas flows (in the space between the nozzle assembly and the bucket ring of the turbine) is $p_1 \geq p_{cr}$, or $p_1/p_z^* \geq \pi_{cr}$, the nozzle must be convergent, in other words, its outlet cross-section must be smaller than the preceding cross-sections (see figure 89, a). In that case the gas expands completely in the convergent nozzle to an external pressure p_1, and the outflow velocity $c_1 \leq c_{cr}$.

If the pressure in the space into which the gas flows is $p_1 < p_{cr}$, in other words, if $p_1/p_z^* < \pi_{cr}$, the nozzle must terminate with a divergent part (see figure 89, b) in order to accomplish complete gas expansion to the pressure p_1 in the nozzle and to obtain a supersonic outflow velocity (greater than critical velocity).

In the convergent nozzle represented in figure 89, a, if $p_1/p_z^* < \pi_{cr}$, the gas cannot expand completely to an external

pressure $p_1 < p_{cr}$ because the nozzle flow area is not sufficiently increased.

In that case a critical pressure $p_{cr} > p_1$ and a critical velocity are established in the outlet (minimum) cross-section of the nozzle that remain constant no matter how much the external pressure p_1 is reduced, under otherwise unchanged conditions, in comparison to critical pressure.

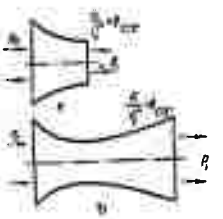

Figure 89: Nozzle configurations:
a - convergent (subsonic); b - divergent (supersonic)

Continued gas expansion from pressure p_{cr} takes place outside the convergent nozzle. During this process the energy that corresponds to the expansion of the gas from pressure p_{cr} to p_1 is consumed primarily for the jet spreading out under the effect of its excess internal pressure and for generating wave-type flow oscillations, and consequently there is no substantial increase in gas velocity above c_{cr} outside the nozzle under consideration.

Gas turbine nozzles are always inclined under some angle α_1' to the rotational plane of the turbine wheel, and the outlet cross-sections of nozzle ducts are not perpendicular to their axes (see figure 90). Therefore, the so-called oblique nozzle outlet section is formed at the outlet of each nozzle duct, in other words, the half-open part ecd of the duct.

Unlike the nozzle with straight outlet section (as shown in figure 89, a) the convergent nozzle with oblique outlet section makes it possible to obtain, if $p_1/p_z^* < \beta_{cr}$, a gas outflow velocity greater than critical velocity at the outlet (from the oblique outlet section). This is explained by the fact that the oblique outlet section has the effect of a divergent nozzle. In other words, if $p_1/p_z^* < \beta_{cr}$, a critical pressure $p_{cr} > p_1$ and a critical velocity are established in the minimum cross-section cd that is perpendicular to the nozzle axis, or in the initial cross-section of the oblique outlet section (see figure 90), and continued gas expansion with gas velocity increasing above critical velocity takes place in the oblique outlet section itself.

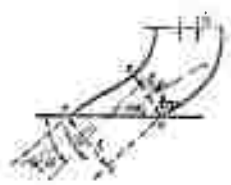

Figure 90: Nozzle with oblique outlet section.

When gas expands in an oblique outlet section the gas pressure is decreased gradually along the wall ce while in point d it drops almost abruptly to the external pressure p_1. As a result the gas jet in an oblique outlet section is exposed to greater pressure from the direction of the wall ce, causing the gas mass to move away from this wall in a direction perpendicular to it. Consequently, the gas jet is deflected by a certain angle δ from the nozzle axis and flows from the oblique outlet section de at an angle equaling $\alpha_1 = \alpha_1' + \delta$.

If the pressure ratio is subcritical, the outlet pressure p_1 is established in the narrow nozzle cross-section cd, and there is no subsequent gas expansion and gas jet deflection in the oblique outlet section (angle $\delta = 0$).

Convergent nozzles are used exclusively in the turbines of aviation gas turbine engines, and their oblique outlet sections are exploited to achieve additional gas expansion to the degree that is necessary. These nozzles operate equally well under almost all regimes, while divergent nozzles are very sensitive (from the point of increasing losses) to a change in regime. Moreover, using divergent nozzles also complicates the design of the turbine nozzle assembly.

3. Energy Conversion at the Rotor Blades

The gas flow, after departing at a velocity c_1 from the nozzle ducts through the axial space separating the nozzle assembly from the bucket ring, enters the ducts formed by the rotor blades.

The gas flow has a relative velocity with respect to the rotor blades whose direction is determined by the angle β_1 (see figure 91).

Based on the cosine theorem it follows from the inlet velocity triangle of the turbine wheel that

$$w_1 = \sqrt{c_1^2 - u^2 - 2uc_1\cos\alpha_1}, \tag{7.8}$$

where α_1 is the angle at which the gas jet departs from the nozzle duct (taking into account the deflection in the oblique outlet section, if the gas expands in it).

It is seen from the same velocity triangle that the axial component c_{1a} and the circumferential component c_{1u} of absolute velocity c_1 equal

$$c_{1a} = c_1 \sin \alpha_1 = w_1 \sin \beta_1; \tag{7.9}$$

$$c_{1u} = c_1 \cos \alpha_1 = w_1 \cos \beta_1 + u. \tag{7.10}$$

The angle β_1 is determined with the aid of these relationships and equalities:

$$\sin \beta_1 = \frac{c_1}{w_1} \cdot \sin \alpha_1.$$

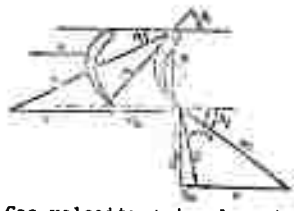

Figure 91: Gas velocity triangles at the inlet and outlet of the turbine rotor blades.

The relative gas velocity w_2 at the outlet of the ducts formed by the rotor blades (see figure 91) is determined with the aid of the energy equation. This equation has the following form, applicable to the relative motion of 1 kg of gas between the rotor blades (not including losses):

$$i_{2\,ad} + A \cdot \frac{w_{2t}^2}{2g} = i_1 + A \cdot \frac{w_1^2}{2g},$$

whence

$$w_{2t} = \sqrt{\frac{2g}{A}(i_1 - i_{2\,ad}) + w_1^2}. \tag{7.11}$$

where w_{2t} is the theoretical relative gas velocity at the rotor duct outlets;

$i_{2\,ad}$ is the enthalpy of 1 kg of gas upon completion of adiabatic expansion to a pressure p_2 behind the turbine wheel.

The flow of the gas through the bucket ring is accompanied by losses, as it was through the nozzle assembly. Therefore, the true relative gas velocity w_2 is less than the theoretical velocity w_{2t}, so that

$$w_2 = \psi w_{2t}, \tag{7.12}$$

where ψ is the velocity coefficient for the rotor blades, a magnitude corresponding to the coefficient φ for the nozzles.

As a rule, the coefficient ψ for turbines of modern turbojet engines is not less than 0.94 to 0.95 and achieves even greater magnitudes in individual instances.

Taking note that the difference between enthalpies in equation (7.11) is the adiabatic heat drop h_r at the rotor blades and

can be expressed on the basis of formula (7.2), by the degree of reaction $h_r = ph_T$, and substituting the numerical values for A and g, we obtain the following expression for the desired relative velocity:

$$w_2 = \varphi \sqrt{2g(h_T - h_r) + w_1^2}. \tag{7.13}$$

The magnitude of absolute gas velocity at the rotor outlet is determined with the aid of the outlet velocity triangle (see figure 91) from which it follows, based on the cosine theorem, that

$$c_2 = \sqrt{w_2^2 + u^2 - 2uw_2 \cos\beta_2} \tag{7.14}$$

The axial and circumferential components of this velocity will be equal to

$$c_{2a} = c_2 \sin\alpha_2 = w_2 \sin\beta_2; \tag{7.15}$$

$$c_{2u} = c_2 \cos\alpha_2 = w_2 \cos\beta_2 \mp u \tag{7.16}$$

The lower signs in the last expression refer to the case where the angle $\alpha_2 > 90^\circ$. This angle determines the direction of the gas flow at the rotor outlet and can be found with the aid of the obvious relationship

$$\sin\alpha_2 = \frac{w_2}{c_2} \sin\beta_2.$$

Let us now determine the force applied by the gas flow to the rotor blades in the rotational direction of the rotor. For this purpose let us use the momentum equation established for the direction of the circumferential velocity u. If we assume the direction of rotor rotation to be positive, and if the gas flow-rate through the turbine equals 1 kg/sec, this equation is written as follows:

$$P_u = -P'_u = \frac{c_{1u} \pm c_{2u}}{g}, \tag{7.17}$$

where P_u is the force applied to the bucket ring by each kilogram of gas flowing through the turbine per second;

P'_u is the action force of the rotor blades applied to the gas flow, equal in magnitude and opposite in direction to the desired force P_u.

There are two signs in front of c_{2u} in equation (7.17). This is due to the fact that the direction of velocity c_{2u} can coincide with the direction of velocity c_{1u} ($\alpha_2 > 90^\circ$), or can be opposite to that direction ($\alpha_2 < 90^\circ$). In the first case there must be a minus sign in equation (7.17), and in the second case a plus sign.

Further, using the equality of (7.10) and (7.17), we can write

$$c_{1u} \pm c_{2u} = w_1 \cos\beta_1 + w_2 \cos\beta_2.$$

Substituting this expression in equation (7.17) we obtain

$$P_u = \frac{w_1 \cos\beta_1 \pm w_2 \cos\beta_2}{g}. \tag{7.18}$$

Multiplying the force P_u by the velocity of blade motion, u, we find the work done by 1 kg of gas at the rotor circumference during a period of one second:

$$L_u = uP_u \qquad (7.19)$$

The force applied by the gas flow to the bucket ring in the axial direction can be determined with the aid of the momentum equation, too.

4. Turbine Efficiency and Turbine Power

The following types of energy losses are encountered in a gas turbine:

losses with outlet velocity, in other words, losses determined by the magnitude of kinetic energy in the gas flow departing from the bucket ring (kinetic energy not used in the turbine);

losses due to overcoming resistance in the nozzle assembly and bucket ring (the effect of these losses was taken into account above, with the aid of coefficients φ and ψ);

losses connected with gas leaks through clearances;

losses due to overcoming the friction of the face surfaces of the turbine wheel against the gas;

losses due to overcoming friction in the turbine shaft bearings.

The first two types of losses are the greatest and are rated by means of the relative efficiency at the rotor circumference, η_u. This efficiency equals the ratio between the work obtained at the rotor circumference (for its mean diameter) and the available work or the adiabatic heat drop h_T for the turbine (stage):

$$\eta_u = \frac{AL_u}{h_T} \qquad (7.20)$$

The adiabatic heat drop that can be accomplished in the turbine (in the stage) can be expressed by the kinetic energy:

$$h_T = A\frac{c_0^2}{2g}, \qquad (7.21)$$

where c_0 is the conditional outlet velocity that could be obtained if the heat drop h_T were completely converted into kinetic energy.

Now, using formulas (7.19), (7.20), and (7.21) we obtain

$$\eta_u = 2g\frac{uP_u}{c_0^2}. \qquad (7.22)$$

A detailed examination of this expression shows that the velocity ratio u/c_0 has the greatest effect on the magnitude of η_u. If u/c_0 is increased, the relative efficiency η_u will increase initially and reach a maximum for a certain value of u/c_0. At this point the total losses assume a minimum. Further increase of u/c_0 is accompanied by a reduction in η_u, primarily due to increasing losses with outlet velocity. At the same time, the greater the degree of reaction p, the greater will be the value of u/c_0 at which a maximum for η_u is obtained.

This is illustrated by the graphs in figure 92 showing (dotted curves) the dependence of η_u on u/c_0 for different values of p and for $\alpha_1 = 20^\circ$, $\varphi = 0.96$, $T_z^* = 1100^\circ$ K.

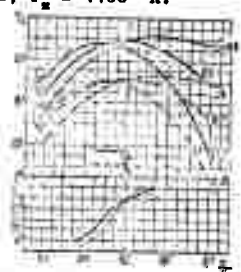

Figure 92: Dependence of turbine efficiency η_u on the velocity ratio.

The kinetic energy that is not used in the turbine is determined by the magnitude of absolute gas velocity at the outlet of the bucket ring (of the last stage), in other words, $c_2^2/2g$ does not represent a loss to the gas turbine engine as a whole. A significant part of this energy (after deducting the loss in the section between turbine and jet nozzle outlet) is used to generate reaction thrust. Therefore, considering the turbine as part of the engine, it is expedient not to use h_T as the available work but the difference

$$h_T^* = h_T - A \cdot \frac{c_2^2}{2g} = c_p (T_z^* - T_{2ad}^*).$$

This difference is the work of the ideal turbine having the same outlet gas velocity by magnitude as the comparable real turbine. Also introduced in this context is the notion of the relative efficiency at the rotor circumference using the outlet velocity, in other words

$$\eta_u^* = \frac{AL_u}{h_T - A \cdot \frac{c_2^2}{2g}} = \frac{AL_u}{h_T^*}. \qquad (7.23)$$

Since $h_T^* < h_T$ it follows that $\eta_u^* > \eta_u$.

Strictly speaking, this efficiency does not describe the effectiveness of the turbine but it will be shown later that the exhaust velocity from the jet nozzle and, consequently, the thrust of the turbojet engine, is directly dependent on precisely the magnitude of this efficiency.

The relative efficiency using the outlet velocity, η_u^*, is dependent on the same factors as the relative efficiency η_u. Like η_u, the relative efficiency η_u^* increases with increasing coefficients φ and ψ.

The dependence of η_u^* on the ratio u/c_0 for different values of p is represented by the solid curves in figure 92. However, there the curve of the most favorable values of p for the given case was plotted as a function of u/c_0.

When we determined the relative efficiency at the rotor circumference and the work L_u we made the assumption that the entire quantity of gas supplied to the turbine flows through the ducts between the rotor blades. Actually, a certain part of the gas leaks through the annular space between bucket ring and turbine casing and escapes the ducts between the rotor blades. Therefore, the work received by the rotor will be slightly less than the work L_u obtained above.

Moreover, part of the work received by the turbine wheel is expended on friction between its face surfaces and the gas.

As a result the work L_{iT} that is transferred to the turbine shaft, or the so-called internal work of the turbine, is always less than the work L_u.

Referring the work L_{iT} and the work losses mentioned above to 1 kg of gas moving through the turbine per second we can write

$$L_{i_T} = L_u - L_{leak} - L_f = L_u \left(1 - L_{leak}/L_u - L_f/L_u\right)$$

where L_{leak} is the work lost due to gas leaks;

L_f is the friction work of the face surface of the turbine wheel.

The ratio L_{leak}/L_u depends on the relative magnitude of the radial clearance between the blades and the turbine casing that surrounds them (when the turbine is hot); for the types of clearance encountered in turbines of modern engines we can roughly use a ratio $L_{leak}/L_u = 0.01$ to 0.02.

As a result of high gas flowrates through the turbine the magnitude of L_f proves to be insignificant and as a rule $L_f/L_u \leq 0.01$.

Thus, we can assume that

$$L_{iT} = (0.97 \text{ to } 0.98)\, L_u.$$

The ratio between the work transferred to the turbine shaft and the adiabatic heat drop in the turbine is called internal relative efficiency or relative indicator efficiency, in other words,

$$\eta_{i_T} = \frac{AL_{i_T}}{h_T^*} = (0.97 - 0.98)\,\eta_{in}$$

or, taking into account the outlet velocity,

$$\eta_{i_T}^* = (0.97 - 0.98)\,\eta_u^*.$$

The work L_T that is removed from the turbine shaft, or the effective work, will be less than the work L_{iT} since part of the latter is expended to overcome friction in the turbine bearings.

Friction losses in the turbine bearings are taken into account by the mechanical efficiency η_{MT}, equaling the ratio between the shaft work L_T and the work L_{iT}.

As a rule, mechanical efficiency is high due to the employment of anti-friction bearings that absorb a relatively small part of the load. Roughly, the following can be used:

$$\eta_{M_T} = \frac{L_T}{L_{i_T}} = 0.98 - 0.99.$$

The ratio between the work removed from the turbine shaft and the adiabatic heat drop in the turbine is called relative effective efficiency, η_T:

$$\eta_T = \frac{AL_T}{h_T}.$$

This efficiency takes into account all the energy losses in the turbine considered above and determines the magnitude of the work that can be removed from the turbine shaft under a given value of adiabatic heat drop.

Taking into consideration the exploitation of the outlet velocity in the jet nozzle, the relative effective efficiency will equal

$$\eta_T^* = \eta_{in_T}\eta_T^* = \frac{AL_T}{h_T^*}.$$

For aviation turbines these efficiency factors are:

$$\eta_T = 0{,}64 - 0{,}80;$$
$$\eta_T^* = 0{,}82 - 0{,}91.$$

It was shown above that an increase in turbine efficiency can be achieved by increasing the velocity ratio u/c_0 to a certain limit. However, under practical circumstances an increase of u/c_0 is limited, for a given heat drop in the turbine, by the value for the circumferential rotor velocity u that can be achieved, considering the strength of the turbine wheel and especially of the rotor blades. The greater the length of the rotor blades for a given turbine wheel diameter, the slower must be, under otherwise equal conditions, the circumferential velocity. Modern turbojet engines have a circumferential velocity at the mean turbine wheel diameter amounting from 270 to 360 m/sec and sometimes more, and a velocity ratio $u/c_0 = 0.4$ to 0.45.

Turbine efficiency is reduced greatly with a reduction in the values of u/c_0. Small values for u/c_0 are obtained when great heat drops must be accomplished in the turbine at a limited circumferential rotor velocity. In that case it can prove necessary to use double-stage or multi-stage turbines in order to ensure the required magnitude of efficiency.

By dividing the heat drop that can be accomplished in the turbine between several pressure stages, it is possible to reduce the circumferential rotor velocity and maintain the most advantageous ratio u/c_0 for each stage individually, or a ratio close to it, thus ensuring a sufficiently great efficiency for the turbine as a whole.

Moreover, building a turbine as a multi-stage configuration (with pressure stages) tends to increase its efficiency for the following additional reasons:

as a result of the reduced heat drop in the stages the gas velocity in the turbine flow section is decreased which leads to a reduction of losses in the nozzle and rotor ducts;

a reduction of gas velocity in the ducts between the blades and a reduction of turbine wheel diameter, resulting in a decrease of circumferential rotor velocity for a given rpm, lead to an increase in blade length, thus reducing the relative losses due to gas leaks through the radial clearances between blades and turbine casing;

the outlet gas velocity of each stage with the exception of the last stage is exploited by the following stage, and the outlet velocity of the last stage is reduced in accordance with the reduction in heat drop attributed to that stage;

the increase in the enthalpy of the gas that is due to internal losses in a stage is partially exploited to produce useful work in the following stages.

The disadvantages of a multi-stage turbine is that the blades of its initial stages, and especially of the first stage, operate under conditions of greater temperatures than the blades of a single-stage turbine having the same heat drop h_T and initial gas temperatu T_z. This is explained by the fact that the reduction in heat drop and, consequently, in pressure drop as well, also has the result that the temperature reduction in a stage (in the nozzle assembly) of a multi-stage turbine is smaller than in a single-stage turbine.

Moreover, increasing the number of stages results in an increase in the length of the turbine which can lead to an increase in turbine weight. However, since the turbine diameter is reduced in the process the transition, for instance, from a single-stage to a double-stage configuration is accompanied by a comparatively small increase in turbine weight.

As an example, let us consider the thermal process of a double-stage turbine with pressure stages and non-cooled blades. This process is represented in the iS-diagram in figure 93. In front of the first turbine stage the pressure p_z, the gas velocity c_z, and the total enthalpy of 1 kg of gas are determined by the point z*. The terminal gas pressure at the rotor outlet of the last, the second turbine stage, equals p_2. Here the adiabatic heat drop h_T that is accomplished in the turbine is measured by the distance z^*2_t.

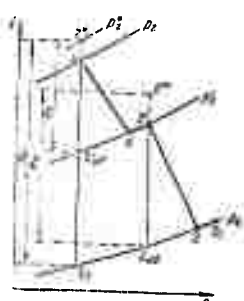

Figure 93: Expansion process in a double-stage turbine with pressure stages.

In the first turbine stage the gas expands from a pressure p_z to a pressure $p_2' > p_2$. As a result of the gas being heated due to friction in the nozzle and rotor ducts this expansion process deviates from the adiabat $z2'_{ad}$ and is represented by the curve z0. Therefore, the true enthalpy of the gas at the outlet of the rotor blades of the first stage is determined by point 0. But the adiabatic heat drop h_I (taking into account the initial velocity c_z) that is accomplished in the first turbine stage, is measured by the distance $z^*2'_{ad}$.

Friction against the rotor face surfaces and leakage of part of the gas through the radial rotor clearances of the first stage have the result that the enthalpy of the gas at the inlet of the second stage is slightly greater than at the outlet from the rotor blades of the first stage, so that it is not determined by point 0 but by point 2'. As a result, and also due to losses in the nozzle and rotor ducts of the second stage, the actual gas expansion process in that stage from a pressure p_2' to a pressure p_2 is represented by the curve 2'2.

The velocity at the inlet of the second stage equals the velocity c_2' at the outlet of the first stage rotor. If we take into account the energy that corresponds to this velocity, the adiabatic heat drop h_{II} that is accomplished in the second turbine stage will be measured by the distance $2'^*2_{ad}$.

If we increase the initial temperature the adiabatic heat drop will be increased for the same pressure drop. Consequently, for a double-stage turbine (see figure 93) $h_I + h_{II} > h_T$, and for a turbine with any number of stages $\Sigma h_{st} > h_T$, where h_{st} is the adiabatic heat drop in each individual stage.

Thus, in a multi-stage turbine the sum of the adiabatic heat drops in the individual stages is greater than the adiabatic heat drop h_T in the turbine as a whole. Physically this is explained by the fact that the losses in each stage, as we showed above, cause an increase in the enthalpy of the gas departing from that stage, thus causing a certain increase of the heat drop in the following stage.

Taking the above into consideration we can write

$$\Sigma h_{st} = (1 + \alpha) h_T$$

where $\alpha > 0$ can also be called the energy recovery factor.

Now, let us assume for simplitiey that the relative efficiencies at the rotor circumferences, $\eta_{u\ st}$, and the adiabatic heat drops h_{st} are identical for all stages. In that case it is obvious that the work $L_{u\ st}$ at the rotor circumferences of all stages will be identical, too, and if z is the number of stages,

$$\Sigma L_{u\ st} = zL_{u\ st} = L_{uT}$$

where L_{uT} is the aggregate work at the rotor circumference of the entire turbine as a whole.

Therefore, in this case the relative efficiency at the rotor circumference of any stage will equal

$$\eta_{u\ st} = zAL_{u\ st}/zh_{st} = \frac{AH_{u_T}}{(1+\alpha)h_T} = \frac{\eta_T}{1+\alpha}.$$

Consequently, $\eta_u = (1+\alpha)\eta_{u\ st}$, in other words, the efficiency of the entire turbine as a whole is greater than the mean efficiency of its stages taken individually.

The energy recovery factor α that enters into the cited relationships increases with increasing number of stages, losses in the stages, and gas expansion ratio in the turbine. For double-stage and triple-stage aviation turbines, this factor in the majority of cases is $\alpha = 0.04$ to 0.08.

The <u>effective power</u> or the power N_T that is removed from the turbine shaft, is determined by the product of the effective work L_T and the weight flowrate per second of combustion products through the turbine, G_g, and is

$$N_T = L_T G_g/75.$$

But since, in accordance with the foregoing,

$$L_T = \frac{h_T}{A}\cdot\eta_T = \frac{h_T^*}{A}\cdot\eta_T^*$$

it applies, correspondingly, that

$$N_T = G_g/75A \cdot h_T\eta_T = G_g/75A \cdot h_T^*\eta_T^*.$$

The effective turbine power of a turbojet engine must be slighly in excess of the power N_k required to drive the compressor, by the magnitude required to drive the auxiliary machinery and to supply cooling air. For modern turbojet engines the mean is $N_T \approx 1.02\ N_k$, whence $L_T G_g \approx 1.02\ L_k G_a$.

However, for a turbojet engine the ratio between the flowrate of combustion products through the turbine and the air flowrate through the compressor usually on the average also equals $G_g/G_a = \frac{1+d_0}{\alpha l_0} \approx 1{,}02$, hence

$$L_T = L_k, \tag{7.24}$$

in other words, for a turbojet engine the effective work of the turbine must be equated to the effective work of the compressor, which is the basic condition for a balanced regime of operation (see below) of a turbojet engine.

With the aid of (7.21), (7.23), and (7.24) we can find the required expansion ratio of the combustion products in the turbine of a turbojet engine, $\varepsilon_T = \frac{p_T^*}{p_2^*}$. Actually, $L_T = \frac{h_T\eta_T}{A} = L_k$

and

$$h_T = c_p' T_z^* \left[1 - \left(\frac{p_2}{p_z^*}\right)^{\frac{k'-1}{k'}}\right].$$

Therefore,

$$\frac{1}{\varepsilon_T} = \frac{p_2}{p_2^*} = \left(1 - \frac{A L_K}{c_p \eta_T T_2^*}\right)^{\frac{k'}{k'-1}}, \tag{7.25}$$

where p_2 is the static pressure behind the turbine, or in front of the jet nozzle of a turbojet engine.

It is seen that, under otherwise equal conditions, the pressure p_2 behind the turbine will decrease with increasing compressor work L_K and decreasing temperature T_2^* in front of the turbine and decreasing turbine efficiency η_T. At the same time the pressure p_2 behind the turbine also depends on airspeed and altitude, since $p_2^* = \varepsilon_{D,c} p_K^* = \varepsilon_{K,c} p_H \pi_c^*$. All of this equally affects the total pressure p_2 behind the turbine.

CHAPTER 8

THE JET NOZZLE OF THE TURBOJET ENGINE

1. Gas Flow in the Jet Nozzle

The final expansion of the combustion products and the conversion of the remaining heat drop behind the turbine into kinetic energy takes place in the jet nozzle. This conversion must be accomplished with a minimum of losses possible under all conditions of engine operation.

As a rule the jet nozzle is located at a certain distance from the turbine and connected with the turbine casing by means of the jet exhaust pipe (exhaust cone), forming the engine exhaust system together with the latter.

If the exhaust system must be lengthened for engine installation in an aircraft an additional extension pipe is installed between jet nozzle and exhaust pipe where, as we mentioned earlier, the gas flow is slowed down. As a result the gas flows along the extension pipe at a reduced velocity which favors a reduction of losses in the pipe. As a rule, the gas velocity at the end of the exhaust pipe or in cross-section e'e' at the jet nozzle inlet is $c'_e = (0.75 \text{ to } 0.90)c_2$.

The walls of the jet nozzle, and very frequently even of the entire exhaust system, are cooled by air. The exhaust pipe walls of some engines have a heat insulation that reduces heat losses to the environment and protects nearby aircraft parts against being heated.

A typical diagram of the exhaust system of a turbojet engine consisting of exhaust cone and air-cooled jet nozzle with fixed discharge area, is shown in figure 94.

Variable area jet nozzles of turbojet engines are usually given an exhaust flap configuration. In these nozzles, as seen in figure 95, the walls consist of a number of flaps or segments (petals) with a variable angle of inclination α_{fl} relative to the longitudinal symmetry axis of the nozzle. If this angle is reduced the nozzle discharge area is increased, and if the angle is increased the area is reduced. The flaps are displaced in the nozzle closing direction by hydraulic or air pressure with the aid of several actuating pistons located in actuating cylinders that are secured to the exhaust cone casing. The flaps open under the effect of the gas flow escaping from the jet nozzle.

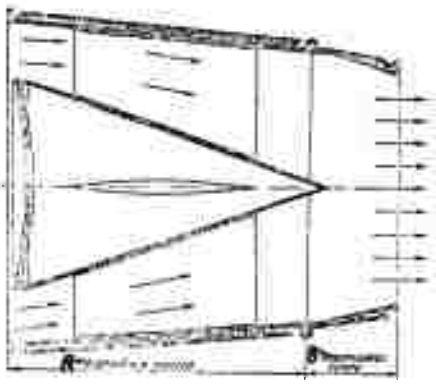

Figure 94: Diagram of the exhaust system of a turbojet engine.

Legends:
A - transition chamber;
B - jet nozzle.

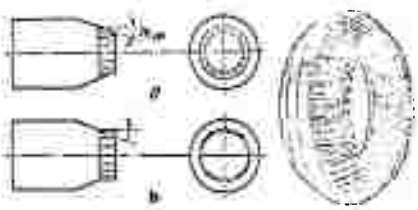

Figure 95: Diagram of a variable area jet nozzle: a - nozzle throttled; b - nozzle opened.

The gas flow is discharged from the jet nozzle at a high velocity and a significant temperature. In modern turbojet engines operating under the designed regime in static operation on the ground the gas velocity c_e at the jet nozzle outlet reaches 550 to 650 m/sec, and the temperature T_e = 830 to 850°K., if no fuel is burned in the afterburner behind the turbine (see below). As the gas flow moves away from the jet nozzle discharge area it is mixed with the surrounding air and gradually dissipates; gas velocity and temperature are reduced. However, the velocity and temperature in the gas flow still remain significant at a fairly considerable distance from the jet nozzle (see figure 96). This requires compliance with the necessary safety measures when the engine is operated on the ground, either in the aircraft or on a test stand. The turbojet engine must be so located in the

aircraft that the danger of the gas flow damaging the fuselage and empennage and the possibility of destroying the runway surface are eliminated.

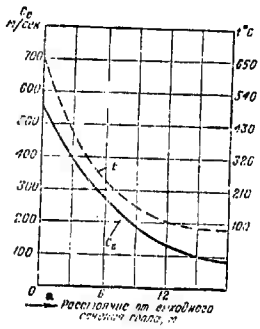

Figure 96. Gas temperature and velocity beyond the jet nozzle of the turbojet engine.

a- distance from nozzle output section, meters.

The gas exhaust velocity from the jet nozzle can be found with the aid of the energy equation written for the gas flow in the section between the turbine outlet cross-section 2,2 and the jet nozzle outlet cross-section ee. If we disregard hydraulical resistance and heat transfer from the gas to the engine exhaust system, this equation can be written as follows, for one kg of gas:

$$i_2^* + A\frac{c_2^2}{2g} = i_{e\,ad} + A\frac{c_{e\,t}^2}{2g}.$$

whence, substituting $i_2^* = i_2 + A\frac{c_2^2}{2g}$, we obtain

$$c_{e\,t} = \sqrt{2g\frac{k}{k-1}RT_2^*\left(1-\frac{T_{e\,ad}}{T_2^*}\right)}. \qquad (8.1)$$

where c_{et} is the theoretical exhaust velocity (not accounting for losses) from the jet nozzle;

i_2^* and T_2^* are the total enthalpy and stagnation temperature of the gas at the turbine outlet;

$i_{e\,ad}$ and $T_{e\,ad}$ are the enthalpy and temperature of the gas in the outlet cross-section of the jet nozzle in the case of adiabatic gas expansion (without losses) from a pressure p_2 to a pressure p_e.

The real gas exhaust velocity from the jet nozzle, c_e, that is directed along the nozzle axis and determines the magnitude of specific engine thrust, is always less than the theoretical velocity $c_{e\,t}$, due to the effect of hydraulic and thermal losses in the exhaust system and as a result of a certain non-uniformity and spin of the flow at the turbine outlet (in other words, velocity c_2 deviates from the axial direction). Taking all these losses into account through the so-called velocity coefficient

of the jet nozzle, $\varphi_{j.n} = c_e/c_{e\ t}$, determined from experience, and expressing the temperature ratio in formula (8.1) by the corresponding pressure ratio, we obtain

$$c_e = \varphi_{j.n}\sqrt{2g\frac{k}{k-1}RT_2^*\left[1-\left(\frac{p_e}{p_2^*}\right)^{\frac{k-1}{k}}\right]}. \qquad (8.2)$$

where p_2^* is the total pressure at the turbine outlet;

p_e is the static pressure in the outlet cross-section of the jet nozzle;

$p_2^*/p_e = \varepsilon_{j.n}$ is the gas expansion ratio in the jet nozzle.

For modern turbojet engines the velocity coefficient of the jet nozzle under the designed regime is $\varphi_{j.n} = 0.96$ to 0.98.

If there is complete gas expansion to atmospheric pressure in the nozzle we must substitute $p_e = p_H$ in formula (8.2), or $p_e = p_0$ if the engine operates on the ground.

If there is a supercritical pressure drop in the jet nozzle the gas in a simple convergent jet nozzle will, as we know, expand only to a critical pressure equaling $p_{cr} = \delta_{cr}p_2^* > p_H$, acquiring a critical exhaust velocity $c_{e\ cr}$ in the process.

If the airspeed is increased the velocity head compression ratio will increase so that under otherwise unchanged conditions the total pressure p_2^* behind the turbine will be increased, as we showed earlier. Consequently, the pressure ratio p_2^*/p_H increases, and at high supersonic airspeeds the pressure drop in the jet nozzle becomes supercritical.

However, in a simple convergent jet nozzle it is impossible to exploit a supercritical pressure drop completely, in other words, to expand the gas to atmospheric pressure p_H if $p_2^*/p_H > 1/\delta_{cr}$, and to obtain an exhaust velocity c_e that is greater than critical velocity $c_{e\ cr}$, or supersonic. Therefore, in a turbojet engine with simple jet nozzle the specific thrust obtained for $p_2^*/p_H > 1/\delta_{cr}$ is less than it could be under otherwise equal conditions. But in the case of complete gas expansion to a pressure $p_e = p_H$, where the exhaust velocity becomes supersonic, this loss in the thrust of the turbojet engine that is due to incomplete gas expansion in a simple jet nozzle becomes appreciable, starting out from an airspeed approximately corresponding to a Mach number of $M_H = 1.5$ to 1.6, and increases rapidly with a further increase in airspeed.

As a result it becomes necessary to use supersonic divergent jet nozzles (see figure 97) for turbojet engines intended for employment at high supersonic airspeeds, in place of the simple convergent jet nozzles.

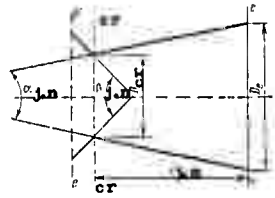

Figure 97: Diagram of a supersonic jet nozzle.

Using a supersonic jet nozzle in place of a simple nozzle makes it possible to increase the specific thrust of a turbojet engine under supercritical pressure drops and a given value for T_2^* and to reduce its specific fuel consumption accordingly, since the supersonic nozzle differs from the simple nozzle in that it is possible to accomplish supercritical pressure drops and to obtain a supersonic gas exhaust velocity.

Thus, for instance, at a Mach number $M_H = 2$ and an altitude of H = 11,000 meters the specific thrust of a turbojet engine with supersonic jet nozzle can be greater by 20 to 25 % than for the same engine with a simple jet nozzle. At still greater airspeeds this gain becomes even more significant.

The length $l_{j.n}$ of the divergent part of a supersonic jet nozzle is determined by the magnitude of the ratio $F_e/F_{cr} = D_e^2/D_{cr}^2$ and by the angle of aperture $\alpha_{j.n}$ of that part of the jet nozzle (see figure 97).

For a given magnitude F_e/F_{cr} the length and weight of the jet nozzle, and also the surface area of its walls, will increase with decreasing angle of aperture $\alpha_{j.n}$. This leads to an increase of gas friction losses in the nozzle and to an increase in the quantity of air required to cool the nozzle walls. Under excessively great angles $\alpha_{j.n}$ the gas flow at the nozzle outlet becomes significantly non-parallel with respect to the longitudinal nozzle axis, and the flow can separate from the nozzle walls, leading to a reduction in engine thrust. As a rule, therefore, $\alpha_{j.n} = 25$ to 30°. However, the subsonic part of a supersonic nozzle is usually designed with an angle $\alpha_{j.n} = 90$ to 120°.

The area ratio F_e/F_{cr} is called the <u>divergence of a supersonic jet nozzle</u> and is uniquely determined by the gas expansion ratio $\varepsilon_{j.n}$ in the jet nozzle.

The dependence of F_e/F_{cr} on $\varepsilon_{j.n}$ for k' = 1.33 is shown in figure 98, where it is seen that the required divergence of a supersonic jet nozzle increases with increasing $\varepsilon_{j.n} = p_2^*/p_e$.

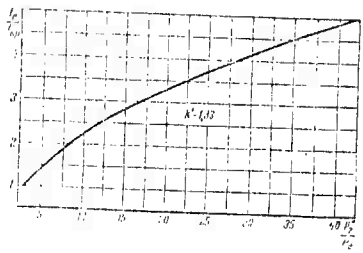

Figure 98: Dependence of the divergence of a supersonic jet nozzle on the gas expansion ratio in the nozzle.

With a change in the gas pressure p_2^* at the inlet of such a nozzle at a given magnitude of nozzle divergence, or with a change in nozzle divergence at a constant pressure p_2^* in front of the nozzle, the pressure p_e in the nozzle outlet cross-section will be changed and can become either greater or less than the atmospheric pressure p_H.

If the nozzle divergence ensures complete gas expansion to atmospheric pressure, in other words, if $p_e = p_H$ and $\varepsilon_{j.n} = p_2^*/p_H$, the regime of nozzle operation is called a <u>designed regime</u>. In that case the engine thrust is determined according to formula (2.7).

If the nozzle divergence is inadequate for complete gas expansion to atmospheric pressure p_H, the nozzle operates under an underexpansion regime where $p_e > p_H$ and $\varepsilon_{j.n} < p_2^*/p_H$. In that case the engine thrust is determined according to formula (2.6).

If the divergence is greater than required for gas expansion to atmospheric pressure p_H, the nozzle operates under an overexpansion regime, in other words, a pressure $p_e < p_H$ is established in the nozzle outlet cross-section, and in that case $\varepsilon_{j.n} > p_2^*/p_H$. Since the gas velocity in the nozzle outlet cross-section is supersonic the gas flow stagnates behind the nozzle under the effect of a counterpressure $p_H > p_e$, and oblique shock waves are formed in the flow where the pressure is increased to p_H, as it is shown schematically in figure 99. In that case, as in the preceding cases, the gas velocity in the nozzle outlet cross-section is determined in accordance with the actual expansion ratio $\varepsilon_{j.n} = p_2^*/p_e$ that corresponds to the given nozzle divergence. The engine thrust is found according to formula (2.6) which can be written as follows, taking into consideration that $p_e < p_H$.

$$P = \frac{G_в}{g}(c_e' - V) - F_e(p_H - p_e).$$

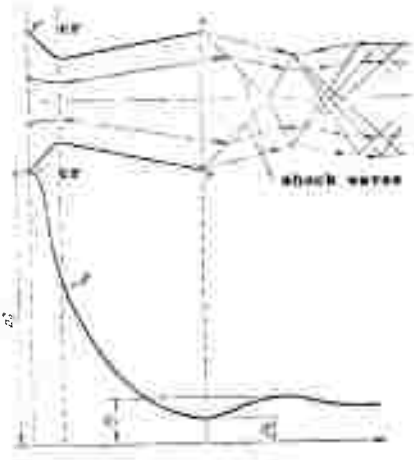

Figure 99: Diagram of the operation of an over-expanded supersonic jet nozzle.

However, experience shows that if the pressure ratio p_e/p_H becomes less than a certain magnitude $(p_e/p_H)_{sep} < 1$ as a result of gas overexpansion, the boundary layer will separate from the nozzle walls and the oblique shock waves described above will move inside the jet nozzle. A gas flow diagram with flow separation from the nozzle walls under an overexpansion regime is shown in figure 100. The pressure ratio $(p_e/p_H)_{sep}$ where flow separation from the nozzle walls begins under an overexpansion regime depends primarily on nozzle divergence and on the angle of aperture $\alpha_{j.n}$. The averaged dependence of this ratio on F_e/F_{cr} for $\alpha_{j.n} \leq 30^\circ$, plotted on the basis of available experimental data, is shown in figure 101.

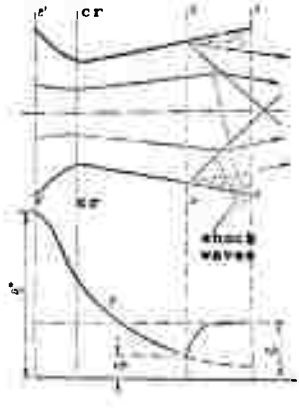

Figure 100: Gas flow diagram with flow separation from the nozzle walls.

The pressure at the internal part of the nozzle surface behind the flow separation plane x x (see figure 100) is close to the external pressure p_H, so that part of the nozzle is practically not involved in thrust generation. Therefore, in case of flow separation under an overexpansion regime the thrust of the engine must be determined according to the formula

$$P = \frac{G_a}{g}(c_x - V) + F_x(p_x - p_H),$$

where c_x, F_x, and p_x are the velocity, flow area, and pressure in the nozzle cross-section x x where flow separation from the nozzle walls begins.

For high supersonic airspeeds, where the pressure ratio p_2^*/p_H is great, it usually proves expedient to use a supersonic jet nozzle with reduced divergence that will not provide full gas expansion to atmospheric pressure p_H for the designed airspeed and altitude. This is explained by the fact that for large values of p_2^*/p_H a reduction in the gas expansion ratio in the nozzle to approximately $\varepsilon_{j.n} \approx 0.75\, p_2^*/p_H$ will result, under otherwise unchanged conditions, in a relatively small reduction of the thrust of a turbojet engine. At the same time the required nozzle divergence and, consequently, the nozzle weight and length as well, are significantly reduced. Moreover, the nozzle outlet diameter D_e is also reduced in the process, contributing toward a reduction of engine drag. The most favorable divergence of a supersonic nozzle is established on the basis of comparative effective thrust and engine weight calculations for different values of F_e/F_{cr}.

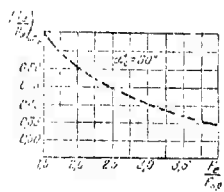

Figure 101: Dependence of $(p_e/p_H)_{sep}$ on nozzle divergence.

If there is a change in the airspeed and altitude and in the regime of engine operation designed for high supersonic airspeeds, the pressure ratio p_2^*/p_H will vary within wide limits. In particular, under otherwise equal conditions the pressure p_2^* as well as the pressure along the engine tract in general and, consequently, p_2^*/p_H as well, will be reduced with a reduction in airspeed, due to a reduction in the aggregate compression ratio π_c^*. Thus, for instance, a turbojet engine with $\pi_{k0}^* = 8$ and $T_z^* = 1300^\circ$ K at an airspeed corresponding to a Mach number $M_H = 3$ and an altitude of 20 km will achieve a pressure ratio of $p_2^*/p_H \approx 20$, while the

same engine operating under a regime of maximum thrust in static operation on the ground (upon take-off) has a value of $p_2^*/p_H \approx 2.9$.

Consequently, if a supersonic jet nozzle is designed so that its divergence ensures complete or close to complete gas expansion at maximum airspeed and altitude, such a nozzle will operate under significant overexpansion regimes at slow airspeeds. The greater the designed airspeed and altitude for the nozzle (the greater its divergence), the more significant will be the overexpansion of the gas in the nozzle and, consequently, the greater will be the thrust degeneration of the turbojet engine at slow airspeeds, especially upon take-off (in comparison to a nozzle designed for this airspeed). The thrust degeneration can be reduced by using a so-called trade-off jet nozzle. This type of nozzle has less divergence than required for maximum airspeed so that it operates under an underexpansion regime at this airspeed, but instead it will not cause significant thrust degeneration at slow airspeeds due to great overexpansion of the gas in the nozzle. However, using a trade-off jet nozzle that ensures sufficient overexpansion of the gas at slow airspeeds can lead to a significant loss of thrust at maximum airspeed (due to great underexpansion), if this airspeed is high.

For most effective use, supersonic jet nozzles must be controlled so that they ensure complete or close to complete gas expansion with a minimum of losses at all airspeeds and altitudes and under all regimes of engine operation. In order to accomplish this type of control it must be possible to vary the nozzle divergence F_e/F_{cr} in accordance with the change in the pressure ratio p_2^*/p_H while the engine is in operation.

The areas of the outlet cross-section F_e and the critical cross-section F_{cr} of a supersonic jet nozzle and the ratio between these areas can be varied by displacing the internal angles 1 (see figure 102,a), by turning the flaps 2 forming the nozzle walls (see figure 102,b), by displacing the internal angles 1 and turning the flaps 2 (see figure 102,c), by turning the flaps 3 to change the nozzle outlet cross-section F_e and injecting air (see figure 102,d) to change the critical flow area (in other words, through pneumatic or gas dynamic nozzle control), and by other means. It is obvious that the most advantageous control of a supersonic nozzle will be achieved if the outlet cross-section and critical cross-section are varied independently (see figure 102, c and d). However, this complicates the nozzle control system. A nozzle designed according to the diagram shown in figure 102,b is simpler and easier to achieve, but in this type of nozzle a change in the outlet cross-section will be accompanied by a simultaneous change in the critical cross-section, which is far from always being favorable.

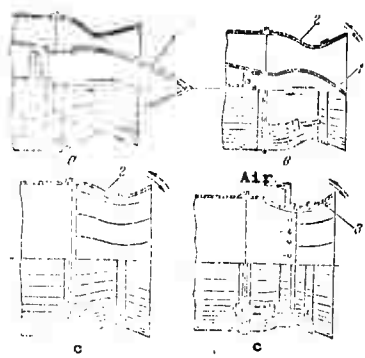

Figure 102: Diagram of the control of supersonic jet nozzles.

2. Concept of the Reverse Thrust of a Turbojet Engine

Reverse thrust is defined as shifting the thrust effect in the opposite direction so that a negative thrust is generated that is directed opposite to the motion of the aircraft and, consequently, causes the aircraft to slow down.

The reverse thrust of a turbojet engine is a very effective means of shortening the hold-off distance and rolling distance of fast aircraft during landings. Thus, for instance, exploiting the reverse thrust of a turbojet engine can shorten the rolling distance of the aircraft on a wet runway and especially on an icy runway 1.5 to 2 times and more, compared to braking with drag chute and brakes. And the hold-off distance of an aircraft prior to landing can be reduced 2 to 2.5 times with the aid of reverse thrust. Also, reverse thrust can be used as a means for slowing down the aircraft in flight, if it is necessary to reduce the airspeed rapidly.

The reverse thrust of a turbojet engine is accomplished by means of suitable reversal of the gas flow departing from the engine, using special devices that can be made in accordance with different designs. Some of the possible designs for these devices are shown in figure 103. Mechanical reversers are used to turn the gas flow, for instance, turning flaps 1 (see figure 103,a) or slides 2 that direct the flow to a grill which turns the flow (see figure 103,b), as well as devices where the flow is initially turned pneumatically. In the last case (see figure 103,c) a jet of compressed air diverted from the compressor and amounting to 3 to 5 % of the total air flow through the engine is injected into the central part of the gas flow through an insert 3. This jet deflects the flow to the grille that turns it into the direction opposite to the motion of the aircraft.

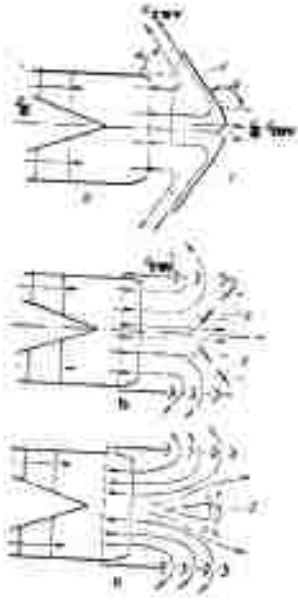

Figure 103: Designs of thrust reversers.

Thrust reversers of turbojet engines must satisfy the following basic requirements:

they must generate a negative thrust amounting to not less than 40 % of the maximum positive thrust generated by the engine in static operation on the ground without thrust reverser;

they must ensure a rapid transition from maximum negative thrust to maximum positive thrust, which is very important in the event of an unsuccessful aircraft landing;

they must not disrupt normal engine operation and must not appreciably affect the weight and size of the power plant;

they must not cause damage to aircraft parts resulting from the effect of the deflected gas jet.

The magnitude of reverse thrust P_{rev} generated by a turbojet engine under reversing conditions depends on the quantity of exhaust gas G_{rev} deflected by the reverser and, as seen from figure 103,a, on the flow deflection angle β of that quantity of gas. As a rule, the relative magnitude of negative thrust P_{rev} is considered, that is P_{rev}/P, where P is the thrust of the turbojet engine under the normal regime with disengaged reverser. The ratio P_{rev}/P is called the thrust reversing coefficient.

The dependence of the reversing coefficient on the relative quantity of gas G_{rev}/G turned in the reverser under different angles $\beta > 90^{\circ}$ and for V = 0 is shown in figure 104.

Figure 104: Dependence of the thrust reversing coefficient of a turbojet engine on the quantity of deflected gas.

It is seen that the value of the reversing coefficient will increase rapidly with increasing relative quantity of deflected gas and increasing angle β. However, increasing this angle to more than $\beta \approx 150^{\circ}$ is not advantageous since in that case the magnitude of negative thrust will increase only little (see figure 105) and the danger will arise that aircraft parts are strongly heated and damaged by the effect of the deflected gas flow.

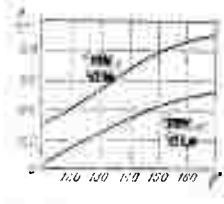

Figure 105: Dependence of the thrust reversing coefficient of a turbojet engine on the deflection angle of the gas flow.

A relatively great quantity of gas must be deflected in the thrust reverser of a turbojet engine in order to obtain the negative thrust required for a landing by a fast aircraft. Thus, for instance, in order to obtain a value of $P_{rev}/P = -(0.4 \text{ to } 0.5)$ at an angle of $\beta = 120^{\circ}$ to 150°, it is necessary to have, accordingly, $G_{rev}/G = 0.8$ to 1.0.

CHAPTER 9

DEPENDENCE OF THE SPECIFIC THRUST AND ECONOMY OF TURBOJET ENGINES ON THE BASIC PARAMETERS OF THE OPERATING PROCESS

1. Specific Thrust

The specific thrust P_{sp} for a given airspeed and altitude is directly dependent on the gas exhaust velocity from the jet nozzle, c_e. If we assume for simplicity that the gas is expanded to atmospheric pressure in the jet nozzle, so that $p_e = p_H$, the specific thrust is expressed by the formula.

$$P_{sp} = \frac{c_e - V}{g}.$$

It was shown in the preceding chapter (see formula 8.2) that the gas exhaust velocity from the jet nozzle of a turbojet engine for a given value of pressure $p_e = p_H$ depends only on the stagnation temperature T_2^* and the total pressure p_2^* at the turbine outlet. The following relationships were obtained in Chapter 7 for the temperature T_2^* and the pressure p_2^* at the turbine outlet:

$$T_2^* = T_z^* - \frac{AL_k}{c_{pg}\eta_{m.T}};$$

$$p_2^* = p_H \sigma_{c.c} \sigma_{c.c}^* \pi_k^* \left(1 - \frac{AL_k}{c_{pg} T_z^* \eta_T}\right)^{\frac{k^*}{k^*-1}}.$$

Moreover, we know that the effective work of the compressor equals

$$L_k = 102{,}57 T_H \frac{\pi_k^{*\frac{k-1}{k}} - 1}{\eta_k}.$$

Thus, it is readily seen that the specific thrust of a turbojet engine for a given airspeed and altitude depends on the gas temperature T_z^* in front of the turbine, on the compressor compression ratio π_k^*, on the efficiencies of compressor and turbine, η_k and η_T, and on the coefficients that take into account the pressure losses in the combustion chambers and in the jet nozzle, $\sigma_{c.c}$ and $\varphi_{j.n}$; in other words, it depends on the basic parameters of the operating process of a turbojet engine.

Let us consider the effect of each of these parameters on the specific thrust of a turbojet engine, assuming that in the event of a change in any one parameter whose effect on specific thrust is clarified, all the other parameters and magnitudes will remain unchanged.

The dependence of specific thrust P_{sp} on the air compression ratio in the compressor, π_k, under different values of T_z^* and for $\eta_T^* = 0.90$, $\eta_k = 0.85$, $\varphi_{j.n} = 0.97$, and $\sigma_{c.c} = 0.95$ at different airspeeds corresponding to Mach numbers $M_H = 0$, 1, and 2, and altitudes of H = 0 and H = 11 km, is shown in figures 106 and 107.

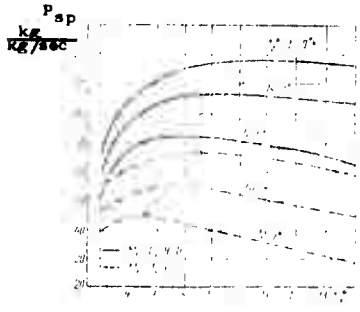

Figure 106: Dependence of the specific thrust of a turbojet engine on the compressor compression ratio on the ground.

It is seen that, under otherwise unchanged conditions, the specific thrust initially increases with increasing compression ratio in the compressor under $T_z^* = \text{const}$, and subsequently begins to decline after reaching a maximum. This type of dependence of P_{sp} on π_k^* is applicable to different airspeeds and explained as follows.

If the compression ratio is increased the thermal efficiency of the cycle or the heat utilization in the engine increases, as we know from Chapter 3, contributing to an increase of exhaust velocity from the jet nozzle and, consequently, also to an increase of specific thrust.

On the other hand, if π_k^* is increased the air temperature T_k^* at the compressor outlet is increased, and if the temperature T_z^* in front of the turbine remains constant this will lead to a reduction in the quantity of heat added to the gas. This must in itself lead to a reduction of gas exhaust velocity from the jet nozzle and, consequently, also to a reduction of specific thrust.

Finally, if there is an increase in the compression ratio π_k^* or, in other words, in the work consumed for air compression, the absolute magnitude of the losses in the compressor and in the turbine will increase, if $\eta_k = \text{const}$ and $\eta_T^* = \text{const}$. Since the total quantity of external heat input is reduced in the process, the relative portion of heat consumed for these losses will increase especially sharply which, of course, must contribute to a reduction of velocity c_e and to a corresponding reduction of specific thrust.

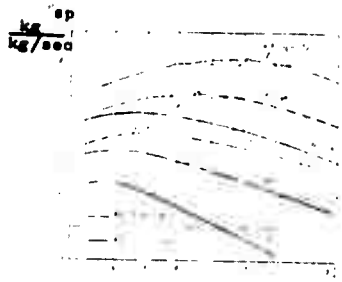

Figure 107: Dependence of the specific thrust of a turbojet engine on the compression ratio of the compressor at an altitude of 11 km.

To the degree that the compressor compression ratio increases the increase in thermal efficiency becomes continuously less intensive and compensates to a continuously lesser degree for the negative effect of the reduction in the quantity of heat input and the increase in the relative quantity of heat expended to make up the losses in the compressor and in the turbine.

In the long run, when the compressor compression ratio exceeds a certain value for the given conditions, the reduction in the quantity of heat added to the gas and the increase of losses in the compressor and in the turbine begin to play a determinative role. This leads to a reduction in the quantity of heat that is convertible into kinetic energy of the flow at the engine outlet, and as a result the specific thrust is reduced.

The optimum value for the air compression ratio in the compressor, $\pi^*_{k\ opt}$, where the specific thrust of a turbojet engine has its maximum, depends on the parameters of the operating process of the engine as well as on flight conditions.

Calculations show that the optimum compression ratio $\pi^*_{k\ opt}$ for obtaining maximum specific thrust increases with increasing gas temperature T^*_g in front of the turbine, compressor efficiency η_k, and turbine efficiency η_T, and with decreasing coefficient $\sigma_{c.c}$ or, in other words, with increasing loss of total pressure in the combustion chambers. Under otherwise unchanged conditions the optimum compression ratio $\pi^*_{k\ opt}$ decreases with increasing airspeed at a given altitude (for T_H = const), since in that case the velocity head compression ratio $\pi^*_{v.h}$ and stagnation temperature T'_H at the engine inlet are increased.

As we know, the velocity head compression ratio $\pi^*_{v.h}$ increases with increasing altitude (with decreasing ambient air temperature T_H) at a given airspeed, but its influence is felt to a lesser degree than the reduction of ambient air temperature T_H. Therefore, under otherwise unchanged conditions the compression ratio $\pi^*_{k\ opt}$ increases with increasing altitude (or with decreasing T_H).

These types of dependence for $\pi^*_{k\ opt}$ are explained as follows. The greater the gas temperature T^*_z in front of the turbine, or the lower the ambient temperature T_H (and, consequently, the lower the temperature T^*_k at the compressor outlet), the greater will be the heat added to the gas in the combustion chamber and, consequently, the later (at greater compression ratios in the compressor) the negative effect of the increasing losses in compressor and turbine on P_{sp} will be felt, and $\pi^*_{k\ opt}$ will be increased. However, this will also cause an increase of the optimum compression ratio with increasing altitude and decreasing airspeed or, in other words, with decreasing T^*_H where T^*_z = const.

If compressor and turbine efficiency are increased, the relative magnitude of the losses in these elements will decrease, so that the effect of losses on specific thrust becomes appreciable only at very great compression ratios. In that case, this will also lead to an increase in $\pi^*_{k\ opt}$.

Under otherwise equal conditions the gas expansion ratio in the jet nozzle of the engine is reduced with decreasing coefficient of pressure loss in the combustion chamber, $\sigma_{c.c}$, which leads to an increase in the temperature T_e of the exhaust gases and, consequently, also to an increase in the quantity of heat carried off by these gases. But since an increase of π^*_k reduces the heat carried off by the exhaust gases, the smaller the coefficient $\sigma_{c.c}$, the greater will be the values of π^*_k up to which the predominant effect of the reduction in the heat removed with the exhaust gases is maintained. As a result the compression ratio $\pi^*_{k\ opt}$ is increased with decreasing $\sigma_{c.c}$.

At high supersonic airspeed the optimum compression ratio of the compressor can even be one. Thus, for instance, if T^*_z = 1200°K, $\eta_k\eta^*_T$ = 0.70, $\sigma_{c.c}$ = 0.95, and if the turbojet engine has a supersonic diffuser with σ_d = 0.75, a value of $\pi^*_{k\ opt}$ = 1 is obtained for an airspeed of V = 2,650 km/h at altitudes of H > 11 km (at a Mach number M_H = 2.5). This means that under these conditions the air compression that is due to the effect of the velocity head is sufficiently great, and that the subsequent air compression in the compressor (π^*_k > 1) does not cover the losses of energy inherent in the compressor and the turbine that drives it. Consequently, using a turbojet engine at high supersonic airspeeds can prove to be unfavorable from the point of achieving the required specific thrust, and in that case the transition to a compressorless engine or ram jet engine must be made. As an example, figure 108 shows the dependence of the optimum compression ratio $\pi^*_{k\ opt}$ on the airspeed at altitudes of H = 0 and H = 11 km, for T^*_z = 1200°K, $\eta_k\eta^*_T$ = 0.70, and $\sigma_{c.c}$ = 0.95.

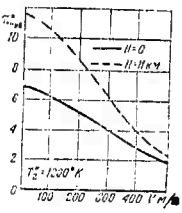

Figure 108: Dependence of the optimum $\pi^*_{k\,opt}$ on the airspeed, for a turbojet engine at maximum P_{sp}.

The nature of the effect of the gas temperature T^*_z in front of the turbine on the specific thrust of a turbojet engine is seen directly from the preceding formulas according to which the specific thrust increases continuously with increasing temperature T^*_z. The dependencies of P_{sp} on T^*_z for two values of π^*_k and for $\sigma_{c.c} = 0.95$, $\varphi_{j.n} = 0.97$, $\eta^*_t = 0.90$, $\eta_k = 0.85$[1] at different airspeeds (flight Mach numbers) and altitudes are shown in figure 109.

Figure 109: Dependence of the specific thrust of a turbojet engine on the temperatures in front of the turbine.

It is seen that increasing the temperature in front of the turbine is a very effective means of increasing the specific thrust, and that its effectiveness will increase with increasing compression ratio in the compressor and increasing airspeed.

If the gas temperature in front of the turbine is too low it can turn out that the heat added to the gas in the combustion chambers is only sufficient to cover the thermal, hydraulical, and mechanical losses in the engine. In that case the gas flow is not accelerated in the engine, and the thrust becomes equal to zero.

---

[1] Unless they are specified, the same values for these magnitudes are also used in the subsequent exmaples to which the graphs in the figures of the present chapter refer.

The dependence of specific thrust on the product of compressor efficiency and turbine efficiency, $\eta_k \eta_T^*$, for $\pi_k^* = 6$ and $T_g^* = 1200^\circ$ K and for different airspeeds and altitudes is shown in figure 110. It is seen that the efficiencies of compressor and turbine have a significant effect on the magnitude of specific thrust.

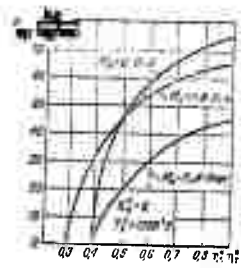

Figure 110: Dependence of the specific thrust of a turbojet engine on compressor efficiency and turbine efficiency.

The effect of the loss in total pressure in the combustion chambers (coefficient $\sigma_{c.c}$) on specific thrust is shown in figure 111, where it is seen that a variation of this loss within the limits from 8 to 10 % has a relatively low effect on the magnitude of specific thrust.

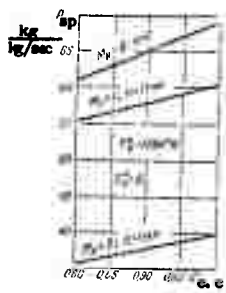

Figure 111: Dependence of the specific thrust of a turbojet engine on resistance in the combustion chambers.

As far as the dependence of specific thrust on the losses in the engine exhaust system (on the coefficient $\varphi_{j.n}$) is concerned, this dependence is obvious from the preceding formulas and requires no special explanations. It should merely be noted that the effect of $\varphi_{j.n}$ increases strongly with increasing airspeed.

2. Economy of a Turbojet Engine

It was shown earlier that the thermal economy of a turbojet engine is determined by the product of effective engine efficiency η_e and propulsive efficiency η_p. At a given airspeed V and calorific capacity H_u of the fuel, the economy is described directly by the specific fuel consumption.

$$C_{sp} = \frac{3600V}{427 H_u \eta_e \eta_p}.$$

Let us examine the effect of the basic parameters of the operating process of the engine on these efficiencies and on specific fuel consumption.

The following formula was obtained earlier for the effective efficiency:

$$\eta_e = \frac{a l_0 A}{2gH_u}(c_e^2 - V^2).$$

If we now determine the ratio al_0/H_u according to formula (6.2) according to which

$$\frac{al_0}{H_u} = \frac{\xi_{c.c}}{c_p'(T_z^* - T_k^*)},$$

we can write as follows for η_e:

$$\eta_e = \frac{\xi_{c.c} A (c_e^2 - V^2)}{2g c_p'(T_z^* - T_k^*)}.$$

It is seen from this formula that the effective efficiency of a turbojet engine depends on the same parameters of the operating process as the specific thrust (η_e as well as P_{sp} are functions of the velocity c_e) and, in addition, on the heat release coefficient $\xi_{c.c}$ or, in other words, on the heat losses during combustion.

At the same time, if the turbine efficiency η_t^* and the compressor efficiency η_k as well as the coefficient $\varphi_{c.c}$ are increased, the effective efficiency will increase at a faster rate than the specific thrust, since the magnitude of η_e is determined, under otherwise equal conditions, by the kinetic energy of the gas at the engine outlet, $c_e^2/2g$, while only the gas exhaust velocity c_e at the engine outlet enters into the expression for specific thrust.

The effect of the compressor compression ratio π_k^* on the effective efficiency η_e for different temperatures T_z^* in front of the turbine and different flight Mach numbers M_H is illustrated by the curves shown in figure 112. Analysis of these curves shows that if the compression ratio in the compressor is increased, the effective efficiency, unlike the thermal efficiency η_t (see Chapter 3), increases only until a certain value for π_k^* is reached and subsequently begins to decline. This type of dependence of η_e on π_k^* is explained by the same causes as the dependence of specific thrust on π_k^*; in other words, simultaneously with the increase in π_k^* for T_z^* = const there is an increase in thermal efficiency, a reduction in the quantity of heat added to the cycle, and an increase in the absolute magnitude of the losses in compressor and turbine.

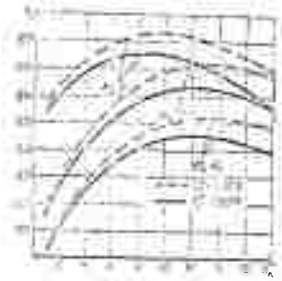

Figure 112: Dependence of the effective efficiency of a turbojet engine on the compression ratio in the compressor.

If we compare the graphs shown in figures 112, 106, and 107 we can note that, under otherwise equal conditions, the maximum of effective efficiency is reached at a greater compressor compression ratio than the maximum of specific thrust. This is due to the fact that the magnitude of effective efficiency is determined by the ratio between the increase in the kinetic energy acquired by the gas flow in the engine and the expended heat, while the magnitude of specific thrust depends only on the increase of gas velocity in the engine. If the compression ratio is increased with $T_z^* = \text{const}$, the heat added to the gas in the combustion chambers is continuously reduced, and consequently, it is obvious that the maximum of η_e sets in at greater values of π_k^* than the maximum of $c_e^2/2g$, c_e, or P_{sp}.

The effect of the temperature T_z^* in front of the turbine on the effective efficiency η_e for different flight Mach numbers M_H is shown in figure 113. It is seen that the effective efficiency increases continuously with increasing T_z^*. Physically this is explained by the fact that if T_z^* is increased with $T_k^* = \text{const}$, $\eta_k = \text{const}$, and $\eta_T^* = \text{const}$, the absolute magnitude of heat losses in the engine increases at a slower rate than the quantity of heat input, since in this case the losses in compressor and turbine remain unchanged due to $\pi_k^* = \text{const}$. Consequently, under these conditions the relative magnitude of the heat lost in the engine is reduced with increasing T_z^*, and the effective efficiency η_e increases accordingly.

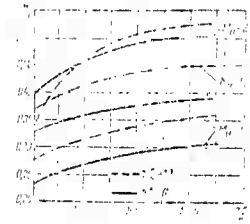

Figure 113: Dependence of the effective efficiency of a turbojet engine on the temperature in front of the turbine.

The dependence of the propulsive efficiency η_p on the basic parameters of the operating process can be examined in a general form with the aid of the already known formula

$$\eta_p = \frac{2}{1 + \frac{c_e}{V}}.$$

Let us express the exhaust velocity from the jet nozzle in this formula by the specific thrust, so that

$$c_e = gP_{sp} + V.$$

Consequently, the propulsive efficiency is expressed by the following formula:

$$\eta_p = \frac{1}{1 + \frac{gP_{sp}}{2V}}.$$

This expression implies that an increase of specific thrust at a given airspeed (due to an increase in T_z^*, π_k^*, η_k, η_T^*, and others) leads to a reduction of propulsive efficiency (as a result of the increase in velocity c_e at V = const) and, conversely, a decrease of specific thrust (due to the increase of π_k^* above $\pi_{k\,opt}^*$ or the reduction of T_z^* and others) leads to an increase of propulsive efficiency.

Characteristic dependencies of propulsive efficiency η_p on η_k^* and T_z^* for a given airspeed (M_H = 2) and otherwise unchanged conditions are shown in figures 114 and 115 where the corresponding curves for effective efficiency η_e and economic efficiency $\eta_{econ} = \eta_e\eta_p$ are also plotted (dotted curves) for comparison purposes.

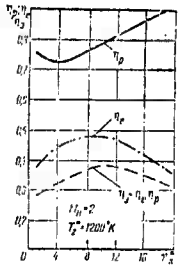

Figure 114: Dependence of the efficiencies η_e, η_p, and η_{econ} of a turbojet engine on the compression ratio in the compressor.

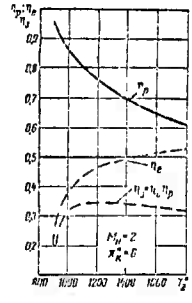

Figure 115: Dependence of the efficiencies η_e, η_p, and η_{econ} of a turbojet engine on the temperature in front of the turbine.

Let us now establish a direct connection between the specific fuel consumption and the basic parameters of the engine operating process. For this purpose we use the already known formula for the specific fuel consumption which is

$$C_{sp} = \frac{3600}{a_0 P_{sp}}.$$

Expressing αl_0 according to formula (6.2) by the temperature difference $T_z^* - T_k^*$, we obtain

$$C_{sp} = \frac{3600\, c_p' (T_z^* - T_k^*)}{\xi_{c.c} H_u l_{sp}}.$$

Thus, in addition to the same parameters of the operating process on which the specific thrust depends, the specific fuel consumption also depends on the calorific capacity H_u of the fuel and on the heat release coefficient in the combustion chambers, $\xi_{c.c}$, increasing with decreasing H_u as well as decreasing $\xi_{c.c}$.

If the turbine efficiency η_T^* and the coefficients $\varphi_{j.n}$ and $\sigma_{c.c}$ are increased, the specific fuel consumption will decrease at the same rate as the specific thrust increases during this process. However, if the compressor efficiency η_k is increased, the specific fuel consumption is reduced to a lesser degree than it is for the same increase of turbine efficiency. This is explained by the same causes that were shown when we considered the dependence of effective engine efficiency η_e on η_k and η_T^*.

As an example, figure 116 shows the dependence of specific fuel consumption on the compressor efficiency η_k and turbine efficiency η_T^* for $\pi_k^* = 6$ and $T_z^* = 1200^\circ K$; $M_H = 0$ and $M_H = 2$. The solid curves in this figure represent the dependence of C_{sp} on η_T^* at a constant compressor efficiency $\eta_k = 0.85 = \text{const}$, while the dotted curves correspond to the dependence of C_{sp} on η_k for $\eta_T^* = 0.90 = \text{const}$. Comparable dependencies for C_{sp} are obtained for different values of π_k^*, T_z^*, and M_H.

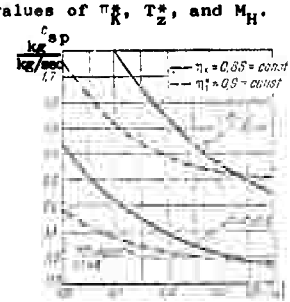

Figure 116: Dependence of the specific fuel consumption of a turbojet engine on compressor and turbine efficiencies.

The dependence of specific fuel consumption on the compressor compression ratio for $M_H = 0$ and $M_H = 2$ and different gas temperatures in front of the turbine is shown in figure 117. Examination of these dependencies permits the following conclusions:

an increase in compressor compression ratio can reduce the specific fuel consumption significantly;

the specific fuel consumption decreases with increasing compressor compression ratio only up to the known limit where it reaches a minimum, and subsequently begins to increase with a further increase of π_k^*;

the greater the gas temperature in front of the turbine, T_z^*, the greater will be the optimum compressor compression ratio $\pi_{k\ opt}^*$ where the minimum of specific fuel consumption is reached;

for identical values of T_z^* and under otherwise equal conditions the compressor compression ratio at which a minimum of fuel consumption is obtained will be significantly greater than the compression ratio that corresponds to the maximum of specific thrust, as well as to the maximum of effective efficiency.

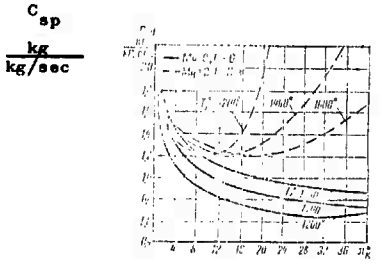

Figure 117: Dependence of the specific fuel consumption of a turbojet engine on the compression ratio.

The nature of these dependencies of the specific fuel consumption C_{sp} on the compressor compression ratio that remain valid even under flight conditions where $M_H > 0$, is explained as follows.

If the compression ratio π_k^* is increased at V = const, the effective efficiency η_e increases initially (see figure 112), and the propulsive efficiency η_p, as we showed above (see figure 114), is reduced, but to a lesser degree than the increase of η_e. Therefore, the economic efficiency $\eta_{econ} = \eta_e\eta_p$ increases, and the specific fuel consumption decreases accordingly. A further increase in the compressor compression ratio is accompanied by an insignificant change and subsequently even by a reduction of effective efficiency, and by a comparatively small increase in propulsive efficiency. Consequently, the product $\eta_{econ} = \eta_e\eta_p$ is reduced, causing an increase in specific fuel consumption. Obviously, the minimum specific fuel consumption is obtained at a compressor compression ratio corresponding to the maximum value of economic efficiency η_{econ}. Since the minimum propulsive efficiency (or the maximum specific thrust) sets in at lower compression ratios than the maximum of effective efficiency, the maximum value of the product $\eta_{econ} = \eta_e\eta_p$ will shift toward even greater values of π_k^*.

Calculations show that the compressor compression ratio which ensures a minimum of specific fuel consumption decreases with increasing airspeed and decreasing altitude. This is explained by the same reasons as the increase in the value of $\pi_{k\ opt}^*$ at which

a maximum of specific thrust is obtained, with increasing airspeed.

Figure 118 shows the dependence, on the airspeed, of the optimum compressor compression ratios at which a minimum of specific fuel consumption is obtained, at the altitudes H = 0 and H = 11 km and for $T_z^* = 1200^\circ K$.

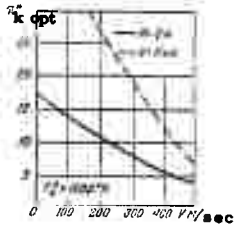

Figure 118: Dependence of the optimum $\pi_{k\ opt}^*$ required for the minimum C_{sp} of a turbojet engine, on the airspeed.

At high supersonic airspeeds the compressor compression ratio is unable to "compensate" for the losses in compressor and turbine, as we mentioned earlier, so that using a compressor with the given parameters cannot increase the economy of a turbojet engine in comparison to a ram-jet engine, and in that case $\pi_{k\ opt}^* = 1$. The airspeed at which the $\pi_{k\ opt}^*$ corresponding to the minimum of C_{sp} becomes equal to one, is usually somewhat greater than the airspeed at which the value of $\pi_{k\ opt}^* = 1$ is obtained that corresponds to the maximum of P_{sp}.

Depending on the purpose of a turbojet engine the most advantageous magnitude for the compression ratio π_k^* is established on the basis of comparative calculations, taking into consideration the effect of π_k^* not only on the specific fuel consumption but also on specific thrust, compressor efficiency and characteristics, engine weight and dimensions, and the weight of the aircraft power plant as a whole, including the required fuel supply.

Let us now consider the effect of the gas temperature in front of the turbine on the magnitude of specific fuel consumption. It turns out that, to the degree of gas temperature increase in front of the turbine and under otherwise equal conditions, the specific fuel consumption decreases initially and, after reaching a minimum for a certain value of $T_{z\ opt}^*$, begins to increase again. This is seen well in figure 119 showing the dependence of specific fuel consumption C_{sp} on T_z^* for two different values of compressor compression ratio.

Figure 119: Dependence of the specific fuel consumption of a turbojet engine on the temperature in front of the turbine.

This type of dependence of the specific fuel consumption C_{sp} on the temperature T_z^* is explained by the different change in effective efficiency η_e and propulsive efficiency η_p when there is a change in temperature. As we showed above, the first of these efficiencies increases continuously with increasing T_z^* at V = const, while the second decreases continuously. Initially, the effect of the increase of effective efficiency η_e predominates so that the product $\eta_{econ} = \eta_e\eta_p$ is increased and the specific fuel consumption reduced. Subsequently, as the temperature continues to increase, the reduction in propulsive efficiency η_p begins to predominate, the product $\eta_{econ} = \eta_e\eta_p$ is decreased because the increase in effective efficiency is slowed down, and the specific fuel consumption begins to increase after reaching a minimum at a value of $T_{z\ opt}^*$ corresponding to a maximum of that product.

Calculations show that the optimum temperature $T_{z\ opt}^*$ in front of the turbine with respect to a minimum of specific fuel consumption will increase with increasing compressor compression ratio and increasing losses in the engine or, in other words, with decreasing compressor and turbine efficiency and decreasing coefficient $\sigma_{c.c}$. Moreover, it turns out that, under otherwise unchanged conditions, the temperature $T_{z\ opt}^*$ increases with increasing airspeed and decreases with increasing altitude, which is seen well in figure 120 showing the dependence of the temperature $T_{z\ opt}^*$ on the airspeed for two altitudes (0 and 11 km) and for two different values of π_k^*.

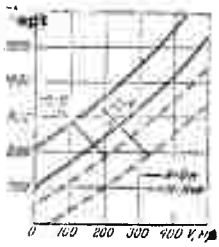

Figure 120: Dependence of the optimum temperature in front of the turbine of a turbojet engine, on airspeed and altitude.

In conclusion let us note that the losses of total pressure in the combustion chambers have the same effect on specific fuel consumption that they have on specific thrust.

CHAPTER 10

EQUILIBRIUM REGIMES OF TURBOJET ENGINES

1. General Considerations

An engine installed in an aircraft must operate under different regimes. A regime of engine operation is defined as a certain set of internal and external conditions under which it operates. The internal conditions are characterized by the given rpm of the engine rotor and the gas temperature in front of the turbine. The external conditions include the airspeed and altitude, and the temperature and pressure of the atmospheric air.

Each regime of a turbojet engine corresponds to its combination of rpm, parameters for the operating process, and air flowrate and, consequently, to certain magnitudes of thrust, specific fuel consumption, and to loads and temperatures of engine parts. Any change in the regime of a turbojet engine has the end result of a change in thrust and specific fuel consumption as well as in the stresses and temperatures in engine parts.

The regime of a turbojet engine that is required under given external conditions is established by adjusting the fuel input into the combustion chambers, and in a number of cases also by a simultaneous adjustment of the magnitude of the flow areas of individual engine elements (for instance, the jet nozzle area, and others).

All the parameters of the operating process of a completed turbojet engine are closely interrelated, as we shall show later. Therefore, in order to determine the changes in thrust and specific fuel consumption of a completed turbojet engine that are associated with a change in its regime or, in other words, in its operating conditions, it is first necessary to establish not only the direct effect of these conditions on the corresponding parameters of the engine operating process, but definitely also the interaction between these parameters.

In order to form a judgement on the operating qualities of a turbojet engine it is also necessary to know the special features of its operation under all practically possible regimes.

In this chapter we shall consider the interaction and change in the parameter of a turbojet engine that are associated with its control and with a change in external conditions, and the special features of turbojet engine operation under different equilibrium regimes.

The equilibrium or steady-state regime of a turbojet engine is defined as a regime where the rpm of the engine rotor and all the parameters of the operating process are constant over time.

In order to accomplish a certain equilibrium regime of a turbojet engine its turbine power must be equal to the power required to

drive its compressor and auxiliary assemblies at the given rpm. This basic condition for equilibrium regimes also corresponds, as we showed earlier, to an equality of turbine work and compressor work, or $L_T = L_K$ (if all the air from the compressor enters the combustion chambers located in front of the turbine).

The special features of turbojet engine operation under equilibrium regimes for different operating conditions can be clarified with the aid of the compressor characteristics with superimposed lines of the constant values for the ratios between the temperature T_z^* in front of the turbine and the temperature T_H^* at the compressor inlet, or the so-called $T_z^*/T_H^* = \text{const}$ lines. These lines are plotted on the basis of a certain relationship between the weight flowrates of air through the compressor and the turbine nozzle assembly (for instance, under the assumption that all the air from the compressor enters the combustion chambers). Under critical and supercritical pressure drops in the turbine nozzle assembly, which is the most frequent condition in turbojet engines, the $T_z^*/T_H^* = \text{const}$ lines are obtained in the form of straight lines and are located on the compressor characteristics as shown in figure 121. In this case, the smaller the temperature ratio T_z^*/T_H^*, the greater will be the distance of these lines from the surge limit (to the right and downward).

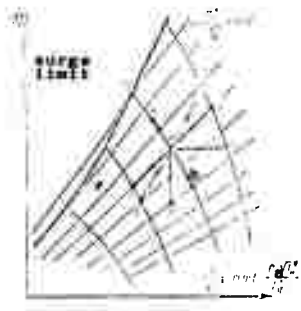

Figure 121: Possible equilibrium regimes of a turbojet engine.

Physically, each $T_z^*/T_H^* = \text{const}$ line under constant conditions at the compressor inlet ($T_H^* = \text{const}$ and $p_a^* = \text{const}$) represents the dependence of the air flowrate through the compressor of the turbojet engine on the compressor compression ratio π_k^* at constant gas temperature in front of the turbine (corresponding to this line) or, in other words, at $T_z^* = \text{const}$.

The intersection points between the $T_z^*/T_H^* = \text{const}$ lines and the lines of constant values for the rpm parameter $n/\sqrt{T_H^*}$, for

instance the points a, b, and c, etc. in figure 121, represent those combinations of the gas temperature T_g^* in front of the turbine and the rpm of the turbojet engine where the given relationship of the weight flowrates of air through compressor and turbine is observed.

In order for each of these combinations of rpm and temperature T_g^* to be also an equilibrium regime of turbojet engine operation, there must be, in addition, a certain relationship between effective turbine work and effective compressor work, or they must be equal, $L_T = L_K$, if all the air from the compressor enters the combustion chambers in front of the turbine.

We know that the effective turbine work L_T depends (see Chapter 7) on the gas temperature T_g^* in front of the turbine, on the gas expansion ratio $\epsilon_T = p_g^* / p_2$ in the turbine, and on turbine efficiency η_T, so that

$$L_t = \frac{c_p'}{\lambda} T_g^* \left[1 - \left(\frac{p_2}{p_g^*} \right)^{\frac{k'-1}{k'}} \right] \eta_t. \qquad (10.1)$$

The gas expansion ratio in the turbine of a turbojet engine in turn depends on the relationship between the minimum flow areas of the turbine nozzle assembly, F_{NA}, and of the jet nozzle, F_e, and also on the losses in these elements. This dependence is obtained on the basis of the continuity condition, in other words, on the equality of the weight flowrates of combustion products through the turbine of a turbojet engine and its jet nozzle. Under critical and supercritical pressure drops in the jet nozzle of a turbojet engine and in the nozzle assembly of its turbine the following relationship is obtained from the corresponding flow equation:

$$\left(\frac{p_2}{p_g^*} \right)^{\frac{k'-1}{k'}} = \left(\frac{\varphi_{NA} F_{NA}}{\varphi_{j.n} F_e} \right)^m,$$

where $m \approx 1.13$ (for $k' = 1.32$, which is characteristic for the turbine of a turbojet engine).

The significance of this relationship consists of the following. If the area F_e of the jet nozzle and $\varphi_{j.n}$ are increased under otherwise unchanged conditions, the resistance to the departure of the gas from the turbine and the corresponding counterpressure p_2 behind the turbine will be reduced, which for a given p_g^* leads to an increase in the gas expansion ratio $\epsilon_T = p_g^* / p_2$ in the turbine. Decreasing F_e and $\varphi_{j.n}$ will increase the resistance to the turbine exhaust so that the pressure p_2 behind the turbine will increase at $p_g^* = \text{const.}$ and the expansion ratio ϵ_T will decrease.

Increasing the area F_{NA} of the nozzle assembly and φ_{NA} leads to a reduction in its resistance so that the pressure drop required to provide the given gas flowrate through the turbine is reduced, causing an increase in the pressure p_2 at $p_g^* = \text{const.}$, and $\epsilon_T = p_g^* / p_2$ will be reduced. Accordingly, if F_{NA} and φ_{NA} are reduced, and under otherwise equal conditions, $\epsilon_T = p_g^* / p_2$ will be increased.

Now we can write for the effective work of the turbine of a turbojet engine

$$L_T = \frac{c_p}{A} T_T^* \left/ 1 - (\varphi_{NA} F_{NA} / \varphi_{j.n} F_e)^m \right/ \eta_T \qquad (10.2)$$

Thus, the effective work of a turbine in a turbojet engine system can change not only due to the gas temperature in front of the turbine but also due to a change in the areas of jet nozzle and turbine nozzle assembly causing a change in the gas expansion ratio in the turbine.

Also, this makes it possible to accomplish different equilibrium regimes of a turbojet engine, corresponding to given points on its compressor characteristics, for instance to points a, b, c, and others in figure 121.

The compressor characteristics with superimposed T_z^*/T_H^* = const lines in conjunction with expression (10.2) make it possible to establish the special features of turbojet engine operation under equilibrium regimes for different engine operating conditions.

2. Special Features of Equilibrium Regimes of a Turbojet Engine under Independent Changes in rpm and Temperature in Front of the Turbine

First, let us consider the greater part of the cases encountered where all the air from the compressor enters the combustion chambers in front of the turbine, assuming that external conditions remain constant.

Let us assume that it is necessary to change the gas temperature in front of the turbine of a turbojet engine, keeping the rotor rpm constant, or in other words, that it is necessary to obtain the equilibrium regime of the turbojet engine to which the points correspond that are located on the same $n/\sqrt{T_H^*}$ = const line (points a, b, c in figure 121).

If we increase the gas temperature in front of the turbine of the turbojet engine (by means of increasing the fuel input) the turbine work L_T will increase, the equality $L_T = L_k$ will be disturbed, so that $L_T > L_k$, and the engine rpm will increase. In order to maintain the previous rpm the increase in turbine work L_T that is associated with the increase in temperature in front of the turbine must be prevented, which according to formula (10.1) can be accomplished only be means of reducing the gas expansion ratio ε_T in the turbine. For this purpose it is necessary, as seen from formula (10.2), either to reduce the (minimum) outlet cross-section area F_e of the jet nozzle, or to increase the minimum cross-section area F_{NA} of the turbine nozzle assembly.

However, although the reduction of jet nozzle area F_e and the increase of turbine nozzle assembly area F_{NA} have the same effect on ε_T, the parameters of the operating process of the turbojet engine change differently during this process.

In the first case (reduction of the jet nozzle area F_e at a constant turbine nozzle assembly area F_{NA}), the weight flowrate of gas through the turbine nozzle assembly is reduced as a result of the reduction in the density of combustion products due to their increased temperature T_z^* in front of the turbine, since F_{NA} = const. Correspondingly, in accordance with the flow continuity condition, the weight flowrate of air through the compressor is reduced, too. However, in this case the rpm remains constant, as we mentioned above. Therefore, the operating point on the compressor characteristics, for instance point a in figure 121, that determines the equilibrium regime of the turbojet engine, shifts along the $n/\sqrt{T_H^*}$ = = const line in the direction of lower air flowrates, approaching the surge limit or, in other words, approaching point c and so on, which is accompanied, as seen from figure 121, by an increase in the compression ratio π_k^*.

In the second case (increasing the turbine nozzle assembly area F_{NA} for F_e = const), calculations show that in order to maintain a constant rpm so that $L_T = L_K$ when the gas temperature in front of the turbine increases, it is necessary to increase the area F_{NA} always at a greater rate than the density of the combustion products is decreased during this process. Therefore, their flowrate through the turbine nozzle assembly and, accordingly, the air flowrate through the compressor are increased. As a result, in this case the initial operating point shifts along the $n/\sqrt{T_H^*}$ = const line in the direction of greater air flowrates, moving away from the surge limit (for instance, point a in figure 121 shifts to point b and lower), which is accompanied by a reduction in the compressor compression ratio π_k^*.

Reducing the temperature in front of the turbine of a turbojet engine at constant rotor rpm requires, obviously, a corresponding increase in the jet nozzle area F_e or a reduction in the area F_{NA} of the turbine nozzle assembly. Here, the changes in the regimes of the turbojet engine will take place in directions opposite to those described above. In particular, the reduction in temperature in front of the turbine at n = const that is associated with an increase in F_e at F_{NA} = const, will be accompanied by a shift of the compressor operating point away from the surge limit or, in other words, by an increase in the air flowrate through the compressor and a decrease in π_k^*, while a reduction in temperature associated with a decrease in F_{NA} at F_e = const will be accompanied by a shift of this point toward the surge limit or, in other words, by a reduction in the air flowrate through the compressor and an increase in π_k^*.

By changing both areas F_e and F_{NA} simultaneously when there is a change in the temperature in front of the turbine it is possible to maintain not only the rpm of a turbojet engine but also the location of the operating point on the compressor characteristic.

In order to change the rpm of a turbojet engine at constant gas temperature in front of the turbine, or in other words, to obtain equilibrium regimes corresponding to the operating points located on T_z^*/T_H^* = const lines in the field of compressor characteristics (for instance, on the line a, 1 in figure 121), it is necessary again to change the area F_e or F_{NA}. Actually, in order to reduce the rpm of a turbojet engine (in order to shift its regime from point a to, for instance, point 1 in figure 121), the turbine work L_T must be reduced since the compressor work is reduced with decreasing compressor rpm. But in this case it was stipulated that T_z^* = const. Therefore, the turbine work can be reduced only by means of increasing the gas expansion ratio ε_T in the turbine, which requires either a reduction of area F_e or an increase of area F_{NA}. However, in the second case (F_{NA} is increased at T_z^* = = const) the air flowrate as a result of the increase of F_{NA} is reduced to a lesser degree, so that the compressor operating point does not shift along the line a,1, as in the first case, but along the line a, 1'; in other words, it moves away from the surge limit (here, the same temperature T_z^* is obtained in point 1' and in point 1, due to the displacement of the T_z^*/T_H^* = const line when F_{NA} is changed).

In order to increase the rpm of a turbojet engine at T_z^* = = const it is necessary to increase the area F_e or to reduce the area F_{NA} accordingly. But when F_{NA} is reduced at constant T_z^* the air flowrate will increase at a slower rate, and the compressor operating point will shift further (along the line a, 2' instead of a, 2) toward the surge limit than they would for an increase in F_e and T_z^* = const at the same increase in engine rpm.

Through the proper selection of the jet nozzle area F_e, turbine nozzle assembly area F_{NA}, and fuel input into the combustion chambers, it is also possible to accomplish any other equilibrium regimes for a given turbojet engine or, in other words, regimes that differ from each other by their rpm, temperature in front of the turbine, and other parameters at the same time, for instance, regimes corresponding to the points on lines a, 3 and a,3' (see figure 121), and so on.

Thus, by simultaneously changing the jet nozzle area or the turbine nozzle assembly area and the fuel input into the combustion chambers it is possible to change, independently of each other, the rpm of a turbojet engine, the gas temperature in front of its turbine, and a number of other engine parameters (for instance, π_k^*, G_a, and others).

On a completed engine the (minimum) outlet cross-section area of the jet nozzle can be changed relatively simply in the required direction. Therefore, changing the area F_e is a procedure

used in practical application for both, controlling a turbojet engine in operation by using variable area jet nozzles, and for the required adjustment of turbojet engine parameters during final experimental development by also using simple interchangeable jet nozzles of different diameters.

Adjusting the area F_{NA} of the turbine nozzle assembly of completed turbojet engines (for instance, by pivoting the nozzle blades) is not used today, since this involves a significant complication of the design of the greater "hot" part of the turbine and can sometimes cause an appreciable reduction in turbine efficiency. If it becomes necessary to change the area F_{NA} during final experimental development of a turbojet engine, this is accomplished by replacing the turbine nozzle assembly.

The acceptable equilibrium regimes for a given turbojet engine during operation in the aircraft are limited by the following:

the maxima of rpm n_{max} and temperature $T^*_{z\ max}$ in front of the turbine, considering the strength and heat resistance of engine parts;

the minima of rpm n_{min} and temperature $T^*_{z\ min}$ in front of the turbine required to ensure stable combustion chamber operation, the required turbine power, and a sufficiently high compressor efficiency;

the surge region of the compressor.

Under practical circumstances, not nearly all the equilibrium regimes are employed that are acceptable for a given turbojet engine, and only those are used that the control system installed in the engine permits under operating conditions in the aircraft. These regimes are called the operating equilibrium regimes of an engine.

The geometrical location of the points corresponding to the operating equilibrium regimes of a turbojet engine in the field of compressor characteristics is called line of operating regimes or operating line of a turbojet engine.

The operating line of a turbojet engine must never pass beyond the area of acceptable regimes and must be located at a sufficient distance from the compressor surge limit.

The shape and location of the operating line of a turbojet engine are determined primarily by the control system selected for the engine and by the nature of its compressor characteristics.

3. Equilibrium Regimes of a Turbojet Engine with Fixed Area Jet Nozzle

Very frequently the rpm of turbojet engines is changed or maintained constant when there is a change in, for instance, external conditions, merely by controlling the fuel supply to the combustion chambers, without changing the area of the jet nozzle.

Therefore, we must also examine the special features of the operating lines of turbojet engines with fixed area jet nozzle or, in other words, for F_e = const and also for F_{NA} = const, considering the statements made above.

Let us consider the case where there is a critical or supercritical pressure drop in the turbine nozzle assembly and in the jet nozzle at the same time, which is characteristic for the greatest part of all regimes of modern turbojet engines.

Since, by stipulation, F_e = const and F_{NA} = const, and assuming for simplicity that η_T, $\varphi_{j.n}$, and φ_{NA} are constant, too (this is close to reality), we obtain the following expression for equilibrium regimes from formula (10.2):

$$\frac{L_t}{T_z^*} = \frac{L_k}{T_H^*} = \text{const.} \tag{10.3}$$

Substituting in this expression the value for the effective work of the compressor, which equals

$$L_k = 102{,}57 T_H^* \frac{\pi_k^{*\frac{k-1}{k}} - 1}{\eta_k},$$

we obtain

$$\frac{T_z^*}{T_H^*} C = \frac{\pi_k^{*\frac{k-1}{k}} - 1}{\eta_k}, \tag{10.4}$$

where C is a constant magnitude.

Equation (10.4) contains only the compressor parameters and the temperature ratio T_z^*/T_H^* as variables. The constant C entering its left side is determined in accordance with data corresponding to the design point selected for the compressor characteristics. This means that in the case under consideration (F_e = const) the operating line of the given turbojet engine is represented in the field of its compressor characteristics by only one curve 0,0 (solid line in figure 122) whose shape and location remain constant under any changes of rpm, atmospheric conditions, airspeed, and altitude.

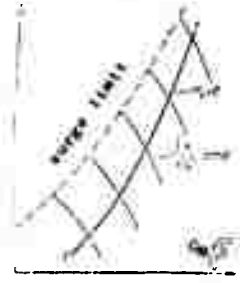

Figure 122: Operating line of a turbojet engine with F_e = const.

A change of the jet nozzle area F_e leads to a corresponding shift of the operating line of the turbojet engine in question. If the area F_e is increased, the equilibrium regimes of the turbojet engine and, consequently, its entire operating line, shift into the area of lower temperatures T_z^* and greater air flowrates, moving away from the compressor surge limit. If the area F_e is reduced, the operating line of the turbojet engine shifts, accordingly, into the area of higher temperatures T_z^*, moving toward the compressor surge limit.

By and large, the slopes of the operating line of a turbojet engine with F_e = const in the field of compressor characteristics will become steeper with increasing designed compression ratio $\pi_{k\,des}^*$ of the compressor. In other words, for the same relative change in π_k^* the resulting change in the flowrate parameter will increase with increasing $\pi_{k\,des}^*$.

Typical cases for the location of the operating lines of turbojet engines with F_e = const in the field of their compressor characteristics, without special anti-surge measures, are shown in figures 123 and 124, where the points a denote equilibrium regimes corresponding to the designed compressor compression ratios.

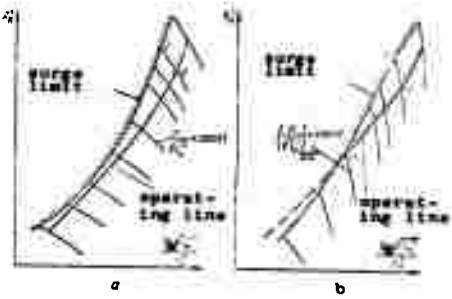

Figure 123: Operating lines of turbojet engines with axial-flow compressors, for F_e = const.

If the designed compressor compression ratio of a turbojet engine is relatively small ($\pi_{k\,des}^*$ = 3.5 to 4.5), the operating line of the turbojet engine (see figure 124) will move away from the surge limit when the rpm is reduced in comparison to its designed values, so that stable engine operation without surging is usually ensured in this area of regimes. If the rpm parameter is increased beyond the designed value, the operating characteristic will move closer to the surge limit, which in a number of cases can lead to the development of surging.

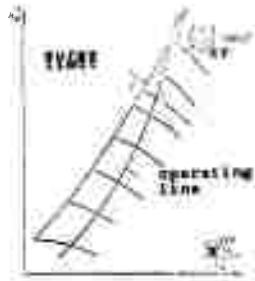

Figure 124: Operating line of a turbojet engine with radial-flow compressor, for F_e = const.

Experience shows that the compresso. surge limit becomes continuously more critical with increasing designed compressor compression ratio. In that case the slope of the operating line of a turbojet engine with F_e = const becomes steeper, as we mentioned above. Therefore, the operating line of a turbojet engine with F_e = const and a significant designed compression ratio ($\pi^*_{k\ des} \geq$ $\geq$ 6 to 8) moves close to the surge limit (see figure 123 a) or even intersects it (see figure 123 b) in the area of rpm parameters below designed values. In the first case the transition of the engine from low rpm values to the designed regime can become difficult or impossible (see below). In the second case it is obvious that, as a result of surging, it is not only impossible to operate the engine at reduced values of the rpm parameter but even to start it.

Consequently, dangerous regimes from the point of compressor surging can be those regimes of a turbojet engine with F_e = const where the rpm parameter is either greater or smaller than its designed value. The first is characteristic for turbojet engines with radial-flow compressors or axial-flow compressors with relatively low compressor head, while the second is characteristic for turbojet engines with axial-flow compressors with high compressor head.

Compressor surging of a turbojet engine with F_e = const under off-design regimes with respect to its operating line develops for the following reasons.

If the rpm is reduced in comparison to designed values at T^*_H = const (in other words, where $\pi^*_k < \pi^*_{k\ des}$), the air flowrate and its corresponding axial air velocity c_a at the compressor inlet of a turbojet engine with F_e = const and with a high designed compression ratio, is decreased at an appreciably faster rate than the circumferential rotor velocity (see figure 125). As a result the angles of attack of the blades in the first compressor stage are increased and can become so great at the reduced rpm values

that an intensive flow separation from the backs of the blades develops, causing compressor surging.

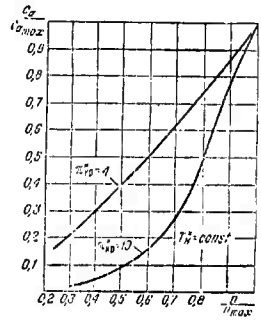

Figure 125: Relative change of air velocity with rpm at the compressor inlet of a turbojet engine with F_e = const.

The greater the designed compression ratio of the compressor, the greater will be the increase in the angles of attack of the blades in its first stage with decreasing rpm of a turbojet engine with F_e = const and, consequently, the faster will the operating line of the engine move toward the compressor surge limit in this case.

The same picture will be found in the last stages of an axial-flow compressor with high compressor head. In accordance with the flow continuity condition the weight flowrate of the air through these stages will be reduced to the same degree as in the first stages. But the air density in the last stages decreases due to the reduction in compressor compression ratio, and as a result the axial air velocity in these stages decreases at a slower rate than the circumferential velocity of the rotor.

As a result the angles of attack of the blades in the last compressor stages of a turbojet engine with F_e = const are reduced at decreased rpm, and can become negative. However, if the blades have large negative angles of attack there will already be air expansion rather than compression in the interblade ducts (turbine-type regime of the compressor stage), resulting in a reduction of compressor head and efficiency but not causing compressor surging.

Exactly the same changes in the angles of attack of the blades in the first and the last compressor stages of a turbojet engine with F_e = const are obtained if the rpm parameter $n/\sqrt{T_H^*}$ and, accordingly, also the compression ratio are reduced as a result of an increase in the temperature T_H^* of the inlet air at constant rpm n. In that case the only difference will be that the circumferential

velocity of the rotor remains constant, and the changes in the angles of attack for the individual stages mentioned above are determined only by the corresponding changes in the axial velocities of the air in these stages (see figure 126).

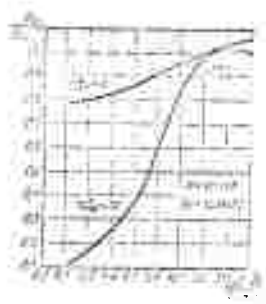

Figure 126: Relative change of air velocity with the rpm parameter (for n = const) at the compressor inlet of a turbojet engine with F_e = const.

If the rpm parameter of a turbojet engine with F_e = const is increased above its designed value ($\pi_k^* > \pi_{k\,des}^*$), the axial air velocity c_a at the compressor inlet will increase slightly at n = const (see figure 126), and consequently the angles of attack of the blades in the first compressor stages will be reduced. At the same time, the axial air velocity in the last stages can also decrease as a result of an increase in its density due to the increased compression ratio, so that the angles of attack of the blades in these stages are increased. Therefore, in this case flow separations that cause surging can develop primarily in the last stages of an axial-flow compressor (or at the diffuser vanes of a radial-flow compressor).

Thus, if surging develops under off-design regimes of a turbojet engine with F_e = const where the compressor compression ratio becomes less than its designed value, the first stages will always be the source of surging, and under off-design regimes with a compression ratio above its designed value, it will be the last stages of an axial-flow compressor (or the diffuser vanes of a radial-flow compressor).

The following means are used to prevent surging in modern turbojet engines with compressors with high compressor head:

increasing the jet nozzle area under off-design regimes;

bypassing part of the air from a point behind one stage or several of the first stages of the compressor into the atmosphere (or to the engine inlet);

pivoting the straightening (guiding) blades of one or several of the first compressor stages.

Let us examine the effect of each of these anti-surging techniques on the profile of the operating line of a turbojet engine.

Obviously, <u>increasing the jet nozzle area</u> only under those regimes of a turbojet engine where the danger of surging develops, requires the employment of a variable-area jet nozzle.

If the control system of such a nozzle permits the elements that change its area F_e to be set in two positions (two-position nozzle), the operating line of the turbojet engine can have a shape represented by the solid line ab'bc in figure 127. The section cb of this line is obtained for a jet nozzle area F_{e1} that is greater than the designed area $F_{e\ des}$, so that this section shifts in the direction of lower temperatures T_z^* and greater air flowrates (the angles of attack of the blades in the first stages are reduced) which means that it moves away from the compressor surge limit. At the rpm parameter where the danger of surging disappears, the jet nozzle area is reduced (section bb' in figure 127) to its designed magnitude $F_{e\ des} < F_{e1}$ and is kept constant for the remaining part of the operating line of the turbojet engine (section b'a in figure 127).

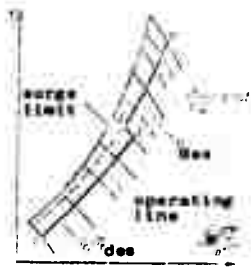

Figure 127: Operating line of a turbojet engine with a two-position variable-area jet nozzle.

For a three-position jet nozzle the operating line of the turbojet engine can have a profile as shown in figure 128. Here the section cb of the operating line is obtained at the maximum nozzle area F_{e2} = const; for the section b'a' the nozzle area is reduced to F_{e1} = const, and when the maximum rpm is reached the nozzle area is finally reduced (section a'a) to its designed magnitude $F_{e\ des}$ that ensures the required maximum gas temperature in front of the turbine.

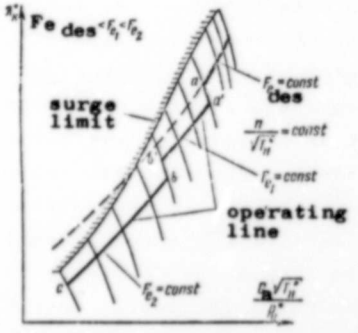

Figure 128: Operating line of a turbojet engine with a three-position variable-area jet nozzle.

However, increasing the jet nozzle area alone will not always succeed in preventing compressor surging of a turbojet engine. This is due to the fact that the gas pressure behind the turbine can be close to atmospheric pressure at reduced rpm of the turbojet engine. At that time the turbine already reacts poorly (in the sense of an increase of ϵ_T and the associated reduction of T_z^*) to the increase in jet nozzle area, so that the operating line of the engine moves insignificantly away from the surge limit. In these cases it is necessary to take recourse to additional anti-surging techniques.

Under otherwise equal conditions, bypassing part of the air from an intermediate compressor stage into the atmosphere will result in an increase in the air flowrate and axial air velocity in the preceding first stages. As a result the angles of attack of the blades in these stages will be reduced for a given rotor circumferential velocity, preventing the flow separations from the backs of the blades that cause compressor surging. The air flowrate through the last compressor stages and through the turbine decreases, and turbine power is reduced accordingly. In order to maintain the engine rpm constant while air is being bypassed from the compressor, the gas temperature in front of the turbine must be increased. This increase in T_z^* is determined from the condition of maintaining the equality of turbine power and compressor power which in this case will have the following form:

$$G_{aT}L_T = G_{aT}L_k + (G_a - G_{aT})L_k'.$$

Designating $G_a/G_{aT} = K$, we find the turbine power from this expression:

$$L_T = L_k\left[1 + \frac{L_k'}{L_k}(K-1)\right],$$

where G_a is the quantity of air entering the compressor;

G_{aT} is the air flowrate through the turbine;

$(G_a - G_{aT})$ is the quantity of air bypassed from the compressor into the atmosphere;

L_k' is the work expended on the compression of 1 kg of bypassed air.

Whence we find, in analogy with formula (10.5)

(10.5)

However, if air is bypassed into the atmosphere from a point behind the compressor (between compressor and combustion chambers) in order to eliminate surging in the last stages of an axial-flow compressor or in the diffuser of a radial-flow compressor, $L_b' = L_b$, and in that case

whence

(10.6)

It follows from formulae (10.5) and (10.6) that the temperature T_g^* in front of the turbine for which compressor power equals turbine power at given values of [illegible] and π_c^*, will increase with increasing magnitude of $k = G_a/G_{aT}$. This means that when air is being bypassed the lines of the given values of $T_g^*/T_H^* = \text{const}$ shift in the direction of large air flowrates in the field of compressor characteristics.

Now it is not difficult to arrive at the conclusion that, when air is being bypassed, the operating line of a turbojet engine with $F_a = \text{const}$ shifts in the direction of large flowrates of air (of the air entering the compressor) or, in other words, that it moves away from the surge limit, but unlike the preceding case this takes place under increased gas temperatures in front of the turbine. This type of displacement of the lower part of the operating line of a turbojet engine and of the $T_g^*/T_H^* = \text{const}$ lines when air is being bypassed from the compressor at less than designed rpm, is shown in figure 129 (section cb).

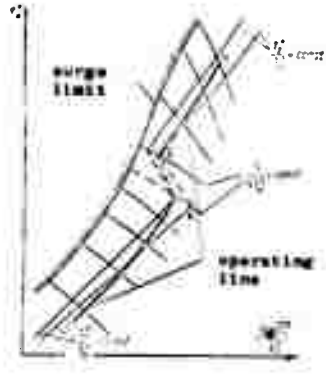

Figure 129: Operating line of a turbojet engine with an air bypass from the compressor.

Pivoting the straight- ing blades in the direction of rotor rotation reduces, as we know from compressor theory, the angles of attack of the rotor blades located behind them for a given circumferential velocity of the rotor, thus displacing the surge limit in the direction of small air flowrates. In that case the compression ratio is reduced for a given rpm.

Therefore, pivoting the straightening (guiding) blades of the first compressor stages can displace that area of the compressor characteristics where these stages are a source of surging, to the left and downward, or, in other words, it can shift the surge limit away from the operating line of a turbojet engine with P_e = const, as indicated by the dotted lines in figure 130. It is obvious that, in order to eliminate surging in the last stages of an axial-flow compressor, the straightening blades of these stages (or the diffuser vanes of a radial-flow compressor) must be pivoted in the direction of rotor rotation.

Since it improves flow conditions around the blades of one or the other stage under off-design regimes, pivoting the straightening blades can increase compressor efficiency under these regimes. As a result, the required temperature in front of the turbine is reduced, as this is seen from expression (10.4), and the operating line of a turbojet engine with P_e = const is displaced accordingly in the direction of greater air flowrates, shifting away from the surge limit (dotted part of the line cbb'a in figure 130).

The greater the distance between the operating line of a turbojet engine and the compressor surge limit, the greater will be the "stability margin" or "surge margin", whose magnitude is determined from the following relationship:

$$\sigma_{stab} = (\bar{G}_a \pi^*_{k\,lim} / \pi^*_k \bar{G}_{a\,lim} - 1)\ 100\ \%$$

where $\bar{G}_a$ and π^*_k are the air flowrate parameter and the compressor compression ratio that correspond to the equilibrium regime of the turbojet engine (for instance, in points a in figures 123 and 124);

$\bar{G}_{a\,lim}$ and $\pi^*_{k\,lim}$ are the flowrate parameter and the compression ratio in corresponding points on the surge limit in points 1 in figures 123 and 124).

Stability margins are determined experimentally during static and in-flight engine tests, and must be not less than 12 to 17 % under all practially possible conditions of engine operation.

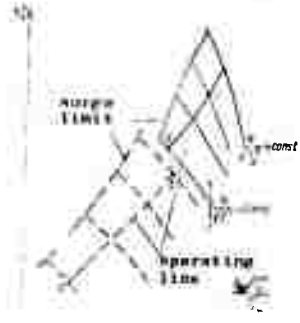

Figure 130.

Operating line of a turbojet engine with pivoting straightening blades.

CHAPTER 11

THE EFFECT OF OPERATING CONDITIONS ON THE REGIMES OF A TURBOJET ENGINE

1. The Effect of the rpm on the Parameters of the Operating Process of a Turbojet Engine

Let us consider the effect of rpm on the regime of a turbojet engine, assuming that atmospheric conditions as well as airspeed and altitude are constant.

In that case the rpm parameter is reduced with a reduction in rpm, so that the point corresponding to the equilibrium regime of a turbojet engine with P_e = const is displaced downward and to the left along its operating line, which means that the compressor compression ratio π_k^* and the flowrate parameter a' are reduced. The reduction in the compression ratio π_k^* is due to the fact that the work L_k that is consumed for the compression of 1 kg of air in the compressor, is reduced approximately proportionally to the square of rpm, and the reduction in the flowrate parameter is caused by the decrease in the weight flowrate of the air through the engine.

If the rpm parameter of a turbojet engine with P_e = const is reduced below its designed magnitude, the compressor efficiency η_k^* as a rule will at first increase slightly, and subsequently begin to decrease at a rate becoming faster with rising designed compression ratio. A certain increase of compressor efficiency for a comparatively small reduction in rpm below its designed value is due to a reduction of losses as a result of the decrease of air flow velocity in the compressor. A reduction of compressor efficiency for a great decrease in rpm is caused by the increasingly significant deviations of the angles of attack of the blades in the first and last compressor stages from their designed values during this process.

However, as far as the turbine efficiency η_t^* is concerned, it remains practically constant when the rpm parameter changes within broad limits.

The possible nature of the dependencies of π_k^*, η_k^*, T_k^*, G_a, and η_t^* on the rpm in the case under consideration are shown in figure 131, where the designed values of all the magnitudes are assumed to be equal to one.

If the rpm is reduced at supercritical drops in the jet nozzle, the temperature T_z^* in front of the turbine that is required in order to accomplish equilibrium regimes of a turbojet engine with P_e = const, is reduced, according to formula (10.3), in direct proportion to the compressor work L_k, as long as the turbine efficiency remains constant (see figure 131).

Figure 131. Variation of the parameters of a turbojet engine with P_e = const, with changing rpm.

However, if the pressure drop in the jet nozzle is subcritical, the reduction in the compression ratio π_k^* will lead to a decrease in the gas expansion ratio ϵ_T in the turbine of a turbojet engine with P_e = const. At the same time, turbine efficiency and compressor efficiency will be reduced if there is a significant reduction in rpm. As a result, the temperature T_z^* in front of the turbine that is required for the equilibrium regimes of the turbojet engine, is reduced with decreasing rpm, initially at a slower rate than the work L_k, subsequently achieves a minimum, and finally, upon further significant reduction in rpm, increases due to the great decrease in ϵ_T and the reduction in turbine efficiency and compressor efficiency.

In order to explain such a change in the temperature T_z^* we turn to the dependencies of the compressor work L_k and the available turbine work L_T, meaning the work that could have been obtained from the turbine of a turbojet engine with P_e = const if the temperature T_z^* in front of the turbine were kept constant, on the rpm.

The compressor work, as we mentioned above, is increased almost proportionally to the square of rpm. But the available turbine work of a turbojet engine not only depends on the rpm but also on the temperature T_z^* in front of the turbine. The lower this temperature, the smaller will be the available turbine work L_T for a given rpm (for a given ϵ_T). Figure 132 shows the nature of the dependence of the compressor work L_k (solid curve) and the available turbine work of a turbojet engine on the rpm, at different temperatures T_z^* maintained constant in front of the turbine (dotted curves), where the designed values of L_k and L_T are assumed to be equal to one. In this figure the topmost dotted curve A refers to the available turbine work at a constant maximum acceptable temperature $T_{z\ max}^*$

in front of the turbine, while the dotted curves B and C refer to the available work of the same turbine at constant temperatures lower than $T^*_{g\,max}$, or at $T^*_{g1} < T^*_{g\,max}$ and $T^*_{g2} < T^*_{g1}$, respectively. It is obvious that, as long as the gas expansion ratio π_T in the turbine remains constant in spite of the reduction in $\dot{m}_k$ and L_k with decreasing rpm (supercritical pressure drop in the jet nozzle), and if η_T = const during this process, the available work of the turbine will not change, either (for instance, section AA' of curve A in figure 132), since T^*_g = const. However, if the expansion ratio π_T is reduced with decreasing rpm (subcritical drop in the jet nozzle) and the turbine efficiency is reduced at the same time, the result will be that the available turbine work is reduced even though T^*_g = const is the same as before.

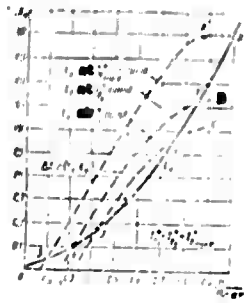

Figure 132: Establishing the equilibrium regimes of a turbojet engine.

The condition $L_T = L_k$, as we know, is mandatory for equilibrium regimes of a turbojet engine. But this condition is precisely satisfied by the intersection points of the lines of available turbine work L_T for different values of T^*_z = const with the line that determines the dependence of the compressor work L_k on the rpm (points 0, 1, 2, 3, 4, and 5 in figure 132).

Consequently, these points determine that combination of rpm and temperature T^*_z in front of the turbine where equilibrium regimes of a turbojet engine with F_e = const are obtained.

It is readily noted that, here, each rpm corresponds to its quite specific temperature T^*_z in front of the turbine; this temperature, as shown in figure 133, is initially reduced with decreasing rpm, and subsequently increases after reaching a minimum.

It is obvious that this increase in the temperature T^*_z at low rpm will be even greater if air is bypassed from the compressor into the atmosphere. However, if a supercritical pressure drop is maintained in the jet nozzle at all engine rpm values, the temperature in front of the turbine under equilibrium regimes of a turbojet engine with F_e = const will only decrease with decreasing rpm.

Points 0 and 5 in figures 132 and 133 determine the maximum rpm, n_{max}, and minimum rpm, n_{min}, where equilibrium regimes of a turbojet engine with F_e = const can be obtained at a temperature equaling the maximum temperature $T^*_{z\,max}$ that is acceptable for the turbine.

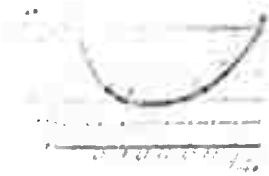

Figure 133: Variation of the temperature in front of the turbine of a turbojet engine with changing rpm, under equilibrium regimes.

At rpm values greater than n_{max} the compressor work L_k becomes greater than the work L_T that the turbine can deliver at $T^*_{z\,max}$ (see figure 132). Consequently, exceeding the maximum rpm of a turbojet engine with F_e = const involves the necessity of increasing the temperature in front of the turbine beyond $T^*_{z\,max}$, which leads to turbine overheating and can cause turbine blade destruction. Therefore, this type of engine operation is not acceptable.

This type of unfavorable relationship between compressor work and turbine work is also obtained at low rpm. Actually, at rpm values below n_{min} of a turbojet engine with F_e = const the turbine work L_T at $T^*_{z\,max}$ is less than the compressor work L_k, as seen in figure 132. In that case, in order to obtain equilibrium regimes of a turbojet engine at rpm values of $n < n_{min}$ it would be necessary to increase the turbine work which for F_e = const can be accomplished only by means of increasing the temperature in front of the turbine beyond $T^*_{z\,max}$. But this is not acceptable because of the danger of overheating the turbine blades.

Thus, a very high gas temperature in front of the turbine of a turbojet engine and, consequently, the danger of overheating the turbine blading, can develop at maximum and close to maximum rpm, as well as low rpm.

Therefore, continuous operation of a turbojet engine, not only at maximum, but also at low rpm, is acceptable only for a limited period of time.

2. The Effect of External Conditions on the Parameters of the Operating Process of a Turbojet Engine

Let us now consider the effect of external conditions, which includes airspeed and altitude as well as the temperature and pressure of the atmospheric air, on the parameters of the operating process, assuming in this case that the engine rpm remains constant and that the pressure drop in the jet nozzle is supercritical.

If the airspeed is increased under otherwise unchanged conditions, the temperature $T_a^* = T_H^*$ and pressure $p_a^* = p_H = \pi_{v.h}^* p_H$ of the air at the compressor inlet of a turbojet engine will increase as a result of the increase in the velocity head compression ratio $\pi_{v.h}^*$.

An increase in the temperature T_H^* leads to a reduction of the rpm parameter $n/\sqrt{T_H^*}$ at $n = \text{const}$. As a result, the point that determines the equilibrium regime of a turbojet engine with $P_e = \text{const}$ is displaced downward and to the left (exactly as in the case of a reduction of n at $T_H^* = \text{const}$), which leads to a reduction in the compressor compression ratio π_k^* and the flowrate parameter $q(\lambda_1)$. Exactly the same displacement of the equilibrium regime will take place, of course, if only the temperature T_H of the atmospheric air is increased under otherwise unchanged conditions.

The change in the compressor compression ratio π_k^* that accompanies a change in the air temperature T_H^* at the compressor inlet for $n = \text{const}$ is due to the following. The compressor compression ratio π_k^* depends on the product of compressor work L_k and compressor efficiency η_k and on the initial temperature T_H^* of the compression process, so that

$$L_{ad\,k}^* = c_p(\kappa - 1)AT_H^*(\pi_k^{*\frac{\kappa-1}{\kappa}} - 1),$$

whence

$$\pi_k^* = \left(1 + \frac{\eta_k L_k}{AT_H^* c_p(\kappa-1)}\right)^{\frac{\kappa}{\kappa-1}}.$$

But experience shows that, if the rpm is kept constant, the product $\eta_k L_k$ is practically almost independent of the temperature T_H^*. Therefore, the compression ratio π_k^* decreases with increasing T_H^* at $n = \text{const}$, and increases with decreasing T_H^*.

The reduction of the parameter $q(\lambda_1)$ in this case occurs because, as we know from compressor theory, it is uniquely determined by the Mach number M_a or λ_1 at the compressor inlet, so that the flowrate parameter is reduced with a reduction in the Mach number M_a (if $M_a < 1$). It was shown earlier (see figure 126) that the air velocity c_a at the compressor inlet of a turbojet engine with $P_e = \text{const}$ decreases or remains approximately constant with increasing temperature T_H^* at $n = \text{const}$ and, consequently, also with increasing T_a. Therefore, if the temperature T_H^* increases as a result of an increase in airspeed or increased temperature of the atmospheric air under otherwise unchanged conditions, the Mach number M_a (or λ_1) and, consequently, also the flowrate parameter, are reduced.

However, the weight flowrate G_a of the air through the engine changes differently during this process. If the airspeed is increased at $n = \text{const}$ and under otherwise unchanged conditions, the overall compression ratio π_0^* is increased due to the increase in the velocity head compression ratio, in spite of the decrease of π_k^* during this process, which leads to an increase of pressure p_z^* in front of the turbine and to a corresponding increase in the density of the air flowing through the engine. As a result, the

weight flowrate G_a of the air through a turbojet engine with F_e = const increases while the flowrate parameter is reduced. However, if only the temperature T_H of the atmospheric air is increased, the compressor compression ratio and p_B^* are reduced, so that the weight flowrate G_a of the air through the engine is also reduced in these cases.

With increasing altitude the temperature of atmospheric air decreases (up to H = 11 km), barometric pressure drops, and the density of atmospheric air is reduced. Therefore, the rpm parameter increases with decreasing altitude at V = const and n = const, and the equilibrium regime of a turbojet engine with F_e = const shifts upward and to the right along its operating line, which corresponds to an increase in the compression ratio π_K^* and the flowrate parameter resulting from the causes noted above. However, the weight flowrate of the air through the engine, G_a, is reduced in this case as a result of the decreasing density of atmospheric air with increasing altitude.

This type of displacement of the equilibrium regime of a turbojet engine with F_e = const or, in other words, this increase in π_K^* and [illegible] also occurs if only the temperature of the atmospheric air is reduced under otherwise unchanged conditions. But this case differs from the preceding case in that the weight flowrate of air through the engine will be increased as a result of the increase in the density of the air flowing through the engine which is due to the reduction of T_H at p_H = const.

With increasing altitude or decreasing atmospheric air temperature at n = const, the equilibrium regime of a turbojet engine with F_e = const will be located at a point on its operating line whose height increases with increasing engine rpm and decreasing airspeed. Therefore, if the engine operates at maximum or close to maximum rpm, an increase in altitude (climbing) at relatively slow airspeed, or simply a reduction in atmospheric air temperature during static operation (upon take-off) can lead to compressor surging (in point b, see figure 124).

A large increase in airspeed or a significant increase of atmospheric air temperature at V = const (or V = 0) will cause a significant downward shift of the equilibrium regime of a turbojet engine with F_e = const along its operating line and, consequently, can also lead to compressor surging (in point H, see figure 123).

In order to eliminate surging it is necessary, in the first case, to reduce the engine rpm or the altitude and, if possible, to increase the airspeed and in the second case to reduce (to limit) the airspeed or, if possible, to increase the engine rpm simultaneously with the airspeed.

The change in the temperature in front of the turbine that is required in order to maintain a constant rpm of a turbojet engine with P_e = const when there is a change in the temperature T_H^* at the compressor inlet, is determined primarily by the nature of the change in compressor work L_k which in the majority of cases does not remain constant here, as experience shows.

The relative change in the compressor work L_k of a turbojet engine with P_e = const is shown in figure 134 as a function of air temperature T_H^* at the compressor inlet for constant rpm and different values of designed compression ratio $\pi_{k\,des}^*$. It is noted that, if there is a change in the temperature T_H^* at n = const, the work L_k of a turbojet engine with P_e = const can change in different ways. Thus, for instance, under high values of $\pi_{k\,des}^*$ the work L_k as a rule will increase with increasing T_H^*, while it will decrease under low values of $\pi_{k\,des}^*$.

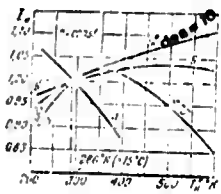

Figure 134: Dependence of the compressor work of a turbojet engine with P_e = const on the air temperature at the inlet, at n = const.

If there is a supercritical pressure drop in the jet nozzle, the temperature T_z^* in front of the turbine of a turbojet engine with P_e = const will change, according to formula (10.3), in direct proportion to the work L_k. Therefore, in this case an increase in the temperature T_H^* (regardless of its causes) at n = const will result in an increase of the temperature T_z^* in front of the turbine of turbojet engines with high values of $\pi_{k\,des}^*$, and a decrease for turbojet engines with low values of $\pi_{k\,des}^*$. Accordingly, a reduction of T_H^* at n = const will cause a decrease of the temperature in front of the turbine under high values of $\pi_{k\,des}^*$, and an increase under low values of $\pi_{k\,des}^*$.

However, if the pressure drop in the jet nozzle is subcritical, an increase of air temperature T_H^* at n = const and P_e = const will be accompanied by a reduction of the gas expansion ratio ε_T in the turbine and, consequently, also of the ratio L_k/T_z^* (due to the reduction of π_k^*), while a decrease of T_H^* will cause it to increase. Here, calculations and experience show that the ratio L_k/T_z^* changes to a greater degree than the work L_k. Therefore, in this case an increase in the temperature T_H^* (as well as in T_H) at n = const always (under all possible changes of L_k shown in figure 134) leads to some degree of increase of the temperature T_z^* in front of the

turbine of a turbojet engine with P_e = const, while a decrease of T_H^* (or T_H) leads to a reduction of the temperature T_g^*.

). Dependence of the Thrust and Economy of a Turbojet Engine on Atmospheric Conditions

In considering the dependence of the thrust and specific fuel consumption of a completed turbojet engine with P_e = const on the temperature and pressure of atmospheric air, let us assume that the rpm and airspeed remain constant here (or that V = 0).

If there is a change in atmospheric pressure p_H at T_H = const and V = const, the pressure at the compressor inlet and the counter-pressure at the jet nozzle outlet of the turbojet engine will change proportionally. But the parameters that determine the regime of the compressor (that is π_k^* and $\frac{n}{\sqrt{T_H^*}}$) and the turbine (for instance, T_g^*/T_H^*) are not dependent on atmospheric pressure. Therefore, if there is a change in atmospheric pressure p_H under otherwise equal conditions, the point in the field of compressor characteristics that corresponds to the equilibrium regime of the turbojet engine is not displaced, and all the parameters of the operating process of the turbojet engine, such as π_k^*, T_g^*, and so on, remain constant.

It follows from the foregoing that, if there is an increase in atmospheric pressure p_H under otherwise equal conditions, the pressures in all cross-sections of the flow section of the turbojet engine will increase proportionally to the pressure p_H, while the temperatures, including those in front of the turbine, will remain constant. As a result, there will be no change in the exhaust velocity from the jet nozzle and, consequently, in the specific thrust and specific fuel consumption. But as far as the weight flow-rate of the air through the engine is concerned, it will be increased in direct proportion to the increase in atmospheric pressure p_H, due to the increase of pressure p_g^* in front of the turbine and because of T_g^* = const, which also leads to a corresponding increase of engine thrust.

Thus, it is not difficult to form the conclusion that, at a given rpm and under otherwise unchanged conditions, the thrust of a turbojet engine will increase proportionally to the increase in atmospheric pressure p_H, and that this is due exclusively to the associated increase in the weight flowrate of air through the engine, while the specific fuel consumption remains constant. And the thrust of a turbojet engine decreases with decreasing atmospheric pressure p_H.

Moreover, it must be taken into consideration that a significant reduction of atmospheric pressure and, consequently, also of the density of the air and combustion products in the engine, that is due to flight at very great altitudes, can lead to a reduction in the Reynolds number in the engine flow section which, under

otherwise equal conditions, already causes an appreciable increase of friction losses, and in particular a corresponding reduction of turbine and compressor efficiency. In that case, obviously, the gas temperature T_g° in front of the turbine must be increased in order to keep the rpm constant. Consequently, if p_H is reduced together with a reduction in the thrust of a turbojet engine, the specific fuel consumption will be increased, and the regime of the turbojet engine will shift along the [illegible] line toward the surge limit, which means that all the parameters of the operating process change, too, and that the stability margin of the engine becomes smaller.

A change in atmospheric air temperature along will always result in a change in the thrust of a turbojet engine and in its specific fuel consumption.

It was shown above that, if the rpm of a turbojet engine remains constant during a reduction of ambient temperature T_H, the weight flowrate of air through the turbojet engine and the compression ratio π_k° of its compressor will increase while the temperature T_g° in front of the turbine, if it also changes in either direction, will do so to a lesser degree than π_k and G_a. Moreover, it is obvious that the temperature T_k° at the compressor outlet will be reduced.

As a result of the increase in the compressor compression ratio the gas expansion ratio in the jet nozzle and, consequently, also the specific thrust of a turbojet engine, will increase with decreasing T_H. Since, in this case, the weight flowrate of the air is increased at the same time, engine thrust will increase at an even greater rate than specific thrust.

Due to the increase in specific thrust, the specific fuel consumption of a turbojet engine will decrease with decreasing T_H. But since, in this case, the excess of air coefficient α is reduced due to the increasing temperature difference $(T_g^\circ - T_k^\circ)$, the specific fuel consumption will change at a lesser rate than the specific thrust when there is a change in ambient temperature.

Thus, at a given rpm and under otherwise equal conditions, the thrust delivered by a turbojet engine will increase, and its specific fuel consumption will decrease, with decreasing ambient air temperature. And if the ambient temperature increases, the thrust of a turbojet engine at n = const will decrease accordingly, while the specific fuel consumption is increased.

The relative changes in the thrust and specific fuel consumption of a turbojet engine with P_e = const and for n = const are shown as functions of ambient air temperature T_H in figure 135, where the values for P and C_{sp} are assumed to be equal to one for T_H = 273°K (0° C).

Figure 135: Dependence of P and C_{sp} of a turbojet engine with F_e = const, on ambient air temperature at n = const.

The significant effects of atmospheric conditions on the parameters of the operating process and, in the long run, on the thrust and specific fuel consumption of a turbojet engine, make it necessary to reduce the results of engine tests to identical, standard atmospheric conditions which, at an altitude of H = 0 (at sea level), correspond to a barometric pressure of p_o = 760 mm mercury column (1.033 kg/cm^3) and an air temperature of T_o = 288°K (+ 15°C).

Obviously, without this reduction it is impossible to compare data obtained at different times for one and the same turbojet engine, to judge correctly whether a turbojet engine meets technical specifications, or to compare the data of different turbojet engines.

Special formulas based on the application of the theory of the similarity of gas flows to turbojet engines are used to reduce the thrust, specific fuel consumption, and other parameters of turbojet engines to standard atmospheric conditions. These formulas and their derivation shall be discussed in the following chapter.

4. The Effect of the Geometry of, and Losses in the Elements of a Turbojet Engine on Thrust, Economy, and Temperature in Front of the Turbine

The following are subject to change in a turbojet engine during operation in the aircraft:

the minimum flow areas of the jet nozzle, F_e, and of the turbine nozzle assembly, F_{NA}, as a result of their control, deformation, or damage;

the velocity coefficient $\varphi_{j.n}$ of the jet nozzle (or rather, of the exhaust system), for instance when an extended exhaust pipe is installed;

the efficiencies of compressor, η_k, and turbine, η_T, as well as the coefficient φ_{NA} of the turbine nozzle assembly, as a result of blade damage or a deviation of radial clearances;

the pressure coefficient $\sigma_{c.c}$ in the combustion chambers, due to deformation of flame tubes and flame stabilizers;

the pressure coefficient σ_{in} at the engine inlet, due to modifications or damage on aircraft air intake assemblies or ducts, or as a result of the installation of a given engine into an aircraft of different design.

Also, an immediate change in the magnitudes and coefficients listed above is very frequently found during final testing of a completed turbojet engine, as a result of design modifications made on engine elements.

In this context, let us consider the effect of the areas F_e and F_{NA} as well as of the coefficients indicated above that are defined as losses in the engine elements, on the thrust and specific fuel consumption of a completed turbojet engine, assuming that the rpm, airspeed, altitude, and atmospheric conditions are constant.

It was established earlier that a change in the jet nozzle area F_e or in the turbine nozzle assembly area F_{NA} at n = const and under otherwise equal conditions will cause a change in the temperature T_z^* in front of the turbine and a shift of the regime of the turbojet engine along the $\overline{V}\tau_H^n = \text{const.}$ line. As a result, all other parameters of the operating process, π_k^*, η_k, η_T, and so on, will change, too. However, the determinative effect on thrust and specific fuel consumption here is still the gas temperature in front of the turbine.

If only the area F_e of the jet nozzle is increased, the gas expansion ratio ε_T in the turbine will increase, the temperature T_z^* in front of the turbine will be reduced if n = const is maintained, and the regime of the engine will shift into the area of lower values of π_k^* and η_k and greater air flowrates G_a. An increase in ε_T accompanied by a simultaneous decrease of temperature T_z^* will lead to a reduction of gas temperature T_2^* in front of the jet nozzle. Moreover, due to the reduction in π_k^* and the increase in ε_T, the gas pressure p_2^* in front of the jet nozzle will drop and, consequently, the gas expansion ratio $\varepsilon_{j.n}$ in the jet nozzle will be reduced. As a result, the specific thrust P_{sp} will decrease, and so will the thrust P of the engine, in spite of a certain possible increase in the flowrate G_a.

A reduction in specific thrust leads to an increase in specific fuel consumption. But at the same time, due to the decrease in the temperature T_z^* in front of the turbine and the insignificant change in the temperature at the compressor outlet that is involved the excess of air coefficient α will increase, contributing to a reduction in specific fuel consumption. However, at the same time there is a decrease in η_T^* and $\varphi_{j.n}$. Therefore, if the jet nozzle area F_e is increased, the specific fuel consumption C_{sp} can decrease slightly at first, achieving a minimum for a certain magnitude F_e determined by the turbojet engine in question and can subsequently increase.

The nature of the relative change in thrust, specific fuel consumption, specific thrust, and other parameters of a completed turbojet engine, as functions of its jet nozzle area F_e and for n = const, is shown in figure 136 where the designed values of all these magnitudes are assumed to be equal to one.

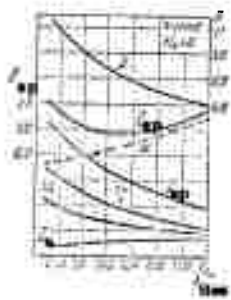

Figure 136: Dependence of the thrust and specific fuel consumption of a turbojet engine on the jet nozzle area, for n = const.

A reduction in the area F_{NA} of the turbine nozzle assembly at n = const also leads to a reduction in the temperature T_z^* in front of the turbine, due to the increase of the gas expansion ratio ε_T in the turbine. Therefore, if the area F_{NA} is reduced, engine thrust and specific fuel consumption will change qualitatively in the same manner as for an increase in the jet nozzle area F_e. But in this case the effect of F_{NA} on thrust proves to be less than the effect of F_e. This is due to the fact that, if F_{NA} is reduced, the reduction in the temperature T_z^* will be accompanied by a shift of the regime of the turbojet engine into the area of greater values of π_k^* and η_k and lower flowrates G_a (it will move toward the surge limit).

Calculations and experience show that, under otherwise equal conditions, a 1 % change in the area F_e can cause the thrust to change by 1 to 2 % in the direction indicated above, the specific fuel consumption by 0.5 to 1 %, and the temperature T_z^* in front of the turbine by 0.75 to 1.5 %, while a 1 % change in the area F_{NA} corresponds to a change of 0.8 to 1.3 % in thrust, 0.5 to 1.1 % in specific fuel consumption, and 0.4 to 1.0 % in T_z^*, for static engine operation on the ground. The effect of F_e becomes stronger with increasing airspeed.

At n = const, a change in the losses in the engine exhaust system that are determined by the coefficient $\varphi_{j.n}$ must result, as seen from formula (10.2), in exactly the same change of the parameters of the operating process as a change in the jet nozzle area F_e.

If the losses in the exhaust system are increased or, in other words, if $\varphi_{j.n}$ is reduced, the exhaust system will show greater gas

flow resistance, so that the pressure p_2^* behind the turbine will increase and ε_T decrease, requiring an increase of gas temperature T_z^* in front of the turbine in order to maintain n = const. Consequently, a reduction in $\varphi_{j.n}$, like a reduction in F_e, will cause the regime of the turbojet engine to shift toward the surge limit along the $\overline{V}_{\text{II}} = \text{const}$ line (π_k^* is increased), and the stability margin of the engine will be reduced.

The change in the thrust of a turbojet engine when $\varphi_{j.n}$ is reduced and n = const, is a result of the increase of the temperature T_z^* and the simultaneous increase of the expansion ratio $\varepsilon_{j.n}$ in the jet nozzle that is due to the increase in π_k^* and the reduction of ε_T during this process.

As a rule, the increase in T_z^* and $\varepsilon_{j.n}$ has a decisive effect that results in an increase in the thrust of a turbojet engine at n = const and a reduction of $\varphi_{j.n}$, in spite of the increase of losses in the exhaust system (see figure 137). Moreover, the increase in the temperature T_z^* that is associated with the increasing losses in the exhaust system of the turbojet engine, also leads to an increase, at n = const, in the specific fuel consumption (see figure 137), since the specific thrust increases at a significantly lesser rate during this process (due to the reduction in $\varphi_{j.n}$) than it does for a reduction in F_e.

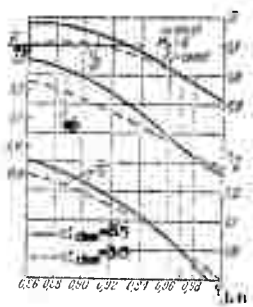

Figure 137: Dependence of the thrust and specific fuel consumption of a turbojet engine on the losses in the exhaust system (on $\varphi_{j.n}$), for n = const.

A 1 % increase of losses in the exhaust system of a turbojet engine at n = const and under otherwise equal conditions, can cause the thrust to increase by about 0.5 to 1.7 % and the specific fuel consumption by 0.7 to 1.4 %.

It is readily noted from the description given above that a change in the velocity coefficient φ_{NA} or, in other words, in the losses in the turbine nozzle assembly, must lead to exactly the same change in the parameters of a completed turbojet engine as a change in the area F_{NA} of the turbine nozzle assembly. In particular, the expansion ratio ε_T increases with decreasing φ_{NA},

resulting in a reduction of temperature in front of the turbine for n = const (if η_T = const during this process), and accordingly in a reduction of engine thrust and of the stability margin.

If the turbine efficiency η_T is increased, the temperature in front of the turbine that is required to maintain the previous rpm of the turbojet engine will increase, which follows directly from formula (10.2), and the air flowrate through the engine will decrease. Therefore, the regime of the engine shifts to the left and upwards along the $\frac{n}{\sqrt{T_H}}$ const line, approaching the surge limit, meaning that π_k^* increases. At the same time, the increase of the hydraulic losses in the turbine that are associated with the reduction in turbine efficiency η_T will cause a reduction of the adiabatic (polytropic) exponent of expansion, which also contributes to a reduction in the gas expansion ratio ϵ_T in the turbine. The increase in π_k^* and the reduction in ϵ_T lead to an increase of the gas expansion ratio in the jet nozzle, $\epsilon_{j.n}$. As a result of the simultaneous increase of T_z^* (and, accordingly, of $T_{\bar{z}}^*$) and $\epsilon_{j.n}$, the specific thrust and the thrust of a completed turbojet engine will increase with decreasing turbine efficiency η_T^* (see figure 138). The specific fuel consumption will increase, too, since in this case the reduction of that is due to the increase in the temperature T_z^* predominates over the increase in specific thrust.

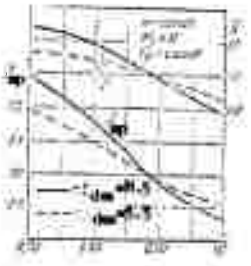

Figure 138: Dependence of the thrust and specific fuel consumption of a turbojet engine on turbine efficiency, at n = const.

If the compressor work L_k is increased with increasing compressor efficiency η_k at n = const, the temperature in front of the turbine must be increased, too. As a result, the regime of the turbojet engine will be displaced along the $\frac{n}{\sqrt{T_H}}=\text{const}$ line toward the surge limit, and the gas expansion ratio $\epsilon_{j.n}$ in the jet nozzle will increase because of the increase in π_k^*. Therefore, in this as in the preceding case, the thrust and the specific fuel consumption of the turbojet engine will be increased.

A 1 % reduction of turbine efficiency at n = const can lead to an increase in the temperature T_z^* of an existing turbojet engine by about 1.3 to 1.45 %, and by 0.8 to 1.8 % in the thrust and the

specific fuel consumption. And a 1 % reduction of compressor efficiency, or a 1 % increase of L_k at n = const, can cause T_z^* to increase by about 1.1 to 1.3 %, and the thrust and specific fuel consumption by 0.6 to 1.3 %.

If the loss in total pressure in the combustion chambers is increased or, in other words, if the coefficient $\sigma_{c.c}$ is reduced, the weight flowrate of air, G_a, will be reduced for a given value of π_k^*, due to the reduction of pressure in front of the turbine and, consequently, the entire operating line of a turbojet engine with F_e = const will be displaced to the left, toward the compressor surge limit.

Therefore, an increase in $\sigma_{c.c}$ at n = const leads to a reduction in the air flowrate through the compressor (unless the $\bar{V}_{\Gamma_H}^{n}$ line is vertical) and to an increase in both, the compression ratio π_k^* and the compressor work L_k. In that case, if the pressure drop in the jet nozzle, for instance, is supercritical so that ε_T = const, the temperature T_z^* in front of the turbine must be increased in accordance with the increase in L_k, if n = const is to be maintained. It is obvious that an increase in the temperature T_z^* at ε_T = const will in turn cause an increase in the temperature T_z^* in front of the jet nozzle. In order to explain how the gas expansion ratio $\varepsilon_{j.n}$ in the jet nozzle is changed in this case, let us revert to expression (10.2) on whose basis we can write

$$\varepsilon_{j.n} = p_z^*/p_H = p_z^*/p_H \, (\varphi_{NA} F_{NA}/\varphi_{j.n}/F_e)^m.$$

Substituting

$$p_z^*/p_H = \pi_{v.h}^* \pi_k^* \sigma_{c.c}$$

and taking into consideration the conditions used above, where $\pi_{v.h}^*$ = const, we obtain

$$\varepsilon_{j.n} = \sigma_{c.c} \pi_k^* \text{ const}.$$

Depending on the slope of the $\bar{V}_{\Gamma_H}^{n} = \text{const}$ line, the increase in the compression ratio π_k^* can be greater or smaller than the reduction in $\sigma_{c.c}$ that causes this increase. Therefore, the expansion ratio $\varepsilon_{j.n}$ in the jet nozzle can either increase or decrease with decreasing $\sigma_{c.c}$. Calculations show that this leads, respectively, to an increase or a decrease of engine thrust within the limits of about ± 0.5 % for a 1 % decrease in $\sigma_{c.c}$.

The specific fuel consumption increases with decreasing $_{c.c}$ (up to 0.5 % for 1 % of $\sigma_{c.c}$) as a result of the increase of the temperature T_z^* in front of the turbine (or decrease of α) which is decisive in this case.

An increase of losses at the engine inlet, or a decrease of the pressure coefficient σ_{in}, regardless of its causes leads to a reduction of air pressure $p_a^* = \sigma_{in} p_H^*$ at the compressor inlet.

However, the flowrate parameter does not depend on this pressure, since the weight flowrate of air at $T_H^* = \text{const}$ is proportional to the pressure p_a^*. Therefore, if σ_{in} is reduced and $n = \text{const}$, the compression ratio π_k^* and the compressor work L_k will remain constant, while the pressure $p_z^* = \sigma_{c.c} p_a^* \pi_k^*$ in front of the turbine will be reduced at the same rate as the pressure p_a^* in front of the compressor.

If there is a supercritical pressure drop in the jet nozzle, the expansion ratio ϵ_T in the turbine will be determined only by the magnitude of the ratio $\varphi_{NA} F_{NA} / \varphi_{j.n} F_e$, and will not depend on the pressure p_z^* in front of the turbine or, in other words, it will not be dependent on p_a^*, either. As a result, in this case the reduction in $_{in}$ leads to an identical reduction in both, the pressure p_z^* in front of the turbine and the pressure p_2^* behind the turbine, and the gas expansion ratio $\epsilon_{j.n}$ in the jet nozzle will be reduced.

Consequently, if there is a supercritical pressure drop in the jet nozzle, a reduction in σ_{in} under otherwise equal conditions will not violate the equality of $L_T = L_k$, and therefore no change in the temperature T_z^* in front of the turbine is required in order to maintain $n = \text{const}$ or, in other words, if there is a change in σ_{in}, the point that determines the equilibrium regime of the turbojet engine will maintain its previous position on the $\frac{n}{\sqrt{T_H^*}} = \text{const}$ line.

Moreover, the thrust of the engine and its specific thrust will decrease with decreasing σ_{in} and $n = \text{const}$, and the specific fuel consumption will increase, which is due to the reduction of the weight flowrate of air through the engine and of the gas expansion ratio $\epsilon_{j.n}$ in the jet nozzle.

However, if there is a subcritical pressure drop in the jet nozzle of a turbojet engine, the reduction of σ_{in} at the inlet and, consequently, of the pressure p_z^* in front of the turbine as well, will cause a reduction of the gas expansion ratio ϵ_T in the turbine or, in other words, if there is a reduction in σ_{in} the pressure p_z^* will drop at a faster rate than the pressure p_2^*, so that the temperature T_z^* must be increased in order to maintain $n = \text{const}$, which follows from equation (10.2). This leads to a simultaneous decrease of thrust and increase of specific fuel consumption, and to a displacement of the regime of the engine to the left and upwards along the $\frac{n}{\sqrt{T_H^*}} = \text{const}$ line, or toward the surge limit (see figure 139), and the stability margin of the turbojet engine will be decreased which frequently proves to be an inacceptable consequence of a reduction in σ_{in}.

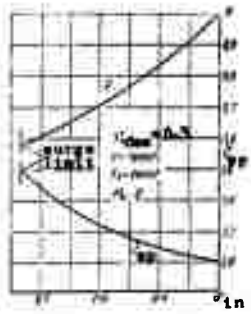

Figure 139: Dependence of the thrust and specific fuel consumption of a turbojet engine on the losses at the engine inlet, for n = const.

CHAPTER 12

CHARACTERISTICS OF TURBOJET ENGINES

1. General Considerations

An engine installed in an aircraft is operated at different rpm, airspeed, and altitude. Therefore, an exhaustive evaluation of all the qualities and capabilities of a turbojet engine requires that the dependencies of its thrust and specific fuel consumption on rpm, airspeed, and altitude be known. These dependencies are called the primary characteristics of a turbojet engine.

The dependencies of the thrust and specific fuel consumption of a turbojet engine on the rpm are called the rpm characteristics or throttling characteristics.

The dependencies of the thrust and specific fuel consumption of a turbojet engine on airspeed and altitude are called, respectively, airspeed characteristics and altitude characteristics or, combined, flight characteristics or altitude-airspeed characteristics.

The primary characteristics of a turbojet engine are established either by means of testing the engine on special test stands or in special aircraft or airborne laboratories, or they are obtained with more or less accuracy on the basis of calculations.

The profile of the primary characteristics of a turbojet engine, or the rate of change of its thrust and specific fuel consumption with changing airspeed and altitude as well as rpm, depends strongly on the control schedule selected for the engine.

The control schedule is defined as the rules for varying the primary parameters or control parameters of an engine (such as n, T^*_z, and others) that determine its thrust and specific fuel consumption.

It is obvious that the control schedule must ensure the most advantageous and reliable utilization of the engine during flight.

Consequently, in order to consider the characteristics of turbojet engines it is first of all necessary to examine the basic problems associated with their control schedules.

2. Concept of the Control Schedules of Turbojet Engines

The primary tasks of turbojet engine control are:

to provide the maximum possible thrust at all required airspeeds and altitudes (take-off, climbing, acceleration, maximum airspeed, maximum possible altitude);

to ensure a minimum possible fuel consumption during flight under reduced thrust regimes (maximum range or maximum endurance flight);

to protect the engine against dangerous or instable regimes or, in other words, against exceeding n_{max} and $T^*_{z\,max}$, against surging, against instable fuel consumption, and other conditions.

Under otherwise equal conditions the maximum thrust of a given turbojet engine is obtained at maximum rpm (maximum air flowrate) and at the maximum acceptable gas temperature in front of the turbine. Therefore, in order to ensure maximum possible thrust, it is necessary to maintain the maximum rpm of the engine and the maximum gas temperature in front of the turbine that is acceptable for it when there is a change in airspeed and altitude or, in other words, to accomplish a control schedule corresponding to

$$n_{\ldots} = \text{const}, \quad T^{\circ}_{\ldots} = \text{const} \tag{12.1}$$

Two governors are required to accomplish the control schedule of a turbojet engine: a governor acting on the engine rpm by means of varying the fuel input into the combustion chambers (rpm governor) and a governor acting on the minimum flow area of the jet nozzle (nozzle governor).

As a rule, modern turbojet engines have a supercritical pressure drop in the jet nozzle during stationary operation on the ground, not only at maximum rpm but frequently also at a lower rpm. A subcritical pressure drop in the jet nozzle of a turbojet engine at maximum rpm in static operation on the ground is obtained only if the designed compression ratio is $\pi^{*}_{k\,des} \approx 3.5$ and if $T^{\circ}_{g\,max} \leqslant 1050^{\circ}K$. But in that case a supercritical pressure drop in the jet nozzle will set in after only a small increase in airspeed and altitude, or at a Mach number of $M_H \geqslant 0.20$ to 0.30.

Moreover, as shown in the preceding chapter, the condition $L_k/T^{\circ}_g = \text{const}$ is satisfied for supercritical pressure drops in the jet nozzle. Therefore, if the fuel flow governor ensures a constant rpm when there is a change in airspeed and altitude, and if the compressor work L_k does not depend on the temperature T°_H of the air entering the compressor, so that $L_k = \text{const}$, the condition $T^{\circ}_g = \text{const}$ will be satisfied at the same time.

Consequently, in the particular case where there is a supercritical pressure drop in the jet nozzle and $L_k = \text{const}$, the control schedule $n_{max} = \text{const}$ and $T^{\circ}_{g\,max} = \text{const}$ will be ensured by only one fuel flow governor.

However, if the compressor work L_k at $n = \text{const}$ depends on the temperature T°_H of the air entering the compressor (see figure 134) and, consequently, also on the airspeed and altitude, the jet nozzle area F_e must be changed in order to keep both $n = \text{const}$ and $T^{\circ}_g = \text{const}$ when there is a change in airspeed and altitude, even if there is a supercritical pressure drop in the jet nozzle.

In fact, if the compressor work L_k decreases with increasing airspeed or with decreasing altitude (in other words, with increasing T°_H) at $n = \text{const}$, and if $F_e = \text{const}$, even the temperature T°_g in front of the turbine must be reduced, according to formula (10.3), in order to maintain $n = \text{const}$, which no longer satisfies

the condition for obtaining maximum thrust. Consequently, in that case the jet nozzle area F_e must be reduced in order to accomplish n_{max} = const and $T^*_{g\,max}$ = const schedules or, in other words, the turbine work L_T must be reduced (in accordance with the reduction of L_k), not by reducing the temperature T^*_g in front of the turbine but by reducing the gas expansion ratio in the turbine.

Conversely, if the compressor work L_k increases (with increasing T^*_H) under the conditions indicated above, the temperature T^*_g in front of the turbine must be increased, according to formula (10.1), in order to maintain n = const if F_e = const. It is obvious that the jet nozzle area F_e must be increased in order to prevent this increase of T^*_g and thus to accomplish n_{max} = const and $T^*_{g\,max}$ = = const schedules under these circumstances. Otherwise the temperature T^*_g can exceed the acceptable magnitude.

Thus, to accomplish control schedules at maximum thrust, or at n_{max} = const and $T^*_{g\,max}$ = const, turbojet engines with axial-flow compressors in the majority of cases require the use of a jet nozzle with variable minimum cross-section area. This nozzle must be "infinitely variable" in order to maintain the n_{max} and $T^*_{g\,max}$ schedules accurately; in other words, its area F_e must be varied gradually, always in accordance with the change in airspeed and altitude. However, such a control of the jet nozzle area significantly complicates the engine control system. Moreover, in the majority of cases, turbojet engines with axial-flow compressors show a comparatively small variation of temperature T^*_g in front of the turbine when there is a change in airspeed and altitude at n = const and constant jet nozzle area.

Therefore, an infinitely variable jet nozzle is not usually employed. In certain cases, where this is necessary, a "stepped" jet nozzle control is used. But in the majority of existing turbojet engines the net nozzle area is not controlled in accordance with airspeed and altitude.

It follows from the foregoing that the following control schedules can be accomplished under a fixed jet nozzle area:

$$n_{max} = \text{const}, \quad F_e = \text{const} \tag{12.2}$$

and

$$T^*_{g\,max} = \text{const}, \quad F_e = \text{const} \tag{12.3}$$

The first of these (12.2) is mostly used in existing turbojet engines, since it requires the simplest control system (one governor reacting to rpm deviations and acting on the fuel flow) and since with respect to results, meaning the available maximum thrust of the turbojet engine, it comes usually close to schedule (12.1). However, in the case of schedule (12.2) the temperature T^*_g in front of the turbine can rise with increasing airspeed or ambient temperature (due to the associated increase of L_k), which must be taken

into consideration by selecting the temperature T_g^* for maximum rpm under standard atmospheric conditions on the ground at V = 0.

The second schedule (12.3) is more difficult to accomplish since it requires the use of a fuel flow governor reacting directly to the gas temperature T_g^* in front of the turbine, while the temperature field in the gas flow in frontof the turbine is always characterized by an appreciable and inconstant irregularity. And the variations in the rpm of a turbojet engine with changing airspeed and altitude that are possible under schedule (12.3) lead to a greater degree of poor engine utilization with respect to thrust than the corresponding variations of the temperature in front of the turbine under schedule (12.2).

The required control schedule and the profile of the characteristics of a turbojet engine depend to a large degree on the designed compression ratio $\pi_{k\,des}^*$ of the compressor and on the designed air temperature $T_{H\,des}^*$ at the compressor inlet, that is the temperature for which the designed regime of the compressor is established.

As a rule the designed regime of a compressor is so selected that it corresponds to the maximum air flow capacity of the compressor at the required stability margin with respect to π_k^* (that is, $\Delta n_k^* = 12$ to 17 %).

As we know, the maximum capacity of a compressor is obtained at the limiting acceptable Mach number M_a at the compressor inlet or, in other words, at that Mach number $M_{a\,cr}$ which cannot be exceeded without causing a large drop in compressor efficiency so that the air flowrate is practically no longer increased (so-called compressor "choking"). As a rule, $M_{a\,cr}$ is located within the range from 0.6 to 0.7.

If the air temperature T_H^* at the compressor inlet is reduced below its designed magnitude $T_{H\,des}^*$ at n = const, the rpm parameter will be increased, and the point that determines the compressor regime will shift along the operating line of the turbojet engine in the direction above and to the right of the operating point of the compressor. As a result, the Mach number M_a at the compressor inlet becomes greater than its limiting value $M_{a\,cr}$ that corresponds to the designed regime, and the compressor efficiency is greatly reduced, while small values of $\pi_{k\,des}^*$ can also result in compressor surging, as we showed earlier. Consequently, the designed temperature $T_{H\,des}^*$ is selected close to the minimum air temperature T_H^* at the compressor inlet that is possible during engine operation in the aircraft.

In that case, the air temperature T_H^* at the compressor inlet will be increased in comparison to its designed magnitude $T_{H\,des}^*$ with increasing airspeed (or flight Mach number M_H). If n = const is maintained during this process, the Mach number M_a at the compressor inlet will become smaller than $M_{a\,cr}$ as a result of the

reduction in the rpm parameter and the resulting shift of the compressor regime to the left and downward along the operating line of the turbojet engine. The decrease in the Mach number M_a in turn leads to a reduction of compressor capacity, so that the air flowrate and, consequently, the thrust of the engine as well, become less than they could be if $M_{a\ cr}$ = const were maintained (curve 1,1 in figure 140).

However, in turbojet engines intended for comparatively slow supersonic airspeeds the temperature T_H^* at the compressor inlet will not increase that much with increasing airspeed, so that the rpm parameter and, accordingly, the Mach number M_a are reduced to a relatively small degree at n = const. Thus, for instance, if the flight Mach number M_H is increased to as much as 1.8 to 2 at an altitude of 11 km, the rpm parameter will be reduced by only 12 to 14 %, and the Mach number M_a to about 20 to 25 %, depending on the designed compression ratio of the compressor. Therefore, using the control schedules (12.1) and (12.2) that ensure a constant rpm with changing airspeed and altitude at low values of $T_{H\ des}^*$, will yield completely satisfactory results for this type of engine.

The temperature T_H^* at the compressor inlet of turbojet engines intended for fast supersonic airspeeds will change within broad limits. Therefore, at maximum and close to maximum airspeeds the rpm parameter will be reduced significantly at n = const and for a low value of $T_{H\ des}^*$, resulting primarily in a large reduction of M_a and of compressor capacity (point 1 in figure 140). This will already reduce the maximum thrust value significantly, so that the compressor flow areas must be increased (to increase the air flowrate) in order to provide the required thrust at fast supersonic airspeeds, and consequently, the compressor weight will increase.

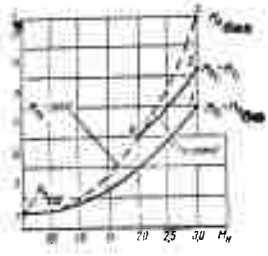

Figure 140: Relative variation of the air flowrate through a turbojet engine with changing flight Mach number M_H (1,1 - n = const; 2,0,1 - combined control schedule; 3,0,1 - V_{pr} = const; F_e = const).

Moreover, if the rpm parameter of a turbojet engine with a significant designed compression ratio $\pi_{k\ des}^*$ is greatly reduced, the stability margin, as we know, will decrease with decreasing

rpm, and compressor surging will develop, requiring special controls in the compressor (for instance, with the aid of pivoting blades in some stages).

One of the possible means of increasing the compressor capacity and, consequently, of increasing the thrust, reducing the compressor weight, and preventing compressor surging at fast supersonic airspeeds, is to design the compressor for maximum capacity at maximum airspeed, that is at $M_{H\ max}$ (point 3 in figure 140). For this purpose the designed air temperature $T^*_{H\ des}$ at the compressor inlet must be equal to the air temperature T^*_H that corresponds to the maximum flight Mach number $M_{H\ max}$.

However, in that case it already becomes impossible to maintain the engine rpm constant with decreasing flight Mach number M_H since the rpm parameter is increased as a result of the reduction of inlet air temperature, and since the Mach number M_a at the compressor inlet is increased and exceeds its limit value $M_{a\ cr}$. Compressor "choking" and a sharp drop in compressor efficiency are the result. Compressor surging is possible, too, if $\pi^*_{k\ des}$ is a small value.

Consequently, the engine must be controlled so that the Mach number M_a at the compressor inlet will not remain above its limiting value at less than maximum airspeeds (curve 3,0,1 in figure 140).

For this purpose the control schedule

$$\frac{n}{\sqrt{T^*_H}} = \text{const};\quad F_e = \text{const} \tag{12.4}$$

can be used where it also applies, of course, that $T^*_z/T^*_H = \text{const}$ so that the point which determines the compressor regime in the field of compressor characteristics will not shift with a change in the flight Mach number M_H (in the temperature T^*_H) or, in other words, so that $\pi^*_{k\ des} = \text{const}$ and $G_a\sqrt{T^*_H}/P^*_a = \text{const}$ are maintained.

In order to ensure this control schedule (12.4) the engine rpm must be reduced in proportion to $\sqrt{T^*_H}$ with decreasing airspeed, resulting in a reduction of the gas temperature T^*_z in front of the turbine that is proportional to T^*_H. But a reduction of rpm and temperature in front of the turbine with an accompanying significant reduction in the air flowrate (curve 3,0,1 in figure 140) results in a sharp reduction of thrust at slow airspeeds and particularly under conditions of takeoff and acceleration of the aircraft, that is at the very moment when a maximum of excess thrust is demanded of the engine. This is the very considerable disadvantage of designing a compressor for maximum capacity at high supersonic airspeed and of the associated control schedule (12.4). The sharp reduction of thrust in this case can be prevented to a significant degree if $T^*_z = \text{const}$ is maintained at the same time with $F_e = \text{const}$. However, for this purpose it is necessary to control the area of the turbine nozzle assembly, F_{NA}, which is associated with significant design complications.

For these reasons a combined control schedule is more advantageous from the point of turbojet engines intended for fast supersonic airspeeds, a schedule representing a combination of schedule (12.1) or (12.2) with schedule (12.4).

This type of combined control schedule can be accomplished in the case where the Mach number M_a at the compressor inlet is lower at maximum airspeed (at $M_{H\ max}$) than its limiting value $M_{a\ cr}$ (point 2 in figure 140). For this purpose the designed air temperature $T^*_{H\ des}$ at the compressor inlet is selected lower than the air temperature T^*_H obtained at $M_{H\ max}$, but at the same time greater than the minimum temperature T^*_H that is possible under operational conditions.

This will make it possible to accomplish, initially, the control schedule (12.1) or (12.2) at decreasing flight Mach number M_H or, in other words, to maintain the rpm constant until the Mach number M_a at the compressor inlet reaches its limiting value $M_{a\ cr}$ as a result of the reduction in air temperature from $T^*_{H\ max}$ to $T^*_{H\ des}$ (point 0 in figure 140). Subsequently, as the flight Mach number M_H continues to increase, the $\frac{n}{\sqrt{T^*_H}} = \text{const}$ and F_e = const control schedule sets in already, and the limiting Mach number $M_{a\ cr}$ that is reached at the compressor inlet is kept constant.

It is readily noted that with the transition from control schedule (12.4) to this combined schedule the compressor capacity and, consequently, the thrust of the turbojet engine as well, are reduced at maximum airspeed and under otherwise equal conditions, but on the other hand the thrust can be increased considerably during take-off and at slow airspeeds.

Under reduced thrust regimes or throttled regimes the primary task of the controls of a turbojet engine is to ensure maximum economy or, in other words, a minimum of specific fuel consumption.

Under given environmental conditions the thrust of an existing turbojet engine can be reduced by different means, for instance by reducing the rpm at constant jet nozzle area, by reducing the gas temperature in front of the turbine at n = const, by reducing the rpm at T^*_z = const, and by other means.

We know that each combination of compression ratio and efficiency of a compressor corresponds to an optimum gas temperature in front of the turbine of a turbojet engine, a temperature where a minimum of specific fuel consumption is obtained.

But at the maximum rpm of a turbojet engine the temperature in front of the turbine is not established at the optimum level from the point of minimum specific fuel consumption, but at a higher, limiting acceptable level for the turbine. This is done in order to obtain the maximum possible specific thrust that is required to reduce the specific weight and drag area of the engine.

Reducing the thrust of a turbojet engine by means of reducing its rpm at F_e = const will lead to a rapid drop in compression ratio as well as to a considerable drop in compressor efficiency, if the designed compression ratio is significant. At the same time, for each new, reduced equilibrium rpm the associated temperature in front of the turbine will be $T_z^* < T_{z\,max}^*$, establishing the equality $L_T = L_k$ of turbine work and compressor work. The magnitude of this temperature will not always correspond to its optimum value for given values of π_k^* and η_k from the point of minimum specific fuel consumption. Therefore, controlling the magnitude of the thrust of a turbojet engine by means of changing the rpm (the fuel flow at F_e = const) is not always best from the point of economy, although it is widely used because of its simplicity.

Reducing the thrust of a turbojet engine by means of reducing only the gas temperature in front of the turbine requires an increase in jet nozzle area in order to keep the rpm constant. Sometimes this can achieve a better combination of temperature in front of the turbine and compression ratio than the preceding technique, so that the economy of the engine at reduced thrust regimes is increased. However, it must be kept in mind that, if the temperature T_z^* is reduced significantly at n = const, the equilibrium regime of the turbojet engine, shifting along the $\frac{n}{\sqrt{T_H^*}} = \text{const}$ line, can prove to be located in the area of appreciably reduced values of compressor efficiency and, in addition, it is not impossible for the turbine efficiency to be reduced, too. Consequently, where this means of reducing the thrust is used it is usually combined with the preceding technique so that, initially, the thrust is reduced by means of reducing T_z^* at n = const (F_e is increased), and subsequently by reducing the rpm at F_e = const.

Also in a number of cases an increase of jet nozzle area and a reduction of rpm of a turbojet engine for the purpose of reducing its thrust is advantageously combined with a control of the compressor (for instance, with the aid of pivoting blades in the straightening rigs) that prevents the considerable drop in compressor efficiency which is possible here; this technique is used in some turbojet engines.

Reducing the thrust of a turbojet engine at reduced rpm and T_z^* = const involves a reduction of the air flowrate and the compression ratio of the compressor. In that case the jet nozzle area F_e must be reduced in order to maintain T_z^* = const. But as a rule, a reduction in the compression ratio and efficiency of the compressor at T_z^* = const will lead to a significant increase of specific fuel consumption. Moreover, if T_z^* = const, the temperature regime will remain almost as strained at reduced thrust as it is under maximum thrust. Consequently, a transition to a reduced thrust regime at T_z^* = const has no practical application.

3. Throttling Characteristics of Turbojet Engines

The throttling characteristics of a turbojet engine are defined as the dependencies of thrust and specific fuel consumption on rpm at a given airspeed and altitude. As a rule, the following engine regimes are recorded for these characteristics or mentioned with reference to them.

1. The maximum power regime, that is the maximum acceptable rpm, n_{max}, and its corresponding maximum thrust P_{max} where reliable, uninterrupted, but temporary engine operation (usually not more than 5 to 10 min) is guaranteed. This regime is used for take-off, sometimes for aircraft acceleration, for reaching maximum altitude, as well as for a temporary increase of airspeed.

2. The rated power regime, that is the rated rpm, $n_{com} \leq n_{max}$, and its corresponding rated thrust where a longer and more reliable engine operation (without interruption for a period of not less than 30 min) is guaranteed. When the engine operates on a test stand, $n_{nom} = (0.96 \text{ to } 1.0)n_{max}$, and $P_{nom} \approx 0.9\ P_{max}$. This regime is used for extended climbing and for flight at close to maximum airspeed.

3. The cruising power regime, that is the rpm reduced to $n = 0.9\ n_{max}$ under test stand conditions and its corresponding thrust $P_{cruise} = (0.70 \text{ to } 0.75)\ P_{max}$. This regime guarantees uninterrupted and reliable engine operation over its established period of service (service life). This regime is frequently called the maximum cruising power regime. In addition, an even more reduced regime is frequently recorded, that is the rpm corresponding to a thrust of about $(0.5 \text{ to } 0.6)\ P_{max}$ under test stand conditions. Cruising power regimes are used for flights at great endurance or long range.

4. The low throttle regime or low throttle rpm, $n_{l.t}$, that is the minimum rpm where the engine can still operate at complete stability. The engine thrust at low throttle rpm must not exceed 3 to 5 % of maximum thrust to ensure that the rolling distance of the aircraft in a power landing will not be increased. The low throttle rpm of modern turbojet engines under ground (test stand) conditions amounts to $(0.2 \text{ to } 0.4)n_{max}$. As a rule, the duration of the uninterrupted operation of a turbojet engine at a low throttle regime is limited to some degree because of the reasons mentioned in the preceding chapter.

The specific fuel consumptions established for a given engine and guaranteed by the manufacturer are indicated for all the regimes listed above (with the exception of low throttle).

Typical rpm characteristics acquired on the test stand for one of the existing turbojet engines with $F_e = \text{const}$ are shown in figure 141. It is seen that engine thrust decreases rapidly with decreasing rpm, while the specific fuel consumption slightly decreases at first and subsequently increases rapidly. Let us consider the causes for these rpm profiles of the thrust and specific fuel consumption of a turbojet engine with $F_e = \text{const}$.

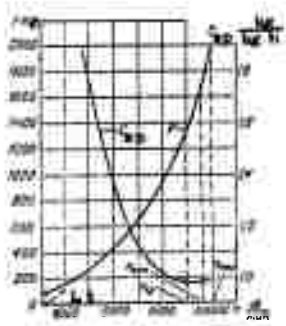

Figure 141: Throttling characteristics of a turbojet engine.

The compression ratio, and consequently the efficiency of the compressor as well, decrease with decreasing rpm of a turbojet engine. Also, the gas temperature in front of the turbine decreases during this process and begins to rise only at rpm values comparatively close to idling rpm. The reduction in π_k^*, η_k, and temperature in front of the turbine causes a reduction of gas exhaust velocity from the jet nozzle and, consequently, of specific thrust, too (see figure 142); during this process the specific thrust continues to decrease with the transition to low rpm where the temperature T_z^* already begins to increase. This is due to the determinative effect of the reduction in π_k^* (and, consequently, also of $c_{j.n}$), η_k, and η_T on specific thrust.

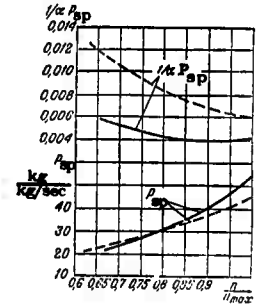

Figure 142: Dependence of the specific thrust of a turbojet engine on rpm.

Since the air flowrate through the engine decreases with decreasing rpm, the thrust will drop at a faster rate in this case than the specific thrust. A 1 % reduction in rpm under test stand conditions will reduce the thrust of a turbojet engine by about

3 to 4 %. As the rpm is reduced its effect on thrust becomes less. However, under airborne conditions the effect of rpm on the magnitude of turbojet engine thrust becomes significantly greater.

The nature of the rpm variation of specific fuel consumption is determined by the dependence of specific thrust and the excess of air coefficient on rpm, since $C_{sp} = 3600/\alpha l_o P_{sp}$.

A reduction of specific thrust at reduced rpm will cause an increase in specific fuel consumption.

However, the temperature difference $(T_z^* - T_k^*)$ and the heat release coefficient $\xi_{c.c}$ and, consequently, the excess of air coefficient α that depends on these magnitudes, will change at varying degrees for the same relative rpm reduction in different engines. This is primarily due to the differences in the characteristics of the compressors and combustion chambers used. To illustrate this, figure 142 shows the dependence of the difference $(T_z^* - T_k^*)$ and coefficient α on the rpm for two engines with different values of designed compression ratio. For the same two engines, figure 142 shows the rpm variation of P_{sp} and the ratio $1/\alpha P_{sp}$ that is proportional to specific fuel consumption. It is seen that, if the excess of air coefficient increases significantly with decreasing rpm, the magnitude $1/\alpha P_{sp}$ and, consequently, C_{sp} as well, in spite of the reduction of specific thrust involved here will first decrease appreciably and subsequently increase, but at a slower rate than the specific thrust decreases. However, if the excess of air coefficient changes little with decreasing rpm, the specific fuel consumption C_{sp} will rise at about the same rate as the specific thrust decreases.

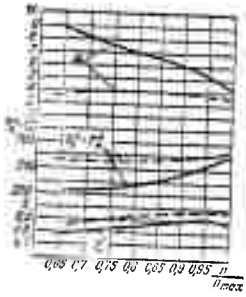

Figure 143: Determination of the dependence of C_{sp} on the rpm of a turbojet engine.

The rpm characteristics of a turbojet engine with F_e = const and with an axial-flow compressor controlled by bypassing part of the air into the atmosphere have a slightly different profile than the one described above. These characteristics are shown in figure 144. It is seen that the thrust of the engine is reduced immediately and the specific fuel consumption increased at the rpm value of

n_{byp} where the bypass ducts open so that part of the air can be passed from the compressor into the atmosphere. In this case the reduction in thrust is a direct result of the reduction in the gas flowrate through the turbine and, consequently, through the jet nozzle as well.

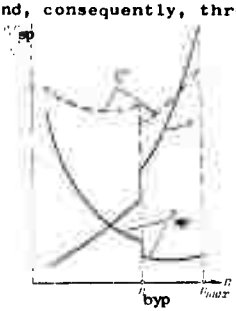

Figure 144: Throttling characteristics of a turbojet engine with air bypass from the compressor.

In spite of the increase of the temperature T_z^* in front of the turbine that is involved, the specific thrust (referred to the air flowrate through the turbine) and, consequently, the temperature T_2^* in front of the jet nozzle as well, will practically not change since the gas expansion ratio in the jet nozzle is reduced at the same time as a result of the decrease in the compression ratio. And the increase in specific fuel consumption when air is being bypassed from the compressor is due to the increase in the temperature in front of the turbine and the simultaneous reduction in the compressor compression ratio, resulting in a reduction of the excess of air coefficient α.

The profile of the rpm characteristics of a turbojet engine with a triple step variation of the jet nozzle area F_e is shown in figure 145. In this case the thrust is initially reduced at n_{max} = const as a result of a reduction of the temperature in front of the turbine, which is accomplished by increasing the jet nozzle area over its designed magnitude $F_{e\ des}$ that corresponds to maximum thrust, to $F_{e1} < F_{e\ des}$. Here the specific fuel consumption is slightly reduced since a more favorable relationship between temperature in front of the turbine and compressor compression ratio is obtained. As the engine rpm is decreased further at F_{e1} = const, the thrust is reduced, too, and the specific fuel consumption drops a little more and then rises rapidly. At reduced rpm n_{byp} the jet nozzle area is increased a second time to $F_{e2} < F_{e1}$, in order to increase the surging margin. Consequently, the thrust decreases again because of the reduction of the temperature in front of the turbine at n = const. But in this case the relationship between temperature in front of the turbine and compressor compression ratio becomes less favorable, and the specific fuel consumption increases. Subsequently, a further reduction of thrust and the transition to

the low throttle regime is accomplished by reducing the rpm at F_{e2} = const, and in that part the rpm characteristic has the profile described above.

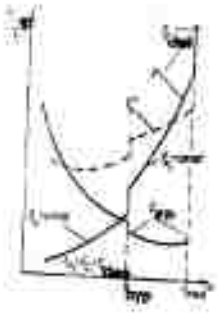

Figure 145: Throttling characteristics of a turbojet engine with triple-step variation of the jet nozzle area.

4. Airspeed Characteristics of Turbojet Engines

The airspeed characteristics of a turbojet engine are defined as the dependencies of thrust and specific fuel consumption on the airspeed (flight Mach number M_H) at a given altitude and for the control schedule selected for the engine.

Typical airspeed characteristics of a turbojet engine with an n = const and T_z^* = const control schedule are shown for different altitudes in figure 146, where the values for the thrust, P_0, and the specific fuel consumption, $C_{sp\ 0}$, obtained during static engine operation on the ground (V = 0), are assumed to be equal to one.

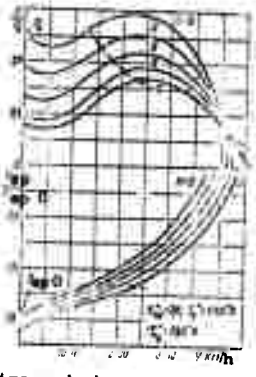

Figure 146: Airspeed characteristics of a turbojet engine for n = const and T_z^* = const.

It is seen from figure 146 that, if the airspeed is increased at n = const and T_g° = const and at a given altitude, the thrust of the turbojet engine at first decreases slightly, subsequently increases, and after reaching a certain maximum decreases again, down to a value of zero. The specific fuel consumption increases continuously with increasing airspeed.

This nature of the dependence of thrust on airspeed is due to the following causes.

The velocity head compression ratio increases with increasing flight Mach number M_H. At the same time the compressor compression ratio decreases as a result of the increase in the air temperature T_H° at the compressor inlet and because n = const. But the effect of the velocity head compression ratio is always predominant in this case, so that the overall compression ratio π_0° increases with increasing Mach number M_H (airspeed). As a result, the air pressure p_k° behind the compressor and, consequently, the gas pressure p_g° in front of the turbine and p_2° at the turbine outlet are increased.

An increase of the pressure p_g° in front of the turbine at T_g° = const will result in an increase of the air flowrate through the engine. At the same time the gas expansion ratio in the jet nozzle will increase as a result of the increase in pressure behind the turbine, so that the gas exhaust velocity from the jet nozzle is increased (in the case of a converging nozzle, up to the moment when a critical pressure drop is established in the nozzle). However, as it can be seen from figure 147, the gas exhaust velocity c_e from the jet nozzle increases at a slower rate than the airspeed, so that the velocity difference and, consequently, the specific thrust that is proportional to this difference, decrease with increasing airspeed.

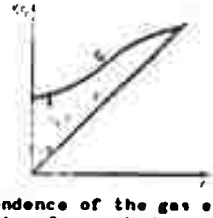

Figure 147: Dependence of the gas exhaust velocity from the jet nozzle of a turbojet engine on the airspeed.

The temperature at the compressor outlet increases with increasing airspeed at n = const (due to the increase in T_H°), while T_g° = const, so that the temperature difference $(T_g^\circ - T_k^\circ)$ and, accordingly, the quantity of heat added to one kg of air in the engine, are reduced. This is also the cause for the decrease of specific thrust when the airspeed increases. At high airspeed the temperature difference $(T_g^\circ - T_k^\circ)$ and the quantity of heat input that is determined

by it can become so small that this heat will be sufficient only to cover the losses in the engine, and in that case the specific thrust becomes equal to zero. It is obvious that the airspeed where the specific thrust and, consequently, the thrust of the engine become equal to zero, will increase with increasing gas temperature in front of the turbine; under otherwise equal conditions.

Thus, if the temperature in front of the turbine remains constant at increasing airspeed, the weight flowrate of air through the engine will increase, while the specific thrust will decrease (see figure 148).

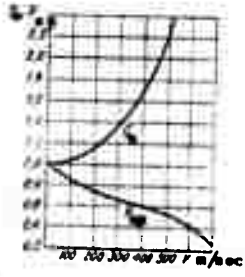

Figure 148: Relative variation of the specific thrust and air flowrate of a turbojet engine with changing airspeed.

In the beginning, as the airspeed increases, the air flowrate will increase at a slower rate than the specific thrust decreases, and the thrust of the engine will be reduced. Subsequently, the increase in the air flowrate begins to predominate over the reduction in specific thrust, and the thrust of the engine will increase. Finally, when there is a very great increase in airspeed, the specific thrust is reduced so significantly that this reduction is no longer compensated by the additional increase of the air flowrate, and the thrust of the engine begins to decrease rapidly.

In order to explain the causes for the increase of specific fuel consumption with increasing airspeed we can use the known expression $C_{sp} = 3600/\gamma_1 P_{sp}$, from which it follows that the specific fuel consumption must change inversely proportional to the product γP_{sp}.

Since the temperature difference $(T_z^o - T_k^o)$ decreases with increasing airspeed, the excess of air coefficient α will increase. But since the decrease of specific thrust is more significant, the product γP_{sp} will continue to decrease in spite of the increase in α (see figure 149), which also leads to the continuous increase of specific fuel consumption mentioned above.

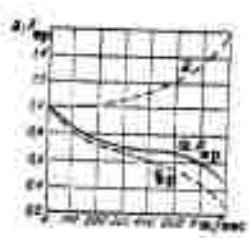

Figure 149: Relative variation of α and P_{sp} with changing airspeed.

The total fuel consumption per hour, G_{fuel}, must also increase with increasing airspeed, since the air flowrate through the engine increases so that the fuel flow into the combustion chambers must be increased in order to heat it to the required temperature T_z^*. At the same time, when the airspeed is increased the required fuel consumption G_{fuel} will increase at a slower rate than the air flowrate G_a through the engine, since the excess of air coefficient α increases during this process, and $G_{fuel} = G_a/\alpha l_o$.

Consequently, the specific fuel consumption will actually increase with increasing airspeed because the fuel consumption per hour increases while the thrust of the engine is decreased during this process, and if it does increase it will rise at a lesser rate than G_{fuel} (due to the reduction of P_{sp}).

However, it must be taken into consideration that an increase of specific fuel consumption with increasing airspeed does not at all indicate a simultaneous deterioration of heat utilization in the engine.

From the point of effective utilization of the consumed heat the economy of a turbojet engine in flight is determined, as we showed earlier, by the value of economic efficiency η_{econ} which is equal to the product of effective efficiency η_e and propulsive efficiency η_p, that is the relative magnitude of that part of the consumed heat that is converted into external work performed by the thrust force.

The dependence of economic efficiency η_{econ} and, separately, of η_e and η_p on the airspeed at $T_z^* = 1200^\circ K = const$, is shown in figure 150. It is seen that these efficiencies and, consequently, the economy of a turbojet engine, increase with increasing airspeed and begin to decrease only after a very high airspeed is reached (the propulsive efficiency decreases continuously).

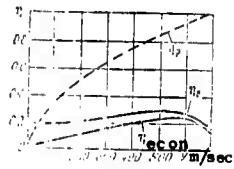

Figure 150: Dependence of the efficiencies of a turbojet engine on the airspeed.

The increase and subsequent decrease of effective efficiency with increasing airspeed that is noted in figure 150, is due to the following causes.

The pressure in front of the turbine increases with increasing airspeed, so that the overall expansion ratio of the combustion products in the engine after yielding their heat is increased. This contributes toward improved heat utilization in the engine and, consequently, toward an increase of η_e.

On the other hand, since the quantity of heat added to one kg of air decreases with increasing airspeed at T_z^* = const, due to the reduction of the difference $(T_z^* - T_k^*)$, the relative portion of this heat that is used to cover the losses in the engine will increase, which contributes to a reduction of η_e.

In the beginning the first cause will play the decisive role, and the effective efficiency will increase with increasing airspeed. Subsequently, when the airspeed becomes very significant, the reduction of the heat input will have the predominant effect, and η_e will decrease.

The increase of propulsive efficiency with increasing airspeed is due to the fact that the exhaust velocity c_e increases at a slower rate than the airspeed, that is the ratio c_e/V is reduced and, therefore, the unconsumed kinetic energy of the flow $(c_e-V)^2/2g$, is reduced.

If the airspeed is increased at a given altitude, the velocity head $\gamma_H V^2/2g$ of the air flow entering the engine will increase, so that the pressure and density of the air inside the engine will increase at n = const. Therefore, the mechanical loads on the compressor and turbine blades and on the casings of all engine elements will increase. Moreover, as a result of the increase in the weight flowrate of air through the engine the turbine power and the compressor capacity, and at n = const also the shaft torque, will increase. Consequently, the maximum limiting airspeed up to which reliable utilization of a turbojet engine from the point of strength is possible at n = const for a given altitude, is limited by the magnitude of velocity head $\gamma_H V^2/2g$ that is acceptable in this respect. It is obvious that the acceptable airspeed, limited by the strength of the engine parts, will increase with increasing altitude. To exceed the limiting airspeed for a given turbojet engine is possible only at a corresponding reduction of rpm (and, consequently, of π_k^* and π_o^*), ensuring the necessary strength margins for the engine parts. But in that case the thrust of a turbojet engine will decrease sharply, and the specific fuel consumption will increase. As an exmaple, in figure 146 these limiting airspeeds are indicated by dotted lines on whose right-hand side those parts of the characteristics of a turbojet engine at n = const are located that can practically not be utilized because of an inacceptable increase of mechanical stresses in engine parts.

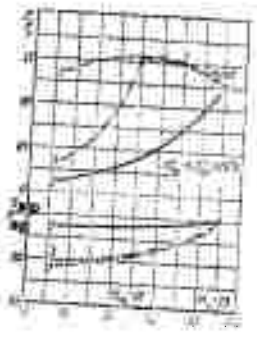

Figure 151: Velocity characteristics of a turbojet engine for three control schedules: 1 - n = const and T_z^* = const; 2 - $n/\sqrt{T_H^*}$ = const and F_e = const; 3 - combined schedule.

The profile of the airspeed characteristics of a turbojet engine with an $\frac{n}{\sqrt{T_H^*}} = \text{const}$ and F_e = const control schedule is shown in figure 151 (for H = 11 km). In this case the engine thrust increases continuously at a fast rate up to an airspeed corresponding to a Mach number $M_{H\ des}$ = 2.8 in this example that is the designed value for the compressor; in other words, it increases to an airspeed where the compressor has a maximum capacity (that is $M_{a\ cr}$). As we already know, this type of uninterrupted increase of thrust with airspeed under this control schedule is the result of the simultaneous increase of rpm (the air flowrate increases at a faster rate than for n = const) and gas temperature in front of the turbine (so that the specific thrust increases, too) reaching their maximum values only at maximum airspeed. For comparison the airspeed characteristics of a turbojet engine with an n = const and T_z^* = const control schedule and of a turbojet engine with a combined control schedule are plotted in the same figure 151 for a designed compressor air temperature $T_{H\ des}^*$ corresponding to a Mach number of $M_{H\ des}$ = 2. All the characteristics that are compared here refer to engines having, at maximum airspeed (M_H = 2.8), identical magnitudes of thrust, temperature in front of the turbine, $T_{z\ des}^*$ = 1,200°K., and compression ratio, $\pi_{K\ des}^*$ = 4. It is seen that the $\frac{n}{\sqrt{T_H^*}} = \text{const}$ and F_e = const control schedule actually leads to the very significant reduction in thrust at slow airspeeds that was mentioned at the beginning of this chapter, compared to the n = const and T_z^* = const control schedule, while the combined schedule yields an intermediate result in this respect.

5. Altitude Characteristics of Turbojet Engines

The altitude characteristics of a turbojet engine are defined as the dependencies of thrust and specific fuel consumption on the altitude at a given airspeed and for the control schedule selected for the engine.

Typical altitude characteristics of a turbojet engine with $T^*_{z\ des} = 1,200^\circ K$ and $\pi^*_{kdes} = 7$ (at $M_H = 0$) and with an $n_{max} = const$ and $T^*_{z\ max} = const$ control schedule are presented for different airspeeds in figure 152. The values of thrust and specific fuel consumption obtained under ground conditions (H = 0 and V = 0) are assumed to be equal to one.

It is seen that the engine thrust decreases continuously with increasing altitude at V = const. This is due to the reduction in the weight flowrate of air through the engine as a result of the decrease in the density of atmospheric air with increasing altitude.

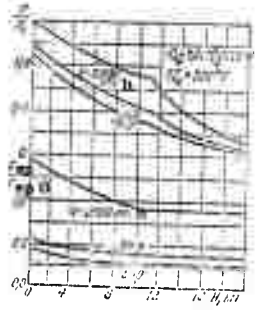

Figure 152: Altitude characteristics of a turbojet engine.

But the ambient air temperature T_H decreases with increasing altitude up to 11 km, resulting in an increase of both, velocity head compression ratio and compressor compression ratio at n = = const and V = const and, consequently, in an increase of the overall compression ratio. Therefore, when the altitude is increased, the pressure p^*_z in front of the turbine and the pressure p_2 behind the turbine are reduced at a slower rate than the pressure p_H of the atmospheric air, so that the weight flowrate of air through the engine at $T^*_z = const$ is also reduced at a slower rate than the ambient air pressure.

Moreover, since the ambient air temperature decreases with increasing altitude, the temperature at the compressor outlet decreases accordingly at V = const and n = const, and the temperature difference $(T^*_z - T^*_k)$ increases at $T^*_z = const$, that is the quantity of heat added to one kg of air in the combustion chambers increases. As a result, and also due to the increase in the overall compression ratio, the effective efficiency of the engine is increased. The increase of effective efficiency and of the quantity of heat input in the engine in turn causes an increase in the gas exhaust velocity from the jet nozzle (the pressure behind the turbine, p_2, decreases at a slower rate than the atmospheric pressure p_H, and $\varepsilon_{j.n}$ increases), resulting in an increase of specific thrust with increasing altitude at V = const.

As a result of these causes the engine thrust decreases at a slower rate than the density of the ambient air, up to an altitude of 11 km.

Atmospheric air temperature does not change at altitudes above 11 km; therefore, the overall compression ratio and the specific thrust remain constant under the control schedule under consideration, and the engine thrust varies proportionally to the density of the ambient air.

The specific fuel consumption decreases up to an altitude of 11 km. This is due to the increase in specific thrust. But at the same time the excess of air coefficient is reduced (see figure 153) as a result of the increase in the temperature difference $(T_z^* - T_k^*)$. Therefore, up to an altitude of 11 km the specific fuel consumption decreases at a lesser rate than the specific thrust increases.

At altitudes above 11 km the specific fuel consumption remains constant so that at these altitudes not only P_{sp} = const but also the temperature difference $(T_z^* - T_H^*)$ will remain constant, and, consequently, α = const, too.

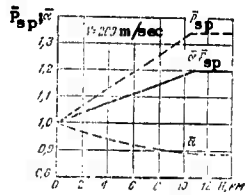

Figure 153: Relative variation of the excess of air coefficient α and of P_{sp} with changing altitude.

Figure 154 shows the dependencies of the engine efficiencies η_{econ}, η_e, and η_p on altitude at constant airspeed and for the same initial data used for the graph in figure 152.

It is seen that the effective efficiency increases significantly with increasing altitude up to 11 km, because of the reasons mentioned above. The propulsive efficiency decreases during this process. This is due to the fact that the gas exhaust velocity from the jet nozzle increases, as we explained above, while V = const and, consequently, the velocity ratio c_e/V is increased, that is the remaining unconsumed kinetic energy in the flow, $(c_e - V)^2/2g$, is increased, again resulting in a reduction of η_p.

However, in this case the reduction of propulsive efficiency is more than compensated by an increase of effective efficiency, and the economic efficiency η_{econ} will increase, as seen from figure 154.

Thus, under otherwise equal conditions the economy of a turbojet engine will increase with increasing altitude.

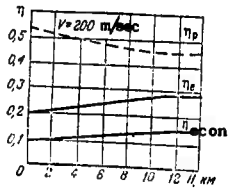

Figure 154: Dependence of the efficiencies of a turbojet engine on altitude.

6. The Concept of Turbojet Engine Characteristics in Similarity Parameters

Similar regimes of a turbojet engine as a whole, as well as of the compressor (and turbine) in particular, are defined as regimes where a dynamic similarity of the gas and air streams flowing through the engine is encountered, that is a similarity with respect to pressure, friction, and inertial forces that can be accomplished only if the flight Mach number and Reynolds number (Re) are equal in all similar cross-sections of comparable streams. Dynamically similar streams are geometrically and kinematically similar at the same time. Therefore, similar regimes can exist not only for a given engine, if its flow section geometry is constant, but also for a family of geometrically similar engines, that is engines where all the similar dimensions are proportional. In the majority of cases the Re numbers in the flow section of a turbojet engine have values (so-called supercritical Re numbers) where the friction force has a very small effect on the flow characteristics of the gas stream. Therefore, as a rule the equality of only the Mach numbers is entirely adequate for satisfying the similarity of the regimes of turbojet engines, as this is done below. Let us assume that, during turbojet engine operation at very great altitudes and at relatively slow airspeeds, the Re numbers in the flow section of the engine are significantly reduced due to low inlet air density, reaching their subcritical values. In these cases the friction force already has a considerable effect on the flow of the gas streams, and since the equality of the Re numbers is not satisfied the similarity of the streams is violated, which can lead to considerable errors. But this is a special problem that is not discussed here.

In addition, it is assumed in approximation that under similar regimes of turbojet engines the heat losses in the combustion chambers ($\zeta_{c.c}$) are identical, and that the specific heat of the combustion products (and the air) is not dependent on their temperature and composition. These assumptions do not result in appreciable errors and simplify the calculations considerably.

All magnitudes whose numerical values remain constant under similar regimes of turbojet engines are called similarity parameters of turbojet engines.

It is established that there are two independent, determinative similarity parameters for turbojet engines with F_e = const: the flight Mach number M_H and the rpm parameter $n/\sqrt{T_H^*}$, that is proportional to the Mach number M_u determined with respect to the circumferential velocity of the rotor of a turbojet engine. This means that, if the values M_H and $n/\sqrt{T_H^*}$ remain constant during any change in the operating conditions of a turbojet engine (rpm, airspeed, and altitude, atmospheric conditions, temperature in front of the turbine, and others), the regimes of the turbojet engine remain similar. It is obvious that only one determinative similarity parameter, $n/\sqrt{T_H^*}$, remains during static turbojet engine operation, where $M_H = 0$.

It is proved in the technical literature that the ratio P/p_H^* between engine thrust and total air pressure, called the thrust parameter, and the ratio $C_{sp}/\sqrt{T_H^*}$ between specific fuel consumption and the stagnation temperature of the air, called the specific fuel consumption parameter, remain constant under similar regimes of a turbojet engine. Also, it can be shown that the temperature ratios (for instance, T_z^*/T_H^* and T_2^*/T_H^*) and pressure ratios ($\pi_k^* = p_k^*/p_a^*$) and all the efficiencies of an engine remain constant under similar regimes of turbojet engines.

Using the dependencies explained above it is possible to reduce significantly the number of the characteristics of a turbojet engine that are required to determine its thrust and specific fuel consumption under different flight conditions and rpm.

Thus, for instance, if the rpm characteristics of a turbojet engine that are applicable only for certain atmospheric conditions (that is p_H and T_H) are plotted in the form of dependencies of P/p_H^* and $C_{sp}/\sqrt{T_H^*}$ on $n/\sqrt{T_H^*}$, they will become applicable for any atmospheric conditions at M_H = const (and also at $M_H = 0$).

A great number of airspeed and altitude characteristics of a turbojet engine that refer to different rpm values can be reduced to a small family of curves expressing the dependence of P/p_H^* and $C_{sp}/\sqrt{T_H^*}$ on the flight Mach number M_H and the $n/\sqrt{T_H^*}$ parameter, as shown in figure 155.

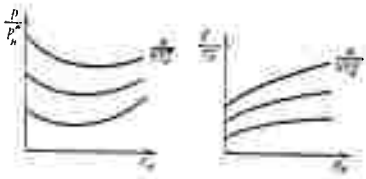

Figure 155: Turbojet engine characteristics in similarity parameters.

The dependencies of the thrust and specific fuel consumption parameters on the flight Mach number M_H and the rpm parameter are called turbojet engine characteristics in similarity parameters.

It must be kept in mind that the characteristics in similarity parameters can be plotted only for turbojet engines where the geometry of the flow section of all engine elements remains constant (that is, F_e = const and F_{NA} = const, and no pivoting blades, and the like) or where a variation of this geometry is uniquely dependent on the parameters $n/\sqrt{T_H^*}$ and M_H.

Having the characteristics of a turbojet engine in similarity parameters we can readily plot from them the airspeed or altitude characteristics of the engine for any given rpm or rpm characteristic at the given airspeed and altitude. For instance, if it is necessary to plot the airspeed characteristics at n = const and H = = const, and given the different values for the airspeed V, the corresponding values are determined for the given altitude:

$$M_H = \frac{V}{\sqrt{gkRT_H}};$$

$$\frac{n}{\sqrt{T_H^*}} = \frac{n}{\sqrt{T_H(1+0{,}2M_H^2)}};$$

$$p_H^* = p_H(1+0{,}2M_H^2)^{3.5}.$$

Subsequently, the values P/p_H^* and $C_{sp}/\sqrt{T_H^*}$ are found on these characteristics, and the actual thrust P and specific fuel consumption C_{sp} are determined from them.

7. Reducing the Results of Turbojet Engine Tests to Prescribed Conditions

Using the concept of the similar regimes of a turbojet engine, the task of reducing test stand results to prescribed atmospheric conditions can be solved with sufficient accuracy and simplicity.

This task consists of determining, on the basis of data obtained through turbojet engine tests under any atmospheric conditions, the data that the engine would have if it operated at the prescribed rpm, but under standard atmospheric conditions, that is at P_0 = 760 mm mercury column, and T_0 = 288°K (+ 15°C), or under any other conditions.

Let us suppose that a turbojet engine was tested on a test stand at an atmospheric air temperature T_{md} and barometric pressure P_{md} and at a certain rpm, n_{md}. The thrust measured during this test was equal to P_{md}, and the specific fuel consumption was $C_{sp\ md}$.

In order for this engine to operate under standard atmospheric conditions at a regime that is similar to the test regime, only one condition must be satisfied (since M_H = 0):

$$n_{cor}/\sqrt{288} = n_{md}/\sqrt{T_{md}};$$

whence

$$n_{cor} = n_{md}\sqrt{288/T_{md}} \qquad (12.5)$$

where n_{cor} is the corrected rpm of the engine.

In order to determine the corrected thrust P_{cor} that this engine would generate if it operated under standard atmospheric conditions at the corrected rpm, n_{cor}, we use the condition of the equality of the thrust parameters under similar regimes of turbojet engines, that is

$$P_{cor}/760 = P_{md}/P_{md}$$

whence

$$P_{cor} = 760/P_{md}\ P_{md}.$$

Furthermore, from the equality of the specific fuel consumption parameters for these two similar regimes of the turbojet engine,

$$C_{sp\ cor}/\sqrt{288} = C_{sp\ md}/\sqrt{T_{md}}$$

we determine the corrected specific fuel consumption, $C_{sp\ cor}$, that corresponds to the thrust P_{cor} and rpm n_{cor} found above, that is,

$$C_{sp\ cor} = C_{sp\ md}\ \sqrt{288/T_{md}}.$$

Subsequently, equating the air flowrate parameters and the products of thrust parameters and specific fuel consumption parameters for the same similar regimes of the turbojet engine, we can obtain the following formulas:

$$G_{a\ cor} = G_{a\ md}\ 760/P_{md}\sqrt{T_{md}/288}$$

$$G_{fuel\ cor} = G_{fuel\ md}\ 760/P_{md}\sqrt{288/T_{md}}$$

where $G_{a\ cor}$ is the corrected air flowrate;

$G_{fuel\ cor}$ is the corrected fuel consumption per hour, that is the air flowrate and specific fuel consumption that would be encountered if the given engine operated under standard atmospheric conditions and at an rpm equal to n_{cor}.

The formulas for determining the corrected values of any turbojet engine parameters can be obtained through this approach. Thus, for instance, the formulas for the corrected gas temperatures in front of the turbine, $T^*_{z\ cor}$, and behind the turbine (in the jet nozzle), $T^*_{2\ cor}$, are obtained from the conditions $T^*_z/T_0 = \text{const}$ and $T^*_2/T_0 = \text{const}$ for similar regimes; these formulas are

$$T^*_{z\ cor} = T^*_{z\ md}\ 288/T_{md}$$

and

$$T^*_{2\ cor} = T^*_{2\ md}\ 288/T_{md}.$$

The results of test stand trials of a turbojet engine are reduced to standard atmospheric conditions in the following sequence:

1. in accordance with formula (12.5) that rpm is determined where an engine regime for the prevailing atmospheric conditions

and similar to the test regime is obtained, that is the regime under which the engine data for standard atmospheric conditions must be determined;

2. after establishing the obtained rpm on the operating engine, the thrust, fuel consumption, gas temperature in the jet nozzle, and so on are measured;

3. with the aid of the formulas obtained above, the corrected thrust, specific fuel consumption, and other engine data that already correspond to standard atmospheric conditions, are determined from the measured magnitudes.

However, if the air temperature exceeds 288°K (+ 15°C) the engine must not be allowed to operate at the revolutions where its regime at this temperature becomes similar to its maximum regime (with respect to rpm) under standard conditions, since these revolutions are obtainéd at a higher level than the maximum engine rpm. During the hot season this circumstance makes it necessary to limit the verification of engine data through tests to correspondingly reduced regimes, while maximum and close to maximum regimes are verified in approximation through graphical extrapolation from the characteristics acquired during these tests.

As a rule, turbojet engine testing is not confined to the acquisition of one or several regimes; rather, all the rpm characteristics of the engine are acquired and also reduced to standard atmospheric conditions. Usually these characteristics are plotted in the form of dependencies of corrected engine parameters on corrected rpm, and therefore they are called corrected characteristics. The accuracy of all measurements performed during engine tests must be: for thrust, ± 0.5 %; for fuel consumption, ± 1 %; for rpm, ± 0.25 %, and for temperature behind the turbine, ± 1 %.

8. Thrust Augmentation of Turbojet Engines through Fuel Combustion behind the Turbine

Thrust augmentation is defined as increasing the thrust of a given engine beyond the magnitude that corresponds to the maximum regime, that is the magnitude obtained at maximum acceptable rpm, n_{max}, and temperature in front of the turbine, $T^*_{z\,max}$. Thrust augmentation makes it possible to increase engine thrust without exceeding the safe mechanical and thermal loads on turbine and compressor parts, and without appreciably increasing the weight of the power plant. Thrust augmentation frequently proves necessary in order to shorten the rolling distance of the aircraft during takeoff, to increase the climbing speed and ceiling of the aircraft, to increase the airspeed rapidly, and to fly supersonic airspeeds at high altitudes.

At the present time the most widely used means of thrust augmentation for turbojet engines consists of burning additional fuel

between turbine and jet nozzle. Fuel combustion behind the turbine takes place as a result of the presence of free oxygen that is available in significant quantity in the combustion products departing from the turbine. As a result the gas temperature in front of the jet nozzle is increased so that the gas exhaust velocity from the jet nozzle increases under otherwise equal conditions and, consequently, the specific thrust and the engine thrust are increased. By nature, such a means of thrust augmentation represents the exploitation of a cycle with heat input in two stages that was described in Chapter 3.

A so-called afterburner is installed for burning additional fuel between turbine and jet nozzle, whose diagram is shown in figure 156.

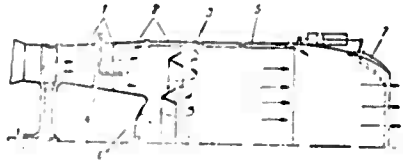

Figure 156: Diagram of the afterburner of a turbojet engine: 1 - diffuser; 2 - afterburner casing; 3 - flame stabilizers; 4 - fuel nozzle; 5 - flame tube; 6 - starting nozzles; 7 - jet nozzle.

The primary elements of an afterburner are: the diffuser 1, used to reduce the gas velocity to a magnitude corresponding to a Mach number of M = 0.25 to 0.3, which is necessary to ensure stable fuel combustion; the afterburner casing 2 in the form of a cylindrical or conical tube with a slight divergence toward the outlet in which the combustion of the additional fuel takes place; the flame stabilizers 3, usually designed in the form of rings with angular cross-section behind whose edges a zone of reverse streams of burning gases is created; and the fuel nozzles 4. A flame tube 5 is installed in afterburners with high combustion temperature, and part of the gas departing from the turbine is directed into the space between flame tube and casing 2 in order to reduce the temperature of the walls of the afterburner casing. A starting device consisting of a sparkplug and starting nozzles 6 is frequently used for reliable fuel ignition in the afterburners.

Turbojet engines with afterburners are given the abbreviated designation TRDF.

The regime of an afterburning turbojet engine that corresponds to the maximum rpm and maximum gas temperature in front of the turbine during afterburner operation is called the afterburning regime.

When an afterburning turbojet engine operates under the afterburning regime the gas temperature T^*_{aft} in front of the jet nozzle (at the afterburner outlet) usually reaches 1600 to 1700°K, and for

some engines can even rise to T°_{aft} = 1800 to 2000°K. In static engine operation on the ground (V = 0 and H = 0) this makes it possible to increase its thrust by 30 to 50 %, compared to the thrust that can be obtained at the maximum regime.

In order to ensure that the regime of the engine is not disturbed in other respects when the afterburner is started or in other words, to ensure that the temperature in front of the turbine and the engine rpm are maintained at their previous levels (n = = const and T°_{z} = const), the pressure p_2 at the turbine outlet and, accordingly, the gas expansion ratio ϵ_T in the turbine, must be kept constant. This requires an increase of the minimum cross-section F_e of the jet nozzle when the afterburner is started, so that the weight flowrate of the combustion products through the jet nozzle remains at its previous level in spite of the decrease in their density due to the increase of temperature in the afterburner.

However, if the jet nozzle area F_e remains constant when the afterburner is started (or if its increase lags behind), the pressure behind the turbine will increase as a result of the increasing temperature in front of the jet nozzle, and the gas expansion ratio in the turbine will decrease, leading to a reduction of turbine work and, consequently, also to a reduction of engine rpm. As a result, the rpm governor will increase the fuel flow into the primary combustion chambers in order to restore the previous rpm level, and the gas temperature in front of the turbine will be increased. But an increase of temperature in front of the turbine is inacceptable at a time when the engine already operates under the maximum regime, since this will result in dangerous turbine blade overheating and, in addition, can cause compressor surging (due to the reduction of the air flowrate through the compressor at n = const).

Thus, starting the afterburner absolutely must be accompanied by a simultaneous increase of the jet nozzle area, in order to maintain the afterburning turbojet engine at constant maximum rpm and to prevent the danger of turbine blade overheating and the development of compressor surging.

If the temperature in front of the turbine at maximum or close to maximum rpm is selected somewhat lower than the maximum acceptable level for the turbine, and if the available stability margin with respect to temperature permits, the afterburner can be started even without increasing the jet nozzle area. However, in that case the temperature in the afterburner cannot be increased significantly for the reasons indicated above, so that a comparatively small thrust augmentation is obtained. Therefore, modern afterburning turbojet engines usually have a variable area jet nozzle 7, as shown in figure 136.

Let us now consider to what degree the magnitude of thrust and specific fuel consumption is affected, under otherwise equal conditions, by an increase of gas temperature in front of the jet nozzle, accomplished by burning additional fuel in the afterburner.

Figure 157 shows the relative increase of the thrust and specific fuel consumption of a turbojet engine as a function of the temperature increase in the afterburner (of the ratio $T^*_{2\ aft}/T^*_2$) at a compression ratio $\pi^*_k = 7$ in the compressor, gas temperature $T^*_z = 1150^\circ K$ in front of the turbine, and airspeed V = 0.

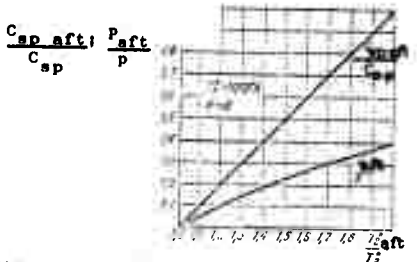

Figure 157: Relative variation of thrust and specific fuel consumption as a function of afterburner temperature.

It is seen that, if the afterburner temperature is increased during static engine operation (V = 0), the specific fuel consumption increases at a significantly faster rate than the thrust of the engine. Thus, for instance, if the thrust is increased by 30 %, the specific fuel consumption will increase by 70 %, which means that the economy of the engine deteriorates significantly.

Modern afterburning turbojet engines during static operation with afterburner on the ground have a specific thrust of 80 to 100 kg · sec/kg, and a specific fuel consumption of 1.8 to 2.2 kg/kg thrust per hour.

Consequently, this means of thrust augmentation proves to be uneconomical at slow airspeeds. But this has no decisive significance for its temporary use.

However, with increasing airspeed and altitude the gain in engine thrust for the same increase in afterburner temperature will rise rapidly, and the increase in specific fuel consumption will slow down considerably. This is due to the pressure increase behind the turbine with increasing airspeed, improving the utilization of the heat added in the afterburner.

Thus, for instance, at an airspeed corresponding to $M_H = 2.5$ a temperature increase to 1800 to 1900°K in the afterburner can increase the thrust of an afterburning turbojet engine almost 2.5 times, as seen in figure 158, while the specific fuel consumption increases by only 10 to 15 %, compared to the P and C_{sp} of the same engine with non-operating afterburner and under otherwise equal conditions.

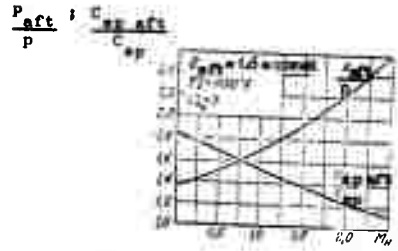

Figure 158: The effect of airspeed on the profile of the thrust and specific fuel consumption of an afterburning turbojet engine.

Thrust augmentation of a turbojet engine by means of burning additional fuel behind the turbine has a very telling effect on the profiles of the airspeed characteristics of the engine, especially at high altitudes. To illustrate this, figure 159 shows the airspeed characteristics (solid curves) of an existing afterburning turbojet engine (the French ATAR engine), and as dotted curves for comparison the airspeed characteristics of the same engine without afterburner. It is seen that, at an airspeed corresponding to $M_H = 2$ and an altitude of 11 km, augmentation through additional fuel combustion behind the turbine will increase the thrust almost 4 times, at an increase in specific fuel consumption of about 30 %. But at the same time the specific weight of the engine is reduced considerably, since the presence of the afterburner increases its weight by about 25 to 30 % while the thrust is increased several times. This latter factor can compensate significantly for the increased fuel consumption (depending on flight endurance). As a result of the special features mentioned above, thrust augmentation of a turbojet engine through additional fuel combustion behind the turbine (that is, employment of an afterburning turbojet engine) in a number of cases not only proves to be an advantageous but even a necessary means for accomplishing flights at supersonic airspeeds and high altitudes.

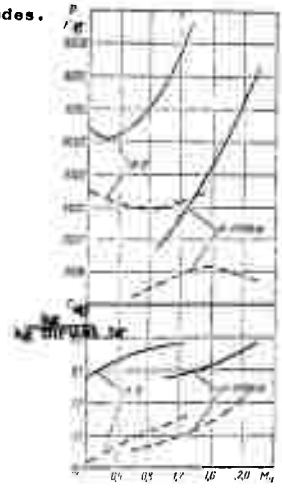

Figure 159: Airspeed characteristics of an afterburning turbojet engine.

An important advantage of using afterburners is the possibility of significantly increasing engine thrust without increasing the gas temperature in front of the turbine.

The additional weight and design complication of the engine must range among the disadvantages of using afterburners. Moreover, when the afterburner is not operating the thrust of the engine will be slightly less, and the specific fuel consumption higher, than the thrust of the same engine without this afterburner (due to the additional resistance created by the afterburner).

9. Thrust Augmentation of Turbojet Engines through Cooling Liquid Injection

Thrust can be augmented by cooling the air that is compressed in the compressor.

As a rule, if the compressed air in aviation gas turbine engines is also cooled, this is accomplished only through the evaporation of liquids (water, alcohol, a mixture of both, and others) injected into the air stream through special nozzles installed in front of the compressor. Other possible means of cooling the air, for instance with the aid of heat exchangers and the like, lead to an inadmissible increase of engine weight and size and are not used for this reason.

When liquid is evaporated in air, heat is removed from the latter equaling the evaporation heat of the liquid. As a result, the polytropic exponent of compression, the work required to compress the air to a given pressure, as well as the temperature at the end of compression, are reduced. Consequently, if the work expended on air compression remains constant, the pressure at the compressor outlet, that is the compressor compression ratio, will rise accordingly.

As a result, the pressure behind the turbine is increased, which in turn leads to an increase of the gas expansion ratio in the jet nozzle.

Consequently, the exhaust velocity from the jet nozzle and the associated specific thrust are increased. In addition, the weight flowrate of the gas (air) through the engine also increases with increasing pressure in front of the turbine at the same temperature T_z^*.

Thus, if liquid is injected that evaporates in the compressed air, the thrust of the engine will increase as a result of an increase of both, specific thrust and air flowrate.

At the same time the quantity of fuel required for a corresponding temperature increase in the combustion chambers at $T_z^* = \text{const}$ will increase as a result of the reduction of the compressor outlet temperature, so that the specific fuel consumption can change, too.

The relative variation of thrust and specific fuel consumption as a function of the ratio between the quantity of evaporated water and the quantity of consumed fuel is shown in figure 160. It is seen that the injection of evaporating liquid, especially of water, into the compressor can be an effective means of engine thrust augmentation.

However, it must be taken into consideration that the quantity of liquid that can evaporate in good time is practically limited to a significant degree by the short period that it remains in the compressor. And when the partial pressure of the vapors of the given liquid reaches vapor pressure for the temperature prevailing at the compressor outlet, evaporation in the compressor will cease completely.

The quantity of liquid that can evaporate in and in front of the compressor increases with increasing air temperature at the compressor inlet (increasing ambient air temperature, fast supersonic airspeed). This can lead to a considerably greater thrust augmentation than shown in figure 160.

Using this relatively simple means of augmenting the thrust of an engine requires large relative flowrates of injection liquid. Thus, for instance, the water consumption required to augment the thrust of a turbojet engine by 20 to 25 % during take-off will exceed the fuel consumption by about 2.2 to 2.4 times.

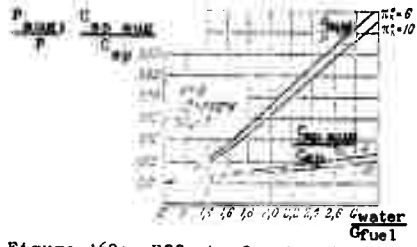

Figure 160: Effect of water injection into the compressor of a turbojet engine on its thrust and specific fuel consumption.

Water injection for the purpose of augmenting engine thrust is also possible directly into the combustion chambers. At the same time the fuel flow must be increased to prevent a drop in gas temperature in front of the turbine. When water is injected into the combustion chambers the generated steam obstructs the air intake into the chambers, resulting in a reduction of the air flowrate through the compressor, so that its compression ratio increases [1]

[1] This effect increases with increasing curvature of the compressor characteristics.

Thus, if water is injected into the combustion chambers, the thrust of the engine is increased as a result of the increase of pressure in front of the turbine (if $T_z^* = const$ is maintained) and of the increase in the gas flowrate. Moreover, the increase of thrust (exhaust velocity from the jet nozzle) contributes to a certain increase in the specific heat of the combustion products resulting from the increased quantity of water vapor contained in them.

For the same increase of engine thrust, augmentation by means of injection into the combustion chambers requires a significantly greater water flowrate than injection into the compressor. Moreover, as the water flow into the combustion chambers increases, the compressor can get into an area of instable regimes since the air flowrate through the compressor is reduced during this process. But at the same time, water injection directly into the combustion chambers instead of into the compressor eliminates the possibility of ice formation and damage to compressor blading under the effect of water particles.

10. Special Features of the Characteristics of Double-Compound Turbojet Engines

Double-compound turbojet engines (see figure 19) have a compressor consisting of two consecutively located compressors for low and high pressure. The first of these is located on the same shaft with the second low pressure turbine (as seen from the combustion chambers) and makes up the low pressure or outer rotor with that turbine, while the second is located on the same shaft with the first, high pressure turbine and makes up the high pressure or inner rotor with that turbine. Low pressure and high pressure rotor are not mechanically connected so that they can rotate at different rpm.

The compression ratios of the low pressure and high pressure compressors in double-compound turbojet engines are small individually and will not exceed 3.5 to 4 even at a high overall compression ratio of 12 to 16.

Therefore, under off-design regimes, where the overall compression ratio is reduced as a result of the reduction of the rpm parameter, flow conditions around the blades of the individual stages of low pressure and high pressure compressor under correspondingly matched rpm will differ to a significantly lesser degree from designed conditions than they will for a single-spool compressor with the same overall compression ratio.

In single-shaft turbojet engines with a high designed compression ratio and $F_e = const$, the transition to reduced regimes, that is the reduction of the rpm parameter, is accompanied, as we already explained, by a significant increase of the angles of attack of the blades in the first compressor stages and a reduction of the angles of attack of the blades in the last compressor stages. As a result, the compressor efficiency is considerably reduced, and compressor operation can become instable, making it necessary to use anti-surging devices.

It is obvious that, in order to prevent a significant increase of the angles of attack of the blades in the first stages during the transition to reduced regimes of a double-compound turbojet engine, the rpm of the low pressure compressor should be reduced at a greater rate, and that, in order to prevent an excessive decrease of the angles of attack of the blades in the last stages, the rpm of the high pressure compressor should be reduced at a lesser rate than the rpm of a single-spool compressor with the same overall designed compression ratio as the double-compound turbojet engine.

This rpm variation of the low pressure and high pressure compressor of double-compound turbojet engines during their transition to reduced, off-design regimes takes place automatically, as shown by Prof. K.V. Kholshchevnikov.

Thus, for instance, the Bristol "Olymp" double-compound turbojet engine has a ratio between high pressure rotor rpm, n_{hi}, and low pressure rotor rpm, n_{lo}, equal to $n_{hi}/n_{lo} = 1.3$ under the designed regime, and increasing to $n_{hi}/n_{lo} = 2$ under the low throttle regime.

This unequal rpm variation between low pressure and high pressure rotor is precisely what is required to improve flow conditions around the blades of the first and the last compressor stages under off-design regimes. As a result, the angles of attack of the first and the last stages of the compound compressor of a double-compound turbojet engine differ from their designed magnitudes to a significantly lesser degree when the rpm (or the rpm parameter, if n = = const) is reduced, than they will in the compressor of a single-shaft turbojet engine with the same overall designed compression ratio.

For these reasons, double-compound turbojet engines have the following principal advantages.

1. The compressor of a double-compound turbojet engine can operate in a stable manner without surging in a significantly broader range of different regimes than the compressor of a single-shaft turbojet engine with the same designed compression ratio. As an example, figure 161 shows the location of the operating lines with respect to the compressor characteristics for a single-shaft turbojet engine (see figure 161 a) and a double-compound engine (see figure 161 b,c) with F_e = const and with the same overall designed compression ratio and no anti-surging devices in either case. It is seen that the operating lines of the double-compound turbojet engine on the characteristics of the low pressure (see figure 161 b) and the high pressure (see figure 161 c) compressor never intersect the surge limit of these compressors. On the other hand, a reduction of the rpm parameter of the single-shaft turbojet engine by about 30 % already causes the operating line to intersect the surge limit of its compressor.

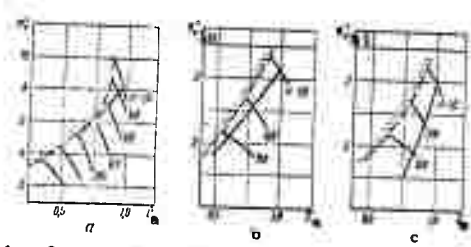

Figure 161: Operating lines of a single-shaft (a) and a double-compound (b and c) turbojet engine.

2. Under reduced regimes, where the rpm parameter (the rpm) is significantly reduced, the efficiency of the compressor of a double-compound turbojet engine will decrease little from its designed magnitude. Therefore, under otherwise equal conditions a double-compound turbojet engine under these regimes will be more economical than a single-shaft turbojet engine whose compressor efficiency will be reduced significantly during this process if it has a high desig ed compression ratio.

3. At low rpm, equilibrium regimes of a double-compound turbojet engine are achieved at lower gas temperatures in front of the turbine, due to its greater compressor efficiency, than for a single-shaft turbojet engine with the same designed parameters.

The disadvantage of double-compound turbojet engines is the more complicated design in comparison to a single-shaft turbojet engine.

The same conditions are required for the equilibrium regimes of double-compound turbojet engines as well as for single-shaft turbojet engines, that is equality must exist between the work, respectively, of the low pressure turbine and compressor ($L_{T\ lo} = L_{k\ lo}$) and of the high pressure turbine and compressor ($L_{T\ hi} = L_{k\ hi}$).

Changing the area of the minimum cross-section of the jet nozzle has an effect on the counterpressure to the gas outflow from the low pressure turbine of a double-compound turbojet engine and results in a corresponding change of the overall gas expansion ratio in its turbines. But this change extends primarily to the gas expansion ratio in the low pressure turbine, while the expansion ratio of the high pressure turbine remains almost constant. Thus, for instance, if the gas expansion ratio in the low pressure turbine is reduced by 15 to 20 % when the jet nozzle area is reduced under otherwise equal conditions, the gas expansion ratio in the high pressure turbine can decrease by at most 2 to 3 %.

Therefore, equilibrium regimes of a double-compound turbojet engine that differ appreciably with respect to gas temperature in front of the turbine at constant high pressure rotor rpm cannot be obtained by means of controlling the jet nozzle area. To obtain

such regimes requires either a corresponding change in the work of the high pressure compressor, $L_{k\ hi}$ (for instance, by means of pivoting its blades), or a change in the area of the nozzle assembly of the high pressure turbine.

Consequently, if the jet nozzle area F_e is reduced, the increase in the temperature in front of the turbine, even though required to maintain the rpm n_{hi} of the high pressure rotor constant, will by very insignificant. And the work of the low pressure turbine, $L_{T\ lo}$, will decrease as a result of the reduction of $\epsilon_{T\ lo}$, so that the rpm n_{lo} of the low pressure rotor will decline. As a result, the air flowrate through the engine will be reduced, but to a lesser degree than the rpm n_{lo}, since n_{hi} = const.

Consequently, the angles of attack of the blades in the first stages of the low pressure compressor will decrease, and its regime will shift away from the surge limit.

However, increasing the jet nozzle area of a double-compound turbojet engine at n_{hi} = const will lead to the opposite result, that is to a shift of the regime of the low pressure compressor toward its surge limit.

In order to maintain a constant rpm n_{lo} of the low pressure rotor when the jet nozzle area is reduced, the gas temperature $T^*_{z\ hi}$ in front of the high pressure turbine and, accordingly, the temperature T^*_z, must be increased so as to compensate for the reduction of $\epsilon_{T\ lo}$. But then the work $L_{T\ hi}$ of the high pressure turbine will be increased (since $\epsilon_{T\ hi}$ = const), and the rpm of the high pressure rotor will rise. This leads to an increase of the air flowrate through the engine, so that the regime of the low pressure compressor moves away from the surge limit, that is, it shifts to the right along the $n_{lo}/\sqrt{T^*_H}$ = const line. Accordingly, with increasing F_e and n_{lo} = const, the regime of the low pressure compressor moves toward its surge limit, shifting to the left along the $n_{lo}/\sqrt{T^*_H}$ = = const line.

Thus, in order to increase the stability margin or to prevent the low pressure compressor from surging, the jet nozzle area F_e of a double-compound turbojet engine must be <u>reduced</u> rather than increased,as for a single-shaft turbojet engine, although the temperature T^*_z in front of the turbine will be increased if n_{lo} = const.

In order to obtain as large a thrust as possible, both rotors of a double-compound turbojet engine in flight should be maintained at their maximum possible rpm, $n_{lo\ max}$ and $n_{hi\ max}$, and gas temperature in front of the turbine, $T^*_{z\ max}$. However, in a double-compound turbojet engine with fixed area jet nozzle, when flight conditions change only one of these parameters can be kept constant (for instance, n_{hi} = const), while the remaining two (n_{lo} and T^*_z) will be changed in the process.

If the gas temperature in front of the turbine of a double-compound turbojet engine is maintained constant with changing airspeed and altitude by means of controlling the fuel flow so that $T^*_{z\ max}$ = const, the work of the high pressure and low pressure turbines will not be changed, either. But if there is, for instance, an increase in airspeed, the temperature T^*_H at the compressor inlet will be increased, causing a reduction in the compressor compression ratio due to the decrease in the rpm parameter and the corresponding increase in the angles of attack of the blades in the first compressor stages and decrease in the angles of attack of the blades in the last compressor stages. As a result, the rpm of the low pressure rotor, n_{lo}, will be reduced, and the n_{hi} of the high pressure rotor increased. The opposite phenomenon is observed with increasing altitude at T^*_z = const, F_e = const, and V = const: an increase of n_{lo} and a decrease of n_{hi}. This type of rotor rpm variation will not cause any peculiarities in the airspeed and altitude characteristics of double-compound turbojet engines. These characteristics are approximately identical to the characteristics for T^*_z = const and constant adiabatic work of the compressor as a whole, since the compressor efficiency of a double-compound turbojet engine varies little with changing compressor regime and flight conditions.

If the low pressure rotor rpm of a double-compound turbojet engine with F_e = const is kept constant, n_{lo} = const, the angles of attack of the blades in the first compressor stages will increase with increasing airspeed (due to the decrease of $n_{lo}/\sqrt{T^*_H}$), so that the work required to drive the low pressure compressor is increased, requiring an increase of gas temperature in front of the turbine in order to maintain n_{lo} = const. But then the rpm n_{hi} of the high pressure rotor will be increased as a result of the rise in T^*_z and decrease in the angles of attack of the blades in the last stages of its compressor. In this case, n_{hi} will be increased at a significantly faster rate than in the preceding case, if T^*_z = const. However, with increasing altitude (up to H = 11 km) the temperature T^*_z, conversely, must be reduced in order to maintain n_{lo} = const, and the rpm n_{hi} will be increased.

The nature of the rpm variation of the high pressure rotor with changing altitude and flight Mach number M_H at n_{lo} = const is shown in figure 162 a.

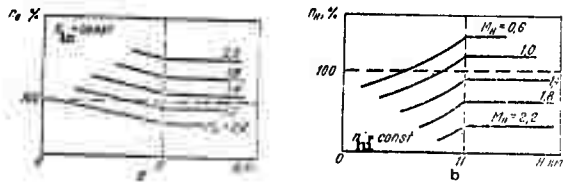

Figure 162: Rpm variation of a double-compound turbojet engine with changing altitude and flight Mach number M_H: a - for n_{lo} = const; b - for n_{hi} = const.

If the airspeed is increased at n_{lo} = const and under otherwise equal conditions the thrust of a double-compound turbojet engine as a result of the increase in temperature in front of the turbine will increase at a greater rate than it will for the T_z^* = const control schedule. However, if the altitude is increased at n_{lo} = const and V = const, the thrust of the engine as a result of the decrease in T_z^* will be reduced at a faster rate than for T_z^* = const.

Since the rpm n_{hi} of the high pressure rotor increases with increasing airspeed at T_z^* = const, the gas temperature, obviously, must be reduced with increasing airspeed in order to maintain n_{hi} = = const. This will lead to a faster decrease in the rpm of the low pressure rotor than for T_z^* = const, and to a corresponding reduction of engine thrust.

In order to maintain n_{hi} = const with increasing altitude, the gas temperature in front of the turbine must be increased, so that the rpm of the low pressure rotor will be increased at a faster rate than for T_z^* = const; as a result, the thrust of the engine will decrease at a slower rate with increasing altitude than for T_z^* = const.

The nature of the rpm variation of the low pressure rotor with changing altitude and flight Mach number M_H at n_{hi} = const is shown in figure 162 b.

Figures 163 and 164 show the relative variation of the temperature T_z^*, rpm of the low pressure and high pressure rotors, n_{lo} and n_{hi}, and the thrust of a double-compound turbojet engine with F_e = const, for changing airspeed and altitude and for the three control schedules under consideration, where the values of all magnitudes for these three cases are assumed to be equal to one at H = 0 and M_H = 0.

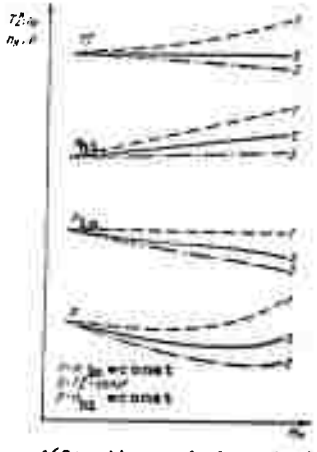

Figure 163: Airspeed characteristics of a double-compound turbojet engine for three control schedules.

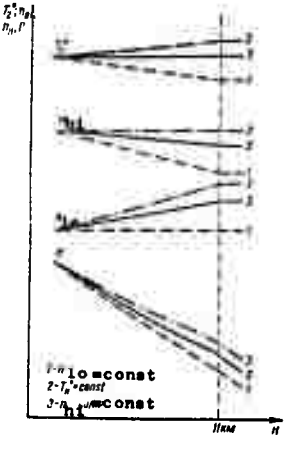

Figure 164: Altitude characteristics of a double-compound turbojet engine for three control schedules.

It should be kept in mind that one of the magnitudes n_{lo}, n_{hi}, or T_{Σ}^{*} can be kept constant only until the values of the two other magnitudes exceed their maximum acceptable values with changing airspeed and altitude.

Figure 165 shows the relative variation of thrust with changing flight Mach number M_H for a double-compound turbojet engine with F_e = = const whose maximum thrust at $M_H < 1$ is limited by the acceptable rpm of the low pressure rotor, so that the limit with respect to acceptable temperature in front of the turbine sets in first with increasing airspeed (at $1 \leq M_H \leq 1.7$), and subsequently the limit with respect to acceptable rpm of the high pressure rotor.

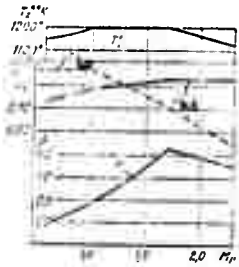

Figure 165: Airspeed characteristics of a double-compound turbojet engine for a combined control schedule.

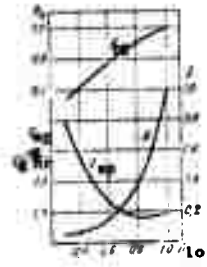

Figure 166: Throttling characteristics of a double-compound turbojet engine.

The rpm characteristics of double-compound turbojet engines can be represented in the form of the dependencies of thrust and specific fuel consumption on the rpm of low pressure rotor as well as high pressure rotor.

Figure 166 shows the test stand characteristics of a double-compound turbojet engine with F_e = const as functions of the relative rpm of the low pressure rotor. If the rpm of either rotor at the maximum regime is assumed to be 100 %, the increase of the angles of attack in the first stages during the transition to reduced regimes (as well as the reduction of $\varepsilon_{T\ lo}$ if the engine is throttled significantly) will lead to a more rapid decrease of the rpm of the low pressure rotor than of the high pressure rotor. It is seen from figure 166 that for an rpm of the low pressure rotor of 0.5 $n_{lo\ max}$, the rpm of the high pressure rotor amounts to about 0.7 $n_{hi\ max}$.

The effect of atmospheric air temperature on the thrust of a double-compound turbojet engine differs slightly from the effect on the corresponding data of a single-shaft engine and can be evaluated by analogy with the effect of airspeed and altitude (that is, of T_H^*) on the regime of the engine under different control schedules.

If the given rpm of the high pressure rotor, n_{hi} = const, is maintained at M_H = 0 and H = 0, the gas temperature in front of the turbine and the rpm of the low pressure rotor will decrease with increasing atmospheric air temperature T_H, so that the thrust of the engine will be reduced at a slightly greater rate than the thrust of a single-shaft turbojet engine.

If the rpm governor of the engine maintains a constant rpm of the low pressure rotor (n_{lo} = const), an increase in T_H, conversely, will be accompanied by an increase of temperature in front of the turbine and high pressure rotor rpm, leading to a less intensive reduction of engine thrust in comparison to a single-shaft turbojet engine.

However, if the engine control system ensures a constant value of gas temperature in front of the turbine, a change in atmospheric air temperature will be accompanied by a change in the rpm of both rotors, so that the rpm of the low pressure rotor will be reduced with increasing T_H, while the rpm of the high pressure rotor is increased.

CHAPTER 13

TRANSIENT REGIMES AND START-UP OF TURBOJET ENGINES

1. Basic Dependencies. Pick-Up of Turbojet Engines

Transient (irregular) regimes of turbojet engines are defined as regimes where all or a certain part of the engine parameters vary over time. Under these regimes the engine shifts from one equilibrium regime to another.

Transient regimes of turbojet engines where the rpm varies over time have the greatest practical significance, since the thrust control of turbojet engines is accomplished primarily by means of changing its rpm.

Transient regimes with increasing rpm are called rotor run-up regimes, while transient regimes with decreasing rpm are called slow-down regimes or rpm reduction regimes.

The primary condition for transient regimes of turbojet engines that are accompanied by a change in rpm is the inequality of turbine power and the power required to drive the compressor and the auxiliary assemblies.

If the turbine power exceeds the power required for the compressor, the engine rpm will increase over time, and an engine run-up transient regime will be obtained. The excess turbine power, $\Delta N_T = N_T - N_k$, is consumed for increasing the kinetic energy of the engine rotor in its rotary motion. When $N_T < N_k$, the engine rpm will be reduced, and an rpm reduction transient regime will be obtained. During this process the kinetic energy of the rotor is reduced, since it is consumed for overcoming the aerodynamic forces and friction forces that impede its rotation.

The time required for the engine rotor to run up from low throttle rpm to maximum rpm is called pick-up time and defines that important operational quality of an engine called pick-up, that is the capability of rapidly increasing the rpm when the fuel flow into the combustion chambers is increased. The shorter the time required for the rotor to run up from $n_{l.t}$ to n_{max}, the better will be the pick-up of the engine, the faster will its rpm increase and, consequently, the thrust generated by the engine. And a rapid increase of thrust, that is a good engine pick-up, is required for a safe go-around of the aircraft in the event of an unsuccessful landing, for completing aerobatic maneuvers, for fast maneuvering in aerial combat, for following an aircraft in formation (for chase aircraft), and so on.

The pick-up time of a turbojet engine is proportional to the moment of inertia of the rotor and must decrease with increasing air flowrate through the engine and increasing excess of turbine work over compressor work: $\Delta L_T = L_T - L_k$ (see figure 132).

This means that the pick-up time will decrease with increasing temperature T_z^* in front of the turbine during the run-up process of the turbojet engine and with increasing jet nozzle area.

However, the temperature increase during the run-up process that is required in order to improve significantly the pick-up of a turbojet engine, is limited by the temperature stability margins $\Delta T^*_{z\ pickup}$, especially at low and intermediate rpm. It is obvious that, with decreasing temperature stability margin, that is with decreasing distance between the equilibrium operating line of a turbojet engine and its compressor surge limit, the temperature increase in front of the turbine that can be achieved during the run-up process in comparison to its values under equilibrium regimes will be reduced and, consequently, the pick-up of the engine will deteriorate under otherwise equal conditions.

Moreover, a significant, although temporary increase of temperature in front of the turbine during the run-up process (provided that the temperature stability margins permit it) can cause inacceptable turbine blade overheating.

For these reasons, turbojet engines have an available excess of turbine power over compressor power that is comparatively small at all revolutions below maximum rpm; it is considerably less than the excess power of a reciprocating engine (with respect to its external characteristics) over the power required to drive the propeller. This primarily explains the significantly poorer pick-up of turbojet engines compared to reciprocating aviation engines. Thus, the pick-up time of modern turbojet engines during static operation on the ground is usually not less than 8 to 10 sec, while reciprocating engines require a total of only 1.5 to 2 sec.

The air flowrate through a turbojet engine decreases with increasing altitude or increasing temperature and with decreasing atmospheric air pressure, and also with decreasing airspeed; under otherwise equal conditions, this contributes to a deterioration of engine pick-up. But, as we showed earlier, the low throttle rpm of a turbojet engine increases with increasing altitude as a result of the employment of a minimum fuel flow limiter in front of the injection nozzles (minimum fuel consumption), so that the low throttle rpm increases with increasing altitude, and the difference $(n_{max} - n_{l.t})$ is reduced. As a result, the pick-up of a turbojet engine in flight can be either worse or better than its pick-up under ground conditions.

2. Special Features of the Transient Regimes of Turbojet Engines

In order to shift a turbojet engine to a new equilibrium regime with increased rpm an excess of turbine power over the level prevailing at the intermediate equilibrium regimes must be generated. In other words, under run-up regimes the turbine power at each

intermediate rpm must be greater than the turbine power at the same rpm but under equilibrium regimes, where it always applies that $N_T = N_K$. This can be achieved only (if F_e = const) by means of increasing the fuel flow, and accordingly, the temperature in front of the turbine over their values under the intermediate equilibrium regimes.

However, in order to shift a turbojet engine to a new equilibrium regime with reduced rpm the turbine power must be reduced, that is, the temperature in front of the turbine must be reduced by reducing the fuel flow, below its values under the intermediate equilibrium regimes.

To illustrate this, figure 167 shows the variation of fuel consumption G_{fuel} and temperature T_z^* in front of the turbine with changing rpm under run-up regimes (curves 1 and 1') and under rpm reduction regimes (curves 3 and 3') for one of the existing turbojet engines. For comparison, the dependencies of fuel consumption and temperature in front of the turbine on the rpm are shown in this figure for the equilibrium regimes of the same engine (curves 0 and 0'). It is seen that the fuel consumptions G_{fuel} and temperatures T_z^* in front of the turbine differ considerably at the same intermediate (transient) rpm under run-up and slow-down regimes and under equilibrium regimes.

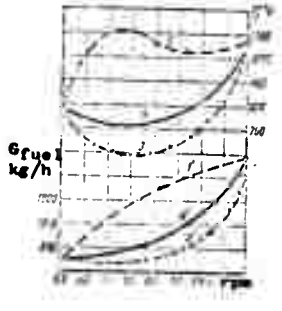

Figure 167: Variation of temperature in front of the turbine and fuel consumption with changing rpm under transient regimes of a turbojet engine.

Let us consider the basic peculiarities of turbojet engine operation under run-up regimes from low throttle rpm, $n_{l.t}$, to maximum rpm, n_{max}. For this purpose we start out by using the graphs in figures 168 and 169, where the solid lines represent, respectively, the dependence of G_{fuel} and T_z^* on the rpm under equilibrium regimes of the turbojet engine.

Depending on the fuel flow schedule the run-up regimes will take a different course. A small increase in fuel flow over fuel consumption under equilibrium regimes (line 1 in figure 168) results in a comparatively small increase of temperature T_z^* in front

of the turbine (curve 1 in figure 169), yielding a small excess of turbine power, ΔN_T, and the pick-up time of the engine will be longer. At a stronger increase of fuel flow (curve 2 in figure 168) the run-up regime will proceed at higher gas temperatures in front of the turbine (curve 2 in figure 169); this results in a greater excess of turbine power, and the pick-up time will be shortened. With a strong fuel flow under a run-up regime the temperature in front of the turbine can also become "overheated", that is $T^*_{z\ max}$ will be exceeded at n_{max} (curve 2' in figure 169, and curve 1 in figure 167), which is acceptable up to a certain limit because of the temporary nature of the run-up process.

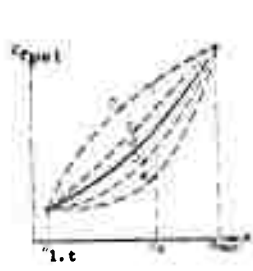

Figure 168: Variation of fuel consumption in a turbojet engine under transient regimes.

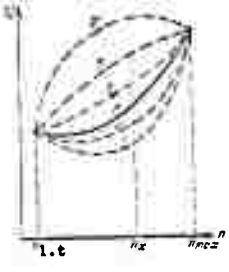

Figure 169: Variation of temperature in front of the turbine of a turbojet engine under transient regimes.

From the known values of temperature in front of the turbine that are obtained for each intermediate rpm, n_x, during run-up, the run-up lines of the engine can be plotted in the field of compressor characteristics. This was done in figure 170, where the curve 0 represents the equilibrium operating line of the engine and the curves 1, 2, and 2' the run-up characteristics, the first of these corresponding to a small increase in fuel flow during the run-up process, and the second to a stronger increase of fuel flow.

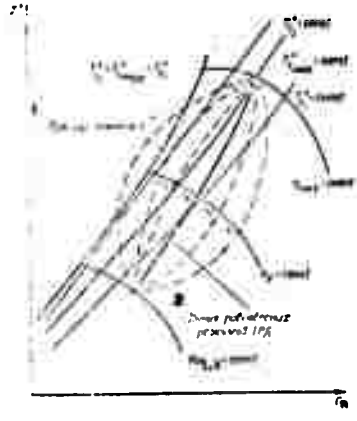

Figure 170: Lines of the transient regimes of a turbojet engine in the field of compressor characteristics.

Legends to figure 170:

1 - surge limit
2 - line of the equilibrium regimes of the turbojet engine

It is seen that the run-up regimes as a result of the higher temperatures in front of the turbine are located closer to the compressor surge limit than the equilibrium regimes of the engine and that their distance from the surge limit will decrease with increasing fuel flow and, accordingly, increasing temperature T_z^*. Therefore, with a strong fuel flow under a run-up regime of a turbojet engine (curve 2' in figure 170) compressor surging can develop, which creates the danger of flameout and spontaneous engine shutdown.

The location of the run-up lines in the field of compressor characteristics also shows that the run-up regimes take place at lower air flowrates through the engine (for the same n) than equilibrium regimes. The greater the fuel flow during the run-up process, the smaller will be the air flowrate at which this process takes place, as illustrated by curves 1 and 2 in figure 171, where the solid curve 0 describes the equilibrium regime.

Consequently, under all run-up regimes the mixture in the engine is enriched, or, in other words, the excess of air coefficient α is reduced in comparison to the equilibrium regimes of the same engine, since $\alpha = G_z/l_o G_{fuel}$. Figure 172 shows the nature of the rpm variation of α for equilibrium regimes (curve 0) and for run-up regimes with a small increase of fuel flow (curve 1) and with a stronger increase of fuel flow (curve 2). The limits of stable combustion chamber operation with respect to α (α_{max} and α_{min}) are plotted as dotted curves in this figure.

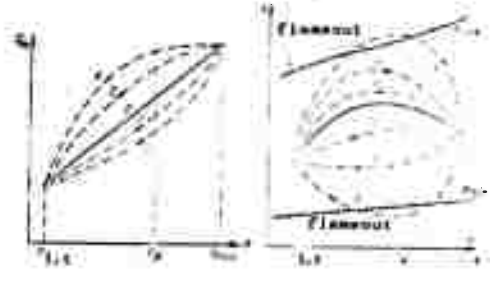

Figure 171: Variation of the air flowrate in a turbojet engine under transient regimes.

Figure 172: Variation of the excess of air coefficient in the combustion chambers of a turbojet engine under transient regimes.

It is readily noted that the enrichment of the mixture in the combustion chambers will increase with increasing rate of increase of the fuel flow during engine run-up. If the fuel flow is too

strong, the magnitude of the excess of air coefficient α can be reduced so much that it becomes less than α_{min} (curve 2' in figure 172) so that instable combustion and flameouts develop in the combustion chambers that can lead to spontaneous engine shut-down.

Thus, a strong increase of fuel flow during the run-up of a turbojet engine can lead to compressor surging as well as to flame-out in the combustion chambers as a result of overenrichment of the fuel and air mixture.

In order to prevent these phenomena, the fuel flow into the combustion chambers during rotor run-up of a turbojet engine must be limited by acceptable boundary values that are safe for the engine. For this purpose the control and regulating systems of all modern turbojet engines are equipped with special automatic maximum fuel flow limiters that are called automatic pick-up systems.

Under reduced rpm regimes the dependencies considered above are of the opposite type, as indicated by lines 3 and 4 in figures 168 and 169. The curves 3 in these figures refer to a small fuel flow reduction accompanied by a relatively small temperature change in front of the turbine, compared to equilibrium regimes, so that the revolutions are reduced slowly. The curves 4 refer to a stronger fuel flow reduction where the temperature in front of the turbine is reduced at a more significant rate than in the preceding case, increasing the difference $(N_K - N_T)$ and reducing the time required for the rpm reduction or, in other words, resulting in a faster decline of engine rpm.

It is obvious that the temperature in front of the turbine is decreased in comparison to the intermediate equilibrium regimes and that the rate of engine rpm reduction is accelerated with increasing rate of fuel flow reduction during the slow-down process. As a result, the location of the reduced rpm line in the field of compressor characteristics (lines 3 and 4 in figure 170) will be further removed from the surge limit with increasing rate of fuel flow reduction and, consequently, of temperature reduction in front of the turbine. Consequently, compressor surging cannot develop during rpm reduction of a turbojet engine.

The location of the reduced rpm lines in the field of compressor characteristics indicates that these regimes take place at greater air flowrates through the engine than for equilibrium regimes. The greater the rate of fuel flow reduction, the greater will be the air flowrates at which the rpm reduction of the engine takes place (lines 3 and 4 in figure 171).

This means that the mixture in the combustion chambers of the engine will become leaner under reduced rpm regimes or, in other words, the excess of air coefficient α will be increased in comparison to the intermediate equilibrium regimes.

The rate of this fuel richness reduction will be comparatively small for a small fuel flow reduction (curve 3 in figure 172). A greater fuel flow reduction will cause the mixture to become considerably leaner (curve 4 in figure 172). An excessive rate of fuel flow reduction during a drop in rpm can make the mixture so lean (curve 4' in figure 172) that the excess of air coefficient α becomes greater than the acceptable α_{max} and flameouts begin in the combustion chambers, resulting in spontaneous engine shut-down. It should be noted that this danger increases with increasing altitude, since in that case, as we explained earlier, the maximum value α_{max} where flameout begins in the combustion chambers will be reduced.

Thus, an abrupt fuel flow reduction during an rpm drop of a turbojet engine can lead to spontaneous engine shutdown as a result of flameout in the combustion chambers due to excessive leanness of the mixture. Therefore, an automatic limitation of the minimum acceptable fuel flow is required not only under equilibrium regimes, as explained earlier, but also under reduced rpm regimes.

In the case of double-compound turbojet engines the rpm run-up and slow-down regimes of the high pressure rotor are qualitatively equivalent to the regimes of single-shaft turbojet engines, but for the low pressure rotor of a double-compound turbojet engine these regimes take place differently, for the following reasons.

As a rule, the moment of inertia of the low pressure rotor, J_{lo}, is greater than the moment of inertia of the high pressure rotor, J_{hi}. Therefore, if the fuel flow is reduced and F_e = const, the rpm and, accordingly, the compressor compression ratio of the second rotor will drop at a faster rate than for the first rotor, and the air flowrate through the engine will be reduced to a greater degree than it would be in the case of, for instance, an identical drop in the rpm of both rotors. This will have the result that the decline of the rpm of the low pressure rotor takes place at lesser air flowrates than for the same revolutions of its intermediate (reduced) equilibrium regimes where the rpm of the high pressure rotor exceeds, as we know, the rpm of the low pressure rotor. In other words, the line of declining rpm of the low pressure rotor in this case is located closer to the surge limit in the fiel of compressor characteristics than the operating line of its equilibrium regimes.

In this case, the faster the rpm of the high pressure rotor drops in comparison to the rpm of the low pressure rotor, the closer will the line of declining rpm of the latter shift toward the compressor surge limit.

Consequently, in the case of double-compound turbojet engines with $J_{hi} < J_{lo}$ even a drop in rpm can cause compressor surging (of the low pressure rotor).

During run-up of a double-compound turbojet engine with $J_{hi} < J_{lo}$ the rpm of the high pressure rotor will increase at a faster rate than the rpm of the low pressure rotor, providing an additional increase of the air flowrate through the compressor of the latter in comparison to its equilibrium regimes, so that no surging can develop in this compressor. But surging can develop, generally speaking, in the high pressure compressor, for the same reasons that apply to the run-up of a single-shaft turbojet engine.

3. Start-Up of Turbojet Engines

The start-up process of a turbojet engine is also included among its transient regimes and represents an engine rotor run-up from zero rpm to low throttle rpm.

It was shown in Chapter 11 that turbojet engines have minimum revolutions n_{min} where the same temperature is required in order to obtain an equilibrium regime that is required under the maximum regime of the engine, that is $T^*_{z\,max}$. These minimum equilibrium revolutions n_{min} amount to about 10 to 20 % of n_{max}. At revolutions below n_{min} the available turbine work L_T at $T^*_{z\,max}$ is less as we know (see figure 132), than the compressor work L_k, so that self-sustained operation of a turbojet engine at revolutions $n < n_{min}$ is not possible without exceeding the maximum acceptable temperature in front of the turbine. Therefore, an additional source of power is required to start a turbojet engine, that is a starting motor or starter that is capable of running up the engine rotor to that rpm where the engine can already make the transition to self-sustaining operation at $T^*_z \leq T^*_{z\,max}$.

Electric starters operating on electric batteries or special airfield power networks and gas turbine starters are mostly used today. The latter are low-power gas turbine engines of small dimensions consisting of a compressor, combustion chambers, and a turbine whose power exceeds the power required to drive its compressor by the magnitude that is necessary to run up the rotor of the turbojet engine. The gas turbine starter itself is started with the aid of a small electric motor. Also, gas turbines operating on the combustion products of a powder charge, on decomposition products of hydrogen peroxide, on compressed air stored in tanks, and others can be used as starting engines.

Also, reliable initial fuel ignition in the combustion chambers must be ensured when a turbojet engine is started, in addition to running up its rotor with a starter.

For this purpose special starting devices are used that consist of an electrical spark plug and a starting injector combined into one assembly. These devices generate the initial starting flame jets that subsequently ignite the fuel fed through the primary operating injectors.

The starting devices of turbojet engines with tubular and cannular combustion chambers are installed only in some of the flame tubes from which the flame is transferred to the remaining flame tubes through a pipe system that interconnects all the flame tubes. In annular combustion chambers several starting devices are installed along the circumference of the common annular flame tube.

Either the primary fuel, kerosene, or a starting fuel, gasoline, is used to start a turbojet engine. The latter facilitates start-up, but complicates the fuel system of the engine.

When the engine is started the starting devices are turned on and off automatically.

Also, the starting system of a turbojet engine must ensure a fuel flow dosage into the combustion chambers that exclude the danger of turbine overheating and instable combustion.

A non-operating turbojet engine in flight is in autorotation, meaning that its rotor is driven by the counterflowing air stream. During this process the rotor rpm is usually greater than the minimum equilibrium revolutions, n_{min}. Therefore, in order to start a turbojet engine in flight it is adequate merely to ignite the fuel fed into the combustion chambers, and it is not necessary to run up the rotor with the starter. However, in flight the conditions for igniting the fuel in the combustion chambers of a non-operating turbojet engine are considerably aggravated, for the reasons discussed at length in Chapter 6. Consequently, reliable air starts of turbojet engines at great altitudes are ensured by using starting devices that generate a starting flame jet of greater power and duration than required for starting a turbojet engine under ground conditions.

The entire process of starting a turbojet engine with the aid of the starter consists of the three following phases taking place one after the other without interruption (see figure 173).

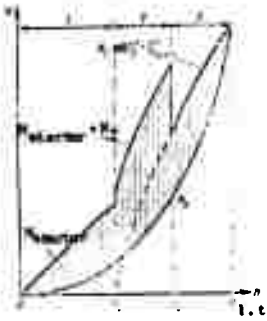

Figure 173: Diagram of the variation of starter power, turbine power, and compressor power of a turbojet engine during start-up.

First phase. Without feeding fuel into the combustion chambers the rotor of the engine is run up by the starter only, to an rpm of $n_1 < n_{min}$ where the turbine of the engine begins to operate as a result of fuel flow and ignition in the combustion chambers, generating a net power of $N_T > 0$ (at $T_z^* < T_{z\ max}^*$).

Second phase. The engine rotor is run up simultaneously by both, the starter and the already operating turbine, to an rpm of n_2 where the starter is disengaged. The rpm where the starter is disengaged usually amounts to $n_2 = (0.12 \text{ to } 0.26)n_{max}$ in order to speed up the starting process and achieve better reliability as well as to reduce the temperature in front of the turbine during the starting process.

Third phase. The rotor is run up independently by the engine to low throttle rpm, $n_{l.t}$, as a result of the engine's excess turbine power. As a rule, starters are used whose power $N_{starter}$ at n_1 revolutions exceeds by several times the power N_{rotor} required to drive the entire rotor of the turbojet engine, in order to reduce the time required to start up the turbojet engine and to achieve better reliability.

When starting a double-compound turbojet engine it is adequate to run up only one of its rotors with the starter, while the other rotor will be driven under the effect of the air stream generated by the run-up rotor. But for running up the high pressure rotor a starter of less power is required than for the low pressure rotor. This is due to the fact that the high pressure rotor has less moment of inertia and, moreover, during its run-up with the starter rotates in air of reduced density (due to the drop in air pressure when the air flows through the low pressure compressor).

CHAPTER 14

TURBOPROP ENGINES

1. General Observations

The most important advantage of a turbojet engine is that its thrust varies gradually with increasing airspeed and subsequently increases up to a certain supersonic airspeed, while the thrust generated by a reciprocating engine and propeller plant (VMU) decreases rapidly all the time. As a result, the turbojet engine provides the thrust required at high airspeeds for a low engine weight, and its specific weight is considerably less than that of a reciprocating engine. This is also the reason why the use of turbojet engines makes it possible to reach airspeeds that cannot be achieved with reciprocating engine and propeller plants.

The disadvantage of a turbojet engine as compared to a reciprocating engine and propeller plant is its lower economy at relatively slow airspeeds. To illustrate this, figure 174 shows the dependence of the specific fuel consumptions, C_{sp}, and economic efficiencies (dotted curves) of a turbojet engine and a reciprocating engine and propeller plant[1] on the airspeed. It is seen that, in the example considered here, these engines are equivalent with respect to economy only at an airspeed of about 900 km/h (this airspeed depends in particular on the altitude). At greater airspeeds the economy of a turbojet engine is greater, and at airspeeds less than indicated above it is considerably less than the economy of a reciprocating engine and propeller plant.

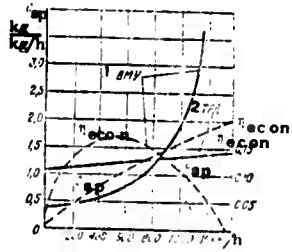

Figure 174: Dependence of the specific fuel consumptions and efficiencies η_{econ} on the airspeed of the aircraft, for a turbojet engine (TRD) and a reciprocating engine and propeller plant (VMU).

Legends:
1 - reciprocating engine and propeller plant;
2 - turbojet engine.

---

[1] The economic efficiency of a reciprocating engine and propeller plant is equal to the product of the effective efficiency of the engine and the efficiency of the propeller; the specific fuel consumption of a reciprocating engine and propeller plant is obtained by dividing the per hour fuel consumption of the engine by the thrust (in kg) generated by the propeller.

As a result of the disadvantages of turbojet engines mentioned above a requirement arises for a certain category of aircraft (of long range and not very high maximum airspeed) to have an engine that would combine the weight and thrust advantages of the turbojet engine at high airspeeds with the advantages of the reciprocating engine and propeller plant during take-off and at relatively slow airspeeds. Turboprop engines (TVD) belong to this category of engines.

A simplified diagram of a turboprop engine is shown in figure 175. This engine differs from a turbojet engine in that its turbine 4 also rotates the propeller 1 via the reducing gear 5, in addition to driving the compressor 2 and auxiliary assemblies.

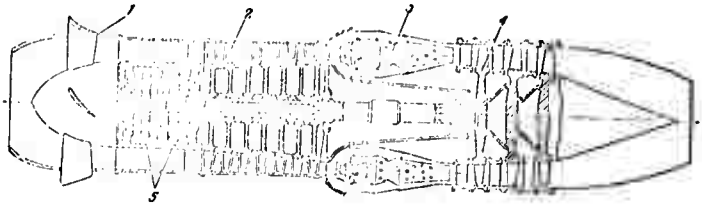

Figure 175: Diagram of a single-turbine turboprop engine: 1 - propeller; 2 - compressor; 3 - combustion chambers; 4 - turbine; 5 - reducing gear.

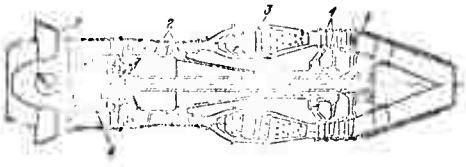

Figure 176: Diagram of a turboprop engine with two separate turbines: 1 - propeller; 2 - compressor; 3 - combustion chambers; 4 - compressor turbine; 5 - propeller turbine; 6 - reducing gear.

In some turboprop engines the propeller is rotated by a separate turbine that is not mechanically connected to the compressor turbine (see figure 176); this makes it possible in a number of cases to accomplish a more flexible engine control. Also, double-shaft (twin-spool) compressors are sometimes used in turboprop engines (see figure 177). In that case, one turbine is used to drive the last compressor stages while the other drives the first compressor stages and the propeller.

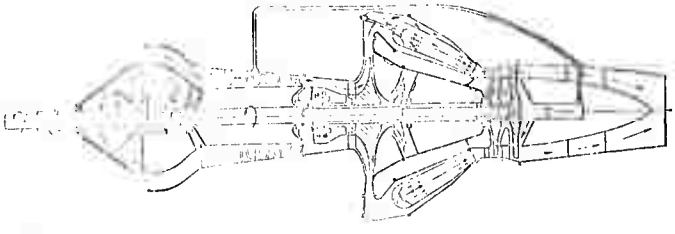

Figure 177: Diagram of a turboprop engine with twin-spool compressor.

The number of turbine stages in modern turboprop engines will not be less than two and will frequently reach five to six. This is due to the necessity of accomplishing a large heat drop in the turbine and the inclination, at the same time, of reducing the turbine rpm for the purpose of reducing the transmission ratio and, consequently, reducing the size and weight of the reducing gear.

Otherwise the primary elements and characteristic crossections of the flow section of a turboprop engine are similar to the descriptions given for turbojet engines.

The useful work of the cycle of a turboprop engine is used to drive the propeller and to accelerate the gas and air stream flowing through the engine, so that we can write for the actual cycle of a turboprop engine

$$L_e = L_{prop}/\eta_{red} + c_e^2 - V^2/2g,$$

where L_{prop} is the work transferable to the propeller and referred to one kg of air flowing through the turboprop engine per second;

c_e is the gas exhaust velocity from the engine;

η_{red} is the efficiency of the reducing gear of the turboprop engine.

However, it is readily noted that the profile of the cycle is not dependent on the nature of the subsequent utilization of the useful work obtained as a result of its realization. Therefore, all the basic relationships and regularities established earlier during the study of the cycles of the turbojet engine remain fully valid for the turboprop engine, as well.

The total thrust P generated by the turboprop engine is composed of the thrust P_{prop} generated by the propeller, and the reactive thrust P_R obtained as a result of the acceleration of the gas and air stream flowing through the engine, that is

$$P = P_{prop} + P_R.$$

In turboprop engines the distribution of the useful work of the cycle or the available energy L_e between propeller rotation, that is the generation of propeller thrust, and acceleration of the gas flow in the engine, that is the generation of reactive thrust, is determined by the relationship $x = L_{prop}/L_e$ and can differ, depending on the purpose and operating conditions of the engine. It is obvious that the thrust generated by the propeller increases and, accordingly, the reactive thrust decreases, with increasing L_{prop} at a given magnitude of L_e, that is with increasing coefficient of energy distribution, x. The magnitude of the energy that is transferable to the propeller is determined by the gas expansion ratio in the turbine: the greater the gas expansion ratio, the greater will be the coefficient x. In the majority of modern turboprop engines the gas is expanded to almost atmospheric pressure in the turbine, so that the reactive thrust is obtained primarily as a

result of the gas outlet velocity from the turbine, without subsequent gas expansion in a jet nozzle. As a rule, in static operation and at slow airspeeds the thrust generated by the propeller of a turboprop engine will exceed the reactive thrust of the turboprop engine seven to nine times.

The distribution of the available energy of a turboprop engine will be optimized at the maximum engine economy under the given conditions.

Calculations show that, with increasing airspeed and decreasing magnitude of available energy, decreasing propeller efficiency, and decreasing turbine efficiency, that part of the available energy which must be transferred to the propeller will decrease, correspondingly increasing the portion of energy used for the generation of reactive thrust or, in other words, reducing $x = L_{prop}/L_e$. Figure 178 shows the dependence of optimum energy distribution x_{opt} on the airspeed for a turboprop engine with a compressor compression ratio $\pi^*_{k0} = 8$, temperature $T^*_z = 1200^\circ K$ in front of the turbine, $\eta^*_T = 0.88$, and $\eta_k = 0.85$. The dotted curve in this figure indicates the dependence of the efficiency η_{prop} used for designing the propeller on the airspeed. It is seen that in this example the coefficient x_{opt} becomes close to zero at an airspeed of about 1,150 km/h so that, consequently, there is no advantage in using such a turboprop engine under these circumstances.

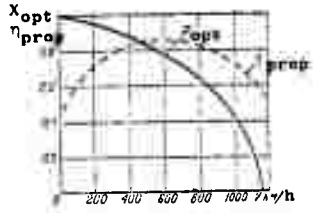

Figure 178: Dependence of the optimum energy distribution (x_{opt}) in a turboprop engine on the airspeed.

2. Power, Thrust, and Specific Parameters of Turboprop Engines

The thrust generated by a propeller in flight can be expressed, as we know, by the power supplied to the propeller, that is by the effective power N_e of the engine, the efficiency η_{prop} of the propeller, and the airspeed, so that

$$P_{prop} = 75\, N_e \eta_{prop}/V.$$

The reactive thrust equals

$$P_R = \frac{G_a}{g}(c_e - V),$$

where G_a is the per second weight flowrate of air through the engine;
c_e is the velocity of the combustion products in the outlet cross-section of the engine.

Thus, the total thrust of a turboprop engine in flight will equal

$$P = 75\ N_e/V\ \eta_{prop} + G_a/g\ (c_e - V). \qquad (14.1)$$

After dividing this expression by G_a we obtain the specific thrust

$$P_{sp} = 75\ N_e/G_a V\ \eta_{prop} + 1/g\ (c_e - V), \qquad (14.2)$$

or

$$P_{sp} = 75 N_{e\ sp}\ \eta_{prop}/V + P_{R\ sp},$$

where $N_{e\ sp} = L_{prop}/75$ is the specific effective power of the engine;

$P_{R\ sp}$ is the specific reactive thrust.

During static operation, $\eta_{prop} = 0$ and $V = 0$, so that the formulas cited above become indefinite. In that case we can use β as the coefficient that determines the static propeller thrust referred to the power N_e that is transferred to the propeller. In that case,

$$P_0 = \beta N_e + \frac{G_a}{g} c_e \qquad (14.3)$$

and

$$P_{sp_0} = \beta N_{e\ sp} + \frac{c_e}{g}.$$

For powerful engines at the rpm for which the propeller is designed, $\beta = 1.05$ to 1.15. As a rule, $\beta = 1.1$ is used for comparative calculations.

The notion of the so-called equivalent power of a turboprop engine is often used for convenience.

The <u>equivalent power</u> N_{eq} is defined as the power that would be required to drive a propeller generating a thrust that is equal to the total thrust of the turboprop engine, that is

$$N_{eq} = PV/75\eta_{prop} = N_e + P_R V/75\eta_{prop} \qquad (14.4)$$

or, at $V = 0$

$$N_{eq_0} = \frac{P_0}{\beta} = N_e + \frac{P_{R_0}}{\beta}.$$

The ratio between N_{eq} and the per second weight flowrate of air through the engine is the <u>specific equivalent power</u>, that is

$$N_{eq\ sp} = N_{e\ sp} + VP_{R\ sp}/75\eta_{prop}. \qquad (14.5)$$

As a rule, the economy of a turboprop engine is evaluated by its specific equivalent fuel consumption, C_{eq}, determined as the ratio between the per hour fuel consumption and equivalent power:

$$C_{eq} = G'_{fuel}/N_{eq}\ (\text{kg/equ. HP per hour}) \qquad (14.6)$$

After dividing the per hour fuel consumption of a turboprop engine by its total thrust we obtain the specific fuel consumption referred to one kg of thrust:

$$C_{sp} = G'_{fuel}/P\ (\text{kg/kg of thrust per hr}) \qquad (14.7)$$

that is convenient to use for comparative evaluation of turboprop and turbojet engines.

Substituting $G'_{fuel} = C_{eq}N_{eq}$ in the last formula, and taking into consideration that $P = 75N_{eq}\eta_{prop}/V$, we obtain the dependence between C_{sp} and C_{eq} which is:

$$C_{sp} = C_{eq}V / 75\eta_{prop} \qquad (14.8)$$

and for $V = 0$

$$C_{sp\ 0} = C_{eq\ 0}/\beta.$$

The thermal economy of a turboprop engine is described by its effective efficiency η_e that is equal to the ratio between the heat converted into useful work, that is, the work corresponding to the equivalent power, and the consumed heat. The useful work of a turboprop engine equals $75N_{eq}$, and the heat consumed in order to obtain it is determined by the calorific capacity H_u of the fuel and the fuel consumption per second which, obviously, equals $C_{eq}N/3600$. Consequently, we can write for the effective efficiency of a turboprop engine

$$\eta_e = 75 \cdot 3600N_{eq}/427H_uC_{eq}N_{eq} = 632/H_uC_{eq} \qquad (14.9)$$

where 632 is the thermal equivalent of one horsepower per hour.

We note that, at a given fuel caloricity, the effective efficiency is the reciprocal magnitude of specific fuel consumption and, consequently, is dependent on the same factors as the latter.

The specific weight g_{eng} of a turboprop engine, too, can be referred to total thrust as well as to effective or equivalent power.

The specific parameters considered above have approximately the following magnitudes for existing turboprop engines operating at the maximum designed regime in static operation on the ground under standard atmospheric conditions:

$N_{e\ sp}$ = 200 to 300 HP/kg of air per sec;
$N_{eq\ sp}$ = 220 to 320 HP/kg of air per sec;
$P_{R\ sp}$ = 20 to 25 kg of thrust/kg of air per sec;
C_{eq} = 0.220 to 0.340 kg/equivalent HP per hour;
g_{eng} = 0.2 to 0.3 kg/equivalent HP.

3. Dependence of the Specific Power and Economy of a Turboprop Engine on the Parameters of the Operating Process

In considering the effect of the parameters of the operating process on the power, thrust, and economy of a turboprop engine we shall assume for simplified reasoning that the engine has one common turbine for compressor and propeller, in which the gas is completely expanded to atmospheric pressure.

The power that can be utilized to drive the propeller of a turboprop engine equals the difference between the shaft power N_T of the turbine and the power required to drive its compressor, N_k, and auxiliary assemblies, N_r.

Therefore, if we take into account the losses in the propeller reducing gear, the effective power of a turboprop engine, or the power that is transferred directly to its propeller, will equal

$$N_e = (N_T - N_k)\eta_{red}$$

The turbine power, as we know, equals

$$N_T = \frac{G_g}{g_{con}} h_T \eta_T$$

and the compressor power

$$N_k = G_a L^*_{ad\ k}/\eta_k.$$

Therefore, assuming that the excess turbine power as a result of $G_g/G_a > 1$ equals the power N_r, we can write for the specific effective power of a turboprop engine

$$N_{e\ sp} = (h_T\eta_T / A - L^*_{ad\ k}/\eta_k)\ \eta_{red}/75. \qquad (14.10)$$

It follows from this expression that the specific effective power of a turboprop engine depends on the same parameters as the specific thrust of a turbojet engine, that is on the temperature T^*_z in front of the turbine, the compressor compression ratio π^*_k, the turbine efficiency η_T, the compressor efficiency η_k, and in addition, on the efficiency of the propeller reducing gear.

Under otherwise equal conditions the specific effective power increases continuously (in accordance with the linearity rule) with increasing temperature T^*_z in front of the turbine, since h_T increases proportionally to T^*_z. The dependence of $N_{e\ sp}$ and $P_{R\ sp}$ on T^*_z for $\pi^*_k = 8$ and $\pi^*_{k0} = 12$; $\eta_T = 0.85$; $\eta_k = 0.85$; $\eta_{red} = 0.97$; $\sigma_{c.c} = 0.95$, under test stand conditions (V = 0) and in flight ($M_H = 0.8$ and H = 11km) is shown in figure 179. It is seen that increasing the temperature T^*_z is a very effective means of augmenting the power of a turboprop engine.

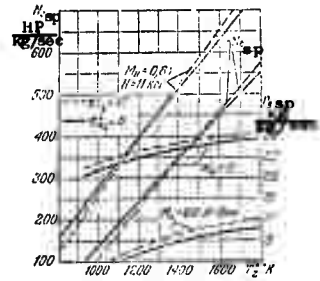

Figure 179: Dependencies of the specific power and specific reactive thrust of a turboprop engine on the temperature in front of the turbine.

The dependence of $N_{e\ sp}$ and $P_{R\ sp}$ on the compressor compression ratio π^*_k for different values of temperature in front of the turbine and otherwise identical magnitudes as used in the preceding

example, is shown in figures 180 and 182. It is seen that the specific effective power initially increases with increasing compression ratio π_k^* and subsequently begins to decrease after reaching a maximum.

This type of dependence of the specific power on π_k^* for $T_z^* = \text{const}$, that is correct at $M_H = 0$ as well as in flight where $M_H > 0$, is due to the same causes as the nature of the dependence of the specific thrust of a turbojet engine on π_k^*. These causes were discussed at length in Chapter 9.

The greater the temperature in front of the turbine, the greater will be the product of turbine efficiency and compressor efficiency, and the greater will also be the compressor compression ratio for which the maximum of specific effective power is obtained. This compression ratio decreases with increasing airspeed and decreasing altitude.

The specific power will increase with increasing efficiency of turbine or compressor, but to a different degree. This is seen directly from formula (14.10). The dependence of $N_{e\,sp}$ on η_T and η_k at $\pi_k^* = 10$ and $T_z^* = 1200$ and $1400^\circ K$ is shown in figure 181 for $M_H = 0$ and $M_H = 0.8$. The solid lines in this figure refer to the case where $\eta_k = \text{const}$ but the turbine efficiency η_T varies; the dotted lines correspond to $\eta_T = \text{const}$ at variable compressor efficiency η_k.

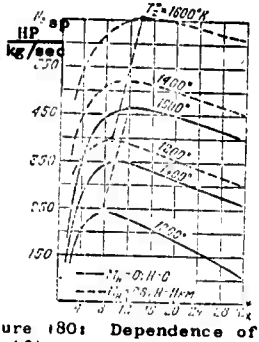

Figure 180: Dependence of the specific power of a turboprop engine on the compression ratio of the compressor.

Figure 181: Dependence of the specific power of a turboprop engine on the efficiencies of turbine and compressor.

It is seen from the graphs in figure 181 that a variation of turbine efficiency and compressor efficiency has a strong effect on the magnitude of effective engine power, and that this effect becomes stronger with decreasing temperature in front of the turbine and decreasing flight Mach number M_H. Moreover, increasing the turbine efficiency will always result in a greater increase of effective engine power than increasing the compressor efficiency by the same amount. This is due to the fact that the turboprop engine differs from the turbojet engine in that its turbine power

considerably exceeds the power required by the compressor so that, at identical compressor efficiency and turbine efficiency, the absolute magnitude of the losses is greater in the turbine than in the compressor.

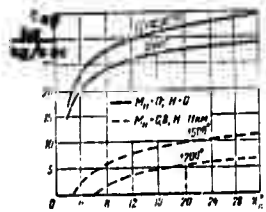

Figure 182: Dependence of the specific reactive thrust of a turboprop engine on the compression ratio of the compressor.

Figures 183 and 184 show the dependencies of the specific fuel consumptions, C_e and C_{ep}, on the temperature in front of the turbine, T_z^*.

It is seen that the specific fuel consumptions of a turboprop engine, unlike those of a turbojet engine, decrease continuously with increasing temperature in front of the turbine. This type of dependence of the specific fuel consumptions of a turboprop engine on the temperature T_z^* is retained under any flight conditions and is explained as follows.

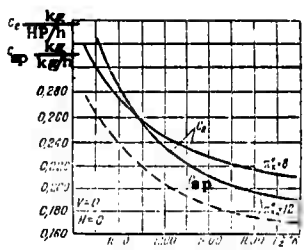

Figure 183: Dependence of the specific fuel consumptions of a turboprop engine on the temperature in front of the turbine, for H = 0; V = 0.

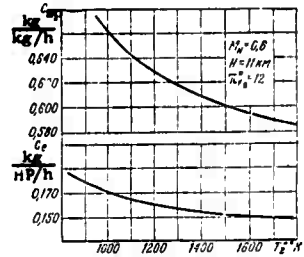

Figure 184: Dependence of the specific fuel consumptions of a turboprop engine on the temperature in front of the turbine, for M_H = 0.8 and H = 11 km.

It is seen from formulas (14.8 and 14.9) that the specific fuel consumption of a turboprop engine depends, under otherwise equal conditions, on the effective efficiency η_e of the engine and the propeller efficiency η_{prop}. But the latter is not dependent on the parameters of the operating process of the engine, including the temperature T_z^*. However, the effective efficiency η_e of a turboprop engine increases with increasing temperature T_z^* and under otherwise equal conditions (for the same reasons as the

effective efficiency of a turbojet engine), with the other direct result, as shown above, that the specific fuel consumptions of a turboprop engine decrease with increasing T_g^*. Thus, increasing the gas temperature in front of the turbine contributes not only to an augmentation of the power and thrust of a turboprop engine, but in addition always leads to an increase in its economy.

Figure 185 shows the dependence of the specific fuel consumptions of a turboprop engine on the compressor compression ratio at different values of temperature in front of the turbine, for $M_H = 0$, $H_0 = 0$, and $M_H = 0.8$, $H = 11$ km, and for the same initial data as in the preceding examples. It follows from these graphs that the specific fuel consumption decreases with increasing compressor compression ratio and subsequently begins to increase after reaching a minimum. Here the optimum compression ratio increases with increasing temperature in front of the turbine.

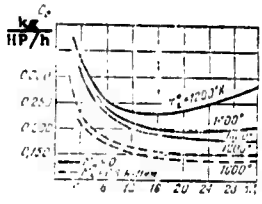

Figure 185: Dependence of the specific fuel consumption of a turboprop engine on the compression ratio of the compressor.

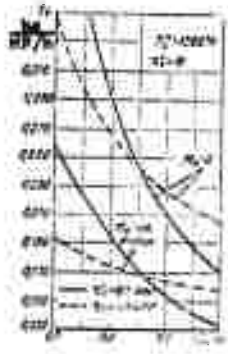

Figure 186: Dependence of the specific fuel consumption of a turboprop engine on the efficiencies of turbine and compressor.

This type of dependence of the specific fuel consumptions of a turboprop engine on the compressor compression ratio π_k^* is due to the direct effect of the latter on the effective efficiency of the engine, η_e. The effective efficiency of a turboprop engine initially increases with increasing π_k^*, reaches a maximum value, and subsequently decreases for the same reasons as the effective efficiency η_e of a turbojet engine (see Chapter 9). It is obvious that the maximum of effective efficiency corresponds to a minimum of the specific fuel consumptions of a turboprop engine.

The nature of the effect of turbine efficiency and compressor efficiency on the economy of a turboprop engine is obvious from the preceding relationship and is shown in figure 186. With increasing turbine efficiency the specific fuel consumption of a turboprop engine decreases at the same rate as the specific power of the engine increases during this process.

However, with increasing compressor efficiency the specific fuel consumption decreases at a slower rate than for the same increase of turbine efficiency, since in this case the temperature T_k^* at the compressor outlet is reduced (at π_k^* = const and M_H = const), resulting in an increase of the temperature difference $(T_z^* - T_k^*)$ if T_g^* = const and, consequently, in an increase of the quantity of heat added to the air in the combustion chambers.

4. Throttling Characteristics of Turboprop Engines

The throttling characteristics of a turboprop engine are defined as the dependencies of the effective power, specific fuel consumption, and reactive thrust on the rpm at a given airspeed and altitude (or at V = 0 and H = 0).

As a rule, these characteristics are provided in the form of curves plotted on the basis of test stand engine trials, and the principal engine data, referred to the maximum (take-off), rated, and cruising regimes as well as the low throttle regime of the engine, are recorded in these characteristics, as in the case of the turbojet engine. All of these regimes are similar to the corresponding regimes of turbojet engines.

The typical rpm profile of turboprop engine characteristics is shown in figure 187. It is seen that the effective power and the reactive thrust and, consequently, the total thrust of a turboprop engine decrease rapidly with decreasing rpm, while the specific fuel consumption increases very significantly during this process. This is due to the reduction of the air flowrate, temperature in front of the turbine, and compressor compression ratio with decreasing rpm, that is to the same causes that result in the reduction of thrust and the increase of specific fuel consumption of a turbojet engine with decreasing rpm.

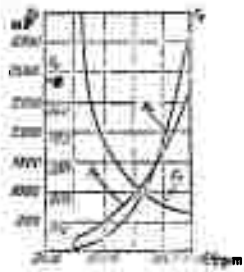

Figure 187: Throttling characteristics of a turboprop engine.

The degree of variation of the effective power, thrust, and specific fuel consumption of a turboprop engine with changing rpm depends very strongly on the control schedule selected for the engine. Let us consider this problem in more detail, assuming for simplified reasoning that the engine has a common turbine for the

compressor and the propeller in which the gas is expanded to atmospheric pressure under all regimes, and that the outlet cross-section area of the engine (of the jet nozzle) is not variable. Let us note that these are the most characteristic conditions for the overwhelming majority of modern turboprop engines.

In order to accomplish an equilibrium regime of a turboprop engine the power N_T generated by its turbine (or turbines) must equal the sum of the powers required to drive the compressor, N_k, the propeller, N_{prop}, and the auxiliary assemblies, N_r. If we determine the turbine power from the air flowrate through the engine (and not from the sum of the flowrates $G_a + G_{fuel}$), and if we neglect the losses in the propeller reducing gear, we can write this basic condition for the equilibrium regimes of turboprop engines as follows:

$$N_T = N_k + N_{prop}.$$

In other words, under equilibrium regimes the effective power of a turboprop engine that is transferred to its propeller must be equal to the power required to drive the propeller, that is

$$N_e = N_T - N_k = N_{prop}.$$

Under given external conditions the turbine power depends, as we know, not only on the rpm but also on the gas temperature in front of the turbine, while the compressor power depends only on the rpm. However, the power required to drive the propeller depends, in addition to the rpm, on the angles of attack of the propeller blades. The greater these angles are, the greater will be the power required to drive the propeller at a given rpm.

Consequently, the regime of a turboprop engine can be varied not only by controlling the fuel flow into the combustion chambers (by changing the gas temperature in front of the turbine) but also by controlling the propeller which, consequently, is an additional controllable element of a turboprop engine. This makes it possible, when necessary, to accomplish also an independent variation of the rpm of a turboprop engine and of the temperature in front of the turbine.

For instance, let it be necessary to change the temperature in front of the turbine of a turboprop engine, keeping the rpm constant. If the temperature in front of the turbine is reduced (by reducing the fuel flow), this will cause a reduction of turbine power, the equality $N_T = N_k + N_{prop}$ will be disturbed, and will take the form $N_T < N_k + N_{prop}$, so that the engine rpm will be reduced. It is obvious that, in order to retain the previous rpm, the power N_{prop} required by the propeller must be reduced, together with the reduction of fuel flow, to such a degree that the equality $N_T = N_k + N_{prop}$ is maintained in spite of the reduction of turbine power. For this purpose the angles of attack of the propeller

blades must be decreased or, in other words, the propeller loading must be reduced. Accordingly, in order to maintain the rpm of a turboprop engine constant at increasing temperature in front of the turbine, the propeller loading must be increased together with the increase in fuel flow, or, in other words, the angles of attack of the propeller blades must be increased.

In order to reduce the rpm of a turboprop engine while keeping the gas temperature in front of its turbine constant, the propeller loading must be increased, resulting in an increase of the power N_{prop} required by the propeller, so that the equality of powers will be disturbed and will become $N_{prop} + N_k > N_T$. As a result, the engine rpm will be reduced in spite of the fact that the gas temperature in front of the turbine is kept constant by means of controlling the fuel flow in accordance with the reduction of the air flowrate through the engine. The reduction in rpm leads to a reduction of all powers, that is N_{prop}, N_k, and N_T, and will take place until the equality of powers is restored at a certain rpm.

The degree of the variation of the turbine power of a given turboprop engine with changing rpm and, consequently, of the gas temperature in front of the turbine, is dependent on the degree of variation of the power required for driving the propeller with changing rpm. The stronger the reduction of the power N_{prop} required for the propeller with decreasing rpm, the greater must be the rate of temperature reduction in front of the turbine.

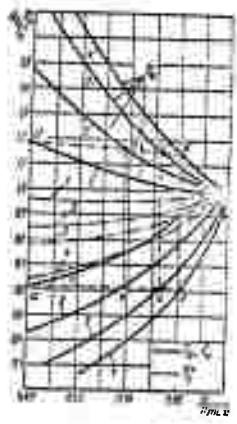

Figure 188: Relative rpm variation of the power and specific fuel consumption of a turboprop engine for different changes of temperature in front of the turbine.

It is possible to accomplish any rule for the variation of propeller power with changing rpm and, consequently, it can also be equated to the effective power of a turboprop engine under equilibrium regimes, by means of a corresponding change of the angle of attack of the propeller blades to accompany a change in rpm. In the exceptional case where the angle of attack of the propeller blades remains constant or, in other words, where the propeller is of the fixed pitch type (VFSh), the variation of the power N_{prop} with changing rpm will take place approximately in accordance with the law of the cubical parabola.

Four cases of the rpm profile of turboprop engine characteristics are represented in figure 188. Curve 1 refers to the case where the propeller loading is increased with decreasing rpm. Curve 2 represents the fixed pitch propeller. Curves 3 and 4 refer to two cases where the propeller loading is reduced with decreasing rpm, in the case of curve 4 at a greater rate than in the case of curve 3.

Let us consider the form that the operating line of the turboprop engine will take for these laws for the variation of propeller power with changing rpm, or rather, more accurately speaking, the operating line of its turbine-compressor assembly. Let us note that the operating line of a turboprop engine is defined, as in the case of the turbojet engine, as the geometric location of the points in the field of compressor characteristics that correspond to the equilibrium regimes of the turboprop engine under a given control schedule.

Since the temperature reduction in front of the turbine with decreasing rpm will be the more significant, the steeper the drop in the power $N_{prop} = N_e$ with decreasing rpm, it is obvious that the operating lines of a turboprop engine that correspond to curves 1,2,3, and 4 in figure 188 will have the profile indicated by the curves with the same numbers in figure 189.

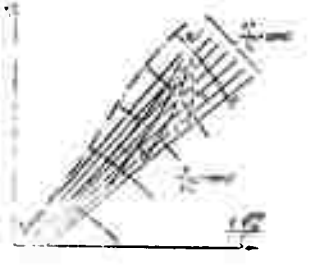

Figure 189: Possible operating lines of a turboprop engine.

It follows from these operating lines of a turboprop engine that the propeller loading must not be strongly increased with decreasing rpm. Generally speaking, the maximum possible propeller loading will be the point where $T^*_{z\ max}$ = const is maintained under decreasing rpm (the straight line Oa in figure 189). An even greater increase of propeller loading will be accompanied, obviously, not only by exceeding the temperature $T^*_{z\ max}$ that is acceptable for the turbine, but also by the danger of the equilibrium regimes of the engines shifting into an area of instable compressor operation which is inacceptable. The limit for the reduction of propeller loading with decreasing temperature in front of the turbine is determined by the condition n_{max} = const. In that case the operating line of the turboprop engine coincides with the constant rpm line, Ob. All the possible operating lines of the turboprop engine that correspond to the different control schedules or, in other words, to the different laws for the variation of the angles of attack of the propeller blades with changing rpm (rpm parameter), are located between the two limiting operating lines Oa and Ob. The following is taken into consideration for the selection of any control schedule.

1. Under reduced power regimes, the same power can be obtained at different rpm and temperature in front of the turbine (points a, b, c, and d in figure 188). The lower the rpm in this case, the greater will be the temperature in front of the turbine, that is $T_a > T_b > T_c > T_d$, and the closer will the equilibrium regime of the turboprop engine shift toward the compressor surge limit. With respect to reliability and engine life the regimes a, b, c, and d are in general approximately equivalent, since, the lower the rpm, the lower will be the forces in the engine parts exposed to centrifugal loads but, on the other hand, the higher will be the temperature regime of the turbine.

2. The stability margins of a turboprop engine with respect to T^*_z and n^*_k will decrease with decreasing distance between the operating line of the turboprop engine and the compressor surge limit.

3. With respect to the start-up and especially the pick-up of a turboprop engine that control schedule is more advantageous that ensures engine start-up and run-up from n_{min} to n_{max} at a minimum of propeller loading. This is due to the fact that the available excess of turbine power, $\Delta N_T = N_T - (N_k + N_{prop})$ at $T^*_{z\ max}$ = const increases with decreasing propeller loading at intermediate revolutions, due to the reduction of the power N_{prop} required by the propeller, and the operating line of the engine will shift away from the surge limit. In this respect, to set a propeller pitch corresponding to the characteristic 4 (see figures 188 and 189) is more advantageous, obviously, than to set a propeller pitch

corresponding to the characteristic 2 or 1 and, even more so, to Oa (see figure 189).

4. The variation of compressor efficiency must be taken into consideration, since the compressor efficiency can be strongly reduced under reduced effective power regimes when the operating line of the engine shifts closer to the n = const line, that is the line Ob (see figure 189).

5. The variation of propeller efficiency under the different laws for the variation of the angles of attack of the propeller blades with changing rpm must be taken into consideration for the final selection of a control schedule. In a number of cases this consideration can have a decisive effect on the selection of one or the other control schedule.

Let us now consider the variation of specific fuel consumption under different laws for the variation of the effective power of a turboprop engine with changing rpm. It is seen from figure 188 that the minimum reduction of temperature in front of the turbine corresponds not only to a minimum reduction of effective power, but also to a minimum increase of specific fuel consumption when the rpm is reduced. On the other hand, the greater the rate of temperature reduction in front of the turbine with decreasing rpm, the stronger will be the increase of specific fuel consumption, and the more significant will be the reduction of effective engine power.

However, it is readily seen that, for the same effective power N_e obtained at different rpm (for instance, points a, b, c, d in figure 188), the specific fuel consumptions are almost identical (points a', b', c', d'). This is due to the fact that the gas temperature in front of the turbine increases with decreasing rpm and at N_e = const (maintained constant by increasing the propeller pitch), but at the same time the compressor compression ratio is reduced as a result of the reduction in rpm. An increase of the temperature T_z^* contributes, as we know, to a reduction of the specific fuel consumption of a turboprop engine, while a decrease of the compressor compression ratio contributes to an increase of specific fuel consumption. As a result, the specific fuel consumption C_e changes very little, if at all. Therefore,at a constant fuel consumption and varying rpm the effective power N_e remains practically constant.

Thus, the same reduced effective power of a turboprop engine (for instance, cruising power) can be obtained at different rpm, or at different propeller pitch settings, with approximately the same economy. However, if we take into consideration the variation of propellor efficiency that is possible here, a different final result can be obtained with respect to the economy of the turboprop engine, and this, too, must be taken into consideration during the selection of a control schedule for the turboprop engine.

Therefore, in the majority of existing turboprop engines the propeller pitch is gradually reduced with decreasing rpm to its minimum value, and a subsequent further reduction of rpm already takes place at constant minimum propeller pitch. Thus, for instance, in the case of the Armstrong-Siddley "Memba" turboprop engine the propeller pitch (the angle of attack of the propeller blades) is reduced from 23° to 12° when the rpm decreases from n_{max} = 15,000 to n = 11,000, and is kept constant at revolutions of n < 11,000.

Also, there is practical interest in a turboprop engine control schedule where the effective power is initially reduced as a result of a reduction of the temperature in front of the turbine at constant rpm (line Ob in figure 189) which is accomplished by reducing the propeller pitch accordingly, to a greater degree than in the preceding case. Subsequently, the transition from some reduced power regime to the low throttle regime is accomplished by reducing the rpm at constant minimum propeller pitch.

The necessary control schedule of a turboprop engine, that is the relationship between temperature in front of the turbine and rpm, is realized practically by means of an appropriate linkage between the fuel flow governor for the combustion chambers and the governor that controls the propeller pitch.

All the relative effects of atmospheric conditions on the thrust and specific fuel consumption of turbojet engines that were discussed earlier, are completely valid for turboprop engines, as well. Therefore, the test results and the rpm characteristics of turboprop engines obtained during these tests must be reduced to standard atmospheric conditions. The correction formulas required for this purpose are obtained from the same conditions for similar regimes of turboprop engines as for turbojet engines, these being:

for corrected rpm

$$n_{cor} = n_{md} \sqrt{288/T_{md}};$$

for corrected reactive thrust

$$P_{R\ cor} = P_{R\ md}\ 760/p_{md};$$

for corrected air flowrate

$$G_{a\ cor} = G_{a\ md}\ 760/p_{md} \sqrt{T_{md}/288}.$$

It can be demonstrated that the ratio $N_e/p_H\sqrt{T_H}$, called the effective power parameter of a turboprop engine, depends only on the rpm parameter $n/\sqrt{T_0}$ if M_H = const, and that it also depends on $n/\sqrt{T_0}$ = const if $N_e/p_0\sqrt{T_0}$ = const.

From this condition the correction formula for the effective power of a turboporp engine is obtained which is

$$N_{e\ cor} = N_{e\ md}\ 760/p_{md} \sqrt{288/T_{md}}.$$

However, as far as the specific effective fuel consumption of a turboprop engine is concerned, it turns out that it remains constant under similar regimes of a turboprop engine, so that it is not necessary to reduce it to standard conditions or, in other words, $C_{e\ cor} = C_{e\ md}$.

In accordance with the formulas obtained above, the corrected fuel consumption per hour of a turboprop engine will equal

$$G_{fuel\ cor} = G_{fuel\ md}\ 760/p_{md}\sqrt{288/T_{md}}.$$

Knowing N_{cor}, $P_{R\ cor}$, and $G_{fuel\ cor}$, it is possible to determine the corrected equivalent power and corrected equivalent fuel consumption:

$$N_{eq\ cor} = N_{e\ cor} + P_{R\ cor}/\rho;$$

$$C_{eq\ cor} = G_{fuel\ cor}/N_{eq\ cor}.$$

However, it must be taken into consideration that the obtained correction formulas can be used only in that case where the angle of attack of the propeller blades of the turboprop engine remains constant. Actually, the power required to drive the propeller during static operation equals, as we know,

$$N_{prop} = \rho n^3\ p_H/T_H\ c,$$

where ρ is the power coefficient that depends on the angle of attack (pitch) of the propeller blades at V = 0;

c is a constant magnitude.

After dividing the individual terms of the last equality by p_H and T_H, we obtain

$$N_{prop}/p_H\sqrt{T_H} = \rho\ (n/\sqrt{T_H})^3 c.$$

But under equilibrium regimes, $N_{prop} = N_e$, so that the effective power parameter of a turboprop engine and, accordingly, its other similarity parameters, will depend not only on the rpm paramoter $n/\sqrt{T_H}$ but also on the coefficient ρ, that is on the propeller pitch. Therefore, in order to maintain the similarity of turboprop engine regimes and, consequently, in order to apply the formulas considered above to the engine, it is necessary to satisfy not only the condition $n/\sqrt{T_H}$ = const, but positively also the condition that ρ = const or, in other words, the propeller pitch must be kept constant.

However, the propeller pitch governors used in modern turboprop engines do not have the capability of simultaneously maintaining n = const and ρ = const, since their task, as we already explained, consists of the opposite: to vary the propeller pitch to a certain degree with changing rpm of the turboprop engine. Therefore, in order to obtain the similar regimes of a turboprop engine that are required to reduce its test data to standard atmospheric conditions, the propeller governor must be disconnected

and the propeller replaced by a hydraulic brake. If no hydraulic brake is available the propeller governor must be especially adjusted so as to satisfy the condition ρ = const under the turboprop engine regimes required for data reduction. This also represents the primary difficulties of reducing the test results of turboprop engines to given conditions.

5. Airspeed and Altitude Characteristics of Turboprop Engines

The airspeed characteristics of a turboprop engine are defined as the dependencies of the effective power, reactive thrust, and specific effective fuel consumption on the airspeed at a given altitude under the control schedule selected for the engine.

The altitude characteristics of a turboprop engine are defined as the dependencies of the effective power, reactive thrust, and specific effective fuel consumption on the altitude at constant airspeed and under the control schedule selected for the engine.

Sometimes the dependencies of the equivalent power of a turboprop engine and of the equivalent specific fuel consumption on the airspeed and altitude are provided, too. In that case the propeller efficiency is conditionally assumed to be independent of airspeed and altitude and is usually taken at a value of 0.80 to 0.85.

Let us consider the airspeed characteristics of a turboprop engine under an n = const and T_g^* = const control schedule that is widely used for these engines and provides for the simultaneous control of fuel flow and propeller pitch.

Typical airspeed characteristics under this control schedule for a turboprop engine with $\pi_{k0}^* = 8$ and $T_g^* = 1200^\circ K$ and having a common turbine for compressor and propeller in which the gas is completely expanded to atmospheric pressure (there is no gas expansion in the jet nozzle) are shown for different altitudes in figures 190 and 191, where all the magnitudes that refer to V = 0 and H = 0 are assumed to be equal to one.

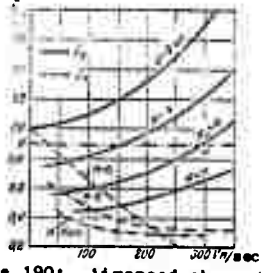

Figure 190: Airspeed characteristics of a turboprop engine (variation of $\bar{N}_e$ and $\bar{P}_R$ as a function of V at different H).

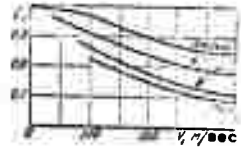

Figure 191: Airspeed characteristics of a turboprop engine (variation of $\bar{C}_e$ as a function of V at different H).

It is seen that the effective power of the turboprop engine increases very intensively with increasing airspeed at n = const and $T_z^* = \text{const}$, while the reactive thrust decreases. However, the specific fuel consumption is reduced significantly during this process. This type of dependence of N_e, P_R, and C_e on the airspeed is due to the following reasons.

The gas expansion ratio in the turbine increases with increasing airspeed as a result of the increase of the total compression ratio, leading to an increase of the heat drop accomplished in the turbine at $T_z^* = \text{const}$. Therefore, the specific effective power of the turboprop engine increases with increasing airspeed. And this cause also has a decisive effect on the specific equivalent power of the turboprop engine, causing it to increase in spite of the reduction of the specific reactive thrust during this process.

At the same time, the weight flowrate of air through the turboprop engine also increases, for the same reasons as in the case of the turbojet engine.

Thus, in this case the increase of the effective power and equivalent power of the turboprop engine with increasing airspeed is the result of a simultaneous increase of both, specific power and weight flowrate of air.

Due to the increase of the heat drop in the turbine with increasing airspeed the gas velocity c_e at the turbine outlet is slightly increased in this case, but at a significantly slower rate than the airspeed. This leads to such a significant decrease of the velocity difference $(c_e - V)$, that is of the specific reactive thrust, that the reactive thrust of the turboprop engine is reduced continuously in spite of the simultaneous increase of the air flowrate (see figure 190).

However, as far as the specific fuel consumption C_e is concerned, it is not difficult to arrive at the conclusion that in the case under consideration this consumption decreases with increasing airspeed as a result of both, an increase of specific power $N_{e\,sp}$ and an increase of the excess of air coefficient α that is due to the decrease of the temperature difference $(T_z^* - T_k^*)$. The physical cause for the decrease of C_e with increasing airspeed is the increase of the total compression ratio and the associated increase of the effective efficiency η_e of the engine.

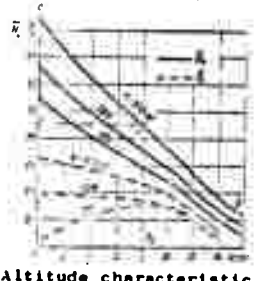

Figure 192: Altitude characteristics of a turboprop engine (variation of $\bar{N}_e$ and $\bar{P}_R$ as a function of H for different V).

Let us now consider the second possible case of turboprop engine control. Let us stipulate that not only $T_z^* = \text{const}$ and $n = \text{const}$ with changing airspeed (and altitude), but also that the heat drop accomplished in the turbine remains constant. The last-named condition can be satisfied by means of reducing the outlet cross-section area of the jet nozzle in accordance with the increase in airspeed.

It is obvious that under these conditions the specific effective power of the engine will remain constant with changing airspeed (and altitude) (if the compressor work $L_k = \text{const}$). Consequently, when the airspeed is increased the effective power of the turboprop engine will increase only as a result of the corresponding increase of the weight flowrate of air through the engine, that is at a slower rate than in the preceding case.

Since $\varepsilon_T = \text{const}$, the gas expansion ratio in the jet nozzle, $\varepsilon_{j.n} = p_z^*/p_H$, increases proportionally to the overall compression ratio π_o^* when the airspeed is increased. For this reason, as well as due to the increase of the air flowrate, the reactive thrust of the turboprop engine in this case varies with increasing airspeed approximately in the same manner as the thrust of a turbojet engine, which means that it changes insignificantly at subsonic airspeeds. As a result, the product $P_R V$ is increased, and the specific equivalent power $N_{eq\ sp}$ will increase in spite of the fact that $N_{e\ sp} = \text{const}$.

Calculations show that in this case the increase of $N_{eq\ sp}$ and the decrease of the specific fuel consumption C_{eq} are greater with a simultaneous increase of airspeed than in the preceding case.

Altitude characteristics of a turboprop engine are shown for different airspeeds in figures 192 and 193. These characteristics show the relative variation of N_e, P_R, and C_e with changing altitude in comparison to their values at V = 0 and H = 0, and are plotted for the same conditions as the airspeed characteristics in figures 190 and 191.

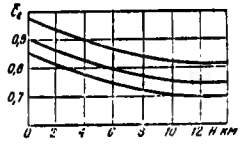

Figure 193: Altitude characteristics of a turboprop engine (variation of C_e as a function of H for different V).

The adiabatic heat drop h_T in the turbine increases with increasing altitude at V = const, as a result of the increase of the overall compression ratio (up to 11 km), so that the specific effective power of the engine is increased, too. But at the same time the weight flowrate of air through the engine is reduced, and

this at a slower rate than the density of the atmospheric air (for the same reasons that apply to a turbojet engine). As a result, up to an altitude of 11 km the effective power of the turboprop engine is reduced at a lesser rate than the density of the atmospheric air. When the altitude is increased beyond 11 km, the overall compression ratio remains π_0^* = const, so that the specific effective power remains constant at T_z^* = const and, consequently, the effective power is already reduced in proportion to the atmospheric air density.

As a result of the increase of the heat drop accomplished in the turbine the gas velocity c_2 at the turbine outlet increases up to an altitude of 11 km and subsequently remains almost constant. This has the result that the specific reactive thrust is increased up to an altitude of 11 km at V = const and n = const, and remains constant at greater altitudes. The increase of the specific reactive thrust and the simultaneous reduction of the air flowrate have the result that the reactive thrust of the turboprop engine either insignificantly decreases or slightly increases with increasing altitude up to 11 km, depending on the airspeed V = const (see figure 192).

The specific fuel consumption C_e of a turboprop engine decreases with increasing altitude up to 11 km at V = const, T_z^* = const, and n = const (see figure 193) as a result of the increase of the effective efficiency η_e due to the increase of the overall compression ratio π_0^*. On the other hand, we know that the excess of air coefficient decreases up to an altitude of 11 km at T_z^* = const but that $N_{e\ sp}$ and $N_{eq\ sp}$ decreases at a greater rate during this process, so that the products of these magnitudes and α increase, while the specific effective fuel consumption and equivalent fuel consumption are reduced. At altitudes of H > 11 km it is obvious that C_e = = const and C_{eq} = const.

If the heat drop accomplished in the turbine is kept constant under all flight conditions (by means of controlling the jet nozzle area), the effective power of the engine will drop at a faster rate with increasing altitude than shown in figure 192, but still at a slower rate than the atmospheric air density. This is due to the fact that the specific effective power remains almost constant while the air flowrate through the engine varies with altitude at the same rate as in the preceding case.

The gas expansion ratio in the jet nozzle increases with increasing altitude and ε_T = const (up to an altitude of 11 km) for the same reasons that apply to an increase of airspeed (due to the increase of π_0^*). As a result, the reactive thrust of the turboprop engine is reduced to a lesser degree than shown in figure 192.

As far as $N_{eq\ sp}$ and C_{eq} are concerned, in this case (at ε_T = const) their degree of variation with changing altitude at V = const is approximately the same as that obtained for complete gas expansion to atmospheric pressure in the turbine (that is, for an increase of ε_T with increasing altitude).

It must be taken into consideration that, in order to fully utilize the airspeed and altitude characteristics of turboprop engines that were considered above, the reducing gear must be designed for the maximum effective power that is obtained at maximum rpm during flight at maximum speed near the ground (or, failing this, at low altitude). But if the propeller reducing gear of a turboprop engine is designed for this maximum possible power that exceeds, at the maximum airspeeds of modern aircraft with turboprop engines, the maximum power of a turboprop engine during static operation on the ground by 50 to 70 %, the weight and size of the reducing gear can become excessively great. Therefore, in order to reduce the weight of the reducing gear and, consequently, to reduce the weight of the engine as a whole, the reducing gear of a turboprop engine is very frequently not designed for the maximum effective power that could be obtained from the engine under flight conditions, but for a lesser power which, however, at the same time provides both, the required airspeed at the given design altitude and the take-off of the aircraft. However, in that case it is also necessary to limit the designed effective power of the turboprop engine with respect to the reducing gear. This type of limit for the effective power of a turboprop engine is indicated in figures 190 and 192 by the dash-dot lines ao for the case where the designed power with respect to the reducing gear is the power (point a) generated by the turboprop engine at an airspeed of 300 m/sec and an altitude H_{des} = 8 km which in this case is called the <u>designed altitude</u> of the engine. It is obvious that the area of the airspeed and altitude characteristics of a turboprop engine that is located above the limiting line oa cannot be utilized.

In this case, the altitude characteristic of the turboprop engine at the given airspeed is already represented by the line oab, rather than cab (see figure 192).

Maintaining the effective power of a turboprop engine constant when the altitude is reduced from the designed value H_{des} (point a) to the ground (point o) can be accomplished by reducing the temperature T_g^* in front of the turbine at n = const, or by reducing the rpm at T_g^* = const and changing the propeller pitch accordingly. The first procedure is more advantageous, for the reasons discussed in the preceding paragraph.

Turboprop engines having the effective power limitation discussed above are called <u>altitude engines</u> and are most widely employed today.

CHAPTER 15

DUAL-FLOW TURBOJET ENGINES

1. General Observations

Dual-flow turbojet engines (DTRD) differ from turbojet engines of conventional design in that the turbine drives a low pressure compressor or secondary circuit fan in addition to the compressor and auxiliary assemblies.

One of the possible designs of a dual-flow turbojet engine is shown in figure 194. In this engine the same turbine 4 drives the compressor 2 and the fan 1 located in an annular duct 3. In this case the function of this fan is performed by the first stages of the axial-flow compressor 2, and for this purpose their blades are lengthened accordingly. The remaining elements and their relative positions remain the same as in a turbojet engine of conventional design.

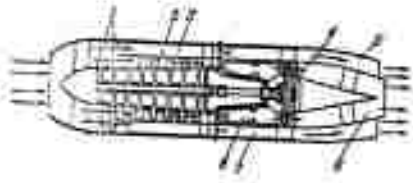

Figure 194: Diagram of a dual-flow turbojet engine: 1 - fan; 2 - compressor; 3 and 7 - annular ducts; 4 - turbine; 5 and 6 - jet nozzles; 8 - combustion chambers.

The flow section of the engine, consisting of the axial-flow compressor 2, the primary combustion chambers 8, the turbine 4, and the jet nozzle 6, is called the primary circuit of a dual-flow turbojet engine, which means that the primary circuit of a dual-flow turbojet engine by nature represents a turbojet engine of conventional design.

The annular duct 7 with the fan 1 located in it represents the secondary circuit of a dual-flow turbojet engine. Only air accelerated by the fan flows through the secondary circuit. This air bypasses the primary combustion chambers and the turbine, and is expelled from the engine parallel to the gas flow departing from the jet nozzle 6 of the primary circuit. In some dual-flow turbojet engines the air from the secondary circuit is mixed with the combustion products of the primary circuit behind the turbine and subsequently departs together with them through a common jet nozzle 5.

The thrust of a dual-flow turbojet engine is made up of the reactive force of the gas flow accelerated in the primary circuit

(that departs from the jet nozzle 6) and the reactive force of the air flow accelerated by the fan in the secondary circuit.

Also, the secondary circuit fan of a dual-flow turbojet engine can be driven by a separate turbine located behind the compressor turbine, as shown in figure 195 or figure 196.

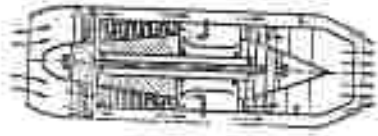

Figure 195: Diagram of a dual-flow turbojet engine with fan located forward.

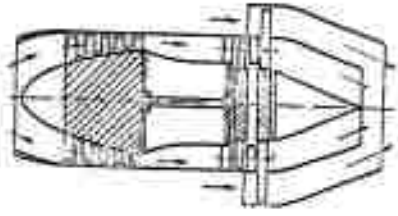

Figure 196: Diagram of a dual-flow turbojet engine with fan attachment aft.

The effect of the secondary circuit fan (in the sense of thrust generation) is similar to the effect of a multi-blade propeller rotating in an annular shroud. We know from propeller theory that such a "fan-type" propeller differs from a normal propeller in that it has greater efficiency at high airspeeds but poor efficiency at slow airspeeds and during take-off, has a lower weight, and requires no reducing gear to reduce the rpm when it is driven by a turbine. Figure 197 shows the approximate dependence of the efficiency of a fan-type and a normal propeller on the airspeed. For comparison purposes the dependence of the propulsive efficiency of a turbojet engine on the airspeed is also provided in this figure. Consequently, the dual-flow turbojet engine (without fuel combustion in the secondary circuit) occupies an intermediate position, with respect to economy and propulsive efficiency, between the turboprop engine and the turbojet engine of normal design. It is inferior in this respect to the turboprop engine during take-off and at slow airspeeds, but superior to it at high airspeeds where the efficiency of a propeller decreases rapidly. At the same time, the dual-flow

turbojet engine is superior with respect to economy to the turbojet engine of normal design at relatively slow airspeeds, since it has a better propulsive efficiency under these conditions, due to the lower exhaust velocity of the air and gas, compared to the turbojet engine. However, at high airspeeds such a dual-flow turbojet engine is inferior to a turbojet engine of conventional design.

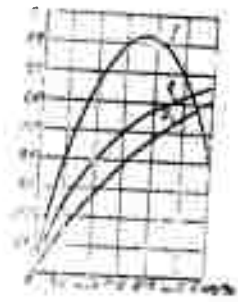

Figure 197: Dependence of the efficiencies of a propeller (1), a fan-type propeller (2), and of the propulsive efficiency of a turbojet engine, on the airspeed.

The thrust of a dual-flow turbojet engine can be augmented by means of burning additional fuel, either in the secondary circuit air flow or behind the turbine of the primary circuit. However, at subsonic and comparatively slow supersonic airspeeds this type of thrust augmentation of a dual-flow turbojet engine will yield a smaller increase of thrust and a significantly greater increase of specific fuel consumption than fuel combustion behind the turbine of an afterburning turbojet engine (TRDF) having the same parameters for the operating process as the primary circuit of the dual-flow turbojet engine.

However, at significant supersonic airspeeds a dual-flow turbojet engine with fuel combustion in the secondary circuit (DTRDF) is already approximately equivalent, under otherwise equal conditions, to an afterburning turbojet engine with respect to its specific thrust (referred to the total air flowrate through both circuits) and specific fuel consumption. Consequently, for the same thrust the diametric dimensions of the axial-flow compressor and turbine of a dual-flow turbojet engine with thrust augmentation can be smaller than those of a turbojet engine or afterburning turbojet engine. The employment of a dual-flow turbojet engine with thrust augmentation at supersonic airspeeds can prove advantageous especially for this reason.

2. Specific Parameters of Dual-Flow Turbojet Engines

The thrust of a dual-flow turbojet engine is made up of the thrust P_1 generated by the primary circuit, and the thrust P_2 generated by the secondary circuit. These thrust components equal

$$P_1 = \frac{G_{a1}}{g}(c_{e1} - V);$$

$$P_2 = \frac{G_{a2}}{g}(c_{e2} - V).$$

Consequently, the total thrust of a dual-flow engine will equal

$$P = \frac{G_{a1}}{g}(c_{e1} - V) + \frac{G_{a2}}{g}(c_{e2} - V), \tag{15.1}$$

where c_{e1} is the exhaust velocity of the combustion products from the jet nozzle of the primary circuit;

c_{e2} is the exhaust velocity of the air from the secondary circuit;

G_{a1} and G_{a2} are the weight flowrates of the air through the primary and the secondary circuit, respectively.

The specific thrust of a dual-flow turbojet engine can be referred either to the air flowrate G_{a1} through the primary circuit only, or to the overall air flowrate through the engine:

$$G_{a\,o} = G_{a1} + G_{a2}.$$

In the first case we obtain from equation (15.1)

$$P_{sp} = \frac{1}{g}[c_{e1} + \kappa c_{e2} - (1 + \kappa)V], \tag{15.2}$$

where $K = G_{a2}/G_{a1}$ is called the dual-flow ratio. Modern dual-flow turbojet engines have a value of K = 0.3 to 2.5 and sometimes more, depending on their purpose.

Under otherwise equal conditions the specific thrust, referred to the air flowrate through the primary circuit, determines the specific fuel consumption of a dual-flow turbojet engine. This is due to the fact that the fuel consumption per hour of a dual-flow turbojet engine depends only on the air flowrate through the primary circuit and on the excess of air coefficient in the primary combustion chambers of that circuit, since

$$G_{fuel\ 1} = 3600\, G_{a1}/\alpha_1 l_o.$$

Accordingly, the specific fuel consumption of a dual-flow turbojet engine will equal

$$C_{sp} = G_{fuel\ 1}/P_1 + P_2 = 3600\, G_{a1}/\alpha_1 l_o (P_1 + P_2).$$

However, $G_{a1}/P_1 + P_2 = 1/P'_{sp}$, so that

$$C_{sp} = 3600/\alpha_1 l_o P'_{sp}. \tag{15.3}$$

Thus, the greater the specific thrust of a dual-flow turbojet engine, referred to the air flowrate through the primary circuit, the lower will be the specific fuel consumption of that engine at a given τ_1.

If we refer the specific thrust to the overall air flowrate through the dual-flow engine we obtain

$$P''_{sp} = P_1 + P_2/G_{a1}(1+K)$$

but since $P_1 - P_2/G_{a1} = P'_{sp}$, it applies that

$$P''_{sp} = P'_{sp}/1 + K. \qquad (15.4)$$

This specific thrust determines the diametric dimensions of a dual-flow turbojet engine. The smaller P''_{sp}, the greater must be the overall air flowrate through the engine for a prescribed total thrust and, consequently, the greater will be the diametric dimensions and weight of the engine under otherwise equal conditions, and the smaller will be its drag-to-thrust ratio.

If additional fuel is burned in the secondary circuit, the gas exhaust velocity from this circuit will increase under otherwise equal conditions, and will become $c_{2aug} > c_{e2}$.

It is obvious that the specific thrust values $P'_{sp\ aug}$ and $P''_{sp\ aug}$ for a dual-flow turbojet engine with thrust augmentation whose secondary circuit afterburner is in operation can be determined in accordance with the same formulas (15.2) and (15.4) that are applicable to the dual-flow turbojet engine, if we substitute c_{2aug} for c_{e2} in these formulas.

The jet nozzle area of the secondary circuit must be increased when additional fuel is burned in the secondary circuit in order to keep the regimes of the secondary and primary circuit constant. Otherwise the air flowrate through the secondary circuit fan will be reduced as a result of the increase in gas temperature between the fan and the jet nozzle of the secondary circuit which, obviously, will lead to a reduction in the power required for driving the fan. But in that case the gas temperature T^*_z in front of the turbine in the primary circuit must be reduced in order to maintain the previous engine rpm, and the thrust of the primary circuit will be reduced. As a result, the increase in overall thrust will be inadequate, and in a number of cases this can even lead to a reduction of the overall thrust of a dual-flow turbojet engine with thrust augmentation in comparison to a dual-flow turbojet engine.

Let us designate by x the energy distribution coefficient in a dual-flow turbojet engine, or the ratio between the energy L_2 consumed to drive the secondary circuit fan and the available energy L_e, that is

$$x = L_2/L_e.$$

That part of the available energy that is attributable to the secondary circuit, $L_2 = xL_e$, is consumed for converting (with the aid of the fan) the kinetic energy of the air stream flowing through this circuit, equaling $\frac{G_{a_2}\left(c_{c_2}^2 - V^2\right)}{2g}$,

and, in addition, is consumed for losses in the turbine, fan, and duct of the secondary circuit. On this basis we can write

$$xL_e\eta_2 G_{a_1} = G_{a_2}\frac{c_{c_2}^2 - V^2}{2g},$$

whence, substituting $G_{a2}/G_{a1} = K$, we obtain

$$c_{c_2} = \sqrt{2gL_e\eta_2\frac{x}{K} + V^2},$$

where η_2 is the efficiency of the secondary circuit that takes into consideration the losses of available energy mentioned above.

The parameters of the operating process of the primary circuit of a dual-flow turbojet engine, that is the compressor compression ratio π_k^* and compressor efficiency η_k, the temperature T_z^* in front of the turbine and the turbine efficiency η_T, and so on, determine the magnitude of available energy L_e. The dependencies of the specific thrust and specific fuel consumption of a dual-flow turbojet engine on these parameters for given parameters x, K, and η_2 of the secondary circuit must be the same by nature as those of a turbojet engine. Therefore, we shall not stop to discuss these dependencies but shall consider the effect of the parameters of the secondary circuit on the thrust and specific fuel consumption of a dual-flow turbojet engine.

In the general case of a dual-flow turbojet engine, where the head of the secondary circuit fan is not a previously established magnitude, the energy distribution coefficient x and the dual-flow ratio K will be independent variables.

The dependencies of the specific thrust P_{sp} and specific fuel consumption of a dual-flow turbojet engine and a dual-flow turbojet engine with thrust augmentation on the energy distribution coefficient x for different dual-flow ratios and for $\eta_2 = 0.75$, V = 0, and H = 0 are shown in figures 198 and 199. Also plotted for comparison purposes in these figures are the values of P_{sp} and C_{sp} for a turbojet engine under the same parameters of the operating process that apply to the primary circuits of the dual-flow turbojet engine and the dual-flow turbojet engine with thrust augmentation, that is for $\pi_{k0}^* = 7$, $T_z^* = 1200^\circ K$, $\eta_T^* = 0.9$, $\eta_k = 0.85$, and $\varphi_{j.n} = 0.96$. In principle the nature of these dependencies is also retained in flight, provided that the condition of the expediency of using a dual-flow turbojet engine is satisfied (see below).

It is seen from figures 198 and 199 that the specific thrust of a dual-flow turbojet engine, and at low values of x and $T_{aug\ 2}^*$ also of a dual-flow turbojet engine with thrust augmentation, is significantly less than that of a turbojet engine (where K = 0). This

is due to the fact that in these cases the shift of part of the available energy to the secondary circuit has the result that the gas exhaust velocity from the primary circuit is reduced, while the exhaust velocity of the air (gas) from the secondary circuit is less than that of a turbojet engine.

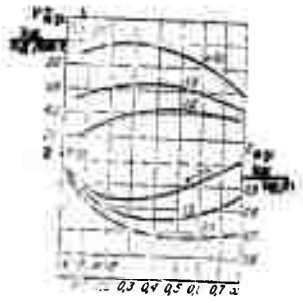

Figure 198: Dependence of the specific thrust and specific fuel consumption of a dual-flow turbojet engine on the distribution of the available energy for different values of K.

Legends:
1 - $P_{sp\ turbojet} = 65$
2 - turbojet engine

Moreover, with increasing dual-flow ratio K at x = const and under otherwise equal conditions, the specific thrust P''_{sp} of a dual-flow turbojet engine is reduced, since in that case the exhaust velocities of the air and gas from the secondary and primary circuits will be reduced. But at the same time the increase of propulsive efficiency that is associated with a reduction of exhaust velocity leads to a reduction of the specific fuel consumption. Thus, for instance, at K = 1.5 and V = 0 the specific thrust P''_{sp} of a dual-flow turbojet engine amounts to 50 to 60 %, and the specific fuel consumption to 70 to 75 %, respectively, of the P_{sp} and C_{sp} of a comparable turbojet engine, as seen from figure 198.

However, the specific fuel consumption of a dual-flow turbojet engine with thrust augmentation increases continuously with increasing dual-flow ratio K and under otherwise equal conditions (see figure 199). This is due to the fact that the air compression ratio in the secondary circuit (that is, L_{fan}) decreases with increasing K at x = const and L_e = const, so that the heat utilization that can be obtained during the combustion of additional fuel in the secondary circuit will deteriorate.

It also follows from figures 198 and 199 that an optimum value of the energy distribution coefficient, x_{opt}, exists in dual-flow

turbojet engines as well as in turboprop engines that corresponds to the maximum specific thrust and minimum specific fuel consumption under given conditions.

Calculations show that, the smaller the dual-flow ratio and the efficiency η_2 of the secondary circuit, and the greater the airspeed and the velocity coefficient of the jet nozzle of the primary circuit, the smaller will be x_{opt} or, in other words, the smaller will be that part of the available energy that must be transferred to the secondary circuit of a dual-flow turbojet engine.

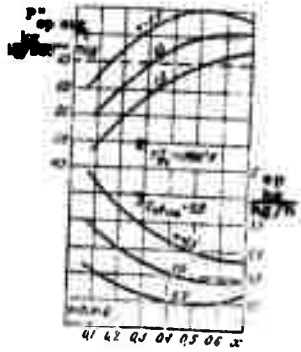

Figure 199: Dependencies of the specific thrust and specific fuel consumption of a dual-flow turbojet engine with thrust augmentation on the energy distribution for different values of K.

Legends:
1 - turbojet engine
2 - T^*_{aug} = 1700°K
3 - C_{sp} turbojet

The dependencies of the coefficient x_{opt} on the dual-flow ratio K for a dual-flow turbojet engine with T^*_g = 1200°K, π^*_{kO} = 7, η^*_t = 0.90, η_k = 0.85, η_2 = 0.75, and $\varphi_{j.n.}$ = 0.96 are shown in figure 200 for two cases, during static engine operation (M_H = 0) and in flight (M_H = 1.2 and H = 11 km). It is seen that, in both cases, the value of x_{opt} increases rapidly with increasing K.

The optimum value of the energy distribution coefficient also increases with increasing gas temperature in front of the turbine, increasing compression ratio (up to a certain limit), and increasing efficiency of the primary circuit compressor.

Since under otherwise equal conditions, each value of the dual-flow ratio K corresponds to an optimum magnitude x_{opt} of the energy distribution coefficient, x must be varied at the same time when there is a change in K in order to obtain a maximum gain of specific thrust.

Calculations also show that the optimum value of the coefficient x_{opt} increases with increasing degree of heat increase of the air in the secondary circuit of a dual-flow turbojet engine with thrust augmentation, under otherwise equal conditions. The dependence on x_{opt} for a dual-flow turbojet engine with thrust augmentation at different values of $\bar{T}_{aug\,2}$ and under different flight conditions is indicated by the dotted lines in figure 200 that are plotted for the same parameters of the operating process that were used for the dual-flow turbojet engine in that graph.

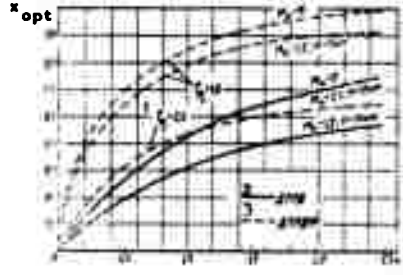

Figure 200: Dependence of the optimum energy distribution on the dual-flow ratio for a dual-flow turbojet engine and a dual-flow turbojet engine with thrust augmentation.

Legends:
1 - $\bar{T}_{aug\,2}$
2 - dual-flow turbojet engine
3 - dual-flow turbojet engine with thrust augmentation

3. Characteristics of Dual-Flow Turbojet Engines and Dual-Flow Turbojet Engines with Thrust Augmentation

The characteristics of dual-flow turbojet engines and dual-flow turbojet engines with thrust augmentation are defined as the dependencies of their overall thrust and specific fuel consumption on the rpm at a given airspeed and altitude (throttling characteristics) and on the airspeed or the altitude under the selected control schedule.

Under identical air flowrates through the compressor (the primary circuit) and equal parameters of the engine operating process (except for the secondary circuit), these characteristics occupy an intermediate position between the corresponding characteristics of turbojet engines and turboprop engines.

The rpm characteristics of a dual-flow turbojet engine differ by the following special features from the rpm characteristics of a turbojet engine having the same parameters for the operating process as the primary circuit of the dual-flow turbojet engine.

The power required to drive the secondary circuit fan of a dual-flow turbojet engine equals

$$N_{fan2} = G_{a2}L_{fan2}/75$$

where L_{fan2} is the effective work of the secondary circuit fan.

Consequently, we must write for the equilibrium regime of a dual-flow turbojet engine

$$N_T = N_k + N_{fan2} + N_r$$

or, determining the turbine power with respect to the airflowrate G_{a1} instead of the gas flowrate, and reducing to G_{a1}, we can write

$$L_T = L_k + KL_{fan2}.$$

As a rule, the designed magnitude for the head or compression ratio of the secondary circuit fan of a dual-flow turbojet engine is always smaller than that of its primary circuit compressor. Therefore, the air flowrate through the secondary circuit decreases with decreasing rpm, for the reasons discussed in Chapter 10, at a slower rate than the air flowrate through the primary circuit compressor, so that the dual-flow ratio K will increase during this process. At the same time, the pressure drop in the primary circuit jet nozzle of a dual-flow turbojet engine is usually subcritical under the maximum regime at V = 0 and H = 0. Therefore, when the rpm is reduced (starting out from maximum rpm) the gas expansion ratio ε_T reduced (starting out from maximum rpm) the gas expansion ratio ε_T in the turbine of a dual-flow turbojet engine with F_e = = const immediately begins to decrease, while in a turbojet engine with F_e = const the ratio ε_T initially remains constant with decreasing rpm.

Increasing the dual-flow ratio K and decreasing ε_T at a faster rate will have the result that, under otherwise equal conditions, the gas temperature in front of the turbine of a dual-flow turbojet engine will decrease at a slower rate with decreasing rpm than that of a turbojet engine, and this rate will slow down with increasing designed value of K at n_{max}.

Therefore, the operating line of a dual-flow turbojet engine with F_e = const will have a greater slope than the operating line of a turbojet engine with F_e = const, as shown in figure 201. Consequently, under reduced rpm the stability margin of a dual-flow turbojet engine with F_e = const will be smaller, and its pick-up poorer than for a turbojet engine with F_e = const and with a designed compressor compression ratio that equals the $\pi^*_{k\,des}$ of the primary circuit compressor of the dual-flow turbojet engine. It is obvious that, under otherwise equal conditions, these stability margins of a dual-flow turbojet engine decrease with increasing designed value of K.

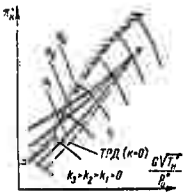

Figure 201: Operating lines of dual-flow turbojet engines for different dual-flow ratios.

Legend:
1 - turbojet engine (K = 0)

Moreover, as a result of the slower rate of temperature decrease in front of the turbine with decreasing rpm, the overall thrust of a dual-flow turbojet engine decreases at a relatively slower rate, and the specific fuel consumption increases at a relatively faster rate, than the thrust and specific fuel consumption of a turbojet engine. As an example, figure 202 shows the relative variation with respect to rpm of the thrust and specific fuel consumption of a dual-flow turbojet engine with K = 2 (solid lines) and of a turbojet engine (dotted lines) having the same $\pi^*_{K\ des}$ = 7, $T^*_{z\ max}$ = 1200°K, η^*_T = 0.9, and η_K = 0.85, where the thrust and specific fuel consumption of both engines are assumed to be equal to one at the maximum regime.

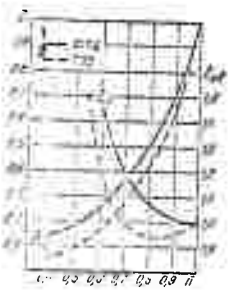

Figure 202: Throttling characteristics of dual-flow turbojet engines.

Legend: 1 - dual-flow turbojet engine;
2 - turbojet engine.

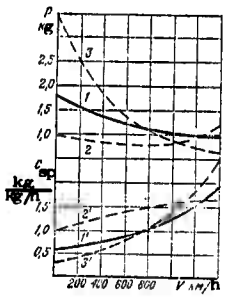

Figure 203: Airspeed characteristics:
1 - dual-flow turbojet engine; 2 - turbojet engine; 3 - turboprop engine.

The profile of the airspeed and altitude characteristics of dual-flow turbojet engines depends on the selected control schedule.

In principle, the control schedules of dual-flow engines at maximum thrust are the same as for turbojet engines, for instance,

$n_{max} = \text{const}$ and $T^*_{3max} = \text{const}$

or

$n_{max} = \text{const}$ and $F_a = \text{const}$,

in addition to T^*_{aug2} = const for dual-flow turbojet engines with thrust augmentation.

As far as the conditions

$$x = x_{opt} \text{ and } K = K_{des}$$

are concerned, their realization under varying airspeed and altitude at the same time with n = const and T^*_z = const(or F_e = const) requires such a great engine control system complication that it is not always practically possible by far.

It can be considerably simpler to accomplish the following control schedules:

for dual-flow turbojet engines:

$$n = \text{const}; \quad T^*_z = \text{const}; \quad K = \text{const};$$

for dual-flow turbojet engines with thrust augmentation:

$$n = \text{const}; \quad T^*_z = \text{const}; \quad T^*_{aug2} = \text{const}; \quad k = \text{const}.$$

But even these schedules require variable area jet nozzles in both circuits of dual-flow turbojet engines.

For comparison, figure 203 shows the airspeed characteristics of a dual-flow turbojet engine for K = 2, η_2 = 0.75 (solid curves), and of a turbojet engine and a turboprop engine under identical control schedules, that is under n = const and T^*_z = const. The values of thrust and specific fuel consumption of the turbojet engine at V = 0 and H = 0 are assumed to be equal to one. The following are equal in all three compared engines: air flowrates through the compressor (in the case of the dual-flow engine, through the primary circuit) under test stand conditions; temperature in front of the turbine, T^*_z = 1200°K; compression ratio and efficiency of the compressor, $\pi^*_{k\,des}$ = 7 and η_k = 0.85; and turbine efficiency η^*_T = 0.9.

TABLE OF CONTENTS

	Page
Introduction	2
CHAPTER 1. Necessary Data from the Thermodynamics of Flow and Gas Dynamics	6
1. Gas Flow and the Equation of Continuity	6
2. The Energy Equation	8
3. Bernoulli's Equation	12
4. Stagnation Parameters. Special Features Involved in Heating Bodies in a Gas Flow	15
5. Sound Velocity and Mach Number	18
6. Propagation of Weak Perturbations in a Gas. Shock Waves	20
7. The Momentum Equation	27
8. Moment of Momentum Equation	32
CHAPTER 2. Turbojet Engines	34
1. General Information	34
2. Turbojet Engine Thrust	39
3. Turbojet Engine Efficiencies	44
4. Specific Parameters of Turbojet Engines	47
CHAPTER 3. Thermodynamic Principles of Turbojet Engine Operation	50
1. General Considerations	50
2. Cycle with Heat Input at Constant Pressure and with Adiabatic Compression and Expansion	51
3. Cycle with Two-Stage Heat Input at Constant Pressure	57
4. Cycle with Heat Input at Constant Pressure and with Isothermic Compression	59
5. Cycle with Thermal Regeneration	61
6. The Real Turbojet Engine Cycle	64
CHAPTER 4. Turbojet Engine Inlets	68
1. Air Compression at the Engine Inlet by the Ram Effect	68
2. Simple Inlets	70
3. Supersonic Inlet Diffusers	72
4. Off-Design Points and Unstable Operation (Surging) of a Supersonic Diffuser	77
5. The Supersonic Diffuser Characteristic Curves and Regulation Concept	81
CHAPTER 5. Aviation Compressors	86
1. Principles of Compressor Arrangement and Operation	86
2. Air Compression in a Compressor	90
3. Compressor Efficiency and Rating	95
4. Fundamentals of Axial-Flow Compressor Theory Velocity Plan and Internal Work Done by a Stage	98

5. Centrifugal Compressor Theory in Brief 107
6. Compressor Characteristic Curves 112
7. Unstable Compressor Operation (Surging), and Preventive Measures 119
CHAPTER 6. Combustion Chambers 127
1. General Observations 127
2. Special Features of Managing the Combustion Process 129
3. Principal Combustion Chamber Parameters 134
CHAPTER 7. Aviation Turbines 137
1. Principles of Turbine Design and Operation 137
2. Gas Outflow from the Nozzle Assembly of a Turbine 142
3. Energy Conversion at the Rotor Blades 146
4. Turbine Efficiency and Turbine Power 149
CHAPTER 8. The Jet Nozzle of the Turbojet Engine 157
1. Gas Flow in the Jet Nozzle 157
2. Concept of the Reverse Thrust of a Turbojet Engine 166
CHAPTER 9. Dependence of the Specific Thrust and Economy of Turbojet Engines on the Basic Parameters of the Operating Process.... 169
1. Specific Thrust 169
2. Economy of a Turbojet Engine 175
CHAPTER 10. Equilibrium Regimes of Turbojet Engines 183
1. General Consideration 183
2. Special Features of Equilibrium Regimes of a Turbojet Engine under Independent Changes in rpm and Temperature in Front of the Turbine 186
3. Equilibrium Regimes of a Turbojet Engine with Fixed Area Jet Nozzle 189
CHAPTER 11. The Effect of Operating Conditions on the Regimes of a Turbojet Engine 199
1. The Effect of the rpm on the Parameters of the Operating Process of a Turbojet Engine 199
2. The Effect of External Conditions on the Parameters of the Operating Process of a Turbojet Engine 202
3. Dependence of the Thrust and Economy of a Turbojet Engine on Atmospheric Conditions 206
4. The Effect of the Geometry of, and Losses in the Elements of a Turbojet Engine on Thrust, Economy, and Temperature in Front of the Turbine 208
CHAPTER 12. Characteristics of Turbojet Engines 216
1. General Considerations 216
2. Concept of the Control Schedules of Turbojet Engines 216
3. Throttling Characteristics of Turbojet Engines 224

4. Airspeed Characteristics of Turbojet Engines 228
5. Altitude Characteristics of Turbojet Engines 233
6. The Concept of Turbojet Engine Characteristics in Similarity Parameters 236
7. Reducing the Results of Turbojet Engine Tests to Prescribed Conditions 238
8. Thrust Augmentation of Turbojet Engines through Fuel Combustion behind the Turbine 240
9. Thrust Augmentation of Turbojet Engines through Cooling Liquid Injection 245
10. Special Features of the Characteristics of Double-Compound Turbojet Engines 247
CHAPTER 13. Transient Regimes and Start-up of Turbojet Engines 255
1. Basic Dependencies. Pick-up of Turbojet Engines 255
2. Special Features of the Transient Regimes of Turbojet Engines .. 256
3. Start-up of Turbojet Engines 262
CHAPTER 14. Turboprop Engines 265
1. General Observations 265
2. Power, Thrust, and Specific Parameters of Turboprop Engines 268
3. Dependence of the Specific Power and Economy of a Turboprop Engine on the Parameters of the Operating Process 270
4. Throttling Characteristics of Turboprop Engines 275
5. Airspeed and Altitude Characteristics of Turboprop Engines 283
CHAPTER 15. Dual-Flow Turbojet Engines 288
1. General Observation 288
2. Specific Parameters of Dual-Flow Turbojet Engines 291
3. Characteristics of Dual-Flow Turbojet Engines and Dual-Flow Turbojet Engines with Thrust Augmentation 296

UNCLASSIFIED
Security Classification

DOCUMENT CONTROL DATA - R & D

(Security classification of title, body of abstract and indexing annotation must be entered when the overall report is classified)

1 ORIGINATING ACTIVITY (Corporate author)
Foreign Science and Technology Center
US Army Materiel Command
Department of the Army

2a. REPORT SECURITY CLASSIFICATION
UNCLASSIFIED

2b. GROUP

3 REPORT TITLE
PRINCIPLES OF THE THEORY OF AVIATION GAS TURBINE ENGINES

4 DESCRIPTIVE NOTES (Type of report and inclusive dates)
Translation

5 AUTHOR(S) (First name, middle initial, last name)
I. I. Kulagin

6 REPORT DATE
15 December 1970

7a. TOTAL NO OF PAGES
302

7b. NO OF REFS
N/A

8a. CONTRACT OR GRANT NO

b. PROJECT NO

c. T702301 2301

d. Requester: AXSMI-YDL

9a. ORIGINATOR'S REPORT NUMBER(S)
FSTC-HT-23- 539-71

9b. OTHER REPORT NO(S) (Any other numbers that may be assigned this report)
ACSI Control Number (None)

10 DISTRIBUTION STATEMENT
Approved for public release; distribution unlimited

11 SUPPLEMENTARY NOTES

12 SPONSORING MILITARY ACTIVITY
US Army Foreign Science and Technology Center

13 ABSTRACT

This is a reprint of RA-017-68 prepared for Missile Intelligence Directorate, Redstone Arsenal.

The ~~text of~~ this book reviewed the principles of the theory of gas turbine engines. The main attention was devoted to the physical significance of the phenomena and behavior patterns reviewed, and especially to those questions of theory directly associated with engine operation in the aircraft, and with bench testing.

DD FORM 1 NOV 68 1473 REPLACES DD FORM 1473, 1 JAN 64, WHICH IS OBSOLETE FOR ARMY USE.

UNCLASSIFIED
Security Classification

KEY WORDS	LINK A		LINK B		LINK C	
	ROLE	WT	ROLE	WT	ROLE	WT
lines of flow						
surface of flow						
flow equation						
flow density						
equation of continuity						
equation of constancy						
heat content equation						